Toute commande sera adressée à:
EDITURA ACADEMIEI ROMÂNE, Calea 13 Septembrie nr. 13, Sector 5, 050711, Bucureşti, România, Tel. 40-21-318 8146, 40-21-318 81 06, Fax. 40-21-318 2444; e-mail: edacad@ear.ro
RODIPET S.A., Piaţa Presei Libere nr. 1, Sector 1, P.O. Box 35-37, Bucureşti, România, Tel. 40-21-318 7001, Fax 40-21-318 7002.
ORION PRESS IMPEX 2000 S.R.L., Şos. Viilor nr. 101, sector 5, bl. 1, sc. 4, ap. 98, parter, P.O. Box 77-19, sector 3, Bucureşti, România, Tel. 40-21-335 0296, 40-21-301 8786, Fax: 40-21-335 0296; e-mail: office@orionpress.ro.

Les manuscrits ainsi que toute correspondance seront envoyés à la rédaction; les livres et les publications proposés en échange seront adressés à: INSTITUTUL DE BIOLOGIE, Splaiul Independenţei 296, P.O. Box 56-53, 060031, Bucureşti.

REVUE ROUMAINE DE BIOLOGIE
SÉRIE DE BIOLOGIE ANIMALE
Calea Victoriei 125
010071, Bucureşti, România
Tél. 650 76 80

REVUE ROUMAINE DE BIOLOGIE

SÉRIE DE BIOLOGIE ANIMALE

TOME 49, N^{os} 1–2 janvier-décembre, 2004

SOMMAIRE

NEW AND RARE EXOCHINAE FOR THE ROMANIAN FAUNA (2nd Note)

IRINEL CONSTANTINEANU, RAOUL CONSTANTINEANU, CAMIL ŞTEFAN LUNGU-CONSTANTINEANU

In this paper the authors present 6 species of Ichneumonidae belonging to the subfamily Exochinae, collected from different counties of Romania. The male of species *Exochus thomsoni* Schm. and the female of *Exochus frontellus* Holmgr. are new for the science. The genus *Periope* Hal. and the following 3 species: *Chorinaeus australis* Thoms., *Triclistus aethiops* (Grav.) and *Periope auscultator* Hal. are new for the Romanian fauna. The other species are rare for the Romanian fauna.

Family **ICHNEUMONIDAE** Latreille, 1802
Subfamily **EXOCHINAE** Dalla Torre, 1901
I. Genus **Chorinaeus** Holmgren, 1856

1. ***Chorinaeus australis*** Thomson 1887, ♀♂
Synonyms:
1887 *Chorinaeus australis* Thomson, Deutsch. Ent. Zeit., **31** (*1*): 201–202;
1925 *Chorinaeus flavifrons* Schmiedeknecht, Opusc. Ichneum., **40–41**: 4158;
1946 *Trieces xanthopsis* Townes, Boll. Ent. Venez., **5**: 61;
1975 *Chorinaeus xanthopsis* Aeschlim., Ann. Soc. Ent. France, **11** (*4*): 3–6.

Material: 2 ♀♀, 19. VII. 1964, 1 ♀ and 1 ♂, 21. VII. 1964, Baia Mare (Usturoi valley), Maramureş county.

♀. Head: dorsally transversal, narrowing beyond eyes, temple not convex. Occipital carina evident. Antennae longer than ½ body; flagellum with 14 articles. Lateral ocelli are situated between eyes at a distance equal to 1, 5 of their diameter. Face moderately convex; little transversal anterior, with a dense, rough, mat punctuation. Clypeus moderately convex, its right margin with a dense, rough punctuation. Genae almost 2 times longer than the width of mandible base.

Pronotum densely punctured, mated. Mesopleuri polished, with a finer punctuation and more rare than that of pronotum. Metapleuri shiny, the most part of their surface is flat and glabrous, lengthways pleural carina and towards hind coxae are hairy. Median longitudinal carinae of propodeum are slightly close near its base, propodeal spiracles are oval, being situated at an equal distance between pleural and lateral carinae. Nervullus oblique, postfurcal, broken below its half, discoideus almost absent.

REV. ROUM. BIOL. – BIOL. ANIM., TOME 49, Nos 1–2, P. 3–10, BUCAREST, 2004

Abdomen margins are parallel, with a dense, rough punctuation. Dorso-longitudinal and lateral carinae of tergite 1 are obvious; lateral carinae of tergite 1 are situated above and below spiracle, towards hind part of tergite are parallel, tergite with a median dorsal carina and two dorso-lateral carinae, obviously at base; tergite 3 without carinae.

Black. Lateral margins of face and frons, the triangular process of face between the antenna base and palpi are yellow; mandibles, with the exception of base and teeth, are dark. Tegulae and flagelli on the dorsal side are reddish-brown, ventral side of flagelli with light colour. Ventral side of coxae and trochanters, base and the apex of anterior and middle femorae, the most part of anterior tibiae and the base of middle and hind tibiae and all tarsi are reddish-brown. The other parts of legs are black. Length: 6.5 mm.

♂. Flagellum with 34–35 segments. The following are yellow: face, clypeus, lateral margins of frons, palpi, mandibles, without teeth and base, scape and the segments of curvature on ventral side, anterior and middle legs, base of hind tibiae; hind coxae and hind femorae are black; dorsal surface of anterior and middle femorae, tip of hind tibiae and hind tarsi are blackish-brown. The rest is similar to the female. Length: 6 mm.

Hosts: *Operophtera brumata* (Lep., Geometridae).

Distribution: England, Germany, Austria, Switzerland, Italy, Hungary, former Czechoslovakia, former Yugoslavia, Russia (Irkutzk, Amursk).

New species for the Romanian fauna.

II. Genus **Triclistus** Foerster 1868

2. ***Triclistus aethiops*** (Gravenhorst, 1829), ♀

Synonyms:

1829 *Exochus aethiops* Gravenhorst, Ichn. Eur., Vratislaviae;

1887 *Triclistus aethiops* Thomson, Deutsch. Ent. Zeit., **31** (*1*): 193–218.

Material: 1 ♀, 17. VII. 1971, Cioclovina mountain (at 640 m. hight), Gorj county.

♀. Head dorsally is slightly transversal, almost squarer, narrowed beyond eyes, laterally it is very long. Temples are long, laterally are longer than the transversal diameter of the eye; plane, with short and dense hairs, more rarely towards the vertex. Antennae longer than ½ body; flagellum with 23–27 segments. Face and clypeus are very convex, with dense and long pubescence. Face transversally, mat, dense punctuated. Clypeus shiny, with more densely punctuation than the face, between dots it is smooth.

Mesonotum with short, abstruse notauli. Mesopleuri are polished, anteriorly with a fine and rare punctuation, with rare hairs; the hind half is smooth and glabrous. Metapleuri are polished, smooth, glabrous, sometimes with a few hairs. Medio-longitudinal carinae of propodeum are almost parallel. Costula obviously only near

lateral carina. Area superomedia and area basalis are flat and glabrous. Lateral areae with pubescence. Propodeal spiracles are small and round. Radial vein begins behind the middle of stigma. Areolet is big, short pedicled, second intercubitus is sometimes missing. Nervulus weakly postfurcal. The small spur of hind tibiae is 1. 7 times longer than the width of the base of the first segment of hind tarsi.

Abdomen dense punctured, with the exception of the middle of tergites 1–3, with long and dense hairs. Tergite 1 with longitudinal obvious carinae, which do not outrun ½ of its length. Subgenital plate of the female presents a cut at the apex, which is 2–3 times longer than its height.

Black. Palps and mandibles are brown to brownish-gray. Antennae are reddish-brown, scape and the first 6 segments of flagellum lighter ventrally than dorsally. Tegulae yellowish-brown to brownish-black, sometimes dark brown; the other parts of fore legs are yellowish-brown; the middle and hind legs are bricky-brown to black; the apex of hind femorae obviously light. Length: 6 mm.

Hosts: *Lathronympha strigata* F. (Lep., Tortricidae), *Agonopterix alpigena* Frey and *A. hypericella* Hb. (Lep., Oecophoridae) [6].

Distribution: Sweden, England, Holland, Switzerland, Austria, former Czechoslovakia, Bulgaria, Russia (St. Petersburg) [6, 7].

New species for the Romanian fauna.

III. Genus **Periope** Haliday, 1839

Synonyms:

1839 *Periope* Haliday, Ann. Nat. Hist. **2**: 114;

1855 *Monoplectron* Holmgren, Svenska Vetensk. Akad. Handl., 1854: 81;

1868 *Oligoplectron* Förster, Verh. Naturh. Ver. Reinlande, **25**: 161, 218, 219;

1949 *Monoplectrochus* Heinrich., 1949 : 109, Münch. Ent. Gesell., Mitt., **35–39**: 109.

Type species of the genus: *Monoplectrochus hoerhammeri* Heirich.

Length = 6.5–9.0 mm.

Head dorsally is transversal, narrowed or widened behind the eyes, in profile is strongly narrowed from the lateral ocelli to the occipital carina. The occipital carina is complete or elongate, not touching the hipostomial carina. Antennae are shorter than the body, more or less knobby. The lateral ocelli do not reach the eyes. The face is convex in transversal sense, more or less visible, separated from clypeus by a transversal, quadratic or elongated groove, with an obvious triangular process between antennae base. Genae are shorter than the breadth of mandible base. Mandibles are widened, narrowed towards the apex, their teeth are big, with the same length, the outer surface of the mandible is roughly punctured.

The upper margin of the end of pronotum is slightly swollen posteriorly, with a superficial excavation. Propleuri are slightly convex. Mesonotum with small

notauli or they are absent. Scutellum convex, without lateral carinae. The dorsal end of the prepectal carina reaches the inferior angle of the pronotum, at a somewhat distance from the anterior margin of the mesopleuron. Sternauli are wide, unobvious or absent. Metapleuri are punctured. Propodeum is short, convex in profile, costula is absent, area superomedia is united with area basalis. The propodeal spiracles are rounded or ellipsoidal. Areolet is small, quadratic, pedicled. Nervullus postfurcal, oblique or vertical. Nervellus is broken beneath the middle. The legs are not so robust, moderately thickened. The trochantereli of the fore and middle legs are partially united with the femorae. The spurs of the middle tibiae are long, the inner spur is longer than the outer one. The hind tibiae with only one spur. The tarsal claws are dentate or not.

Sometimes the abdomen is knobbed, pedicled or sesile. The first tergite is basically more or less narrowed, with 2 dorso-longitudinal carinae not reaching the apex and 2 latero-longitudinal carinae along the whole tergite; the stigmae of the first tergite are situated in the middle, sometimes strongly prominent. The tergite 2 widens gradually backwards, sometimes with 2 dorso-longitudinal carinae at base. The tergites 4-6 are usually transversal. Tergite 7 is hidden at both sexes. The epipleuri of the second tergite are narrow or moderately wide, the tergite 3 is narrow, cuneiform or moderately wide, the tergites 4-6 are moderately wide. The ovipositor is hidden. The entire body is densely punctured.

Black.

Only 4 species are known in genus *Periope,* which are reported only from Holarctic region in the world fauna. Among them *P. auscultator* Hal., *P. hoerhammeri* (Heinr.) and *P. longiceps* Bauer are Palearctic, and *P. aethiops* (Cress.) is Nearctic.

Genus Periope is new for the Romanian fauna.

3. **Periope auscultator** Haliday, 1839, ♀♂

1839 *Periope auscultator* Haliday, Ann. Nat. Hist. **2**: 114;

1855 *Monoplectron zygaenator* Holmgren, Svensk. Vet. Akad. Handl. 1854: 81

Material: 1 ♀ şi 9 ♂♂, 26, 27, 28. VII. 1961, Ciocanu, Dâmbovicioara commune and 1 ♂, 29. VII. 1961, Cheile Dâmbovicioarei, Argeş county.

Head, on dorsal view, is narrower than the thorax, not narrowed transversally behind the eyes. The occipital carina is evident, reaching the hipostomial carina. The antennae are as long as ½ of the body length, obviously knobbed, flagellum with 20 articles, scape is elongated, the articles 2–3 are also elongated but shorter than the scape. The face is slightly transversal, almost quadratic, strongly convex, especially beneath the antennal sockets, which are delicate and densely punctured, strongly polished. Clypeus is evidently separated from face by a wide ridge; it is polished, punctured more rarely than face, its outer side is rounded. Palpi short and thick. The genae length is ½ of the basal width of the mandible.

Pronotum with small epomiae. The mesonotum is densely punctured, with evident notauli, as long as 1/3 of mesonotum length. The mesopleuri and metapleuri are polished, delicate and densely punctuated. The scutellum is convex, polished, delicately punctuated, bounded with carinae only at base. Propodeum with whitish dense, short hairs. Area superomedia and area basalis are united; they are wider than their common length; their surface is roughly-punctured, without setae. The propodeal spiracles are rounded. Areolet is sesile. Nervullus is postfurcal. Tarsal claws are combed.

Abdomen is pedicled, narrowed to the apex and delicately, rarely punctuated, intensely polished. Tergite 1 is elongated; strongly widened at the apex, with 2 dorso-longitudinal carinae; tergite 2 is slightly elongated; it enlarges gradually to the apex, tergites 3–4 are almost square, with parallel lateral margins; the next tergites are transversal, narrowed to the apex. Sternite 1 is united with tergite, almost reaching the stigma.

Black, with whitish, short and dense hairs. The antennae are dark brown. The apex of all femorae, all tibiae, the tarsal articles, except for the last 1–2, the most part of the tergites 2–3 are yellow-red. The last tarsal articles are dark. Pterostigma is bricky-red. Length = 7.0 mm.

The male is similar to the female. The antennae flagellum with 23 articles. Areolet is pedicled. Length = 6.5 mm.

Hosts: unknown.

Distribution: England, Sweden, Germany, Russia (Irkutzk) [6].

New species for the Romanian fauna.

IV. GENUS **EXOCHUS** Gravenhorst 1829

4. **Exochus frontellus** Holmgren 1856, ♀

Material: 1 ♀, 30.VIII.1969, Slătioara, Suceava county.

♀= **new**. The head is polished, slightly narrowed backwards. Frons is convex at the middle. The antennae are filiform, longer than the head and thorax together. The face is slightly convex. Thorax is wider than the head. Mesonotum is punctuated, the sides of the thorax are polished, rarely punctured. Nervullus is postfurcal, nervullus broken beneath the middle. Propodeum evidently areolated, costula not evident. The abdomen is a little longer than the head and thorax together. Tergite 1 with evident dorso-longitudinal carinae. Tergites, starting with tergite 2, are punctuated. Tergite 2 is transversal.

Black. Antennae are reddish at the apex, on the ventral side. The palpi, the mandibles, a spot on the genae and sides of vertex, a large spot on the face beneath the base of the antennae are yellow. The wings are almost colourless, stigma is brown. The legs are red-yellowish; coxae and trochanteri are brown on the dorsal side. Femorae are yellow at the base and apex. The hind tibiae with black apex. Length = 6 mm.

Hosts: unknown.

Distribution: Sweden. It is a rare species in Romania, being reported previously from Gurahonţ, Arad county and from "Hârboanca" natural reservation, Vaslui county [5].

5. ***Exochus thomsoni*** Schmiedeknecht 1925, ♀♂

Synonyms:

1895 *Exochus crassicornis* Thomson, Opusc. Ent., **19**: 2134.

1925 *Exochus thomsoni* Schmiedeknecht, Opusc. Ichneum., **5** (25): 3213.

Material: 1 ♀, 16.VIII.1949, Ivești, Galați; 1 ♂, 13.VIII.1949, Hanu Conachi, Galați county; 1 ♂, 11.VII.1958, Bicaz, Neamț county; 1 ♂, 4.VI.1965, "Valea lui David" natural reservation, Iași county; 1 ♂, 21.VIII.1958, Agigea, Constanța county.

♀: Length = 8 mm.

♂ = **new**. The head is less narrow than the thorax. Antennae are thick, filiform, slightly narrowed at the apex, a little shorter than the body. Notauli are deep and long enough. Costula is evident. The apical extremity of the radial vein is almost straight. Nervullus is slightly antefurcal, a little broken above the middle, almost at the middle. The abdomen is punctured, covered with hairs.

Black. The following are yellow: entire face, two dots on the vertex, the lower margins of the frons, the ventral half of the scape and of the pedicle, a line before and one beneath the base of the wings, the tegulae, the wing roots, pterostigma and mesosternum almost entirely and the ventral part of the abdomen. Pterostigma is brown. Scutellum and postscutellum are brown, with a yellow-whitish spot on the anterior part. The legs are red, with coxae and trochanteri black. The apex of the trochanteri, the anterior and middle coxae are whitish. The hind tibiae with a whitish ring. The hind tarsi are black-brownish, with ¾ of the basis of the articles 1–2 reddish. Length = 6–7.5 mm.

Hosts: unknown.

Distribution: Sweden. It is a rare species in Romania, being reported previously only from Ada Kaleh island, Mehedinţi county [2].

V. GENUS **TRIECES** Townes 1946

Type species: *Exochus texanus* Cresson 1872 [7]

6. **Trieces tricarinatus** (Holmgren 1856) 1856, ♀♂

Material: 1 ♀, 5. VII.1956, Agigea, Constanța county; 3 ♀♀, 11 and 12. VI. 1965, Letea woods (Haşmacul Mare), Tulcea county and 1 ♂, 19, VII. 1963 "Codrul Secular Slătioara" natural reservation, Suceava county.

♀. Head dorsally is transversal, narrowed behind the eyes. Temple convex; occipital carina evident. Antennae shorter than the body; flagellum with 27–31 segments; all flagellum segments a little prolonged. Eyes glabrous; distance between lateral ocelli and eyes is 1.5 times their diameter. Face and clypeus are not convex. Mandibles narrowed towards the apex. Genae evidently shorter than the basal width of the mandible.

Pronotum dense punctured, mat. Mesopleuri polished; metapleuri polished, smooth, with some rugosities near hind coxae, with hairs above rugosities. Pronotum punctured rugged; dorso-longitudinal carinea parallel; superomedia and basal areae are united, glabrous; lateral areae hairy. Propodeal spiracles are small, round, situated at its middle. Nervulus oblique, postfurcal. Hind coxae with long and dense hairs. Hind femorae are 2.4 times longer than wide.

Abdomen is rough and dense punctured. Dorso-longitudinal carinae of third tergite evident only at base; they meet the middle of tergite.

Black. Face, clipeus, genae, mandible base and palpi are yellow. A spot on face processus (situated between the antennae base) and a spot near tentorial grooves are dark brown; usually fore and middle legs, hind tibiae and tarsi yellowish-brown or reddish-brown; stigma dark brown. Length = 4.0–5.5 mm.

♂. Alike female. Genae equal to basal width of mandible. Flagellum with 25–29 segments. Legs, without hind coxae and femorae, with a lighter colour than the female. Length = 4.5–5.7 mm.

Hosts: *Yponomeuta cognatella* Hb., *Y. evonimella* L., *Y. malinella* Zell., *Y. rorella* Hb., *Y. padella* L., *Y. vigintipunctata* Ratz., *Y. mahalebella* Guen. (Lep., Yponomeutidae), *Choristoneura murinana* Hb., *Grapholita funebrana* Tr., *Laspeyresia pomonella* L. (Lep., Tortricidae), *Agonopteriz scopariella* Hein. (Lep., Oecophoridae), *Scythrix knochella* F. (Lep., Scythrididae).

Distribution: Western Europe, Ukraine, Republic of Moldova, Kazakstan, Russia (Iaroslav, Tambov) [6]. In Romania it is a rare species, being recorded previously from Haţeg, Hunedoara county, Ineu, Arad county, Saschiz, Mureş county, Cehu Silvaniei, Sălaj county, Victoria, Iaşi county [5]; Letea woods, Biosphere Reserve "Danube Delta", Tulcea county [1, 4] and Slătioara, Stulpicani commune, Suceava county [3].

CONCLUSIONS

1. Female of species *Exochus frontellus* Holmgr. is new for science;
2. Male of species *Exochus thomsoni* Schm. and *E. citripes* Thoms. is new for science;
3. Genus *Periope* Hal. and species *Periope auscultator* Hal., *Chorinaeus australis* Thoms. and *Triclistus aethiops* (Grav.) are new for the Romanian fauna;
4. Species *Exochus frontellus* Holmgr. and *Exochus thomsoni* Schm. are rare for the Romanian fauna.

REFERENCES

1. Constantineanu M. I., Constantineanu R. M., 1968, *Ord. Hymenoptera (Fam. Ichneumonidae)*, in: *L'Entomofaune de l'île de Letea (Delta du Danube)*, Trav. Mus. Hist. Nat. "Grigore Antipa", **9**: 149 – 183, 1968.
2. Constantineanu M. *et al.*, 1975, *Fauna, Grupul de cercetări complexe "Porțile de Fier" – Seria monografică*, 316 pp., Ed. Acad. Rom. – "*Insecta: Hymenoptera – Ichneumonidae*", p. 112–155.
3. Constantineanu R., *Contribuții la cunoașterea exoehinelor (Hym., Ichneum.) din județul Suceava*, An. Muz. Jud. Suceava, Fasc. Șt. Nat., **7**: 151– 157, 1983.
4. Constantineanu I., Constantineanu R., *Contributions to the Faunistic and Ecological Study of Ichneumonids (Hymenoptera, Ichneumonidae) in the Danube Delta Biosphere Reservation*, Mem. Secț. Șt. Acad. Rom., **21**: 145–188, 1997, București.
5. Pisică C., *Ichneumonidele (Hymenoptera, Insecta) din România și gazdele lor. Catalog*, Edit. Univ. "Al. I. Cuza" Iași, 2001, 406 pp.
6. Tolkanitz V. I., *Fauna Ukrainî*, **11** (*2*): 1–212 : *Paraziticeskie pereponciatokrâlâie, Ihnevmonidî – metopiinî*, Nauk. Dumka, Kiev, 1987.
7. Yu D. S., Horstmann K, 1997, *A Catalogue of World Ichneumonidae (Hymenoptera)*, Mem. Amer. Ent. Inst., **58** (*1–2*): 1–1558, Gainesville.

Received September 20, 2004.

Raoul Constantineanu
Irinel Constantineanu
Institute of Biological Researches
Bd. Carol I, Nr. 20 A
6600 Iași

Camil Ștefan Lungu-Constantineanu
"Al. I. Cuza" University, Iași
Faculty of Biology
Bd. Carol I, Nr. 20 A, 6600 Iași

CAENESTHERIELLA VARIABILIS (DADAY) (CONCHOSTRACA: CRUSTACEA) ESPÈCE NOUVELLE POUR LA FAUNE DE ROUMANIE ET SA VALIDITÉ

AURELIU STOICESCU

L'auteur signale pour la première fois la présence en Roumanie du conchostrace *Spinicaudata Caenestheriella variabilis* et mentionne les différences entre cette espéce et *Cyzicus tetracerus* avec laquelle *C.variabilis* a ètè synonymisée.

INTRODUCTION

L'espèce *Caenestheriella variabilis* a été décrite en 1914 par Daday de Dées, après avoir examiné la collection de Phyllopodes récoltés par Dr.K. Chyzer à Szöllöske et Bereczki en Hongrie, en mai 1884 et en juin 1892. Selon Daday de Dées «cette espèce est intéressante en ce que la forme et la structure de la tête et surtout du rostre des mâles y présentent un assez grand nombre de variations et parce qu'elle forme, pour ainsi dire, la transition entre *Caenestheriella* aux *Cyzicus*». Les recherches entreprises sur le territoire de la Roumanie, ont mis en évidence la présence du genre *Cyzicus* mais le genre *Caenestheriella* n'a pas été signalé. N. Botnariuc et T. Orghidan mentionnent la possibilité de la présence du genre *Caenestheriella* en Roumanie, ce que nous confirmons dans le présent travail. Jusqu'à présent *Caenestheriella variabilis* est l'unique espèce de ce genre trouvée en Roumanie.

MATÉRIEL ET MÉTHODE

Le matériel étudié a été récolté dans des mares temporaires, entre le 9 mai et le 1er juin 1994, dans les localités suivantes du département de Călărași; la forêt Spanțov, le 2.V.1994, 5 mâles, le 10.V.1994, 11 mâles et 3 femelles, le 29.V.1994, 33 mâles et 28 femelles ; la commune Ulmeni, le 28.V.1994, 2 mâles et 2 femelles ; la forêt Tufele Grecului, le 1er juin 1994, 4 mâles et 12 femelles. Il est à remarquer que cette espèce a été trouvée surtout dans de petits trous d'eau limpide et douce de forêt ou à la lisière de la forêt.

Cette étude est basée sur l'examen de 72 exemplaires que l'auteur a collectés personnellement.

REV. ROUM. BIOL. – BIOL. ANIM., TOME 49, N^{os} 1–2, P. 11–18, BUCAREST, 2004

RÉSULTES ET DISCUSSIONS

Mâle. La coquille (fig.1) ressemblante, comme forme et couleur à celle de l'espèce *Cyzicus tetracerus*. La coquille est brune-jaunâtre et présente les dimensions suivantes : longueur 6,2–9,5 mm. ; hauteur 4–6,2 mm.

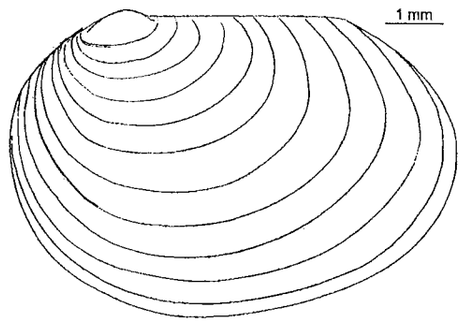

Fig. 1 – Mâle: la coquille vue latéralement.

La coquille recouvre le corps entier de l'animal ; regardée latéralement, elle présente une forme ovoïdale; vue d'en haut elle est fusiforme ayant son maximmum de largeur dans la moitié antérieure. Le bord dorsal de la coquille est droit. L'angle postéro-dorsal est net, et habituellement ovoïdale. L'umbo est bien développé ; les stries d'accroissement varient entre 12–15. La structure de la coquille est granuleuse, son bord présente une série de poils.

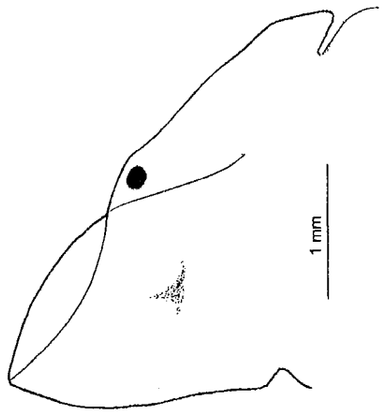

Fig. 2 – Mâle : la tête vue de profil.

La tête de l'animal vue de profil (fig. 2) a une forme triangulaire ; elle est comprimée latéralement et allongée dorso-ventralement. Dans sa partie dorsale, la

tête se continue formant un angle occipital aigu, allongé dorsalement. Le bord antérieur de la tête est habituellement un peu convexe, formant au dessus des yeux composés une proéminence largement arrondie. Ventralement la tête se prolonge par un rostre, qui présente la forme d'une lame, comprimée latéralement, située dans le plan median du corps. Le sommet du rostre est aigu et ne présente pas d'épine. Le bord postérieur du rostre peut être largement arqué (fig. 3a) ou presque droit (fig. 3b). A la base du rostre il y a la tache oculaire bien développée. Le fornix (fig. 4), un pli chitineux, très développé se prolonge jusqu'au sommet du rostre. Les antennules présentent jusqu'à 20 papilles sensitives. Les antennes ont le rameau antérieur composé de 13 à 16 articles et le postérieur de 14 à 16 articles.

Le corps de l'animal est composé de 24 à 25 segments, chacun ayant une paire de pattes. Les 15 à 16 derniers segments du corps sont pourvus à leur partie médio-dorsale d'une série d'épines, soutenues dans chaque segment par un socle commun. Les épines sont dirigées vers l'arrière et leur nombre est variable. Les pattes, sans lame triangulaire, sont au nombre de 24 à 25 paires. Les deux premières paires de pattes sont préhensiles.

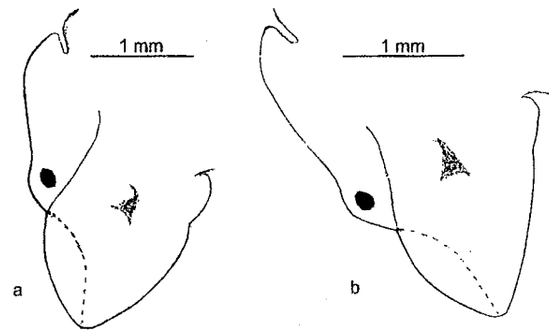

Fig. 3 – Mâle: le rostre avec le bord postérieur arqué (a) et presque droit (b).

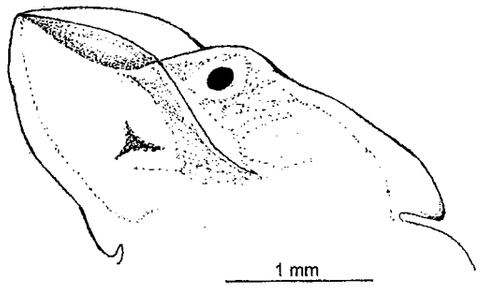

Fig. 4 – Mâle: le fornix.

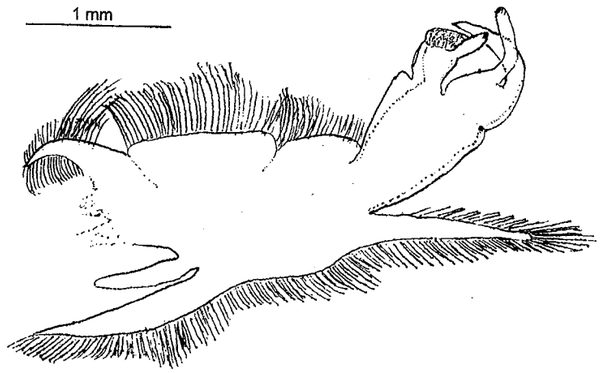

Fig. 5 – La patte I préhensile vue dans l'ensemble.

La patte I préhensile (fig. 5) a le bord interne de la partie apicale enfoncé au dessous de la massue de l'endopodite. Cette enfonçure délimite un petit tubercule (fig. 6). La patte II préhensile, a le bord interne de la partie apicale largement ondulé, le tubercule au dessous de la massue de l'endopodite, étant très faiblement prononcé (fig. 7). La massue de l'endopodite est couverte de petites papilles sensitives ; tant à la pointe de la palpe enditale que de la palpe endopoditale il y a des papilles sensitives. La troisième paire de pattes ne presénte pas de palpe enditale, mais présente une palpe endopoditale qui est plus longue que l'endopodite. Toutes les pattes ont le bord du saccule branchial ou l'épipodite lisse. Les dernières paires des pattes sont rudimentaires.

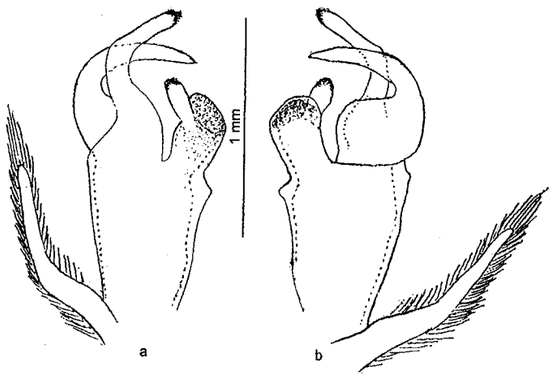

Fig. 6 – La partie apicale de la patte I préhensile ; la face interne (a) ; la face externe (b).

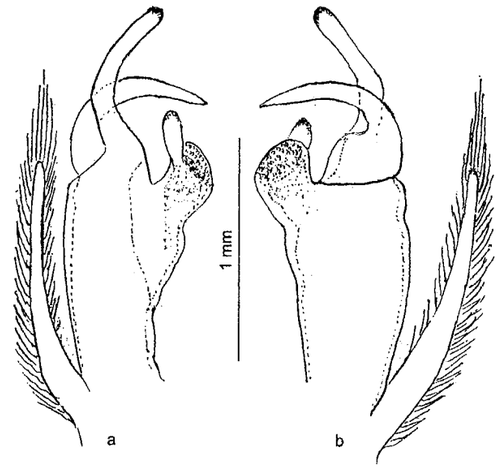

Fig. 7 – La partie apicale de la patte II préhensile ; la face interne (a) ; la face externe (b).

Le telson (fig. 8) présente des épines dorsales en nombre variant de 17 à 23 et qui sont aussi variées comme dimensions. Sur l'angle proximal dorsal du telson il y a une épine plus puissante. Les griffes du telson ne sont pas articulées.

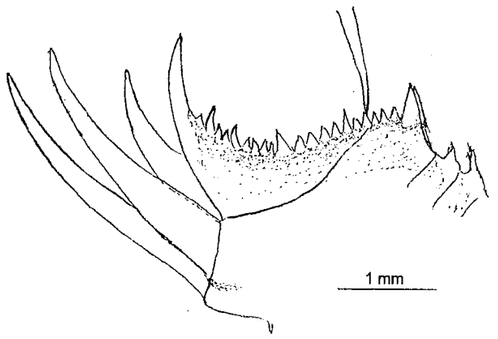

Fig. 8 – Le telson du mâle.

Femelle. La coquille (fig. 9) présente les dimensions suivantes ; longueur 6,5–12,5 mm. ; hauteur 4,5–8,5 mm. Le nombre des stries d'accroissement varie de 12 à 21. La forme, la couleur ainsi que sa structure ne diffèrent pas de celles offertes par le mâle.

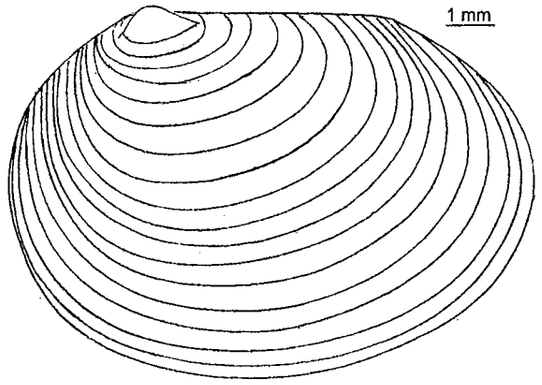

Fig. 9 – Femelle: la coquille vue latéralement.

La tête (fig. 10), vue latéralement, présente une forme triangulaire, le rostre se terminant en pointe avec le bord postérieur droit. Le contour antérieur du rostre et de la tête, aussi bien que l'angle occipital sont semblables à ce qu'on observe chez la mâle. Antennules typiques. Les antennes présentent aux deux branches de 15 à 16 articles chacune.

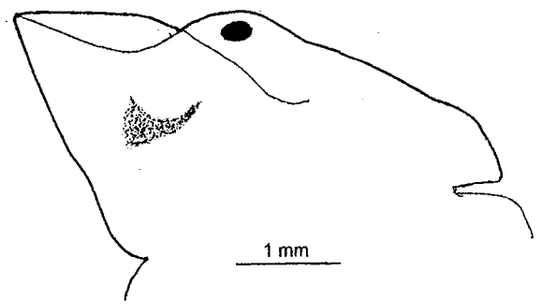

Fig. 10 – Femelle: la tête vue latéralement.

Le corps est composé de 24 à 25 segments, ayant chacun une paire de pattes. Le 16 derniers segments du corps sont pourvus à leur partie médio-dorsale d'épines. La première paire de pattes est sans palpe enditale ; la palpe endopoditale est un peu plus courte que l'endopodite (fig. 11). Les paires IX, X de pattes ont la palpe endopoditale très courte. Le telson (fig.12) est semblable en tant que conformation et nombre d'épines à celui du mâle.

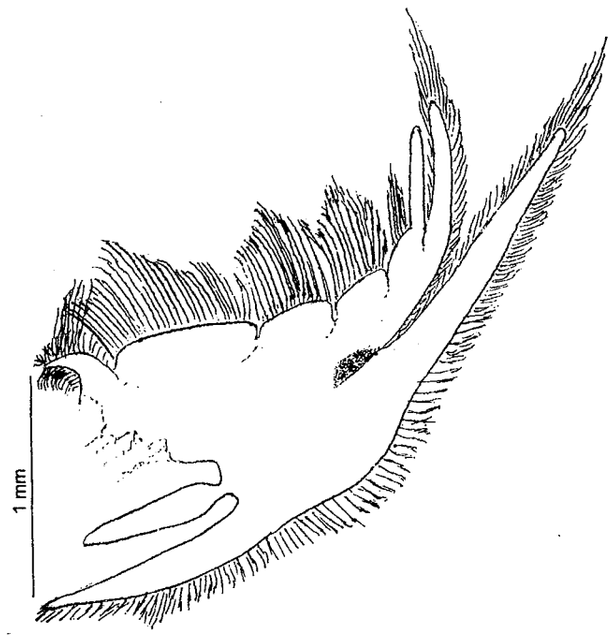

Fig. 11 – Femelle: la patte I vue dans l'ensemble.

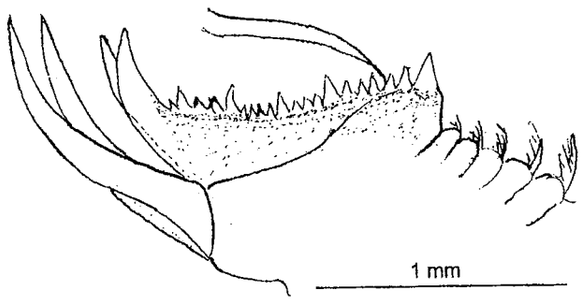

Fig. 12 – Le telson de la femelle.

Brtek et Thierry (1995) considèrent *C.variabilis* un synonyme de *Cyzicus tetracerus*. Nous somes d'avis que c'est un espèce distincte qui differrèe de *C.tetracerus* par les caractères suivants :

- mâles ayant une tête triangulaire (chez *C.tetracerus* quadrangulaire) ;
- l'angle occipital pointu (chez *C.tetracerus* arrondi) ;
- 24–25 le segments du corps (chez *C.tetracerus* 25–27) ;
- troisième paire de pattes sans palpe enditale ;

– carapace avec 12–15 stries de croisance (chez *C.tetracerus* 15–17) ;
– carapace des femelles avec 12–21 stries de croissance (15–17 chez *C.tetracerus* très variables.

Nous mentionnons aussi que *C.variabilis* a été trouvé dans des petites mares avec une eau limpide, bien oxygénée, tandid que *C.tetracerus* vit d'habitude dans les mares à l'eau trouble.

BIBLIOGRAPHIE

1. Botnariuc, N., 1947, *Contributions à la connaissance des Phyllopodes Conchostracés de Roumanie*, 1947.
2. Botnariuc, N., T. Orghidan, 1953, *Fauna Republicii Populare Române*, Phyllopoda, **IV**, 2, 46, 1953.
3. Daday de Dées M, 1926, *Monographie systématique des Phyllopodes Conchostracés*, Annales des Sciences Naturelles Zoologie **IX**, 141–145.
4. Brtek, J., & A., Thiéry, 1995, *The geographic distribution of the European Branchiopods (Anostraca, Notostraca, Spinicaudata, Laevicaudata)*, 298: 263–280.

Reçu mai 15, 2004.

B-dul Republicii 73
Bl. J. Sc. B, Et. I, Ap. 8
Oltenița, Jud.Călărași

ICHTHYOLOGICAL RESEARCHES IN THE BASIN OF THE RIVER LĂPUŞ

ALEXANDRU WILHELM*, GAVRIL ARDELEAN**

During 3–6 September 2003 we made ichthyological researches in the basin of Lăpuş river and tributaries in 40 sampling points. We determined 1 850 specimens of 22 fish species. 19 of these are native species, only 3 are of allochthonous origin.
The low number of species can be explained by the pollution of water with a mine or ore-washer and the organic pollutants of the public sewage and brandy distilleries.
In accordance with the classification of Bănărescu (1994) the majority of species are not endangered, but *Leuciscus leuciscus* is considered on the verge of extinction, *Gobio kessleri* and *Thymallus thymallus* are vulnerable species, *Gobio uranoscopus* is less vulnerable.

Dans la période 3–6 septembre nous avons efectué des investigations ichtyologiques dans le bassin du Lăpuş. Nous avons choisi 40 points de collecte sur la rivière Lăpuş et ses affluents. Nous avons collecté en totalité 1 850 exemplaires de poissons appartenant à 22 espèces, parmi lesquelles 19 autochtones et 3 introduites par l'homme.
Le nombre relativement petit d'espèces est dû à la pollution de l'eau avec les résidus miniers et communaux tels que les substances organiques provenues des distilleries.
Après la classification de Bănărescu (1994) la majorité des espèces trouvées ne sont pas périclitées, mais *Leuciscus leuciscus* est en train de disparition, *Gobio kessleri* et *Thymallus thymallus* sont vulnérables et *Gobio uranoscopus* est peu vulnérable.

Key words: Lăpuş, tributaries, fish fauna, water pollution.

INTRODUCTION

The source of the Lăpuş is situated under the Văratec peak, at 1 200 m above the sea level, and it flows into the Someş at a height of 145 m. It is 114.6 km long, with a surface of the basin of 1 820 km^2. Its water is gathered from the southern slopes of the Gutîi, Ţibleş and Lăpuş mountains.

The main right-hand tributaries of the Lăpuş are the Strâmbu-Băiuţ, the Cavnic together with the Bloaja and the Săsar. Its left-hand tributaries are the Botiz, the Roaia, the Suciu with the Brad and the Rohia. Its average water output is 10.1 m^3, and 18 m^3/s, respectively.

A part of its water network is extremely polluted by the non-ferrous metal mining, as the sewages of the mines and ore-washers contain – besides the great amount of floating sediment – lead-, zinc-, sulphate- and cyanide-chemicals and phenol-derivatives too, which get into the waters and make impossible the surviving of fish. Therefore the upper reaches of the Lăpuş, Suciu and Cavnic and almost the whole Săsar are "dead" waters regarding the fish population.

REV. ROUM. BIOL. – BIOL. ANIM., TOME 49, N^{os} 1–2, P. 19–28, BUCAREST, 2004

The polluting substances are rapidly diluted by the significant water output of the affluents, and additionally the important decline of 10–15 m/km of the bed leads to good oxygenation and thus a fast self-cleaning. In the middle reaches the well-known Lăpuş-defile also enhances the self-cleaning process by narrowing the bed and fastening the water-flow. Unfortunately, in this region fish poaching with explosives is very frequent, which destroys the fish population indiscriminately. The lower reaches of the river are polluted by the public sewage of the city of Baia Mare and by the brandy distilleries of the villages near the riverside. This sad situation is worsened by the periodical ecological disasters, *e.g.* the cyanid-pollution in the spring of 2000, which destroyed the flora and fauna of the lower reaches of the river.

Regarding ichthyological researches, nobody has carried out systematic surveys in the Lăpuş basin. Bănărescu (1964, 1969) in his basic ichthyological works makes mention the Carpathian lamprey *(Eudontomyzon danfordi)* and rainbow-trout *(Oncorhynchus mykiss)* in the Firiza, the rainbow-trout *(Oncorhynchus mykiss)* in the Lăpuş at Buşag, and the Brown trout *(Salmo trutta fario)* in the less polluted tributaries. He lists 28 fish species in the Someş in the neighbourhood of the mouth of the Lăpuş. Bănărescu *et al.* (1999) on the basis of the 1992–96 researches during the Someş make mention about the Carpathian lamprey in the Firiza, the stoneloach *(Barbatula barbatula)* in the Lăpuş at Buşag and the Balcan spined loach *(Sabanejewia aurata)* at the mouth.

MATERIAL AND METHOD

Since there had been no direct surveys until now regarding the basin of the Lăpuş, we considered this very important: during 3–6 September 2003 we surveyed the fish population of the Lăpuş and its tributaries in 40 sampling points (Fig. 1). We were using a type IUP-12 electrofishing aggregate. During the survey we have determined 22 fish species and 1850 specimens (Table 1, Table 2). The gathered fishes were lift back into the water in the same place.

We had 12 sampling points on the Lăpuş:

1. Near Băiuţ, not far from the source. In the water there were floating particles originating from mining. No fish could be found.

2. Under the mouth of the Botiz, at the 48th kilometre mark. The water contained a yellow floating substance. Two fish species were present.

3. Above Lăpuş village. The bed was rocky with a fine muddy coating and the water was transparent. We found three fish species.

4. Above the mouth of the Suciu. There was a wide bed, low water level with big rocks. There were seven fish species.

5. At the mouth of the brook Rohia. There were big black rocks in the wide bed, at low water level. We found five fish species.

6. Beneath the Lăpuş-defile, between the Codru-Butesii village and Buteasa bridge. The bed was rocky, coated with fine mud, the water was clear, transparent.There were nine fish species present.

7. Under the bridge of the village of Coaş. The bed was pebbly-sandy, there were some *Myriophyllum* stocks. We found nine fish species.

8. Above the mouth of the Săsar, at the bridge of Lăpuşel village. The bed was pebbly-sandy with a fine mud coating. It was wide with a thin water layer flowing slowly. We gathered nine fish species.

9. Opposite the mouth of the Săsar. The bed was stony with a thick organic substance level originating from the brandy distillery of Lăpuşel village. There were three fish species.

10. Near Bozânta-Mare village. The bed was stony-sandy, the river changes its bed frequently. The water was low and clear with shallows. Seven fish species.

11. A moor formed in the abandoned river bed. The bottom is stony with a thick mud layer coat. We gathered eight fish species.

12. Above the mouth of the river. The bed was sandy covered with a layer of organic substances. The water is shallow and transparent. Six fish species.

In the basin of the Lăpuş, on the tributaries we had 28 sampling points:

13. The Tocila is a rocky mountain brook with shallow, clear and fast flowing water. We found two fish species.

14. Strâmbu-Băiuţ, mountain brook, near the source. The bed is rocky, with shallow, clear, fast flowing water. We found two fish species.

15. Strâmbu-Băiuţ, beneath the former point. The bed was wide, with big stones and shallow, fast flowing water. Four fish species..

16. The Botiz, above Poiana Botizii village. In this mountain brook with stony and muddy bed we found three fish species.

17. Botiz, beneath Poiana Botizii village. The bed was stony with whirlpools and mud coating. We gathered four fish species.

18.The brook Roaia above its mouth. The bed was pebby with mud and algae. Four fish species were present.

19. Suciu, near its source. The bed was rocky with a fine mud layer. The water was greenish and milky with no fish.

20. Suciu, under the mouth of the Cârligătura brook. The bed was stony, the water clear. We found one species.

21. Suciu, above the mouth of the Vadurile brook. Stony bed, clear water, five fish species.

22. Suciu, above Groşii Ţibleşului village. Stony bed, clear water, four fish species.

23. Suciu, between Suciu-de-Sus and Suciu-de-Jos villages. The bed was wide with stones and shallow water. We found six fish species.

24. Suciu, not far from its mouth. Wide bed with shallows, flat water. Seven fish species.

25. Ţibleş, a mountain brook, a tributary of the Brad. The bed was rocky-stony without coating. The water was fast and clear with three fish species.

26. Brad, beyond the mouth of the Ţibleş. It is a mountain brook with artificial rapids, and rocky-stony bed. Three fish species.

27. Brad, near the forester's lodge. Stony bed with thin mud coating, artificiall falls. We found three fish species.

29. Brad, beneath the mouth of Valea-Mare. The bed was stony, the water fast and clear, and there were eight fish species.

30. Rohia, above its mouth. Stony and muddy bed. Six fish species present.

31. Cavnic brook, above Cavnic village, near the source. The bed was stony, the shallow and fast flowing water seemed clear. No fish were present.

32. Cavnic, under Cavnic village. Stony bed with a yellow coating, turbid and yellow water. Fish were absent.

33. Cavnic, under Făureşti village. The bed was stony with a thick cover of algae and bacteria. We found one fish species.

34. Cavnic, under Copalnic village. There was a rocky-stony bed with a fine mud layer, clear water. With two fish species.

35. Bloaja brook, near its source. There was found a rocky bed with a fine mud coating and four fish species.

36. Bloaja, above Izvoarele village. Rocky bed, artificial rapids, clear water and five fish species gathered.

37. Bloaja, above Ciocotiş village. The bed was rocky with a thin mud layer, the water was clear. Three fish species.

38. Bloaja, between Ruşor and Cernuţi villages. The bed was pebbly, with a fine mud layer. Seven fish species were found.

39. Săsar, above Baia-Sprie. A rocky mountain brook with a layer of algae and bacteria, the water seemed to be clear. No fish found.

40. Săsar, around its mouth. The bed contained a thick layer of blue and green algae and bacteria. There were no fish.

RESULTS AND DISCUSSION

We gathered a total number of 22 fish species: 18 in the Lăpuş (Table 1), and 14 in its tributaries (Table 2). Only three of these, the German carp *(Carassius auratus)*, the pseudokeilfleck barbe *(Pseudorasbora parva)* and the sunfish *(Lepomis gibbosus)* are of allochtonous origin, the rest are native species.

Table 1

The ichthyofauna of the Lăpuş river basin

No.	Fish species	Lăpuş											
		1	2	3	4	5	6	7	8	9	10	11	12
1	*Leuciscus leuciscus*						1						
2	*Leucis cephalus*		25	9	1	23	18	9	28	2	38	14	15
3	*Alburnus alburnus*							8	1		40	25	2
4	*Alburnoides bipunctatus*			2	7	4		4	1				1
5	*Vimba vimba*								5				
6	*Chondrostoma nasus*							1					
7	*Barbus barbus*								30		6		
8	*Barbus petenyi*			2	100	28	16	13	2		2		
9	*Gobio gobio*				1		20	3	4		3	27	2
10	*Gobio uranoscopus*				4	3							
11	*Gobio kessleri*						7	10					1
12	*Pseudorasbora parva*										3	10	
13	*Rhodeus sericeus*							3	23	1	3	17	
14	*Carassius auratus*						1					11	3
15	*Barbatula barbatula*				2	3							
16	*Cobitis elongatoides*						1					1	
17	*Sabanejewia aurata*				16			8	5				
18	*Lepomis gibbosus*		1							1		1	

Table 2a

The ichthyofauna of the Lăpuş river basin

No.	Fish species	Tocila	Strâmbu Băiuţ		Botiz		Roaia	Suciu					
		13	14	15	16	17	18	19	20	21	22	23	24
1	*Leuciscus leuciscus*					2						1	
2	*Leucis cephalus*					8	15					26	13
3	*Phoxinus phoxinus*	19	23	61	23					6	30		
4	*Alburnoides bipunctatus*												
5	*Barbus petenyi*									1		12	1
6	*Gobio gobio*		3	16	5	3	45			3	8	60	40
7	*Gobio uranoscopus*												2
8	*Rhodeus sericeus*											1	2
9	*Barbatula barbatula*	9		11	8		16				4	9	
10	*Cobitis elongatoides*			1			4						2
11	*Sabanejewia aurata*												
12	*Thymallus thymallus*									5			
13	*Salmo trutta fario*												
14	*Cottus gobio*								16	5	10		

Table 2b

The ichthyofauna of the Lăpuş river basin

No.	Fish species	Brad					Rohia			Cavnic			Bloaja			Săsar		
		25	26	27	28	29	30	31	32	33	34	35	36	37	38	39	40
1	*Leuciscus leuciscus*					8	10				17				37		
2	*Leucis cephalus*					4	4			3	12	60	6	14			
3	*Phoxinus phoxinus*			13	16	20	3								55		
4	*Alburnoides bipunctatus*											2	8	14	39		
5	*Barbus petenyi*		2	5	3	10	10								11		
6	*Gobio gobio*					2									10		
7	*Gobio uranoscopus*						2										
8	*Rhodeus sericeus*																
9	*Barbatula barbatula*			4		2	27					13	2	10	5		
10	*Cobitis elongatoides*														9		
11	*Sabanejewia aurata*																
12	*Thymallus thymallus*	1		13	5	1		1					1				
13	*Salmo trutta fario*	5															
14	*Cottus gobio*	52	4	9	5	1		1				25	4				

The spreading and frequency of certain species is different:

Fam.Cyprinidae

Leuciscus leuciscus L., Dace, clean mic.

It is extremely rare. A few specimen were found in the Lăpuş only beneath the defile, and in two tributaries, the Botiz and Suciu.

Leuciscus cephalus L.,Chub, clean.

This species has a wide spreading area, we found it in almost every fishing point in the mountains and plain areas as well. It was absent only in small mountain brooks. It tolerates well water pollution, a great number of specimen were found even in the yellow water with lots of floating substances of the upper reaches of the Lăpuş.

Phoxinus phoxinus L., Minnow, boiştean.

This is a frequent species in the mountain brooks until the neighbourhood of the source, but since it is sensitive to pollution, it disappeared from some reaches of the tributaries and the whole Lăpuş.

Alburnus alburnus L., Bleak, obleţ.

We found it only in the hilly and flat areas of the Lăpuş.

Alburnoides bipunctatus Bloch, Schneider, beldiţă.

We found it to be a frequent species in the mountain brooks with larger water output and in the hilly regions, but it is sensitive to pollution, so it is missing in the affected areas.

Vimba vimba L., Vimba-bream, morunaş.

It proved to be a very rare species in the surveyed area; we found some young specimens only at the bridge near Lăpuşel village.

Chondrostoma nasus L., Nose, scobar.

Despite the favourable conditions, it was very rare in these areas. We caught a single exemplar at the bridge near Coaş village.

Barbus barbus L., Barbel, mreană.

We found a viable population in the hilly regions of the Lăpuş.

Barbus petenyi Heckel, Balcanic Barbe, moioagă.

The balcanic barbe, considered again a genuine species (Kotlik *et al.*, 2002), proved to be one of the most frequent species in the surveyed areas. We found it from the smallest mountain brooks to the end of the hilly area of the river. It has important populations in the majority of the sampling points.

Gobio gobio L., Common gudgeon, porcuşor comun.

It is a common species in the hilly and flat areas of the river, but it was found in only a few points of the tributaries in small numbers.

Gobio kessleri Dybowski, Sand-gudgeon, porcuşor-de-nisip.

It was found in the hilly region of the Lăpuş.

Gobio uranoscopus Vladykov, Stone-gudgeon, porcuşor-de-vad.

We found viable populations in the upper reaches of the hilly part of the Lăpuş and in some tributaries too.

Pseudorasbora parva Schlegel, Pseudokeilfleckbarbe, murgoi-bălţat.

This allochtonous species was found only in the lower reaches of the hilly part of the Lăpuş.

Rhodeus sericeus Bloch, Bitterling, boarţă.

It is a frequent species in the hilly and flat reaches of the Lăpuş, where we could find large populations. It is not sensitive to water pollution, but its spreading is limited by the presence of shells necessary for its reproduction. Regarding the tributaries, only the Suciu contained some specimen.

Carassius auratus Bloch, German carp, caras.

It is a stagnophyl species introduced by man, we found it only around Bozânta-Mare village, in the moors formed as a consequence of the frequent changes of the bed of the Lăpuş, and near the mouth of the river.

Fam. Cobitidae

Barbatula barbatula L., Stoneloach, grindel.

This species usually frequent in mountain and hilly reaches, was absent in the upper reaches of the Lăpuş and the polluted tributaries, which shows that it is markedly sensitive to pollutants.

Cobitis elongatoides Băcescu, Spined loach, zvârlugă.

This species is frequent in other regions, but here it proved to be rare, we found only a few specimen in a few gathering points in the Lăpuş, and in Suciu and Roaia, but in those places it was frequent.

Fam. Salmonidae

Thymallus thymallus L., Grayling, lipan.

We found a relatively large population only in the Brad, but there it appears even near to the source.

Salmo trutta fario L., Brown trout, păstrăv.

Despite the fact that the conditions seem to be favourable in the upper reaches of many brooks, we caught a few exemplars only in the upper reaches of the Brad and the Bloaja, mainly under artificial rapids.

Fam. Centrarchidae

Lepomis gibbosus L., Sunfish, biban-soare.

It is a species imported from North America, and we found here only a few sporadic specimens. One exemplar was caught in the upper reaches of the Lăpuş, in a very polluted water.

Fam. Cottidae.

Cottus gobio L., Bullhead, zglăvoc.

It was found only near the sources of the Suciu, Brad and Bloaja, and it proved to be very frequent in some points.

CONCLUSIONS

With its 100 km length, more than 1850 km^2 reservoir basin, lots of large tributaries, the Lăpuş is an important river of Northwestern Romania. Considering that it has mountain, hilly and flat reaches, the gathered 22 species can be considered a low number. As a comparison we can mention the 80 km long Vişeu river where we found 17 species, the 83 km long Iza with 22 species (Wilhelm *et al.* 2001–2002, Harka *et al.* 2002). We found 31 species in the 94 km long Tur (Wilhelm *et al.* 2001–2002, Harka *et al.* 2003), 28 species in the 193 km long Crasna (Harka *et al.* 2001) and 47 in the 200 km long Barcău (Harka *et al.* 1998). Even in the Ier, which is of the same length (107 km) but has almost only flat reaches, we could gather 27 species (Wilhelm *et al.* 2001–2002).

The fish fauna of the Lăpuş, besides the low number of species, is characterized by the low number of specimens of many of the species, or even sporadic appearance, which indicates that the survival of these species is uncertain.

This alarming situation can be explained by the mentioned pollution, since it is not accidental that the fish fauna is missing in those reaches where there is a mine or ore-washer nearby. On the other hand, the ecological pressure that affects the lower reaches of the river, *e.g.* the repetitive industrial disasters, the organic pollutants of the public sewage and brandy distilleries, has an important negative effect upon the increase in the ecological diversity offered by the recipient river, the Someş. Although in the Someş, around the mouth of the Lăpuş there live diverse fish species, many of which cannot be found in the Lăpuş, pollution stops them in spreading upwards.

Bănărescu (1994), when characterizing the situation of freshwater fish species in Romania, mentions about their spreading areas and frequencies, including them into different groups of conservation status. According to him, among the fish species found in the Lăpuş the spreading area decreased in the last 30 years in the case of *Leuciscus leuciscus, Barbus barbus, Gobio kessleri* and *Thymallus thymallus*. Five species, *Leuciscus leuciscus, Barbus barbus, Gobio uranoscopus, G. kessleri* and *Thymallus thymallus* show a decreasing tendency in their frequency. Accordingly, the *Leuciscus leuciscus* is considered a species on the verge of extinction, the *Gobio kessleri* and *Thymallus thymallus* are vulnerable species, the *Gobio uranoscopus* is less vulnerable, while the situation of the other species is satisfactory.

REFERENCES

1. BĂNĂRESCU P., 1964, *Pisces, Osteichthyes*. in: *Fauna R.P.R.*, **13,** Ed.Acad.R.P.R., Bucureşti.
2. BĂNĂRESCU P.M., 1994, The present-day conservation status of the fresh water fish fauna of Romania. *Ocrotirea naturii şi a mediului înconjurător*, **38** (1): 5–20.

3. BĂNĂRESCU P.M., TELCEAN I., NALBANT T.T., HARKA A., CIOBANU M., 1999, The fish fauna of the River Someş/Szamos basin. in: *The Someş/Szamos River Valley.* Szolnok-Szeged-Târgu Mureş: 249–268.
4. HARKA A., 1997, Halaink. Budapest.
5. HARKA A., GYÖRE K., SALLAI Z., WILHELM S., 1998, A Berettyó halfaunája a forrástól a torkolatig. *Halászat,* **81** (2): 68–74.
6. HARKA A., SALLAI Z., WILHELM S., 2001, A Kraszna/Crasna halfaunája. *Halászat,* **94** (1): 34–40.
7. HARKA A., SALLAI Z., WILHELM S., 2002, A Felső-Tisza romániai mellékfolyóinak (Szaplonca/Săpânţa, Iza, Visó/Vişeu) halfaunája. *Halászat,* **95** (4): 173–179.
8. HARKA A., SALLAI Z., WILHELM S., 2003, A Túr és mellékvizeinek halai. *Halászat,* **96** (1): 37–44.
9. KOTLIK P., TSIGENOPOULOS C.S., RÁB P., BERREBI P., 2002, Two new Barbus species from the Danube River basin, with redescription of *B. petenyi* (Teleostei: Cyprinidae). *Folia Zoologica,* **51** (3): 227–240.
10. UJVARI I., 1972, *Geografia apelor României.* Ed.Ştiinţifică, Bucureşti.
11. WILHELM S., 2000, *Halak a természet háztartásában.* Kriterion Könyvkiadó, Bucureşti.
12. WILHELM A., ARDELEAN G., HARKA A., SALLAI Z., 2001–2002, Fauna ihtiologică a bazinului râului Tur. *Satu Mare – Studii şi comunicări,* II-III: 147–157.
13. WILHELM A., ARDELEAN G., SALLAI Z., 2001–2002, Fauna ihtiologică a bazinului râului Ier. *Satu Mare – Studii şi comunicări,* II–III:137–146.
14. WILHELM A., HARKA A., SALLAI Z., 2001–2002, Contribuţii la cunoaşterea situaţiei actuale a faunei ihtiologice a Depresiunii Maramureş. *Satu Mare – Studii şi comunicări,* II–III: 158–169.

Received September 2, 2004.

*P-ţa Libertăţii 24/7
Săcuieni, Jud. Bihor
wilhelms@rdslink.ro

**Vasile Goldiş University
Str. 1 Decembrie 1918 no. 6
3900 Satu Mare
ardelean gavril@yahoo.com

THE MACROINVERTEBRATES ASSOCIATION OF MAIZE CULTURE, INCLUDING ALIEN INVASIVE SPECIES *DIABROTICA VIRGIFERA VIRGIFERA* (COLEOPTERA-CHRYSOMELIDAE)

IRINA TEODORESCU*, DACIA VÎLSAN**

Personal investigations in maize crops and literature data have been made in order to assess the diversity of macroinvertebrates in maize crop. A number of over 200 macroinvertebrate species, from Phyllums Nemathelminthes, Mollusca and Arthropoda were identified. 140 of these are phytophagous and over 41 are predators and parasitoids. The alien species *Diabrotica virgifera virgifera* comes into direct and indirect competition for the same food sources with a number of macroinvertebrates and microorganism species. Special interrelations can be established with some Insecta and Aranea predators and parasitoid species. Obtained data underline that in Romania *Diabrotica virgifera virgifera* cannot be erradicated, because the direct and indirect competition is not severe, and lack specific natural enemies.

1. INTRODUCTION

In order to survive as any alien organism, *Diabrotica virgifera virgifera* has to become integrated to the new biocenosis. In these new biocenoses, the host plant is the maize, but there are numerous and various fauna and microorganism components. The interrelations with these components are various. With some macroinvertebrates and microorganism species, *Diabrotica virgifera virgifera* comes into direct and indirect competition for the same food sources. Special interrelations can be established with some Insecta and Aranea predators and parasitoid species, "natural enemies" of different pest species, which could also destroy the eggs, larvae, pupae and adults of *Diabrotica virgifera virgifera.*

In Romania, in maize culture, the alien species *Diabrotica virgifera virgifera* integrates to a complex association of macroinvertebrates, including mainly the Phyllums Mollusca, Nemathelminthes and Arthropoda (Lăcătuşu *et al.* 1978), Teodorescu Irina, 1989, Teodorescu Irina, Vădineanu A., 1997, 2001).

Diabrotica virgifera virgifera comes in a **direct competition** to some of them for the same food sources (the maize pollen and silk for adults and the maize roots for larvae) or into **indirect competition** (for other maize organs).

2. MATERIAL AND METHODS

In order to establish macroinvertebrates association of maize crops, there have been used: pitfall traps, entomological net, random sampling on epigean and subterraneous parts of maize plants, hand collecting, visual observations.

Personal investigations have been made between 1978–2003, during the maize development period, in many localities (Giubega, Cioroiaşu, Perişor, Galicea Mare (Dolj district), Sprancenata, Slatina, Balş, Dăbuleni (Olt district), Socol (Mehedinţi district), Băneasa, Braneşti (Ilfov district), Roşiorii de Vede, Alexandria (Teleorman district), Perişani (Râmnicu Vâlcea district). Qualitative analysis was meant to identify the arthropod to species level (except for Aranea, Myrmicidae, Formicidae, some Diptera) and to establish the trophic categories for each of them. Quantitative analysis was made to five samples collected with traps placed at the ground level, along 20 days interval. These analyses were focused especially on the numerical abundance and dominance assessment.

3. RESULTS AND DISCUSSIONS

From personal investigations and literature data (1–4) there was established that in maize crops, a number of over 200 macroinvertebrate species, phytophagous, predators, parasitoids, coprophagous and necropagous, from Phyllums: Nemathelminthes, Mollusca and Arthropoda are present.

The primary consumers (phytophagous species) were numerically dominant. A number of 140 macroinvertebrate species consume the epigean and subterraneous organs of maize plants (Table 1).

From the Phyllum Nemathelminthes, some phytophagous Nematoda, orders Tylenchida and Dorylaimida, feed on maize.

From the Phyllum Mollusca, some Gastropoda species of order Stylommatophora consume especially the maize small plants and the germinating seeds.

The phytophagous Arthropoda species belong to classes Crustacea (of Oniscidae and Porcellionidae families), Arachnida (of Acarina order, Tarsonemidae, Pyemotidae and Eriophyidae families), Myriapoda (Diplopoda of families Polydesmidae, Blaniulidae, Scutigerellidae) and Insecta (of Collembola, Orthoptera, Homoptera, Heteroptera, Thysanoptera, Coleoptera, Lepidoptera orders) (Table 2).

The Insecta (over 67 %) and Nematoda species (over 17%) were numerically dominant (Tables 2, 3). From Nematoda, Tylenchida species were numerically dominant (87.5 %). In the insects group, Homoptera, Coleoptera and Orthoptera species were numerically dominant (Table 3).

70% of the pest species prefer vegetative organs of maize plants (Table 4), especially roots and leaves.

The *Diabrotica* larvae feeding on the maize roots are in **direct competition** with nematode species from orders Tylenchida and Dorylaimida, with some gastropods Stylommatophora, Isopod crustacea, Protospermophora and Megadenopoda miriapod, and insects from orders Orthoptera (*Gryllotalpa gryllotalpa*), Coleoptera (Elateridae), Lepidoptera (Noctuidae).

Table 1

Macroinvertebrate species which feed maize aerial and subterraneous organs

No.	Species	Families	Part of plant
1	2	3	4	5
1.	*Tylenchus davainei*	Tylenchidae	Tylenchida	roots
2.	*Ditylenchus dipsaci*	Tylenchidae	Tylenchida	leaves, roots
3.	*Ditylenchus destructor*	Tylenchidae	Tylenchida	leaves, roots
4.	*Tylenchorhynchus cylindricus*	Tylenchorhynchidae	Tylenchida	roots
5.	*Tylenchorhynchus dubius*	Tylenchorhynchidae	Tylenchida	roots
6.	*Trophurus sculptus*	Tylenchorhynchidae	Tylenchida	roots
7.	*Pratylenchus pratensis*	Pratylenchidae	Tylenchida	roots
8.	*Pratylenchus penetrans*	Pratylenchidae	Tylenchida	roots
9.	*Pratylenchus crenatus*	Pratylenchidae	Tylenchida	roots
10.	*Pratylenchus neglectus*	Pratylenchidae	Tylenchida	roots
11.	*Rotylenchus robustus*	Hoplolaimoidea	Tylenchida	roots
12.	*Helicotylenchus multicinctus*	Hoplolaimoidea	Tylenchida	roots
13.	*Helicotylenchus dihystera*	Hoplolaimoidea	Tylenchida	roots
14.	*Helicotylenchus digonicus*	Hoplolaimoidea	Tylenchida	roots
15.	*Helicotylenchus vulgaris*	Hoplolaimoidea	Tylenchida	roots
16.	*Paratylenchus curvitatus*	Paratylenchidae	Tylenchida	roots
17.	*Paratylenchus aciculus*	Paratylenchidae	Tylenchida	roots
18.	*Hemicycliophora typica*	Hemicycliophoridae	Tylenchida	roots
19.	*Heterodera schachtii*	Heteroderoidea	Tylenchida	roots
20.	*Meloidogyne incognita*	Melodogynidae	Tylenchida	roots
21.	*Meloidogyne hapla*	Melodogynidae	Tylenchida	roots
22.	*Longydorus elongatus*	Longydoridae	Dorylaimida	roots
23.	*Xiphinema americanum*	Longydoridae	Dorylaimida	roots
24.	*Xiphinema diversicaudatum*	Longydoridae	Dorylaimida	roots
25.	*Succinea putris*	Succineidae	Stylommatophora	leaves
26.	*Cecilioidea acicula*	Perussaciidae	Stylommatophora	germinating seeds, leaves, roots
27.	*Limax maximus*	Limacidae	Stylommatophora	roots

Table 1

(continued)

1	2	3	4	5
28.	*Limax cinereoniger*	Limacidae	Stylommatophora	roots
29.	*Deroceras agreste*	Agriolimacidae	Stylommatophora	small plants, leaves
30.	*Deroceras reticulatum*	Agriolimacidae	Stylommatophora	small plants, leaves
31.	*Deroceras laeve*	Agriolimacidae	Stylommatophora	small plants, leaves
32.	*Euconulus fulvus*	Euconulidae	Stylommatophora	germinating seeds, leaves
33.	*Helicella obvia*	Helicidae	Stylommatophora	germinating seeds, leaves
34.	*Cernuella virgata*	Helicidae	Stylommatophora	germinating seeds, leaves
35.	*Helicopsis striata*	Helicidae	Stylommatophora	germinating seeds, leaves
36.	*Zenobiella rubiginosa*	Helicidae	Stylommatophora	leaves
37.	*Oniscus asellus*	Oniscidae	Isopoda	germinating seeds, roots, leaves
38.	*Porcellio scaber*	Porcellionidae	Isopoda	germinating seeds, roots, leaves
39.	*Steneotarsonemus spirifex*	Tarsonemidae	Acari	panicles
40.	*Siteroptes graminum*	Pyemotidae	Acari	leaves, panicles
41.	*Aceria tritici*	Eriophyidae	Acari	leaves
42.	*Polydesmus complanatus*	Polydesmidae	Protospermophora	germinating seeds, roots
43.	*Polydesmus coriaceus*	Polydesmidae	Protospermophora	germinating seeds
44.	*Blaniulus guttulatus*	Blaniulidae	Opistospermophora	germinating seeds, stalk collet
45.	*Scutigerella immaculata*	Scutigerellidae	Megadenopoda	germinating seeds, stalk collet, roots
46.	*Onychiurus armatus*	Onychiuridae	Collembola	germinating seeds
47.	*Ceratophysella armata*	Hypogastruridae	Collembola	roots
48.	*Calliptamus italicus*	Catantopidae	Orthoptera	leaves
49.	*Calliptamus barbarus*	Catantopidae	Orthoptera	leaves
50.	*Polysarcus denticaudus*	Tettigoniidae	Orthoptera	leaves
51.	*Tettigonia viridissima*	Tettigoniidae	Orthoptera	small plants, leaves
52.	*Tettigonia caudata*	Tettigoniidae	Orthoptera	small plants, leaves
53.	*Gryllus campestris*	Gryllidae	Orthoptera	leaves
54.	*Melanogryllus frontalis*	Gryllidae	Orthoptera	leaves
55.	*Melanogryllus desertus*	Gryllidae	Orthoptera	leaves
56.	*Decticus verrucivorus*	Acrididae	Orthoptera	small plants, leaves

Table 1

(continued)

1	2	3	4	5
57.	*Oedipoda coerulescens*	Acrididae	Orthoptera	small plants, leaves
58.	*Acrida hungarica*	Acrididae	Orthoptera	small plants, leaves
59.	*Dociostaurus maroccanus*	Acrididae	Orthoptera	small plants, leaves
60.	*Locusta migratoria*	Acrididae	Orthoptera	small plants, leaves
61.	*Chorthippus parallelus*	Acrididae	Orthoptera	small plants, leaves
62.	*Gryllotalpa gryllotalpa*	Gryllotalpidae	Orthoptera	stalk collet, roots
63.	*Anaphothrips obscurus*	Thripidae	Thysanoptera	flowers
64.	*Chirothrips manicatus*	Thripidae	Thysanoptera	panicles
65.	*Limothrips cerealium*	Thripidae	Thysanoptera	panicles
66.	*Limothrips denticornis*	Thripidae	Thysanoptera	leaves, female flowers
67.	*Haplothrips aculeatus*	Phlaeothripidae	Thysanoptera	female flowers, seeds
68.	*Oliarus leporinus*	Cixiidae	Homoptera	roots, leaves
69.	*Oliarus pallens*	Cixiidae	Homoptera	stalk
70.	*Oliarus panzeri*	Cixiidae	Homoptera	roots, leaves
71.	*Hyalestes obsoletus*	Cixiidae	Homoptera	roots, leaves
72.	*Laodelphax striatella*	Delphacidae	Homoptera	leaves
73.	*Toya propinqua*	Delphacidae	Homoptera	leaves
74.	*Philaenius spumarius*	Cercopidae	Homoptera	leaves
75.	*Macrosteles laevis*	Cicadellidae	Homoptera	leaves
76.	*Macrosteles sexnottatus*	Cicadellidae	Homoptera	leaves
77.	*Macrosteles quadripunctulatus*	Cicadellidae	Homoptera	leaves
78.	*Doratura heterophyla*	Cicadellidae	Homoptera	leaves
79.	*Doratura homophyla*	Cicadellidae	Homoptera	leaves
80.	*Psammotettix striatus*	Cicadellidae	Homoptera	leaves
81.	*Psammotettix alienus*	Cicadellidae	Homoptera	leaves
82.	*Psammotettix provincialis*	Cicadellidae	Homoptera	leaves
83.	*Austroagalia sinuata*	Cicadellidae	Homoptera	leaves
84.	*Cicadella viridis*	Cicadellidae	Homoptera	leaves
85.	*Kyboasca bipunctata*	Cicadellidae	Homoptera	leaves

Table 1

(continued)

1	2	3	4	5
86.	*Anoecia corni*	Anoeciidae	Homoptera	roots
87.	*Anoecia vagans*	Anoeciidae	Homoptera	roots
88.	*Sipha maydis*	Chaitophoridae	Homoptera	leaves, stalk, corn cobs
89.	*Birsocrypta gallarum*	Aphididae	Homoptera	roots
90.	*Rhopalosiphum maidis*	Aphididae	Homoptera	leaves, panicles, corn cobs
91.	*Rhopalosiphum padi*	Aphididae	Homoptera	leaves, panicles
92.	*Aphis fabae*	Aphididae	Homoptera	leaves, panicles
93.	*Schizaphis graminum*	Aphididae	Homoptera	leaves
94.	*Sitobion avenae*	Aphididae	Homoptera	leaves, flowers
95.	*Myzus persicae*	Aphididae	Homoptera	leaves
96.	*Metopolophium dirhodum*	Aphididae	Homoptera	leaves
97.	*Dolycoris baccarum*	Pentatomidae	Heteroptera	leaves
98.	*Lygus rugulipennis*	Miridae	Heteroptera	leaves, flowers
99.	*Lygus pratensis*	Miridae	Heteroptera	leaves, flowers
100.	*Lygus pabulinus*	Miridae	Heteroptera	leaves, flowers
101.	*Palomena prasina*	Pentatomidae	Heteroptera	leaves
102.	*Harpalus azureus*	Carabidae	Coleoptera	germinating seeds, small plants
103.	*Harpalus rufipes*	Carabidae	Coleoptera	germinating seeds, small plants
104.	*Harpalus distinguendus*	Carabidae	Coleoptera	germinating seeds
105.	*Harpalus griseus*	Carabidae	Coleoptera	germinating seeds, small plants
106.	*Harpalus aeneus*	Carabidae	Coleoptera	germinating seeds, small plants
107.	*Amara similata*	Carabidae	Coleoptera	germinating seeds, small plants
108.	*Amara ovata*	Carabidae	Coleoptera	germinating seeds, small plants
109.	*Amara aenea*	Carabidae	Coleoptera	germinating seeds, small plants
110.	*Anisodactylus signatus*	Carabidae	Coleoptera	germinating seeds, small plants
111.	*Anisodactylus binotatus*	Carabidae	Coleoptera	germinating seeds, small plants
112.	*Zabrus tenebrioides*	Carabidae	Coleoptera	germinating seeds
113.	*Agriotes lineatus*	Elateridae	Coleoptera	roots
114.	*Agriotes ustulatus*	Elateridae	Coleoptera	roots

Table 1

(continued)

1	2	3	4	5
115.	*Agriotes obscurus*	Elateridae	Coleoptera	roots
116.	*Agriotes sputator*	Elateridae	Coleoptera	roots
117.	*Athous niger*	Elateridae	Coleoptera	roots
118.	*Athous subfuscus*	Elateridae	Coleoptera	roots
119.	*Athous haemorrhoidalis*	Elateridae	Coleoptera	roots
120.	*Selatostomus aeneus*	Elateridae	Coleoptera	roots
121.	*Selatostomus latus*	Elateridae	Coleoptera	roots
122.	*Melanotus brunnipes*	Elateridae	Coleoptera	roots
123.	*Melanotus punctolineatus*	Elateridae	Coleoptera	roots
124.	*Opatrum sabulosum*	Tenebrionidae	Coleoptera	germinating seeds, stalk collet, leaves
125.	*Anoxia villosa*	Scarabaeidae	Coleoptera	roots
126.	*Melolontha melolontha*	Scarabaeidae	Coleoptera	roots
127.	*Rhizotrogus equinoctialis*	Scarabaeidae	Coleoptera	roots
128.	*Amphimalon solstitialis*	Scarabaeidae	Coleoptera	roots
129.	*Anomala solida*	Scarabaeidae	Coleoptera	roots
130.	*Polyphylla fullo*	Scarabaeidae	Coleoptera	roots
131.	*Pentodon idiota*	Scarabaeidae	Coleoptera	roots
132.	*Tanymecus dilaticollis*	Curculionidae	Coleoptera	stalk collet, young leaves
133.	*Tanymecus palliatus*	Curculionidae	Coleoptera	stalk collet, young leaves
134.	*Ostrinia nubilalis*	Noctuidae	Lepidoptera	flowers, leaves, stalk, corn cobs, seeds
135.	*Scotia segetum*	Noctuidae	Lepidoptera	germinating seeds, stalk collet, leaves
136.	*Scotia ipsilon*	Noctuidae	Lepidoptera	germinating seeds, stalk collet, leaves
137.	*Scotia exclamationis*	Noctuidae	Lepidoptera	germinating seeds, stalk collet, leaves
138.	*Helicoverpa armigera*	Noctuidae	Lepidoptera	germinating seeds, stalk collet, leaves
139.	*Amates c-nigrum*	Noctuidae	Lepidoptera	small plants
140.	*Margaritia sticticalis*	Pyralidae	Lepidoptera	leaves

Table 2

The weight of phytophagous macroinvertebrate species found in the maize crop

No.	Groups	Species number	%
1	Tylenchida	21	15.00
2	Dorylaimida	3	2.14
3	Stylomatophora	12	8.57
4	Isopoda	2	1.43
5	Acari	3	2.14
6	Diplopoda	4	2.86
7	Insecta	95	67.86
	Total	140	

Table 3

The number and weight of phytophagous insect orders found in the maize crop

No.	Groups	Species number	%
1	Collembola	2	2.10
2	Orthoptera	15	15.79
3	Thysanoptera	5	5.26
4	Homoptera	29	30.53
5	Heteroptera	5	5.26
6	Coleoptera	32	33.68
7	Lepidoptera	7	7.37
	Total	95	

Table 4

The number and weight of pests species/plant organs

No.	Attacked organ	Pests number	%
1	roots	46	32.86
2	leaves	29	20,71
3	vegetative organs	23	16.43
4	vegetative and reproductive organs	42	30.71
	Total	140	

The *Diabrotica* adults, consuming the pollen, styles from female blossoms (so-called "silk"), the leaves and the immature seeds on corncobs, are in **direct competition** with numerous species of macroinvertebrates.

The *Diabrotica* adults, consuming the pollen and silk, are in direct competition with *Steneotarsonemus spirifex* acarina, Thysanoptera species, homoptera Aphididae (*Rhopalosiphum maidis* and *Aphis fabae*).

The leaves of maize small plants constitute the food source for Gastropoda, Isopoda, Acarina, Insecta species (belonging to Orthoptera, Homoptera, Coleoptera orders).

The *Diabrotica virgifera virgifera* is **in indirect competition** with species feeding on stalk collet, corn stalks, and germinating maize seeds. The *Gryllotalpa*, *Tanymecus* species **attack the stalk collet** of maize (the last species attack especially seedlings with three leaves).

The germinating maize seeds are consumed by some species of Gastropoda, Isopoda, Diplopoda, Collembola, Coleoptera-Carabidae.

Some species of Nematoda, Acarina and Insecta are vectors for viruses, mycoplasms, yeasts and bacteria species (Table 5). With these viruses, mycoplasms, yeasts and bacteria species, *Diabrotica virgifera virgifera* is in indirect competition. The transferred agents cause maize diseases, which damage the plants and expose them to other pests attacks.

Table 5

Macroinvertebrate species vectors for viruses, bacteria,mycoplasms, yeasts

No.	Species	Virus	Mycoplasms	Bacteria	Yeasts
1.	*Pratylenchus pratensis*	+			
2.	*Longydorus elongatus*	+			
3.	*Xiphinema americanum*	+			
4.	*Xiphinema diversicaudatum*	+			
5.	*Siteroptes graminum*	+			+
6.	*Tettigonia viridissima*	+			
7.	*Limothrips cerealium*	+			
8.	*Haplothrips aculeatus*	+			
9.	*Oliarus leporinus*	+			
10.	*Laodelphax striatella*	+			
11.	*Macrosteles laevis*	+	+		
12.	*Macrosteles sexnottatus*	+			
13.	*Macrosteles quadripunctulatus*		+		
14.	*Psammotettix striatus*	+			
15.	*Psammotettix alienus*	+			
16.	*Austroagalia sinuata*	+			
17.	*Cicadella viridis*	+			
18.	*Rhopalosiphum maidis*	+		+	
19.	*Rhopalosiphum padi*	+			
20.	*Aphis fabae*	+			
21.	*Schizaphis graminum*	+			
22.	*Sitobion avenae*	+			
23.	*Myzus persicae*	+			
24.	*Metopolophium dirhodum*	+			
25.	*Lygus pratensis*	+			

Some species of Tylenchida, Dorylaimida, Thysanoptera and Homoptera are vectors for viruses. The species *Siteroptes graminum* is vector for mycoses, some species of *Macrosteles* are vectors for mycoplasms and *Rhopalosiphum maidis* for bacteria.

No trophic interrelations between *Diabrotica virgifera virgifera* and coprophagous (*Geotrupes*, *Onthophagus*, *Aphodius* species), necrophagous (*Dermestes* species) insects. Other Coleoptera (Nitidulidae, Chrysomelidae), Diptera (Culicidae, Sciaridae, Mycetophilidae, Tabanidae, Calliphoridae, Drosophilidae) species without any connection with maize crop are present.

A number of over 41 predator and parasitoid species were identified. The most of predator and parasitoid species belong to insects (Table 6).

Table 6

Predator and parasitoid arthropods identified in maize crops

No.	Species	Families	Orders
	Aranea		
1.	*Lithobius forficatus*	Lithobiidae	Lithobiomorpha
2.	*Nabis ferus*	Nabidae	Heteroptera
3.	*Orius niger*	Nabidae	Heteroptera
4.	*Trigonotylus ruficornis*	Miridae	Heteroptera
5.	*Dolycoris baccarum*	Pentatomidae	Heteroptera
6.	*Aeolothrips intermedius*	Aeolothripidae	Thysanoptera
7.	*Anaphothrips obscurus*	Thripidae	Thysanoptera
8.	*Cicindela germanica*	Cicindelidae	Coleoptera
9.	*Poecilus cupreus*	Carabidae	Coleoptera
10.	*Pterostichus nigrita*	Carabidae	Coleoptera
11.	*Dolichus halenis*	Carabidae	Coleoptera
12.	*Abax carinatus*	Carabidae	Coleoptera
13.	*Abax ater*	Carabidae	Coleoptera
14.	*Calosoma maderae auropunctatum*	Carabidae	Coleoptera
15.	*Brachinus crepitans*	Carabidae	Coleoptera
16.	*Malachius bipustulatus*	Malachiidae	Coleoptera
17.	*Anthicus antherinus*	Anthicidae	Coleoptera
18.	*Formicomus pedestris*	Anthicidae	Coleoptera
19.	*Cantharis annularis*	Cantharidae	Coleoptera
20.	*Coccinella septempunctata*	Coccinellidae	Coleoptera
21.	*Adalia bipunctata*	Coccinellidae	Coleoptera
22.	*Propylaea quatuordecimpunctata*	Coccinellidae	Coleoptera
23.	*Adonia variegata*	Coccinellidae	Coleoptera
24.	*Hippodamia septemmaculata*	Coccinellidae	Coleoptera
25.	*Hippodamia tredecimpunctata*	Coccinellidae	Coleoptera
26.	*Aleochara lanuginosa*	Staphylinidae	Coleoptera
27.	*Tachyporus hypnorum*	Staphylinidae	Coleoptera
28.	*Oxytelus insecatus*	Staphylinidae	Coleoptera

Table 6

(continued)

No.	Species	Families	Orders
29.	*Aphydoletes aphidimyza*	Itonididae	Diptera
30.	*Episyrphus balteatus*	Syrphidae	Diptera
31.	*Syrphus ribesii*	Syrphidae	Diptera
32.	*Leucopis glyphinivora*	Chamaemyiidae	Diptera
33.	*Chrysopa abbreviata*	Chrysopidae	Neuroptera
34.	*Chrysopa carnea*	Chrysopidae	Neuroptera
35.	*Chrysopa septempunctata*	Chrysopidae	Neuroptera
36.	*Lysiphlebus fabarum*	Aphidiidae	Hymenoptera
37.	*Tryoxis angelicae*	Aphidiidae	Hymenoptera
38.	*Aphidius avenae*	Aphidiidae	Hymenoptera
39.	*Praon dorsale*	Aphidiidae	Hymenoptera
40.	*Aphelinus asychis*	Aphelinidae	Hymenoptera
41.	*Exorista* sp.	Tachinidae	Diptera

Their trophic spectrum must be well known and these organisms must be protected. The integrated pest control measures, applied against *Diabrotica virgifera virgifera*, must favorize their action of pest populations control. Some polyphagous predator species could include in their trophic spectrum the *Diabrotica* stages, thus contributing to the control of pest population to small sizes, acceptable from the economic point of view.

4. CONCLUSIONS

In Romania's conditions, alien species *Diabrotica virgifera virgifera* have been established in the structure of maize agrobiocenoses, which include a high macroinvertebrate and microorganism diversity.

In macroinvertebrate association, *Diabrotica virgifera virgifera* is in direct or indirect competition with some species.

It is in direct competition with phytophagous species consuming especially panicles, silk, roots of maize plants and in indirect competition with phytophagous species consuming the germinating seeds, corn stalks and stalk collets. A special indirect competition has been established with microorganisms producing maize diseases.

The *Diabrotica virgifera virgifera* interrelations with its predators and parasitoids are not well known. Some polyphagous predator species may contribute to control the pest population sizes.

Taking into consideration that in our researches we could not find any autochthonous mortality factors, and competition is not severe, *Diabrotica virgifera virgifera* cannot be eradicated in Romania. Thus, we consider that

maintaining low populations sizes, as well as preventing it from spreading in new zones, will be difficult to manage.

REFERENCES

1. LĂCĂTUŞU, MATILDA, TEODORESCU, IRINA, TUDOR, CONSTANŢA, PAULIAN, FL., 1978, *Structura şi evoluţia entomofaunei în monocultura de porumb*, Probleme de ecologie terestră, Editura Academiei Române.
2. TEODORESCU, IRINA, 1989, *Contributions a la connaissance des effets de la pollution industrielle sur certaines biocenoses des agrosystemes adjacents aux sources d'emission*, An. Univ. Buc., Anul XXXVIII, 71–79.
3. TEODORESCU, IRINA, VĂDINEANU, A., 1997, *Negative action of industrial emission upon ground level arthropod populations*, Rev. Roum. Biol, ser. Biol. anim., **42**, *2*, 237–248.
4. TEODORESCU, IRINA, VĂDINEANU, A., 2001, *Managementul capitalului natural, studii de caz*, Editura Ars Docendi, Bucureşti.

Received October 2, 2004.

*University of Bucharest,
Department of System Ecology,
Splaiul Independenţei 91–95,
76201-Bucharest, Romania
Telephone+40-411.52.07,
e-mail: iteodorescu @ bio.bio.unibuc.ro

**Ministry of Agriculture, Forests, Water and Environment,
24, B-dul Carol I, Bucharest, Romania,
e-mail: dacia.vilsan@maa.ro

EVALUATION OF A BACULOVIRAL PRODUCT EFFICIENCY ON BIOLOGICAL CONTROL OF *HYPHANTRIA CUNEA* DRURY (LEPIDOPTERA:ARCTIIDAE) IN ROMANIA

MARIA IAMANDEI*, T. MANOLE*, IRINA TEODORESCU**, ALINA IAMANDEI*

The aim of the present paper is to discuss the results of two years attempt of biological control of *H. cunea* populations with a baculoviral product (HcVG) previously obtained at the Research-Development Institute for Plant Protection Bucharest. For the first time in Romania a baculoviral product was tested in the field cage conditions against *H. cunea* larvae. The efficiency of biological control was assessed by mortality percent of different larvae instars. The mortality level registered was the highest in the L_1-L_2 and L_2-L_3 instars (89% and 78.67% in 2001, respectively 93% and 86.33% in 2002). The researches point out *H. cunea* critical stage and will be very useful for the baculovirus treatments management.

1. INTRODUCTION

Hyphantria cunea Drury (*Lepidoptera-Arctiidae*) is a very polyphagous *Lepidoptera* and eats a wide range of forest and fruit trees, shrubs and herbaceous plants. Some of 600 host plant species have been recorded (13) as food. In Romania, it was demonstrated that, although *H. cunea* is polyphagous, normal development will occur only on the few preferred food plants: mulberries, maples, apples, cherries, walnut and plums (rather than grapes, strawberries, roses and so on).

There have been many researches on the biological control of this pest. The most of them are referred at the use of antagonistic organisms (insects, bacteria, fungi and viruses).

Preparations of *Bacillus thuringiensis* var. *kurstaki* (Bt) were reported to be the most effective (2, 3, 6, 8).

There were also tested *Beauveria bassiana* and *B. globulifera* fungi and the oophagous parasites *Trichogramma dendrolimi* (18, 9). Parasite nematodes can be also used to reduce *H. cunea* populations level (14).

Natural strains of baculoviruses have a great inoculative augmentation potential and the option of using crude suspensions of virus may result in a greater efficacy in comparison with the more expensive, purified products.

REV. ROUM. – BIOL. ANIM., TOME 49, N^{os} 1–2, P. 41–46, BUCAREST, 2004

2. MATERIAL AND METHODS

The researches were carried out at the Research-Development Institute for Plant Protection Bucharest (R.D.I.P.B.) in the 2001–2002 period.
The experiments were developed in the field conditions in special cages and the results obtained are synthetized in Tables 1 and 2.

The assay technique used was different from other methods recently described (11, 12). The inoculum was sprayed on the natural food (leaves and branches of mulberries trees and maples) on 3 variants, each with 3 replicates:

V_1 – treated with viral product "Inf-Hc";
V_2 – treated with Dimilin 25 WP;
V_3 – untreated (control).

In each cage with treated and untreated leaves, 100 different instars of *H. cunea* larvae were introduced. Virus dosage was 5.6×10^9 SPVC/ml. The purification of the included bodies was carried out by Huger's method (1963) (7). The efficiency of the viral products was expressed in the mortality percent of *H. cunea* larvae of the "Inf-Hc"treated variant (V_1).

Pathological analysis of the midgut epithelium infected cells was made both with light and electron microscope. Investigations with the light microscope were made in 3 steps:

- fixation on Carnoy dilution;
- paraffin inclusion;
- clarified and coloured on Fe hematoxylin buffer.

Electron microscope investigations were carried out by admixed 10 µl of the viral suspension with an equal volume of freshly prepared Na_2CO_3. Following admixing a microdroplet was placed on Formavar coated electron microscope grids. After 4 minutes the grid was placed on a drop of 2% w/v phosphotungstic acid and examined with a Philips 410 LS Electron Microscope.

3. RESULTS AND DISCUSSIONS

The production and registration of a new baculoviral biopreparate for biological control of *H. cunea* larvae need the establishment of standard tests of efficiency of virus strains on the target pest instars larvae. The baculoviruses strains obtained after infection initiated in *H. cunea* larvae were currently described by many authors (1, 4, 5, 9). Some molecular aspects of HcVG baculovirus including polyhedra with occluded virions and the electron dense polyhedron envelope that surrounds each occlusion body are present (Fig. 1). The susceptibility degree decreases with larval age. Neonatae larvae were the most susceptible, while the 5th instar larvae were the least. The HcVG limitative action is optimal to early 2nd instar larvae.

Table 1

Baculovirus product efficiency of biological control of *Hyphantria cunea* larvae (2001)

larval instar	Variant	Mortality (%) registered in the next days after treatment									% pupation
		2	3	4	5	6	7	8	9	10	11	
L_{1-2}	V_1	9.00	28.33	52.33	59.00	61.33	65.33	72.67	65.67	84.00	89.00	11.00
	V_2	82.00	85.67	89.00	89.00	90.67	90.67	90.67	90.67	90.67	90.67	9.33
	V_3	0.00	0.00	0.00	0.00	0.00	0.00	0.00	0.00	0.00	0.00	100.00
L_{3-4}	V_1	4.00	14.67	37.00	51.00	55.33	58.00	62.00	67.67	71.00	78.67	21.33
	V_2	61.33	77.33	78.67	78.67	78.67	79.33	79.33	79.33	79.33	79.33	20.67
	V_3	0.00	0.00	0.00	0.00	0.00	0.00	1.00	1.00	1.00	1.00	99.00
L_5	V_1	0.00	4.00	11.67	19.67	20.00	22.00	28.33	34.00	34.00	34.00	66.00
	V_2	47.67	49.67	51.67	51.67	51.67	51.67	51.67	51.67	51.67	51.67	48.33
	V_3	0.00	0.00	0.00	1.00	1.00	4.00	4.00	4.00	4.00	4.00	96.00

Table 2

Baculovirus product efficiency of biological control of *Hyphantria cunea* larvae (2002)

larval instar	Variant	Mortality (%) registered in the next days after treatment									% pupation
		2	3	4	5	6	7	8	9	10	11	
L_{1-2}	V_1	6.00	29.00	58.67	65.00	69.00	73.67	81.33	85.00	93.00	93.00	7.00
	V_2	79.67	84.33	86.67	86.67	89.33	89.33	89.33	89.33	89.33	89.33	10.67
	V_3	0.00	0.00	0.00	0.00	0.00	1.00	1.00	1.00	1.00	1.00	99.00
L_{3-4}	V_1	2.00	26.33	42.00	51.33	53.33	58.67	74.00	78.00	81.67	86.33	13.67
	V_2	45.33	58.33	62.67	62.67	64.33	64.33	64.33	64.33	64.33	64.33	35.67
	V_3	0.00	1.00	1.00	1.00	5.00	5.00	5.00	5.00	5.00	5.00	95.00
L_5	V_1	0.00	0.00	10.67	11.00	14.33	16.67	20.33	28.67	28.67	28.67	71.33
	V_2	34.67	44.67	46.33	46.33	47.33	47.33	47.33	47.33	47.33	47.33	52.67
	V_3	0.00	0.00	0.00	0.00	2.00	4.00	4.00	4.00	4.00	4.00	96.00

Spraying the viral product directly on the nourishing substratum gives the advantage of the easy administration and of increasing pathogenic action. The larvae eat the virus simultaneously with the food. When spraying the product directly on the nest, only few drops of viral solution reach the surface of larvae because of the compact net woven by larvae.

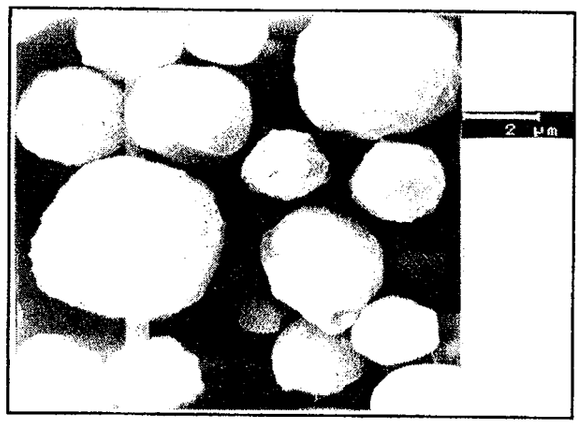

Fig. 1 – The ultrastructure of HcVG isolated from larval tissues of *H. cunea*.

Both years of trials a high percent of larval mortality was registered especially in the first variant (L_1-L_2), in the first days after the treatment. Thus, the mortality percent of L_1-L_2 larvae was over 52% after 4 days in 2001 (Table 1) and respectively over 58% in 2002 (Tables 1 and 2). Less susceptible to the baculovirus action were the L_5 instar larvae. The mortality of L_5 instar larvae was only 11.67% in 2001 and 10.67% in 2002, respectively.

H. cunea larvae instars survival was directly dependant on their susceptibility to the baculovirus action. The high survival level was registered in the untreated variant, expressed by pupation percent (66% in 2001 and 71.33% in 2002).

In the variant treated with Dimilin 25 WP, the larval mortality percent was high on the entire period of trials, and the limitative action of the chemical product was registered as well in the case of L_1-L_2 instars as in L_3-L_4 at the highest levels (between 82 and 96% in L_1-L_2, and 61 to 79% in L_3-L_4, respectively).

The susceptibility of *H. cunea* larvae to the limitative action of HcVG baculovirus was slow: in the first day after treatment, the mortality was very low (under 9%).

The mortality level increased to the end of interval (after 10–11 days of experiment) especially in the L_1-L_2 instars and significantly reduced to next instars.

4. CONCLUSIONS

1. For the first time in Romania a baculoviral product, previously obtained at R.D.I.P.P. Bucharest, was tested in the cage field condition against *H. cunea* larvae.

2. The efficiency of biological control in the two years of experiments was expressed by larval mortality. The degree of mortality registered was the highest in the L_1-L_2 and L_3-L_4 instars, but very low in the last stages.

3. The susceptibility of *H. cunea* larvae to baculovirus action indicates the critical stage (especially L_1 and L_2) and this fact will be very useful both to avoid any damages and for the treatments management.

4. In comparison with the quick action of chemical treatment (Dimilin 25 WP) the baculoviral product HcVG registered a slow response of the pest population. Despite of this, the use of viral product had certain ecological advantages: the baculovirus is active only on its specific "target pest", while Dimilin affects the chitin synthesis process in all arthropods; through their negative action they affected the parasitoids and the predators, natural enemies of the whole pest insects.

REFERENCES

1. BLISSARD, G., W., ROHRMANN, G., F., 1990, *Baculovirus diversity and molecular biology*, Ann. Rev. Entomol., **35**, p. 127–155.
2. BRAVO, A., LORENCE, ARGELIA, RAMIREZ, R.Q., 1995, *Biopesticides compatible with the environment: Bacillus thuringiensis, a unique model*, Biocontrol, **1**, *1*, p. 41–55.
3. CHOI, Y.C., LEE, S.W., SHIN, Y.H., LEE, K.H., 1986. *Studies on the mass production of Bacillus thuringiensis as a microbial insecticide*, Research Reports of the Rural Development Administration, Plant Environment, Mycology and Farm Products Utilization, Korea Republic, **28**, p. 56–59.
4. D'AMICO, V., 2002, *Baculoviruses (Baculoviridae). Insect viruses and pest management*, John Wiley & Sons eds, p. 344–350.
5. FUNK, J., BRAUNAGEL, S., C., ROHRMANN, G., F., 1997, *The Baculoviruses*. Plenum Press, N.Y., p. 7–15.
6. GALANI, Gh., ANA-MARIA ANDREI, 1997, *Microbiological control of some pests by bacteria and entomopathogene fungi. Limitarea populaţiilor de dăunători din culturile agricole prin mijloace biologice şi biotehnice*, Braşov, Ed. DISZ TIPO, p. 258–306.
7. HUGER, A., 1963, *Granuloses of insects. Insect pathology. An advanced treatise*, Ed. E. A. Steinhaus, Acad. Press, **16**, p. 531–574.
8. JASINKA, J., 1984, *Farm studies on application techniques and pesticide efficiency against Hyphantria cunea*, Növenyvedelem, **20**, p. 368–372.
9. SHU, C., R., YU, C., Y., 1985, *An investigation on the natural enemies of Hyphantria cunea*, Natural enemies of insects Kunchong Tiandi, **7**, p. 91–94.
10. TUAN, S., J., CHEN, W., L., KAO, S., S., 1998, *In vivo mass production and control efficacy of Spodoptera litura (Lepidoptera:Noctuidae) nucleopolyhedrovirus*, Chinese J. Entomol., **18**, p. 101–116.

11. VAIL, P., V., JAY, D., L., STEWART, F., D., MARTINEZ, A., J., DULMAGE, T., 1978, *Production of polyhedral inclusion body in a high density insect cell bioreactor*, J. Econ. Entomol., **71**, p. 293–296.
12. WEISS, S., A., DUNLOP, B., F., GEORGIS, R., THOMAS, D., W., VAIL, P., V., HOFFMANN, D., F., MANNING, J., S., 1994, *Production of baculoviruses on industrial scale*, Proceedings of invertebrate pathology & microbial control, **1**, p. 441–446.
13. WORTH, R.A., 1994, *Book of Insect Records*, Chap. 2 Greatest Host Range, p.28.
14. YAMANAKA, S., SETA, K., YASUDA, M., 1986, Evaluation of the use of entomogenous nematode, Steinernema feltiae for the biological control of the fall webworm *Hyphantria cunea* (Lepidoptera: Arctiidae), Journal of Nematology, **16**, p. 26–31.

Received May 2, 2004.

* *Research Development Institute for Plant Protection*
Bucharest, Bvd. Ion Ionescu de la Brad, 8,
Telephone +40.021. 320.88.50
e-mail: icpp@pcnet.ro

** *University of Bucharest, Department of System Ecology,*
Splaiul Independenței, 91–95,
76201-Bucharest-Romania
Telephone +40.021-411.52.07
e-mail: iteodorescu@bio.bio.unibuc.ro

THE ZOOPLANKTON STRUCTURE IN DAM LAKE IRON GATES I (DANUBE km 942–1075) AFTER THREE DECADES OF ITS EXISTENCE

VICTOR ZINEVICI, LAURA PARPALĂ

The lake appearance in 1971 determined irreversible changes of the zooplankton structures of former ecosystems (the Danube river, end section of over 40 of its affluents, springs and ponds). The strongest modifications occurred in the first two years of lake existence, namely: the taxonomic spectrum reduction with more than one third (107→70 taxa), correlated with a high increase of the numerical density and biomass. The colmatage of some areas, together with the submerged vegetation development in littoral zone, determined an increased tendency of the taxonomic diversity, which was also observed in 2002, after three decades of dam lake existence. On the contrary, the numerical density and biomass, after an increase registered in 1971–1972, showed a sharp decrease in the next 7–8 years, reaching somehow low values, characteristic for the dam lakes of river type. The numerical and gravimetrical proliferation of plankton larvae of *Dreissena polymorpha* represented a phenomenon with negative ecological implications. They constituted a clear dominant element of the zooplankton structure in 2002.

Key words: zooplankton, taxonomic diversity, numerical density, biomass, dam lake.

INTRODUCTION

The dam Lake Iron Gates I includes in its perimeter a Danube section of approximate 130 km, the end sections of more than 40 Danube affluents, as well as several springs and stagnant waters. The dam Lake construction in 1971 determined irreversible changes of the biocenosis structures in the mentioned zones. The strongest modifications were registered in the first two years of lake existence. At the request of power station manager, in 2002, there were carried out researches regarding the changes of zooplankton structure, after three decades since the construction of the biggest dam lake on the Danube.

MATERIALS AND METHODS

The samples were collected with 5l Patalas-Schindler device in 24 points situated between km 1072 and 950, in summer and autumn 2002 (Table 1). For each sample 50 l of water were filtered through 65 μm mesh net. The collecting was made on the entire water column. For the biomass calculation (expressed in μg wet weight/l) literature data were used, function of species, sex, development stage and size class.

Table 1

The river sections and zooplaknton sampling stations in dam Lake Iron Gates I in 2002

No	River sections	Station	River km
1	Baziaş	Littoral	1072
2	Baziaş	Medial	1072
3	Kiseljevo	Medial	1062
4	Moldova Veche	Medial	1048
5	Cozla	Medial	1012,5
6	Cozla	Littoral-bay	1012,5
7	Berzasca	Medial	1016
8	Berzasca	Littoral	1016
9	Elişeva	Medial	1007
10	Greben	Medial	998
11	Greben	Littoral	998
12	Sviniţa	Medial	995
13	Sviniţa	Littoral	995
14	Plavişeviţa	Medial	976
15	Plavişeviţa	Littoral	976
16	Dubova	Bay	970
17	Dubova	Littoral	970
18	Cazanele Inferioare	Medial	967
19	Ieşelniţa	Medial	960
20	Ieşelniţa	Bay	960
21	Cerna	Medial	954
22	Cerna	Bay-centre	954
23	Cerna	Bay-upstream	954
24	Bahna	Medial	950

RESULTS AND DISCUSSION

Taxonomic diversity. The Danube zooplankton was characterized by the reduced taxonomic diversity of only 37 components (Table 2) in the river section, in ecological conditions before the lake formation (a high rate of water flow reaching 5 m/sec, the missing of a typical littoral zone). The most numerous taxa belonged to Rotatoria populations (62.16%) (6). From the ecological point of view, the euplanktonic forms were prevalent, to which some nectobenthonic forms were added. Because the high rate of water flow does not allow euplanktonic zooplankton species to complete their development cycles, we assume that these forms were of allochthonous origin.

Table 2

The species diversity numerical density and biomass of zooplankton in dam Lake Iron Gates I before the dam lake formation (1958–1967)

Period	Ecosystem	Taxon number	Ex./l	µg wet matter/l
1958	Danube	37	111	2368
1961–1962	Rivers	12		
1966–1967	Springs	10		
1966–1967	Marshes	54	659	
1958–1967	P.F. zone	105		

Several stagnant waters, with permanent or temporary character, were localized along the left riverbank, especially within km 960–1025, before the dam

construction. In them, the most diverse zooplankton, from the taxonomic point of view, which comprised 54 components, was present (1) (Table 2). Its analysis on taxonomic groups evidenced a uniform distribution of taxa between Rotatoria (31.48%), Cladocera (31.48%) and Copepoda (27.77%).

In spring only 10 taxa were found, exclusively belonging to Copepoda (27.77%). 60% of these belonged to the order Harpacticoida comprising nectobenthonic forms (7).

Very few information exist referring to the zooplankton in the inferior portions of Danube affluents in Iron Gates area. In the case of inferior Cerna river, 12 species were identified (Table 2). 83.33% of these belonged to Rotatoria (2). Their ecological structure reflected the dominance of the forms dependent on vegetal bioderm.

On the whole, the taxonomic spectrum of the zooplankton from the former mosaic of ecosystems of the Lake Iron Gates I comprised 105 components. 45.71% of them belonged to Rotatoria populations.

In the first year of lake existence (1971) the zooplankton taxonomic spectrum underwent the strongest reduction of 30.48% (3). In the second year, the lowest taxonomic diversity (70 taxa) through 32 years of lake existence was registered (8). Then, 112 (1978) and 125 (2002) taxa were noticed showing an increasing tendency of the taxonomic diversity (Table 3). At the beginning, this dynamics was determined by the existence of some available ecological niches, provided by the new ecosystem appearance, and further, by the formation of areas with submerged and emerged vegetation along the littoral zone which favoured the proliferation of the phytophilous forms. 84.80% of all registered species in 2002 belonged to primary consumers, the rest of 15.20% being secondary consumers.

Table 3

The interannual dynamics of species diversity, numerical density and biomass of zooplankton in dam Lake Iron Gates I in 1971–2002

Period	No. taxa	Ex./l	µg wet matter/l
1971	73	1372	21457
1972	70	1095	2697
1973		405	
1974		171	
1975		115	
1976		164	
1978	112	38	239
1979	106	453	923
1980	109	48	213
1981	92	104	2168
1984		128	205
1985		28	69
1986		280	366
1987		153	162
1995		68.5	72.4
2002	125	70	112
1971–2002	322		

The ecological structure consisted in euplanktonic, nectobenthonic, euplanktonic macrophytophilous forms. The high contribution to the taxonomic spectrum had Rotatoria group (51.89%) within C_1 zooplankton, and Cyclopida in the case of C_2 zooplankton.

Although the taxonomic diversity was identical in summer and autumn 2002 (79 taxa in both cases) the composition of their taxonomic spectra significantly differed. Thus, the total number of the identified species in two seasons far depassed the each season value (Table 4). The cause was the existence of an active seasonal succession of the species. By similar reasons, the contribution of systematic groups underwent seasonal changes (Table 5).

Table 4

The seasonal variations of species diversity (taxon number), numerical density (ex./l) and biomass (μg wet matter/l) of whole zooplakton and its trophic levels (C_1, C_2) in 2002

Ecological parameters	Trophic level	Period		
		VI	IX	VI–IX
Taxonomic diversity (no. taxa)	C_1	68	70	106
	C_2	11	9	19
	C_1+C_2	79	79	125
Numerical density (ex./l)	C_1	115	23	69
	C_2	1	1	1
	C_1+C_2	116	24	70
Biomass (μg wet matter/l)	C_1	77	77	77
	C_2	5	62	33.5
	C_1+C_2	82	139	110.5

Table 5

The seasonal variations of species diversity (a), numerical density (b) and biomass (c) of zooplankton, on taxonomic groups (%), in 2002

Taxonomic structure	a		b		c	
	VI	IX	VI	IX	VI	IX
C_1	100	100	100	100	100	100
Ciliata	13.23	8.57	1.22	5.30	0.25	0.71
Testacea	25.00	20.00	1.65	3.76	1.62	0.79
Lamellibranchiata	1.47	1.43	70.85	16.53	65.80	2.09
Rotatoria	48.54	54.28	25.24	39.74	19.28	9.45
Cladocera	8.82	12.86	0.17	7.66	9.45	54.23
Copepoda	2.94	2.86	0.87	27.01	3.61	32.73
C_2	100	100	100	100	100	100
Ciliata	54.55	11.11	87.06	0.88	7.14	0.01
Rotatoria	9.09	11.11	9.00	16.24	14.29	1.88
Cladocera	9.09	11.11	0.07	0.45	78.57	1.64
Copepoda	27.27	66.67	0.00	82.43	0.00	96.47

The spatial dynamics of the taxonomic diversity revealed the season maximum values in Ieşelnița gulf, where the ecosystem trophic level increased, as a result of the anthropic factor action. Values close to them were registered in areas Greben and Baziaş (Fig. 1). In the last case, the high diversity showed the influence of the flooding area of the Nera river, nearby situated.

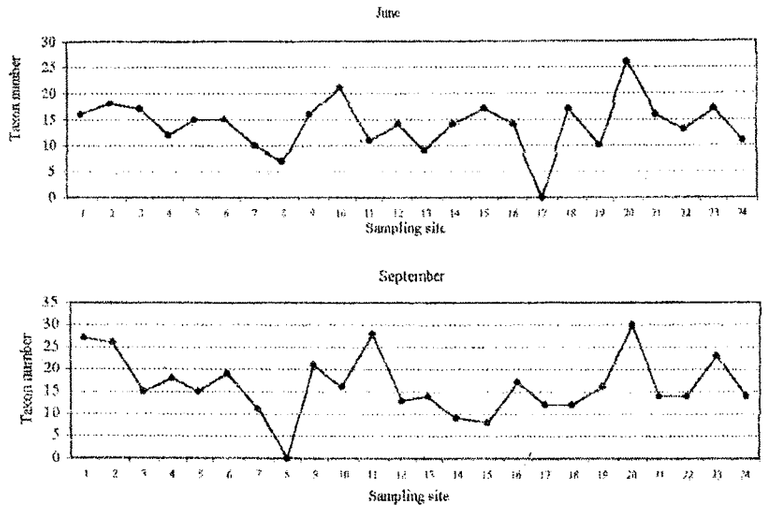

Fig. 1 – Spatial variations of the taxonomic diversity (taxon number), in 2002.

The constant frequency species represented 11.84% during summer and only 8.97% in autumn. To notice that the accessory frequency species were also not so numerous (summer – 13.16%; autumn – 16.67%). As a consequence, the main part of species (75% in summer, 74.36% in autumn) were accidental forms, characterised by a reduced ecological role. The component of most frequency was the plankton larva of *Dreissena polymorpha* (100% in summer, 95.65% in autumn). *Keratella cochlearis*, *K. cochlearis tecta* (in summer), *Bosmina longirostris* and Copepoda g. sp. of nauplial form and I/III copepodit stadies were situated on the next places (Table 6).

Table 6

The frequency constant forms (1) and numerical (2) or gravimetrical (3) dominant forms of zooplankton (%) in dam Lake Iron Gates I, in 2002

Composition	1		2		3	
	VI	IX	VI	IX	VI	IX
Primary consumers						
Testacea						
Arcella arenaria Greef	-	56.62	-	-	-	-
Ciliata						

Table 6

(continued)

Composition	1		2		3	
	VI	IX	VI	IX	VI	IX
Lamellibranchia						
Dreissena polymorpha Pallas	100	95.65	70.85	16.53	65.80	-
Rotatoria						
Brachionus calyciflorus anuraeiformis Brehm	65.22	-	-	-	-	-
Epiphanes clavulata Ehrenberg	52.17	-	-	-	-	-
Keratella cochlearis Gosse	100	-	10.48	-	-	-
K. cochlearis tecta Gosse	100	73.95	-	-	-	-
K. quadrata Müller	78.26	-	-	-	-	-
Synchaeta oblonga Ehrenberg	52.17	60.89	-	-	-	-
S. pectinata Ehrenberg	60.87	-	-	-	-	-
Cladocera						
Bosmina longirostris Schoedler	-	-	-	-	-	34.36
Moina micrura Kurz	-	56.52	-	-	-	-
Simocephalus vetulus (Müller)	-	-	-	-	6.28	-
Copepoda						
Copepoda g.sp. – stadiul nauplius	60.87	100	-	22.14	-	-
Cyclopidae g.sp. Stadiul copepodit I-III	-	100	-	-	-	16.38
Secondary consumers						
Ciliata						
Didinum nasutum (Müeller) Stein	-	-	37.00	-	-	-
Menodinium balbianii Fabre-Domergus	-	-	39.00	-	-	-
Rotatoria						
Asplanchna priodonta Gosse	-	-	-	-	14.29	-
Cladocera						
Leptodora kindti (Focke)	-	-	-	-	78.57	-
Copepoda						
Cyclopidae g.sp. copepodit IV-V	-	78.26	-	60.77	-	15.78
Mesocyclops crassus Fischer	-	-	-	18.00	-	70.12

Numerical abundance. Few information exist as regards the zooplankton numerical abundance in former ecosystems of the dam Lake Iron Gates I. They refer to river sector and swamps located along former Danube course. Their analysis showed a reduced development of numerical effectives of zooplankton in the Danube. The calculation of this parameter average in Orşova area, in 1958, resulted in 111 ex/l (Table 2). Similar values were registered in areas Cazanele Inferioare and Coronini. As spatial dynamics showed, the values obtained near to banks zones were 5 times higher than that in the former Danube course area. In both cases the Rotatoria was the dominant group (6).

In the case of stagnant waters present before the dam lake formation, the zooplankton numerical abundance spatially varied in wide ranges. Thus, for example, the temporary swamps Camenița (km 1025) and Ieşelnița (km 961) distinguished by high values of the mentioned parameter in some moments of annual cycle (2085, respectively 1106 ex/l), while the temporary pond Dubova (km 972) and permanent pond Cozla (km 1015) were situated to the other extreme (42, respectively 112 ex/l) (1). The average of all these values was 659 ex/l (1) (Table 2).

In the first year of dam lake existence (1971) the increased nutrients provided through flooding of large terrestrial areas determined a strong zooplankton proliferation. The 1971 average (1372 ex/l) represented the absolute maximum value among the annual averages during the three decades of ecosystem existence. Spatially, the maximum numerical abundance was observed in littoral area recently flooded. It depassed 5.8 times the value in medial area of the former Danube course. A high numerical development was observed also in 1972 (1095 ex/l), even if it is 1.2 times lower than the 1971 value. The descendant dynamics continued in 1973–1975. Beginning with 1976, the annual averages of the numerical density ranged between 28–453 ex/l (Table 3) (3, 4, 5, 9, 10, 11). It is considered that this range is characteristic for the dam lakes of river type.

The 2002 average (70 ex/l) enclosed in this range. To notice that September 2002 average (24 ex/l) was 4.8 times lower than that of June (116 ex/l), although, the maximum value of the mentioned parameter was usually registered in early autumn, in European lakes. The reduced zooplankton development in September was probably determined by the considerable increase of the river flow in an unusual period of the annual cycle (August).

The numerical ratio between the two zooplankton trophic levels within the 2002 collected material evidenced an extremely reduced number of secondary consumers as compared to the primary ones (Table 4).

The mentioned high floodings caused also changes in spatial numerical distribution. Thus, in June the maximum value was registered in Ieşelnița gulf (347 ex/l) (as a result of anthropic nutrient provision) and the minimum value in upstream extremity of Cerna gulf (24 ex/l) (where the influence of Cerna river waters, usually poor in zooplankton, is present). On the contrary, in September the maximum value (201 ex/l) was registered in the upstream area of the Cerna gulf (because here the negative influence of river high flooding is not present), and the minimum value in Elişeva area (4 ex/l) (Fig. 2).

The primary consumer analysis on systematic groups showed the numerical dominance of Lammellibranchia in June (70.85%) and Rotatoria in September (39.74%). In the case of secondary consumers the numerical dominance belonged to Ciliata in summer (87%) and to Cyclopidae in autumn (82.43%) (Table 5).

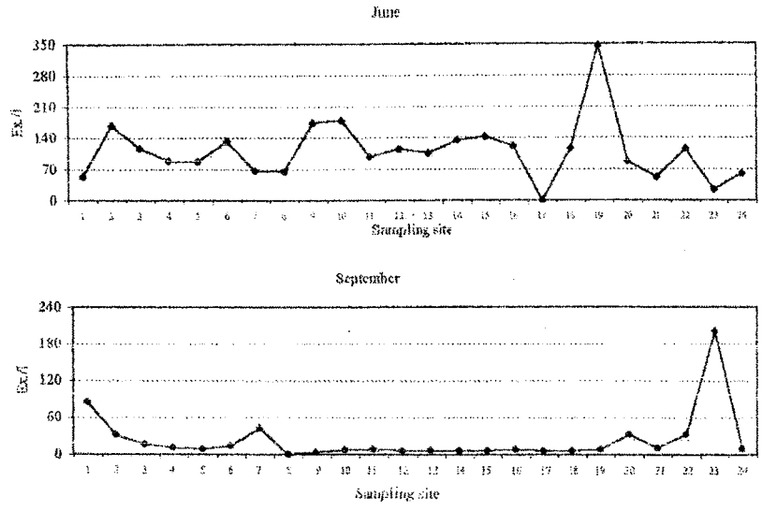

Fig. 2 – Spatial variations of the numerical density (ex/l), in 2002.

The analysis on taxa evidenced the determinant role of larva of *Dreissena polymorpha* (70.85%) during summer, and of Copepoda g. sp nauplial forms (22.14%) in autumn, within the C_1 trophic level. In the case of secondary consumers the numerical dominance was assured by *Didinium nasutum* during summer (37%) and by Cyclopida g. sp. IV–V copepodits in autumn (60.77%) (Table 6).

Biomass. The biomass data before the lake formation are also very scarce and refer only to the river zooplankton. The annual average, calculated with the data obtained by Popescu (6) for the Orşova profile, seems very high (4056 µg wet weight/l). It is not in accordance with the ecological conditions existent in the mentioned section before the river blocking. On the other hand, the data analysis showed that the zooplankton biomass in littoral zone was certainly higher than that in medial area of the former Danube course. Among taxonomic groups, Cladocera represented the main component of biomass (totalizing 63.97% of it).

In the first year of dam lake existence the numerical proliferation of zooplankton directly correlated to the gravimetrical one (average = 21457 µg/l) (Table 3). 8 times lower annual average (2697 µg/l) was registered in the next year. The annual averages in the next period were 1.2–39 times lower than the last value (4, 5, 8, 9, 10, 11).

In the ecological conditions of 2002 the zooplankton of dam Lake Iron Gates I was characterized by reduced values (112 µg/l), on the last place within 1971–2002 period. Besides the causes, which determined the low values of the numerical density, the prevalence of small size species was added too, in this case.

The biomass seasonal dynamics had an ascendant character from summer towards autumn (82→139 µg/l) (Table 4) although the numerical density descendantly evolved.

As in the case of the numerical abundance, the configuration of the spatial dynamics of the zooplankton biomass in the two seasons clearly differed. In the case of both parameters the reasons were nearly similar. As a consequence, the season maximum values were located also in gulf Ieşelniţa (112 µg/l), respectively in profile Baziaş (834 µg/l), and the minimum values in Orşova zone (29 µg/l) and gulf Dubova (12 µg/l) (Fig. 3).

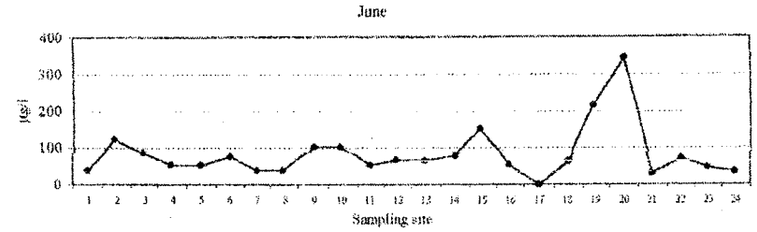

Fig. 3 – Spatial variations of the biomass (µg wet weight/l), in 2002.

The analysis of the gravimetrical contribution of systematic groups evidenced, similar to numerical density, wide seasonal differences. Thus, in June, there was remarked the high contribution of Lammellibranchia within C_1 level (62.86%). In September their role was replaced by Cladocera group (54.23%). Within the C_2 level, the Cladocera dominance (78.57%) in June was replaced by Cyclopida (96.47%) in September (Table 5).

The analysis of the gravimetrical dominance of species showed the following seasonal succession: larvae of *Dreissena polymorpha* (65.80%)→*Bosmina longirostris* (34.36%) for C_1 and *Leptodora kindti* (78.57%) →*Mesocyclops crassus* (70.12%) for C_2 (Table 6).

CONCLUSIONS

• Of 105 taxa evidenced in the Danube (km 942–1075) and afferent waters before the dam Lake Iron Gates I formation, 66.67% remained in the new ecological conditions, while 33.33% disappeared;

• In the first 32 years (1971–2002) of ecosystem existence the taxonomic diversity of the zooplankton totalised 311 taxa;

• The major part of zooplankton taxa (77.49%) appeared after the lake formation, while, the former ones represented only 22.51% of the mentioned total number;

• The interannual dynamics of taxonomic diversity of lacustrine zooplankton showed the lowest values in the first two years of lake existence (73 taxa in 1971 and 70 in 1972) and the maximum values in 2002 (125 taxa);

• The zooplankton numerical density and biomass were characterised by reduced values (70 ex/l, respectively 112 µg wet weight/l), peculiar to dam lakes of river type, in 2002;

• The interannual dynamics of numerical density and biomass registered the highest values in the first two years of new ecosystem existence (1372 ex/l, respectively 2145µg wet weight/l in 1971 and 1095 ex/l, respectively 2697µg wet weight/l in 1972), then far low values, with minimum ones in 1978 (38 ex/l) and 1985 (69 µg/l);

• The component with a determinant role in the structural dynamics of zooplankton community of the lake was the plankton larva of *Dreissena polymorpha*.

REFERENCES

1. Gh. Brezeanu, 1970, *Zooplanctonul zonei Porţile de Fier I (Studiul hidrobiologic al Dunării şi al afluenţilor săi)*: 76-84, 152–156. Ed. Acad. R.S.R., Bucureşti.
2. Gh. Brezeanu, Virginia Marinescu–Popescu, 1964, *Studiul hidrobiologic al bazinului inferior al Cernei*. Hidrobiologia, **5**: 65–94, Bucureşti.
3. Gh. Brezeanu, Marieta Petcu, 1973, *Bazele ecologice ale formării şi evoluţiei zooplanctonului în lacul de acumulare de la Porţile de Fier în primul an de existenţă*. Hidrobiologia, **14**: 177–187, Bucureşti.
4. Gh. Brezeanu, V. Zinevici, 1984, *La formation et l'évolution du zooplankton du lac de barrage "Porţile de Fier" (le Danube inférior) dans l'intervalle 1971–1980*, Verh.Internat.Verein.Limnol., **22**: 1558–1561, Stuttgart.
5. M.T. Gomoiu, D. Secrieru, Gh. Oaie, Melania Cristescu, N. Nicolescu, Virginia Marinescu, 1998, *Ecological state of the river Danube ecosystems in 1995*. Geo-Eco-Marina, **3**: 37–88, Bucuresti-Constanta.
6. Ecaterina Popescu, 1960, *Observaţii asupra planctonului în regiunea de amonte a Dunării inferioare (km 1042-km 957)*. Bul.Inst. de Cerc.Pisc., **19**, **3**: 5–17, Bucureşti.
7. Elena Arion-Prunescu, 1970, *Biocenoze din izvoare*. Monografia zonei Porţile de Fier. Studiul hidrografic al Dunării şi afluenţilor săi: 137–142. Ed.Acad.R.S.R., Bucureşti.

8. B. Rusev, Victoria Cure, Virginia Popescu-Marinescu, 1983, Die *Veranderungen der Strömungrschwindigkeit und ihre Answirkungen auf die Plankton- und Benthosbiozönosen der Donau*. Hidrobiologia, **18**: 93–148, Bucureşti.
9. V. Zinevici, Laura Teodorescu, 1982, *Structura calitativă şi cantitativă a zooplanctonului din partea inferioară a lacului de baraj Porţile de Fier I (1978-1981)*. Bul. De Cerc. Piscicole, **4** (35), 1–2: 5–19, Bucureşti.
10. V. Zinevici, Laura Teodorescu, 1989$_a$, *Structura taxonomică a zooplanctonului din sectorul românesc al Dunării în perioada 1984-1987*. Şt.Cerc.Biol., s.Biol.Anim., **41**, **2**: 93–99, Bucureşti.
11. V. Zinevici, Laura Teodorescu, 1989$_b$, *La structure numérique et gravimetrique du zooplancton dans les secteur roumain du Danube au cours de années 1984-1987*. Rev.Roum.Biol., s.Biol.Anim., **34**, **2**: 155–165, Bucharest.

Received May 22, 2004.

Institute of Biology
Spl. Independenţei 296, Bucharest
E-mail: victor.zinevici@ibiol.ro

TAXONOMIC COMPOSITION AND NUMERICAL DENSITY OF THE ZOOBENTHOS IN THE DAM LAKE IRON GATES I (ROMANIAN SECTION) IN 2002

VIRGINIA POPESCU-MARINESCU

We present the zoobenthos data regarding its composition, taxonomic variability and frequency, numerical density (on zoobenthos groups), as well as the spatial and seasonal variations of the total zoobenthos density, in the damlake Iron Gates I, in 2002. As the table and graphic analysis revealed, a wider diversity of the zoobenthos taxa (but much lower than the value registered before the river damming) existed in the ecosystem upper zone than in the rest of the accumulation. *Hypania invalida. Limnodrilus hoffmeisteri, Tubifex tubifex, Branchiura sowerbyi, Sphaerium sp.* and *Dreissena polymorpha* were the constant-dominant species in the damlake. The Ponto-Caspian elements were present especially in the upper half of the ecosystem. The zoobenthos numerical density was generally high, presenting wide spatial and seasonal variations; the oligochaets and the polychaets were the numerical dominant taxonomic groups.

1. INTRODUCTION

The analysis of the zoobenthos state from the Romanian section of the damlake Iron Gates I was presented. This was performed on the data obtained by the processing of the material gathered in the 2002 summer (June) and autumn (September). The determination and localization of the profiles and stations for the biological sample collection are presented in Table 1.

Alongside the zoobenthos sample collection, some field observations and measurements regarding the benthos facies nature, the water depth and the flow rate were carried out. These environment factors had a special significance for the survival and development of the benthos organisms.

We specify that the researches were performed according to a contract that was concluded with the Iron Gates Hydroelectric station Branch, in 2002.

2. MATERIALS AND METHODS

The benthos sample collection, both on the longitudinal (between Baziaş and the zone near the dam) and the transversal profiles (including the Romanian riparian, the damlake navigable zone and the intermediary portion between the riparian and the damlake navigable zone) was carried out by quantitative methods, with a bodengreiffer, on a 400 cm^2 surface of muddy, sandy, stony or mosaic substratum.

REV. ROUM. BIOL. – BIOL. ANIM., TOME 49, N^{os} 1–2, P. 59–72, BUCAREST, 2004

The collected material was preliminarily washed in the field and fixed in formol 4%. The sample working out in the laboratory consisted in their final washing, sorting, determining, counting and weighting on groups, genera, species, after which the organisms were immersed in alcohol 70°. The zoobenthos species determination was performed using a binocular magnifying glass and an optical microscope. The obtained quantitative data were related to 1 m^2 substratum surface.

Table 1

Profiles and stations of zoobenthos sample collection, in the damlake Iron Gates I, in 2002

Profile name	Danube km	Stations	Station code
BAZIAŞ	1072.4	Left riparian	1
		Intermediary zone	2
		Navigable zone	3
OSTROV	1062.0	Navigable zone	4
MOLDOVA VECHE	1048.7	Intermediary zone	5
		Navigable zone	6
SIRINA	1012.3	Intermediary zone	7
ELIŞEVA	1007.0	Intermediary zone	8
		Navigable zone	9
GREBEN	998.0	Left riparian	10
		Navigable zone	11
SVINIŢA	995.0	Left riparian	12
		Navigable zone	13
PLAVIŞEVIŢA	976.0	Intermediary zone	14
DUBOVA	970.0	Gulf middle	15
		Navigable zone	16
MRACONIA	967.0	Navigable zone	17
IEŞELNIŢA	960.0	Navigable zone	18
ORŞOVA VECHE	957.0	Left riparian	19
		Navigable zone	20
CERNA	954.0	Gulf tail	21
		Gulf middle	22
		Navigable zone	23
BAHNA	950.0	Intermediary zone	24

3. RESULTS AND DISCUSSION

By **spatial distribution** and **frequency** point of view, the benthos fauna in the damlake Iron Gates I was dominated by some pelophilic species, present both on the longitudinal and transversal profiles (Table 2). The representative species, with a frequency higher than 50%, were *Hypania invalida, Limnodrilus hoffmeisteri, Tubifex tubifex, Branchiura sowerbyi, Sphaerium* sp. Both their high frequency and high numerical density were due to the fact that the respective

organisms found in the accumulation suitable conditions for their development, owing to a large surface of muddy facies. With only 50% frequency and reduced populations in 2002, *Dreissena polymorpha* was present in numerous samples such as juveniles and offsprings unfixed on the substratum. In few cases young individuals were fixed on the stones or on the empty shells of the own species. With a limited spreading, almost in the upper half of the ecosystem, the gastropods *Lithoglyphus naticoides, Theodoxus danubialis, Th. fluviatilis, Viviparus acerosus, Bithynia tentaculata* were found on sandy and gravel or sandy-muddy facies, with frequencies under 15%. We specify that especially in autumn, the water transported many empty shells of *Sphaerium, Dreissena* and *Viviparus*, originated from the areas both of the riparian and between the riparian and the damlake navigable zone, towards the damlake navigable zone.

A peculiar category of zoobenthos organisms of the damlake Iron Gates was constituted by the Ponto-Caspian elements, of marine origin, adapted to the fresh water life (1, 6, 7, 9). Among these, we already mentioned the species *Hypania invalida.* It reached the highest numerical density among the Ponto-Caspian elements present in the damlake Iron Gates I and is the unique polychaet representative in the zone (Table 3). *Dreissena polymorpha* was also a Ponto-Caspian species. Crustacea was the zoobenthos group, the richest in Ponto-Caspian elements. Among them, *Jaera istri* was especially bound on the stony facies, as *Corophium curvispinum, C. chelicorne, C. robustum.* Usually, on the sandy-muddy facies or sandy facies with gravel or mud, there were found *Dikerogammarus haemobaphes fluviatilis, D. villosus, D. v. bispinosus, Chaetogammarus tenellus behningi, Obesogammarus obesus, P. sarsi.* On the same facies category *Palaeodendrocoelum romanodanubialis, Otoplana antipai, Oligochaerus limnophyllus* habited. Excepting *Hypania invalida* and *Dreissena polymorpha,* all other Ponto-Caspian elements were spread especially in the upper zone of the damlake Iron Gates I, mainly in the first 25 km from the upper stream, in 2002. There, the sand with gravel substrate enabled a better aeration, the Ponto-Caspian species being oxyphilous.

The benthos fauna presented the largest **taxon diversity** in the profiles Baziaş, Ostrov, Moldova Veche of the Iron Gates I ecosystem, in 2002. In these zones the taxonomic composition was almost dominated by the Ponto-Caspian elements (Table 2). Although the animals were strongly affected by the accumulation construction, they found the ecological niches in which not only resisted, but developed too, in the course of time (3, 4, 6, 7, 9).

But, the taxon diversity, in the damlake Iron Gates I, in 2002, was much reduced against its value registered before the Danube damming. The main factor of its severe diminution was the dominance of the muddy facies and the reduction of the sandy facies, and even the disappearance of the stony facies, in some zones. A sudden structural modification of wide amplitude occurred in the first 2 years

after the accumulation construction, as a consequence of the environment factor changes. The lithorheophilic fauna almost completely disappeared, being replaced by the pelophilic elements. As the taxon diversity decreased, the number of individuals of the taxa, adapted to the new environment conditions, increased (2, 3, 4, 6). The relevant examples are presented in Tables 2 and 3.

Table 2

Taxonomic composition, spatial distribution and frequency of the zoobenthos organisms, in the damlake Iron Gates I, in 2002

Taxonomic unit name	Collection months: J = June; S = September Station code: 1-24 (Table 1)		Frequency (%)
1	2		3
Coelenterata			
Hydra viridis	J: 1 – 4; 6; 10	S: 1 - 4; 6; 7	25.53
Cordylophora caspia	J: 4; 10	S: 4; 7; 9	10.63
Turbellaria			
Dugesia gonocephala	J -	S: 15	2.12
Dugesia lugubris	J -	S: 4	2.12
Oligochaerus limnophyllus	J: 2	S -	2.12
Otoplana antipai	J: 2; 4	S: 2; 6; 7	10.63
Palaeodendrocoelum romanodanubialis	J: 1 - 4; 6; 7; 10	S: 1 - 4; 6; 15; 17	27.65
Oligochaeta*)			
Branchiura sowerbyi	J: 1; 12 - 21; 23; 24	S: 12 - 22; 24	53.31
Limnodrilus hoffmeisteri	J: 1 - 3; 9; 12 - 21; 23; 24	S: 1; 2; 12 - 24	61.70
Tubifex tubifex	J: 1 - 3; 12 - 21; 23; 24	S: 1; 2; 12 - 24	61.70
Polychaeta			
Hypania invalida	J: 1 - 4; 6 - 24	S: 2 - 4; 6 - 10; 16; 17; 22; 23	74.46
Hirudinea			
Erpobdella octoculata	J: 4; 7	S: 1; 3	8.51
Glossiphonia complanata	J: 1; 3; 14	S: 1	8.51
Haemopis sanguisuga	J -	S: 17	2.12
Hirudo medicinalis	J -	S: 21	2.12
Lamellibranchia			
Anodonta piscinalis	J: 16	S -	2.12
Dreissena polymorpha	J: 1 - 4; 6 - 8; 10; 14; 21; 22; 24	S: 1 - 4; 6; 7; 9 - 11; 17; 22; 24	50.00
Pisidium sp.	J: 14; 20	S: 10; 16; 18; 20	12.50
Sphaerium sp.	J: 1 - 3; 9; 11 - 15; 22; 23	S: 1; 2; 4; 6; 8; 13 - 18; 20 - 24	56.25
Unio tumidus	J: 16; 21	S: 2; 16; 18; 22	12.50
Gastropoda			
Bithynia tentaculata	J -	S: 1 - 3	6.25
Lithoglyphus naticoides	J: 1	S -	
Theodoxus danubialis	J: 3; 4; 10	S: 2; 4; 10; 17	14.58

Table 2

(continued)

1	2		3
Theodoxus fluviatilis	J: 1; 4; 7; 9	S: 3; 4; 7	14.58
Viviparus acerosus	J: 1- 3; 16	S: 2; 3	12.50
Isopoda			
Jaera istri	J: 1 - 4; 6 - 8; 10	S: 2 - 9; 17	36.17
Amphipoda			
Corophium chelicorne	J: 2; 4; 6; 7	S: 2; 4; 7; 9; 17	18.75
Corophium curvispinum	J: 1; 3; 4; 11	S: 1 - 3; 5; 6; 8; 9; 17	25.00
Corophium robustum	J: 8	S: 8	4.16
Chaetogammarus telleus behningi	J: 1; 7; 8; 10	S: 1; 2; 11; 17; 21	18.75
Dikerogammarus haemobaphes fluviatilis	J: 1 - 3; 7; 9 - 11	S: 17	14.58
Dikerogammarus villosus	J: 4; 9	S: 1; 4; 17	10.41
Dikerogammarus villosus bispinosus	J: 1 - 4; 6; 7; 9; 10; 15; 17	S: 2; 3 - 6; 9; 17	35.41
Obesogammarus obesus	J: 1 - 4; 6; 7; 9; 10; 13; 17	S: 1- 4; 6 - 8; 17	37.50
Pontogammarus sarsi	J: 1; 4; 8; 9	S: 1; 2	12.50

*) Oligochaeta were not completely identified.

The zoobenthos organism **numerical density**, on **taxonomic groups,** in the damlake Iron Gates I, in 2002 two seasons (summer and autumn), was presented in Table 3. It was observed the dominance, along almost the entire accumulation of the oligochaets with a maximum value at Baziaş (791,375 ex/m^2), being followed by the polychaets with the highest value at Baziaş, too (129,450 ex/m^2). The gammarids (84,475 ex/m^2), isopods (22,575 ex/m^2) and lamellibranchia (31,075 ex/m^2), whose maximum values were also found in Baziaş, followed. The numerical density of the zoobenthos organisms of the mentioned 5 groups was high only till Moldova Veche. Among the main zoobenthos organisms we mention also the corophiids with their highest number (41,755 ex/m^2) found at Moldova Veche, where they begin to drastically decrease. We also mention the great development of coelenterates, especially at Baziaş, where they reached a maximum value (225,150 ex/m^2).

But the same organism groups, which reached the highest numerical density, had also minimum values (oligochaets, polychaets and gammarids, 13 ex/m^2 at Elişeva; isopods, 25 ex/m^2 at Mraconia; corophiids, 50 ex/m^2 at Greben; lamellibranchia and gastropods, 50 ex/m^2 in few zones).

Table 3

Numerical density (ex/m^2) of the zoobenthos organisms on the taxonomic groups, in the damlake Iron Gates I, in June / September 2002

Profiles and stations	Taxonomic group					
	Coelenterata	Turbellaria	Nematoda	Polychaeta	Oligochaeta	Oligochaeta cocoons
0	1	2	3	4	5	6
BAZIAŞ						
Left riparian	50 / 2,500	275 / 150	–	2,100 / –	4,825 / 375	150 / –
Intermediary zone	225,150 / 28,000	22,500 / 100	– / 250	129,450 / 550	791,375 / 9,750	48,750 / 325
Navigable zone	32,875 / 638	325 / 13	–	4,650 / 138	9,975 / 575	–
OSTROV						
Navigable zone	12,850 / 2,050	900 / 125	275 / –	7,200 / 1,525	1,300 / 2,275	–
MOLDOVA VECHE	**In June samples were not collected**					
Intermediary zone					150	
Navigable zone	4,950 / 1,250	125 / 125	25 / 125	5,950 / 2,350	1,725 / 3,500	200 / –
SIRINA						
Intermediary zone	– / 600	8 / 50	–	33 / 150	– / 300	–
ELIŞEVA						
Intermediary zone	–	–	–	775 / 175	275 / 4,100	125 / –
Navigable zone	– / 63	–	–	64,450 / 13	21,975 / 13	5,200 / –
GREBEN						
Left riparian	750 / –	250 / –	–	525 / 900	1,150 / –	–
Navigable zone	–	–	–	25 / –	–	–
SVINIŢA						
Left riparian	–	–	–	1,200 / –	25,800 / 26,825	7,000 / 1,350
Navigable zone	–	–	–	62,575 / –	39,375 / 4,475	2,625 / 150

Table 3

(continued)

0	1	2	3	4	5	6
PLAVIŞEVIŢA						
Intermediary zone	–	–	– / 25	200 / –	4,850 / 21,675	1,750 / 4,850
DUBOVA						
Gulf middle	–	– / 25	1,050 / 50	75 / –	7,725 / 8,150	75 / 3,100
Navigable zone	–	–	7,500 / 3,375	25 / 25	4,475 / 10,275	– / 3,000
MRACONIA						
Navigable zone	–	– / 25	– / 25	3,800 / 450	12,600 / 5,675	– / 325
IEŞELNIŢA						
Navigable zone	–	–	25 / 825	3,700 / –	12,325 / 4,425	2,650 / 2,100
ORŞOVA VECHE						
Left riparian	–	–	– / 5,500	25 / –	21,100 / 16,050	3,525 / 375
Navigable zone	–	–	– / 835	25 / –	24,325 / 12,700	6,300 / 1,925
CERNA						
Gulf tail	–	–	1,750 / 1,275	375 / –	19,725 / 53,200	1,375 / 1,425
Gulf middle	–	–	1,500 / –	1,200 / 50	12,300 / 3,850	– / 225
Navigable zone	–	–	350 / –	350 / 50	2,525 / 4,275	– / 450
BAHNA						
Intermediary zone	–	–	– / 525	400 / –	21,825 / 5,500	3,125 / 5,425

Table 3

(continued)

Profiles and stations	Taxonomic group					
	Lamellibranchia	Gastropoda	Isopoda	Gammaridae	Corophiidae	Varia
0	7	8	9	10	11	12
BAZIAŞ						
Left riparian	650 / 150	225 / 200	150 / –	400 / 150	825 / 200	800 / 525
Intermediary zone	31,075 / 425	8,500 / 2,125	22,575 / 600	84,475 / 3,350	100 / 4,325	25 / 225
Navigable zone	8,200 / 738	250 / 1,013	4,125 / 150	9,500 / 500	225 / 175	950 / 25

Table 3

(continued)

0	7	8	9	10	11	12
OSTROV						
Navigable zone	200/725	200/875	7,200/2,375	11,250/2,375	15,000/4,750	25/25
MOLDOVA VECHE		In June samples were not collected				
Intermediary zone	—/–	—/50	—/650	—/3,925	—/41,775	—/100
Navigable zone	25/1,925	575/–	1,725/75	1,275/2,875	50/75	–
SIRINA						
Intermediary zone	25/75	8/25	67/125	167/175	142/775	–/25
ELIŞEVA						
Intermediary zone	50/2,000	–/50	100/150	75/1,075	100/1,825	–
Navigable zone	475/100	75/75	–/38	425/13	–/100	–
GREBEN						
Left riparian	25/100	875/50	1,175/–	3,250/–	–	1,150/–
Navigable zone	25/50	–	–	50/38	50/–	–
SVINIŢA						
Left riparian	400/100	–	–	–	–	–/25
Navigable zone	75/125	–	–	400/–	–	100/25
PLAVIŞEVIŢA						
Intermediary zone	1,025/275	125/25	–	–	–	400/25
DUBOVA						
Gulf middle	100/100	25/75	–	–	–	150/50
Navigable zone	125/25	25/–	–	–	–	25/50
MRACONIA						
Navigable zone	–/1,750	–/75	–/25	50/1,775	–/7,150	–/25
IEŞELNIŢA						
Navigable zone	–/200	–/75	–	–	–	775/75

Table 3

(continued)

0	7	8	9	10	11	12
ORŞOVA VECHE						
Left riparian	500/–	–	–	–	–	600/225
Navigable zone	950/150	–	–	–	–	150/25
CERNA						
Gulf tail	225/150	–	–	–/150	–	525/1,025
Gulf middle	525/75	–	–	–	–	825/–
Navigable zone	50/50	–	–	–	–	2,350/250
BAHNA						
Intermediary zone	50/250	–	–	–	–	–

The spatial and seasonal variations of the density of different zoobenthos taxonomic groups could be observed in Table 3. It was especially remarked that the coelenterates, turbelariates and crustaceans almost disappeared starting from Greben downstream, in both analyzed seasons.

The spatial and seasonal variations of the total numerical density of the organisms in the benthos zoocoenoses of the **left riparian** along the damlake Iron Gates I were represented by the two curves in Fig. 1. Their lines are almost parallel from Baziaş until Orşova Veche, after that they become divergent towards the Cerna. The summer maximum value was at Svinița (34,400 ex/m^2), where the oligochaets were well developed on a muddy facies, at 4.6 m depth, and at a water flow which could decrease under 0.5 m/sec. The autumn maximum value, determined especially by the same pelophylic oligochaets, was situated at the Cerna gulf tail, at 4.20 m depth and at a very low water flow. The minimum values were registered both in summer and autumn at Greben (9,150 ex/m^2, respectively 1,050 ex/m^2). The total average of the left riparian zoobenthos organisms in the Iron Gates I ecosystem was of 20,745 ex/m^2 in summer, and of 22,595 ex/m^2 in autumn.

The higher autumn value included the high value of the Cerna gulf tail. All other figures were lower in the rest of the accumulation.

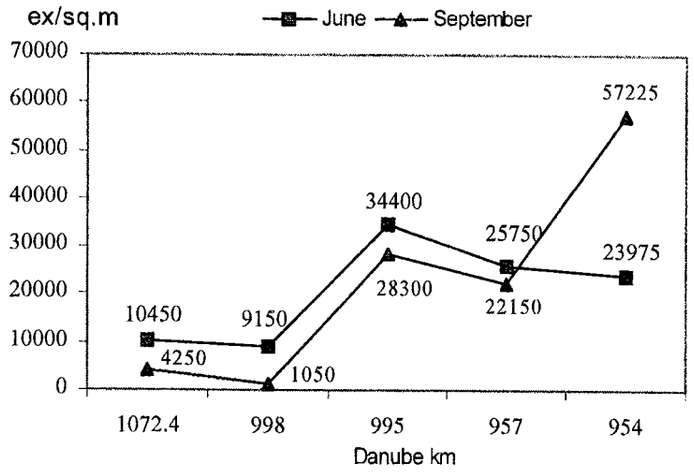

Fig. 1 – Spatial and seasonal variations of the total numerical density (ex/sq.m.) of the zoobenthos organisms in the riparian zone of the damlake Iron Gates I, in 2002.

In the intermediary zone between the riparian and the damlake navigable zone, the spatial and seasonal variation curves presented a maximum at Baziaş, in the intermediary zone, both in summer (1,363,975 ex/m^2) and autumn (50,025 ex/m^2) (Fig. 2). We must mention that in this station on a mosaic facies, at 9.5 m depth and with a low water flow (0.5–0.75 m/sec) the main taxonomic groups found (oligochaets, coelenterates, polychaets, gammarids, lamellibranchia, isopods, turbelariates, gastropods) had a maximum development in June, against all our 2002 data. We specify that the Danube with a large width at Baziaş has a stretching zone toward the Romanian riparian. The minimum values of the numerical density of the benthos organisms in the area between the riparian and the damlake navigable zone were found at Sirina, both in summer (450 ex/m^2) and in autumn (2,300 ex/m^2).

The total average of the benthos organisms in this zone of ecosystem was very high in summer (203,604 ex/m^2) and low in autumn (16,571 ex/m^2); the summer figure was determined by the values at Baziaş station.

The most complete data of the benthos organism density exist in the case of the **damlake navigable zone** on the transversal profiles along the damlake Iron Gates I, in 2002. The two curves of the **spatial and seasonal variations** had generally different courses (Fig. 3).

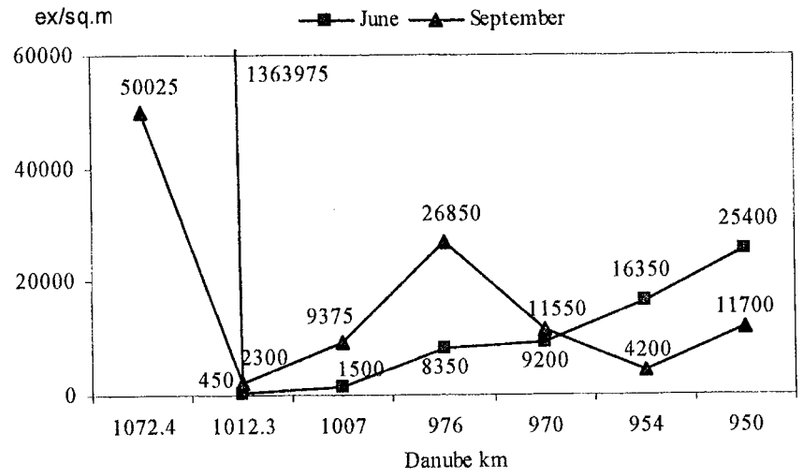

Fig. 2 – Spatial and seasonal variations of the total numerical density (ex/sq.m.) of the zoobenthos organisms in the intermediary zone between the riparian and navigable zone in the damlake Iron Gates I, in 2002.

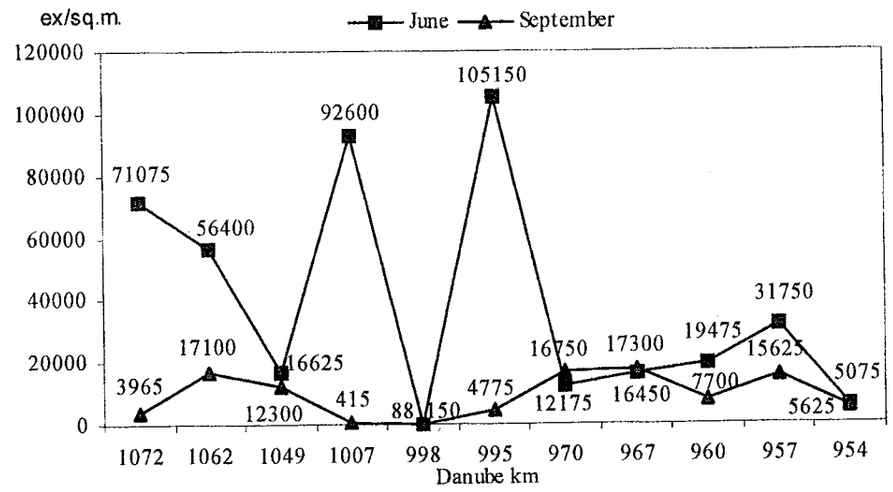

Fig. 3 – Spatial and seasonal variations of the total numerical density (ex/sq.m.) of the zoobenthos organisms in the navigable zone of the damlake Iron Gates I, in 2002.

The summer development maximum was at Svinița (105,150 ex/m^2). There, at water depths of 14 m, on muddy facies the pelophilic species of the main

taxonomic groups present along the entire damlake, namely the oligochaets and polychaets, were very well developed. Also, a second curve peak was situated at Elişeva (92,600 ex/m^2), where on a muddy facies too, at depths of 17 m, the same oligochaets and polychaets as at Svinița were dominant. In autumn the highest density of the benthos organisms was found at Mraconia (17,300 ex/m^2), very close to the Ostrov value (17,100 ex/m^2). In both stations, the corophiids dominated. We must mention that in autumn, at Mraconia, on the damlake navigable zone, the water depth was of 20 m, close to the maximum depth at which the samples (24 m – Orşova and Cerna stations) were collected. But, in the damlake Iron Gates I there exist also depths of 74 m at 974 km and of 50 at 970 km, where we were not able to collect samples. The minimum development values of the entire benthos zoocoenosis on the damlake navigable zone were at Greben, both in summer and autumn (150 ex/m^2, respectively 88 ex/m^2), in 2002.

The benthos organism number average along the entire damlake navigable zone was much higher in summer (38,861 ex/m^2) than that in autumn (9,401 ex/m^2).

The spatial and seasonal variations of the averages of the total benthos numerical density, calculated on the transversal profiles, along the damlake Iron Gates I, were represented by curves of same aspect (Fig. 4).

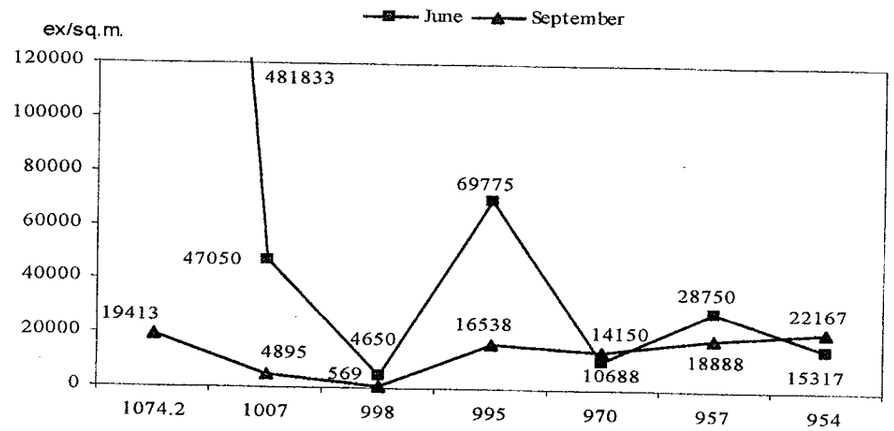

Fig. 4 – Spatial and seasonal variations of the total numerical density (ex/sq.m.) of the zoobenthos organisms, averages on transversal profiles in the damlake Iron Gates I, in 2002.

In summer, the curve presented two peaks: the first at Baziaş (481,833 ex/m^2), the second at Svinița (69,775 ex/m^2) profile. In autumn, the total

zoobenthos values on different transversal profiles were much closer. However, also in this case, the curve presented two peaks: the highest at Cerna (22,167 ex/m^2), followed by the second at Bazias (19,413 ex/m^2). Much lower were the minimum values situated both in summer and in autumn, at Greben (4,650 ex/m^2, respectively 569 ex/m^2).

The general damlake averages (calculated on the Table 3 data) were of 85,062 ex/m^2 in summer and only 14,351 ex/m^2 in autumn.

The zoobenthos values of most studied profiles were higher in summer than in autumn, as very clearly resulted both from Table 3 and Figures 1–4. This situation, characteristic for 2002, was the consequence of the strong flooding, much prolonged in summer, which, together with an increased water flow, washed and dragged the mobile substrata. We must underline that the muddy facies still dominated in the damlake Iron Gates I, even in the 2002 hydrological conditions.

The numerical density of the benthos organisms in the Romanian section of the damlake Iron Gates I, in 2002, related to that registered before the Danube damming, as well as to its values during the three decennia of accumulation existence, showed that in the actual ecosystem there exists an abundance especially of pelophilic elements well adapted to the new conditions (5, 8). But, this high numerical density of zoobenthos organisms shows the increase of the trophic level of the new ecosystem, and also the absence of suitable consumers to use this abundant feed.

4. CONCLUSIONS

1. The structural changes of the benthos zoocoenoses, both the sudden ones, generated by the accumulation construction in the Iron Gate zone, and the slower ones, produced in the course of time in the new ecosystem, led to the decrease of the taxon number, but to the increase of the number of individuals adapted to the new environment conditions.
2. It was concluded that in the damlake Iron Gates I, in 2002:
   - the numerical density of the zoobenthos organisms was high, the oligochaets and polychaets being on the first places. Also, from the numerical density point of view, large spatial and seasonal variations of the damlake benthos organisms were observed.
   - the taxonomic diversity in the ecosystem Iron Gates I was low against that registered before the river damming and it decreased from the upper stream towards the lower stream.
   - the presence of Ponto-Caspian element was found especially in the upper half of the damlake.

REFERENCES

1. Băcesco Mihai, *Quelques observations sur la faune benthonique du defilé roumain du Danube: son importance zoogéographique et pratique;la description d'une espèce nouvelle de mermithide, Pseudomermis cazanica n.sp.*, Ann.sci., Univ.Iassy, **31**: 240–253 (1948).
2. Virginia Popescu-Marinescu, *Componenţa şi structura biocenozelor din Dunăre, C. Biocenozele bentonice din zona litorală şi de adâncime, în Monografia zonei Porţile de Fier. Studiul hidrobiologic al Dunării şi al afluenţilor săi,* Ed. Acad. R.S.R., 85–110 (1970).
3. Cure Victoria, Popescu-Marinescu Virgina, Schneider Adrian, *Dinamica zoobentosului în lacul de acumulare Porţile de Fier în cel de al doilea an de la formare – 1972,* Travaux de la Station "Stejarul", Limnologie: 141–155, Pângăraţi (1975).
4. Popescu Ecaterina, Prunescu-Arion Elena, *Contribuţii la studiul faunei bentonice din Dunăre, în regiunea cataractelor (Km 1042 – 955)*, St. cerc. biol., Seria biol. anim., Ed. Academici RSR, **13;** *2*: 237–256 (1961).
5. Virginia Popescu-Marinescu, *Etappen der Zoobenthos Entwicklung in der Donau, im Gebiet des " Eiserens Tors", Abschnitt Mraconia*, Rev. roum. biol., Biol. anim., Ed. Academiei Române, **31**, *1*: 73–80, Bucharest (1986).
6. Virginia Popescu-Marinescu, *Les populations d'Hypania invalida (Grube) dans la Zone Porţile de Fier, avant et apres la creation du lac d'accumulation*, Rev. roum. biol., Biol. anim., Ed. Academiei Române, **37**, *2*; 134–140, Bucarest (1992).
7. Virginia Popescu-Marinescu, *Evolution of Zoobenthic Ponto-Caspien Elements Populations in the Danube, at the Iron Gates*, Internat. Assoc.Danube Res., Tulcea, Limnological Reports Volume 34, Proceedings of the 34th Conference , Tulcea, România, **34**: 347–355 (2002).
8. Virginia Popescu-Marinescu, Oaie G., *Angaben über die Abundanz und Biomasse der bentischen Wirbellosen in den Stauseen Eisernes Tors I und II*, 31 Konferenz der IAD, Limnologische Berichte Donau 1996, Wissenschaftliche Referate, I: 261–266, Baja/Ungarn (1996).
9. Popescu-Marinescu Virginia, Nastasescu Maria, Marinescu Carmen, Cutaş Florentina, Neagu Elena, *Amphipoda (Gammaridae and Corophiidae) existing in the Danube Romanian Sector before and after the construction of Porţile de Fier I Damlake*, Trav. Mus. nat. Hist. nat., "Grigore Antipa": XLIII, 347–366 (2001).

Received May 20, 2004.

National Institute of Research and Development for Biological Sciences Splaiul Independenţei, 296, Bucharest

RECHERCHES CONCERNANT LA DIVERSITÉ ET L'ÉQUITABILITÉ DES POPULATIONS DE SYMPHYLES *(SYMPHYLA)* DES FORÊTS DE FEUILLUS

RADU GAVA

The author characterizes the associations of symphyles from the oak, beech and alder forests with the help of the log-linear mathematical model proposed by Motomura. These have a diversity and an equitability that come sufficiently close to the log-linear mathematical model, so that they can be considered as nomocenoses, in the sense proposed by Daget, Lecordier and Leveque (4).

1. INTRODUCTION

Les symphyles représentent un groupe de myriapodes moins étudiés sous l'aspect écologique. Pour connaître la distribution qualitative et quantitative des peuplements de symphyles en fonction de facteurs physico-chimiques et biotiques agissant dans les milieux forestiers nous avons choisi trois forêts de feuillus situées dans la zone du bassin moyen de la rivière d'Argeş (Roumanie), une de chênes, une de hêtres et une autre d'aunes. La caractérisation de ces structures a été faite à l'aide du modèle log-linéaire proposé par Motomura (9).

2. MATÉRIEL ET MÉTHODE

Le matériel a été collecté dans une forêt de chêne, une de hêtre et une autre d'aune. Du point de vue climatique, la zone recherchée se situe dans le climat continental. La température moyenne annuelle est de 9,5°C. La moyenne annuelle de la quantité de précipitations est de 685 mm (1).

La forêt de chênes est située sur une terrasse de la rivière d'Argeş, à l'altitude de 370 m. La végétation de bois est dominée par *Quercus petrea.* La couche d'arbrisseaux formée d'églantiers est fragmentée par endroits. La couche herbeuse, dominée par *Carex pilosa*, est presque continue. Le sol est un luvisol litier planique pseudogleisé avec un faible contenu d'humus (1,50–1,80%) et réaction fortement acide (pH = 4,58). Le régime aéro-hydrique est défectueux. Dans les périodes de sécheresse, le sol est compact et dur et dans les périodes humides il gonfle. La litière forme une couche relativement continue.

La deuxième forêt recherchée a été une forêt d'aune de la plaine de la rivière d'Argeş. L'espèce dominante, est représentée par *Alnus glutinosa.* La couche d'arbrisseaux, formée de sureaux et épines, est bien représentée. Le tapis d'herbe est fragmenté. Le sol est un sol gleic typique. La réaction est modérément acide (pH = 4,58) et le contenu en humus (Ct) réduit (1,50–1,80%).

REV. ROUM. BIOL. – BIOL. ANIM., TOME 49, Nos 1–2, P. 73–78, BUCAREST, 2004

L'eau phréatique monte jusqu'à la surface dans les périodes d'excès d'humidité et crée des conditions d'anaérobiose, défavorables à la vie. La couche de litière est mince et fragmentée.

La troisième forêt recherchée est une hêtraie. Elle est située dans la vallée de la Rivière Doamnei, principal affluent de l'Argeş. L'espèce dominante, *Fagus silvatica,* est accompagnée d'exemplaires sporadiques de *Quercus petrea.* L'horizon d'arbrisseaux est formé de rejetons de hêtre. La couche herbeuse, dominée par *Carex pilosa,* est peu développée. Le sol est un erodisol typique. La réaction est modérément acide (pH = 5,6) et la quantité de substance organique (Ct) varie entre 1,50–1,80%. Le régime aérohydrique est bon. La couche de litière est inégale à cause du microrelief accidenté qui favorise l'agglomération de feuillage dans les portions concaves et, parfois, même sa disparition dans les portions convexes.

Dans chaque forêt nous avons établi un stationnaire de travail avec la surface de 10.000 m^2 (100 × 100 m) d'où on a prélevé mensuellement, depuis février jusqu'en novembre y compris, durant trois ans 12 échantillons de litière et de sol, au total 360 échantillons. Les échantillons ont été prélevés de manière randomisée. Chaque échantillon a été rapporté à une surface de 20 cm^2 (1/500 m^2) et il a compris la litière et le sol jusqu'à la profondeur de 10 cm. La litière avec l'humus de litière ont été triés à l'appareil Tulgren et le sol a été trié à l'aide d'un binoculaire. Le matériel a été conservé en alcool éthylique de 70^0. Dans l'ensemble des trois stations, on a identifié 9 espèces de symphyles (7 espèces en chênaie, 9 en hêtraie et 3 en aunaie).

3. RÉSULTATS ET DISCUSSIONS

Le groupement d'espèces, appartenant à une certaine unité taxonomique, d'un biotope approximativement homogène et suffisamment équilibré, forme une nomocénose (4). La nomocénose se caractérise par un mode propre de répartition quantitative des individus aux espèces. Ce groupement est le résultat d'un processus de sélection écologique des espèces du fonds général existant dans la région (Nicolaev, 1977 cité d'après Stugren 1982). La distribution quantitative des individus par espèces dans le cadre de ce groupement est le résultat de l'interaction des facteurs physico-chimiques et biotiques agissant dans le biotope respectif. La caractérisation de ces structures se fait à partir de la connaissance de la distribution en abondance des espèces et la représentation de celle-ci par un modèle mathématique approprié.

Parmi les différents modèles possibles à prendre en considération, nous avons utilisé pour la caractérisation des nomocénoses de symphyles des trois stations recherchées, le modèle mathématique log-linéaire, proposé par Motomura. Celui-ci peut s'appliquer à des groupements d'êtres qui peuplent un milieu approximativement uniforme et peuvent être comparés par leur taille et par leur mode de vie. Il a été déjà utilisé dans l'étude des peuplements benthiques marins et

d'eau douce (9), des peuplements de mollusques terrestres (Motomura, 1935, cité d'après Daget, Lecordier, Leveque, 1972), oribatides (2), melolonthides dans la savane (7), des peuplements de chilopodes et diplopodes de la litière (5, 6). C'est pour la première fois que ce modèle est employé dans l'étude des peuplements de symphyles.

En représentant sur un graphique les logarithmes des effectifs de symphyles en fonction du rang d'espèce $\log q_i = f(i)$, on peut remarquer que les points obtenus s'alignent plus ou moins sur une droite (Fig. 1), fait qui nous permet d'apprécier que ces peuplements ont une distribution de l'abondance numérique qui peut s'ajuster à un modèle log-linéaire proposé par Motomura.

Les peuplements dont la distribution en abondance s'approche suffisamment du modèle Motomura peuvent être considérés comme nomocénoses. Les nomocénoses log-linéaires se caractérisent par une certaine richesse spécifique (diversité) et par la manière dont est distribuée l'abondance relative des espèces (équitabilité) (3).

Les nomocénoses, dans le sens proposé par Motomura, se caractérisent aussi par la constante **m** appelée aussi constante de milieu, qui représente l'antilogarithme de la pente de la droite de régression et qui a toujours des valeurs sous-unitaires. Lorsque la diversité est faible, la pente de la droite est plus forte et la valeur de **m** s'approche de zéro.

Les peuplements de symphyles de la chênaie ont au total 663 individus répartis par 7 espèces (Tableau 1). L'indice de diversité spécifique (l'indice Shannon) est de 1,710 bits à la diversité maximale de 2,321 bits, l'équitabilité égale à 0,737. Le coefficient de corrélation **r'** entre les logarithmes des effectifs théoriques ajustés **(log q'i)** et le rang d'espèce **(i)** est de – 0,958. Pour un tel coefficient, l'ajustement du modèle log-linéaire de Motomura peut être considéré comme approximatif, selon les critères de Inagaki (1967). L'équation de la droite de régression **log q'i** en **i** (droite d'ajustement) est:

$$\log q'i = 2{,}97847 - 0{,}38605\, i \quad \text{(Fig. 1).}$$

Dans l'aunaie, les peuplements de symphyles ont un effectif total de 267 individus appartenant à 3 espèces (Tableau 2). L'indice de diversité Shannon est de 0,584 bits à une diversité maximale de 1,00 bits et équitabilité 0,584. Le coefficient de corrélation **(r')** entre **(log q'i)** et **(i)** est de – 0,985. Pour cette valeur de **(r')** l'ajustement du modèle log-linéaire peut être considéré comme bon (8). La droite de régression est valable pour l'équation:

$$\log q'i = 3{,}58084 - 1{,}18274\, i \text{ (Fig. 1).}$$

L'échantillon total des peuplements de symphyles de la hêtraie est formé de 703 individus et 9 espèces (Tableau 3). L'indice de diversité spécifique Shannon est de 2,419 bits à la diversité maximale de 3,00 bits et l'équitabilité de 0,806. Le coefficient de corrélation **(r')** entre les effectifs théoriques ajustés et le rang

d'espèce est de – 0,9208. Celui-ci est considéré comme insatisfaisant pour l'ajustement de la distribution au modèle log-linéaire de Motomura. L'équation de la droite de régression est:

log q'i = 2,71676 – 0,28944 i (Fig. 1).

Tableau 1

Les caractéristiques de la nomocénose de symphyles de la forêt de chênes

Espèce	Rangs (i)	Effectifs réels (qi)	Effectifs théoriques ajustés (q'i)
Symphylella vulgaris	1	337	391,2
Symphylellopsis subnuda	2	164	160,8
Scolopendrella notacantha	3	137	66,1
Symphylellopsis balcanica	4	10	27,2
Geophylella pyrenaica	5	9	11,2
Hanseniella nivea	6	3	4,6
Scutigerella remy	7	3	1,9
TOTAL		**663**	**663,0**

r'= – 0,958
Log q'i = 2,97843 – 0,38605 i
m = 0,411

Tableau 2

Les caractéristiques de la nomocénose de symphyles de la forêt d'aunes

Espèce	Rangs (i)	Effectifs réels (qi)	Effectifs théoriques ajustés (q'i)
Symphylella vulgaris	1	232	250,1
Symphylellopsis subnuda	2	34	15,8
Symphylellopsis balcanica	3	1	1,1
TOTAL		**267**	**267,0**

r'= – 0,985
Log q'i = 3,58084 – 1,18274 i
m = 0,065

Tableau 3

Les caractéristiques de la nomocénose de symphyles de la forêt de hêtres

Espèce	Rangs (i)	Effectifs réels (qi)	Effectifs théoriques ajustés (q'i)
Symphylellopsis subnuda	1	292	300,1
Symphylella vulgaris	2	146	172,9
Hanseniella nivea	3	81	99,6
Scolopendrella notacantha	4	78	57,4
Scutigerella remy	5	37	33,0
Geophylella pyrenaica	6	29	19,1

Tableau 3

(continued)

Scutigerella carpatica	7	25	11,0
Symphylellopsis balcanica	8	14	6,3
Symphylella isabellae	9	1	3,6
TOTAL		**703**	**703,0**

r'= – 0,920
Log q'i = 2,71676 – 0,23944 i
m = 0,576

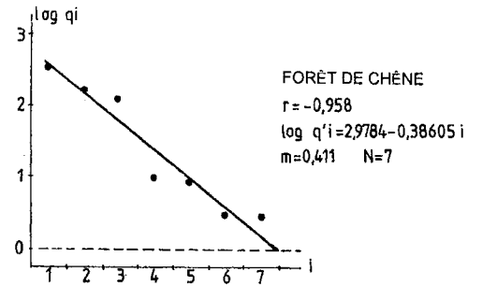

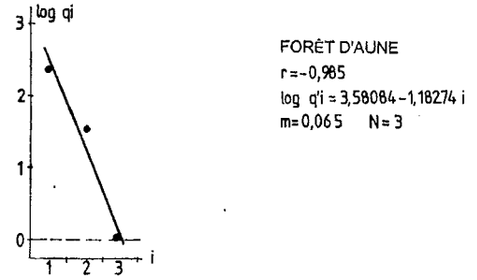

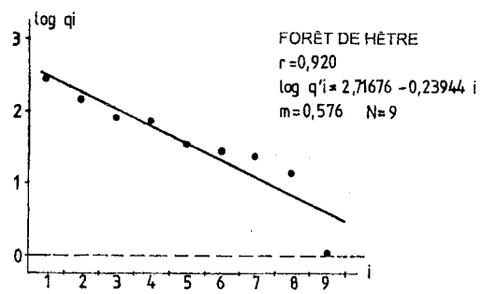

Fig. 1 – Les droites d'ajustement aux distributions réelles des nomocénoses log-linéaires de symphyles de la litière et du sol des chênaies, aunaies et hêtraies recherchées dans le département d'Argeş.

4. CONCLUSIONS

En conclusion, à partir de l'analyse des indices de diversité spécifique, on peut admettre que les peuplements de symphyles des trois stations recherchées sont organisés en structures spécifiques uniques, caractérisées par une certaine combinaison d'espèces (diversité), avec une certaine distribution quantitative des individus (équitabilité), qui peuvent être considérées comme nomocénoses dans le sens du terme proposé par Daget, Lecordier et Leveque, mais sur la base du critère propose par Inagaki, seulement celles de l'aunaie peuvent être assimilées au modèle mathématique log-linéaires proposé par Motomura.

BIBLIOGRAPHIE

1. Barco, Aurelia, Nedelcu E., 1974. *Judeţul Argeş*. Ed. Academiei, Bucureşti.
2. Cancela, da Fonseca, J. P., 1969. *L'outil statistique en biologie du sol. V. Indices de diversité spécifique*. Rev. Ecol. Biol. Sol, **6, 1,** 1–30
3. Daget, J., 1976. *Les modèles mathématiques en écologie*, Masson, Paris, Coll. Ecologie, **8,** 170.
4. Daget, J., Lecordier, C., Leveque, C., 1972. *Notion de nomocénose: ses applications en écologie*, Bull. Soc. Ecol., **3**, 448–462.
5. Gava, R. 1991. *Étude écologique comparative des Myriapodes de quelques types de forêts de feuillus du bassin moyen de la rivière d'Argeş*. Thèse de doctorat, Université de Cluj-Napoca.
6. Geoffroy, J.-J., 1979. *Les peuplements de Chillopodes et de Diplopodes d'une chênaie-charmaie (Station biologique de Foljuif Seine-Marne),* Thèse de doctorat, Université P. et M. Curie, Paris, **6.**
7. Girard, C., Lecordier, C., 1978. *Quelques nomocénoses de Sericines (Col. Melolonthidae) dans la savane de Lamoto (basse Côte d'Ivoire*), Ann. Soc. Ent. France (N.S.), **14, 1,** 73–86
8. Inagaki, H., 1967. *Mise au point de la loi de Motomura et essai d'une écologie évolutive*, Vie et Milieu, **18, 1,** (B), 153–156.
9. Motomura , I., 1932. *Etude statistique de la population écologique*, Doobutugaku Zassi, **44,** 387–393
10. Stugren, B., 1982. *Bazele ecologiei generale*, Ed. Ştinţifică şi Enciclopedică, Bucureşti.

Reçu le 7 octobre 2004.

Université de Piteşti
Faculté de Sciences,
Rue Târgu din Vale nr. 1
PITEŞTI Roumanie
e-mail: gavaradu@yahoo.com

STRUCTURE AND DYNAMICS OF THE GAMASINA MITES (ACARI: MESOSTIGMATA) FROM A FOREST WITH *PICEA ABIES* FROM THE BUCEGI MASSIF

MINODORA STĂNESCU*, J. DARIUSZ GWIAZDOWICZ**

This paper presents the structure and dynamics of the Mesostigmata mites from an ecosystem with *Picea abies*. Species composition of edaphic mites from Mesostigmata showed the presence of the two suborders: Gamasina with 10 families (Parasitidae, Veigaiaidae, Laelapidae, Rhodacaridae, Ascidae, Ameroseiidae, Macrochelidae, Pachylaelaptidae, Eviphididae, Zerconidae) with 42 species and Uropodina with 2 families (Trachytidae, Uropodidae), with 6 species. In temporal dynamics in summer there were identified 27 species of Mesostigmata mites, in autumn 39 species and in winter 31 species. The highest numerical densities of mites were observed in autumn at *Veigaia nemorensis* (1871 ind./sq.m.; CV = 97) and the lowest densities of mites were observed in summer and autumn at *Lysigamasus neoruncatellus* (7 ind./sq.m.; CV = 374) and in winter at *Vulgarogamasus zschokkei* (7 ind./sq.m.; CV = 374). In spatial dynamics the litter and fermentation layer there were identified 36 species of Mesostigmata mites and in humus layer 25 species were recorded. The differences between abiotic factors in all these seasons (pH, humidity and the soil temperature) have determined a higher number of species and numerical densities of all Acari in the litter and fermentation layer than in the humus layer.

Key words: mites, Gamasida, litter, Bucegi Massif.

INTRODUCTION

Mites (Arachnida, Acari) are microarthropods that live in various ecological habitats: plants, animals, on soil and in its levels. In general, species from the Mesostigmata order are detritivorous, predators and endo or ecto parasites.

Species, which live free in soil, depend on its structure and on its composition in detritus, humus. Water from soil is also an important factor for the presence of these mites. Detritivorous species feed with organic matter, predators feed with springtails, earthworms and larvae of small insects (3).

The number of species from Mesostigmata is very increased in the litter and then decreases up to 20 cm depths. Most of these acarine are secondary and tertiary consumers in terrestrial ecosystems. This fauna is influenced by abiotic factors like: temperature, humidity of the soil, precipitation, the content of organic matter. The preference of the mesostigmatid mites for some types of soil allowed us the possibility of separation in groups of species biological indicators. These species regulate the other populations of microarthropods in the soil.

REV. ROUM. BIOL. – BIOL. ANIM., TOME 49, N° 1–2, P. 79–88, BUCAREST, 2004

MATERIALS AND METHODS

The researches were made in 2003, in forests with *Picea abies* from the Bucegi Massif.

Bucegi Massif has two parts in the north-south direction. To the east there is a big wall of stone named "Abruptul Prahovean" and it has a charcoal structure. The highest peak from Bucegi massif is "Omu" by 2507 m altitude.

This massif has many affluents of the Prahova river like: Urlătoarea, Peleşul, Izvorul Dorului, etc. This zone is representative for the forestry ecosystems with *Picea abies*, with *Fagus sylvatica* and the mixture between them.

The ecosystem with *Picea abies* is situated on a slope of 20°, on the east side of the mountain, at 1350 m altitude. The herbaceous layer and the shrub layer are missing. The litter layer is continuous and thin (1–2 cm) and humus is moder-mull.

The relative humidities, the acidity and the temperature of the soil were measured (Tables 1, 2, 3).

Table 1

The relative humidities in soil layers from the studied area

Ecosystem	Layer	Summer	Autumn	Winter
Picea abies	OLF	25.02	31.18	33.70
	OH	64.86	42.71	72.76

Table 2

The acidity in soil layers from the studied area

Ecosystem	Layer	Summer	Autumn	Winter
Picea abies	OLF	4.6	4.5	4.2
	OH	4.9	4.5	4.9

Table 3

The temperature in soil layers from the studied area

Ecosystem	Layer	Summer	Autumn	Winter
Picea abies	OLF	9° C	3° C	–3° C
	OH	9° C	4° C	–5.5° C

Fauna of mites from this area was sampled (14 samples) with MacFadyen soil core. Each sample was divided in OLF-litter and fermentation layer and OH-humus layer (variable weight).

The identification of the mites from the Mesostigmata order was made up to the species level (1, 2, 4, 5, 7, 8, 9, 10, 11)

The extraction was performed with a modified Berlese-Tullgren extractor. After taxonomical identification, numerical abundance was obtained that constituted a database for the statistical analysis: average-x, numerical density-x/m^{-2}, variance-S2, average error-S, and coefficient of variance-CV, relative abundance-Ar, constancy-C (6).

RESULTS AND DISCUSSION

Species composition of edaphic mites from Mesostigmata showed the presence of the two suborders: Gamasina with 10 families (Parasitidae, Veigaiaidae, Laelapidae, Rhodacaridae, Ascidae, Ameroseiidae, Macrochelidae, Pachylaelaptidae, Eviphididae, Zerconidae) with 42 species and Uropodina with 2 families (Trachytidae, Uropodidae), with 6 species.

Table 4

Structural parameters of the Gamasina mites from the *Picea abies* forest in summer, 2003

Species	OLF						OH					
	x	*x*/ sq.m.	S2	S	S'	CV	*x*	*x*/ sq.m.	S2	S	S'	CV
Pergamasus laetus	0.4	36	0.4	0.6	0.05	177	0.2	21	0.2	0.4	0.03	199
Pergamasus athiasae	0.2	21	0.2	0.4	0.03	199	0.4	36	1.8	1.3	0.1	374
Pergamasus sp.	0.1	14	0.3	0.5	0.04	374	0.3	29	1.1	1.1	0.08	374
Leptogamasus parvulus	0.5	50	0.9	0.9	0.07	188	2.1	207	8.1	2.8	0.2	137
Leptogamasus tectegynellus	0.6	57	1.2	1.1	0.08	191	1.9	193	8.2	2.9	0.2	149
Lysigamasus neoruncatellus	0.1	7	0.1	0.3	0.02	374	0.1	7	0.1	0.3	0.02	374
Lysigamasus lapponicus	0.2	21	0.6	0.8	0.06	374	0.1	7	0.1	0.3	0.02	374
Vulgarogamasus kraepelini	0.3	29	0.5	0.7	0.05	254	0.1	14	0.1	0.4	0.03	254
Vulgarogamasus oudemansi							0.1	7	0.1	0.3	0.02	374
Eugamasus magnus	0.1	7	0.1	0.3	0.02	374						
Veigaia nemorensis	2.6	264	29	5.3	0.38	202	3.6	357	22	4.7	0.33	130
Veigaia exigua	0.1	7	0.1	0.3	0.02	374	0.1	7	0.1	0.3	0.02	374
Veigaia propinqua	0.1	7	0.1	0.3	0.02	374	0.1	14	0.3	0.5	0.04	374
Veigaia cervus	0.1	7	0.1	0.3	0.02	374						
Leioseius magnanalis							0.1	14	0.3	0.5	0.04	374
Arctoseius semiscissus	0.4	43	0.9	0.9	0.07	219	0.2	21	0.2	0.4	0.03	199
Arctoseius cetratus	0.1	7	0.1	0.3	0.02	374	0.2	21	0.3	0.6	0.04	270
Melichares pomorum	0.1	14	0.1	0.4	0.03	254						
Macrocheles montanus							0.1	7	0.1	0.3	0.02	374
Geholaspis longispinosus							0.1	7	0.1	0.3	0.02	374
Neopodocinum mrciaki	4.9	493	43	6.5	0.47	132	0.6	57	0.7	0.9	0.06	149
Pachyseius humeralis	0.6	57	1	1	0.07	178	1.2	121	2.5	1.6	0.11	130
Hypoaspis aculeifer	0.1	14	0.3	0.5	0.04	374	1.4	136	2.7	1.6	0.12	121
Hypoaspis praesternalis							0.1	7	0.1	0.3	0.02	374
Eviphis ostrinus	0.6	57	2.1	1.5	0.1	254	0.1	14	0.1	0.4	0.03	254
Zercon triangularis	3.3	329	28	5.3	0.38	162	0.8	79	1.4	1.2	0.08	151
Zercon fageticola	1.4	136	26	5.1	0.36	374	2	200	56	7.5	0.53	374
Trachytes aegrota	0.2	21	0.6	0.8	0.06	374	0.4	43	1.8	1.3	0.1	313

Taking account of spatial distribution, the maximum of numerical density at Mesostigmata order was recorded by *Neopodocinum mrciaki* (493 ind./sq.m.; CV = 132), *Zercon triangularis* (329 ind./sq.m.; CV = 162), in the litter and fermentation layer, in summer and the minimum by *Arctoseius cetratus, Veigaia exigua, Veigaia propinqua, Veigaia cervus* (each with 7 ind./sq.m.; CV = 374) (Table 4).

In the humus layer, the highest value of numerical density was recorded at *Veigaia nemorensis* (357 ind./sq.m.; CV = 130) and the lowest at the *Vulgarogamasus oudemansi, Hypospis praesternalis, Veigaia exigua (* each with 7 ind./sq.m.; CV = 374).

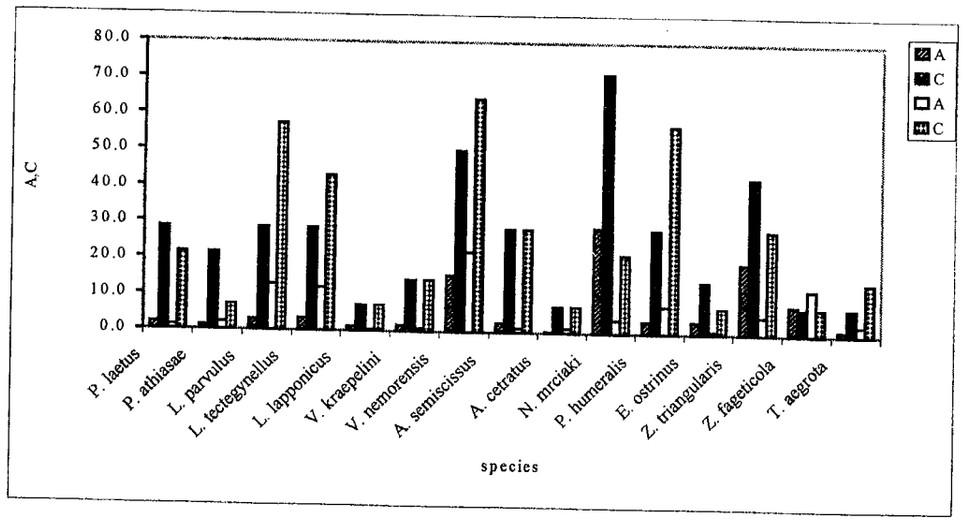

Fig. 1 – Relative abundance (A) and constancy (C) of Mesostigmata at OLF and OH layer, in summer, in *Picea abies* forest.

Neopodocinum mrciaki is the most abundant species in OLF (A= 29%; C=71), in comparison with *Eviphis ostrinus*, which has the lowest representation in OH (A = 0.9%; C = 7.1).

Table 5

Structural parameters of the Gamasina mites from the *Picea abies* forest in autumn, 2003

Species	OLF						OH					
	x	*x*/ sq.m.	S2	S	S'	CV	*x*	*x*/ sq.m.	S2	S	S'	CV
Pergamasus athiasae	2.2	221	3.7	1.9	0.14	87	0.1	7	0.1	0.3	0.02	374
Leptogamasus parvulus	12	1157	127	11	0.81	98	0.6	64	1.3	1.2	0.08	179

Table 5

(continued)

Species	OLF						OH					
	x	*x*/ sq.m.	S2	S	S'	CV	*x*	*x*/ sq.m.	S2	S	S'	CV
Lysigamasus neoruncatellus	0.1	7	0.1	0.3	0.02	374	0.1	7	0.1	0.3	0.02	374
Lysigamasus lapponicus	0.6	57	0.6	0.8	0.05	132	0.4	36	0.9	0.9	0.07	260
Lysigamasus truncus	0.4	36	1.8	1.3	0.1	374						
Lysigamasus conus	0.1	7	0.1	0.3	0.02	374						
Vulgarogamasus kraepelini	0.6	64	1.6	1.3	0.09	199	0.1	7	0.1	0.3	0.02	374
Vulgarogamasus oudemansi							0.1	7	0.1	0.3	0.02	374
Vulgarogamasus zschokkei	0.9	93	1.5	1.2	0.09	130						
Eugamasus sp.	0.1	7	0.1	0.3	0.02	374						
Eugamasus magnus	0.3	29	0.7	0.8	0.06	289						
Gamasodes spiniger							0.1	7	0.1	0.3	0.02	374
Holoparasitus excisus	0.1	7	0.1	0.3	0.02	374						
Veigaia nemorensis	19	1871	329	18	1.3	97	2.5	250	7.2	2.7	0.19	107
Veigaia exigua	0.3	29	0.4	0.6	0.04	214	0.1	7	0.1	0.3	0.02	374
Veigaia propinqua	0.4	43	1.8	1.3	0.1	313						
Leioseius magnanalis							0.1	14	0.1	0.4	0.03	254
Lasioseius sp.	0.1	7	0.1	0.3	0.02	374						
Arctoseius semiscissus	0.1	14	0.3	0.5	0.04	374						
Arctoseius cetratus	0.2	21	0.6	0.8	0.06	374						
Arcoseius sp.	0.1	14	0.3	0.5	0.04	374						
Melichares juradeus	0.1	7	0.1	0.3	0.02	374						
Macrocheles sp.	0.1	7	0.1	0.3	0.02	374						
Macrocheles montanus	0.1	7	0.1	0.3	0.02	374						
Geholaspis longispinosus	0.1	7	0.1	0.3	0.02	374						
Neopodocinum mrciaki	2.3	229	10	3.2	0.23	141	0.2	21	0.2	0.4	0.03	199
Pachyseius humeralis	7	700	25	5	0.36	71	1.5	150	1.7	1.3	0.09	86
Pachylaelaps furcifer	0.1	7	0.1	0.3	0.02	374						
Hypoaspis aculeifer	0.8	79	1.4	1.2	0.08	151	0.3	29	0.4	0.6	0.04	214
Hypoaspis oblonga	5.7	571	422	21	1.47	359	0.1	7	0.1	0.3	0.02	374
Haemolaelaps cubicularis	0.2	21	0.6	0.8	0.06	374						
Eviphis ostrinus	0.7	71	3.5	1.9	0.13	260						
Zercon triangularis	8.3	829	84	9.2	0.65	111	0.7	71	1	1	0.07	139
Zercon fageticola	4	400	65	8.1	0.58	202						
Zercon carpathicus	0.2	21	0.3	0.6	0.04	270	0.1	7	0.1	0.3	0.02	374
Prozercon kochi	0.3	29	0.7	0.8	0.06	289	0.1	7	0.1	0.3	0.02	374
Prozercon traegardhi							0.4	36	1.8	1.3	0.1	374
Trachytes pauperior							0.1	7	0.1	0.3	0.02	374
Trachytes aegrota	0.3	29	1.1	1.1	0.08	374						
Urodiaspis tecta	0.2	21	0.6	0.8	0.06	374						
Urobovella obovata							0.1	7	0.1	0.3	0.02	374

Because of the optimal environmental conditions in litter and fermentation layer, in autumn, the following predatory species are numerically dominant: *Leptogamasus parvulus* (1157 ind./sq.m.; CV = 98), *Veigaia nemorensis* (1871 ind./sq.m.; CV = 97), and *Pachylaelaps furcifer, Macrocheles montanus, Holoparasitus excisus* (each with 7 ind./sq.m.; CV = 374) are in the opposite situation (Table 5).

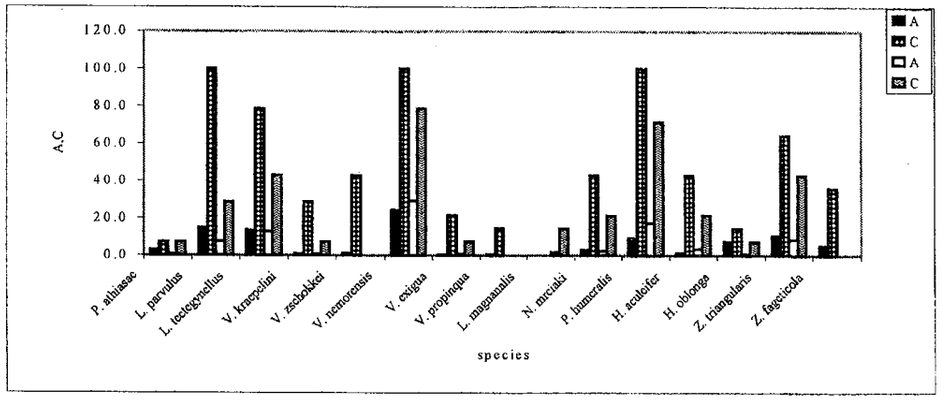

Fig. 2 – Relative abundance (A) and constancy (C) of Mesostigmata mites at OLF and OH layer, in autumn, in *Picea abies* forest.

In spatial distribution, *Veigaia nemorensis* recorded in the humus layer, the highest numerical density (250 ind./sq.m.; CV = 107), in autumn. The lowest values of these parameters had *Zercon carpathicus, Prozercon kochi, Hypoaspis oblonga* (each with 7 ind./sq.m.; CV = 374) in the same layer.

The maximum values of the relative abundance and of the constancy indices were recorded by *Veigaia nemorensis* (A = 24%; C = 100) in OLF, and the minimum by *Veigaia exigua* (A = 0.4%; C = 21.4) in OH.

From the Mesostigmata order the most representative species is *Veigaia nemorensis* (243 ind./sq.m.; CV = 178), in the litter and fermentation layer, in winter and the lowest are: *Vulgarogamasus zschokkei, Parasitus furcatus, Leioseius magnanalis, Hypospis oblonga, Zercon tatrensis, Urodiaspis tecta* (each with 7 ind./sq.m.; CV = 374) (Table 6).

Table 6

Structural parameters of the Gamasina mites from the *Picea abies* forest in winter, 2003

Species	OLF						OH					
	x	x/ sq.m.	S2	S	S'	CV	x	x/ sq.m.	S2	S	S'	CV
Pergamasus athiasae	0.4	43	0.7	0.9	0.06	199	0.1	7	0.1	0.3	0.02	374
Leptogamasus parvulus	0.9	86	4.6	2.1	0.15	250	0.4	36	0.4	0.6	0.05	177
Leptogamasus tectegynellus	1	100	8.6	2.9	0.21	294	0.1	14	0.1	0.4	0.03	254
Lysigamasus lapponicus	1.1	107	7.8	2.8	0.2	260	0.9	86	3.4	1.8	0.13	214
Vulgarogamasus kraepelini							0.1	7	0.1	0.3	0.02	374
Vulgarogamasus zschokkei	0.1	7	0.1	0.3	0.02	374	0.1	7	0.1	0.3	0.02	374
Vulgarogamasus cornutosimilis							0.1	7	0.1	0.3	0.02	374
Parasitus furcatus	0.1	7	0.1	0.3	0.02	374						
Veigaia nemorensis	2.4	243	19	4.3	0.31	178	1.3	129	2.2	1.5	0.11	116
Veigaia exigua	0.1	14	0.1	0.4	0.03	254	0.1	7	0.1	0.3	0.02	374
Leioseius magnanalis	0.1	7	0.1	0.3	0.02	374						
Arctoseius brevicheles	0.1	14	0.3	0.5	0.04	374						
Melichares pomorum	0.1	7	0.1	0.3	0.02	374						
Dendrolaelaps sp.	0.1	14	0.3	0.5	0.04	374						
Neopodocinum mrciaki	1.4	136	8.7	3	0.21	217	0.1	14	0.1	0.4	0.03	254
Pachyseius humeralis							0.8	79	1.7	1.3	0.09	167
Pachylaelaps furcifer							0.1	7	0.1	0.3	0.02	374
Hypoaspis aculeifer							0.4	36	0.6	0.7	0.05	209
Hypoaspis oblonga	0.1	7	0.1	0.3	0.02	374	0.3	29	1.1	1.1	0.08	374
Zercon triangularis	1.1	114	8.4	2.9	0.21	254	0.1	14	0.1	0.4	0.03	254
Zercon tatrensis	0.1	7	0.1	0.3	0.02	374						
Zercon romagniolus							0.1	7	0.1	0.3	0.02	374
Zercon fageticola	0.1	14	0.1	0.4	0.03	254						
Zercon similis	0.1	7	0.1	0.3	0.02	374						
Prozercon kochi	1.3	129	8.8	3	0.21	231	0.7	71	4.7	2.2	0.15	303
Prozercon traegardhi	0.2	21	0.3	0.6	0.04	270	0.4	36	1.8	1.3	0.1	374
Prozercon satapliae	0.1	7	0.1	0.3	0.02	374						
Prozercon sellnicki							0.1	14	0.3	0.5	0.04	374
Trachytes pauperior	0.1	14	0.1	0.4	0.03	254	0.9	86	4.9	2.2	0.16	258
Trachytes aegrota	1.2	121	8.5	2.9	0.21	240	0.5	50	0.9	0.9	0.07	188
Urodiaspis tecta	0.1	7	0.1	0.3	0.02	374						

In the humus layer, in winter, the maximum of numerical density was recorded at *Veigaia nemorensis* (129 ind./sq.m.; CV = 116) and the minimum at the

Vulgarogamasus zschokkei, Vulgarogamasus cornutosimilis, Veigaia exigua, Zercon romagniolus, (each with 7 ind./sq.m.; CV = 374).

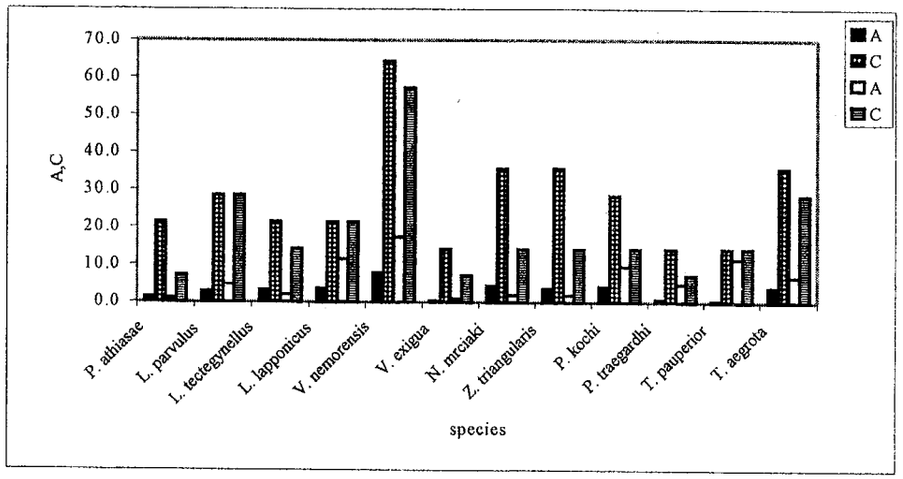

Fig. 3 – Relative abundance (A) and constancy (C) of Mesostigmata mites at OLF and OH layer, in winter, in *Picea abies* forest.

In this ecosystem *Veigaia nemorensis* recorded increased values of the relative abundance and of the constancy indices, (A= 8%; C=64.3) in OLF, and one species from Uropoda suborder – *Trachytes pauperior,* had decreased values of these parameters(A = 0.5%; C = 14.3) in OH.

CONCLUSIONS

The biological and edaphic conditions (temperature, acidity and humidity) of the soil have determined the taxonomic structure of Gamasina community.

In this ecosystem 48 species of Mesostigmata mites were identified: 42 species of Gamasina suborder and 6 of Uropodina suborder.

In temporal dynamics, 27 species of Mesostigmata mites were identified in summer, 39 species in autumn and 31 species in winter.

The highest numerical densities of mites were observed in autumn at *Veigaia nemorensis* (1871 ind./sq.m.; CV = 97) and the lowest densities of mites were observed in summer and autumn at *Lysigamasus neoruncatellus* (7 ind./sq.m.; CV=374), in winter at *Vulgarogamasus zschokkei* (7 ind./sq.m.; CV = 374).

In spatial dynamics the litter and fermentation layer 36 species of Mesostigmata mites were identified and in the humus layer 25 species were recorded.

Taking account of spatial dynamics, the most increased values of numerical densities of mites were observed in the litter and fermentation layer: *Veigaia nemorensis* (1871 ind./sq.m.; CV = 97), *Neopodocinum mrciaki* (493 ind./sq.m.; CV = 132) and the most decreased densities of mites were observed in both layers at the following species: *Lysigamasus neoruncatellus, Lysigamasus lapponicus, Eugamasus sp., Holoparasitus excisus, Vulgarogamasus kraepelini, Vulgarogamasus oudemansi, Pergamasus athiasae, Veigaia exigua, Veigaia propinqua, Veigaia cervus, Macrocheles montanus, Geholaspis longispinosus, Leioseius magnanalis, Melichares juradeus, Hypospis oblonga, Pachylaelaps furcifer, Zercon romagniolus* (each species with 7 ind./sq.m.; CV = 374).

The differences between abiotic factors in all these seasons (pH, humidity and the soil temperature) have determined a higher number of species and numerical densities of all Acari in the litter and fermentation layer than in the humus layer.

REFERENCES

1. Athias Henriot C., 1968, Observation sur le Pergamasus IV. Un essai de coordination de taxonomie et de la chorologie du sous-genre Pergamasus (Acariens Anactiniotriches, Parasitidae). *Acarologia*, **10** (2): 181–190.
2. Blaszak Czeslaw, 1974, Zerconidae (Acari, Mesostigmata), Polski. Monografic Fauny Polski, **3**, pp. 1–315.
3. Evans O.G., 1992, *Principles of acarology*. CAB International Wallingford Oxon OX 10 8De UK.
4. Gwiazdowicz J. Dariusz, 2000, The gamasid mites (Acari, Gamasida) of the Bialowieza National Park. Scientific Papers of Agricultural University of Poznan, Forestry, vol. **3**, pp. 3–37.
5. Gwiazdowicz J. Dariusz, 2003, Description of the male *Leioseius elongatus* (Acari, Gamasida) with a key to males of European species of the genus Leioseius. Biologia, Bratislava, 589/**2**, 151–154.
6. Honciuc Viorica and Minodora Stănescu, 2000, Comparative analysis of the mites (Arachnida-Acari) communities in the fir-beech forest ecosystems from Bucegi and Garbova Massifs. Proceedings of the Institute of Biology, vol **III**, pp.127–135.
7. Hyatt H. Keith, 1980, Mites of the subfamily Parasitinae (Mesostigmata : Parasitidae) in the British Isles. *Bull.Br.Mus. Nat. Hist.* (Zool.), **38** (5): 237–378.
8. Juvara Balş Ilinca, 1974, Sur le Leptogamasus de Roumanie. Sous-genre Ernogamasus Athias (Acarina, Anactinotrichida, Parasitina). *Trav. Inst. Speol. "Emile Racovitza"*, **13**:23–35.
9. Juvara Balş Ilinca, 1976, Contribution à la connaissance des genres Pergamasus Berlese et Amblygamasus Berlese de Roumanie. *Trav. Inst. Speol. "Emile Racovitza"*, **15**:17–52.
10. Karg Wolfgang, 1993, Acari (Acarina), Milben Parasitiformes (Anactinochaeta) Cohors Gamasina Leach, **59**: 1–513.

11. Gilarov M.S., Bregetova N.G., 1977, *Opredeliteli Obitaiuscih v Pocive Clescei, Mesostigmata.* Isdatelistvo "Nauka", Leningratkoe, Otdelenie, Leningrad, 1–717.

Received November 14, 2004.

*Institute of Biology, Department of Ecology and Natural Protection, Splaiul Independenței Street, no. 296, Bucharest, 060031, Fax 004 021 22 19 071 – Ecological Station, Sinaia, Calea Codrului Street. no. 34, 1061000, Romania e-mail address: stanescumina@hotmail.com

**University of Agriculture, Department of Forest and Environmental Protection, 71c Wojska Pollskiego Street, 60–625 Poznan,Poland. e-mail address: dagwiazd@owl.au.poznan.pl

FIBRONECTIN DISTRIBUTION IN THE EXTRACELLULAR MATRIX OF CELLS CULTURED IN DEUTERATED MEDIA

WANDA BUZGARIU* VIORICA COROIU* SIMONA CHERA*
OTILIA ZĂRNESCU**GH. TIȚESCU***

This work refers to the study of deuterated water influence on fibronectin (FN) distribution and organization in the extracellular matrix. The studies intended to reveal the changes occurred at the extracellular matrix level in the case of embryonic fibroblasts cultivation in media with various heavy water concentrations (20%, 40%, and 65%). Fibronectin was identified in the extracellular matrix of fibroblasts by the indirect immunocytochemical technique, using a secondary antibody conjugated with peroxidase. In the presence of heavy water in the culture medium, the arrangement and localization of cellular fibronectin have changed depending on the exposure time, D_2O concentration in the medium and the stage of fibronectin polymerization in the extracellular matrix, which was correlated with the time of monolayer cultivation. Heavy water determined a reduction of fibronectin network, this decrease being the most obvious in 65% D_2O medium following 5 days of exposure. When the network distribution was analyzed after 2 days exposure to heavy water, in an early stage of fibronectin network formation, the deuterated medium led to a pericellular distribution of fibronectin aggregates. Heavy water can act on the process of fibronectin fibril formation both directly, due to the solvent effect exerted on the process of fibronectin polymerization, and indirectly, by the effects upon the metabolic reactions and, implicitly, on proteic synthesis and cellular fibronectin secretion. Thus, the organization as aggregates of fibronectin network in cells cultured in deuterated media may be due to the solvent effect exerted by D_2O, while the reduction in FN could be the result of the disturbance of protein synthesis and biochemical reactions.

1. INTRODUCTION

Cellular adhesion influences cell proliferation, since the cells have to be adhered when the division begins and the cells enter the S phase (1, 2). Fibronectin (FN) is one of the molecules involved in cell adhesion, being a high molecular mass dimeric glycoprotein linked through a disulphide bond at carboxyterminal end (3–5). Fibronectin also plays an important role in other cell processes such as migration, differentiation (6), proliferation (7) and modulation of signal transduction pathways by the interaction with other molecules such as surface receptors (8).

REV. ROUM. BIOL. – BIOL. ANIM., TOME 49, N^{os} 1–2, P. 89–96, BUCAREST, 2004

Fibronectin polymerization in extracellular matrix (ECM) controls the composition and stability of the extracellular matrix and of cell-matrix adhesion sites, being involved in the ECM signalling cascade that regulates some aspects of cell behaviour (9). At the same time, fibronectin matrix assembly nucleates in focal adhesions and has an important role in cell locomotion and adhesion.

Deuterium (D) is the stable isotope of hydrogen and has the mass number two fold higher compared with light hydrogen or protium. The natural abundance of deuterium in water is about 150 ppm. Heavy water (D_2O) is the water in which protium is substituted by deuterium and has distinct physico-chemical properties from H_2O. The H_2O substitution for D_2O either in the environment or in the culture medium of the living systems generates changes in their main functions and composition. At high concentrations, D_2O affects a wide range of biological, biochemical and biophysical activities such as mitosis (10), cell cycle kinetics (11), function of membrane systems (12, 13), metabolic reaction (14).

In our earlier investigations we have evaluated the effects of heavy water on cell proliferation, and the structural and functional alterations of lysosomes (15) and mitochondria (16) induced by D_2O.

The objective considered by us in this paper concerns the study of deuterated water action on fibronectin organization in extracellular matrix *in vitro*. The studies followed to reveal the alterations occurred at the extracellular matrix level when fibroblasts cells are exposed to long-term action of heavy water.

2. MATERIALS AND METHODS

2.1. CELL CULTURE

The experiments were carried out on human embryonic (fetal) fibroblasts between passages 4–7. The cells were cultured in DMEM medium with normal deuterium content (150 ppm) supplemented with 10% bovine fetal serum and antibiotics (100 U/ml penicillin and 100 µg/ml streptomycin) at 37°C in atmosphere with 5% CO_2. For the preparation of deuterated culture media, water samples of various deuterium concentrations (25%, 50%, 75%) provided by NIR-DCIS Râmnicu Vâlcea were used. The media were sterilized by filtration. The final D_2O concentration after the serum addition was of 20%, 40%, 65%. In order to detect the fibronectin in the extracellular matrix and cell morphology, the cultures were seeded on glass coverslips placed in Petri dishes at a density of 7.5×10^4 cells/ml. After 24 hours (the lag period of the cells), the medium was replaced by the deuterated variants (20%, 40%, 65% D_2O). The control was also replaced with fresh medium. The replacement of medium was considered the start of the experiments, from which the counting of days had begun.

2.2. IMMUNOCYTOCHEMICAL IDENTIFICATION OF FIBRONECTIN

At defined times of culture in deuterated media (2 and 5 days) cells on the glass coverslips were washed twice in phosphate buffered saline (PBS), pH 7.4 and fixed with cold (– 20° C) methanol for 5 minutes. The cells were then incubated for 20 min at room temperature with 3% H_2O_2 in methanol for endogenous peroxidase blocking. The coverslips were rinsed and after the incubation with goat serum, the cells were incubated for 1 hour at 37 °C in a moist chamber with the primary antibody diluted in PBS, *i.e.* mouse monoclonal IgG anti-fibronectin (1:400, Sigma). After rinsing, the coverslips were incubated for another 60 minutes with the peroxidase labelled secondary antibody (goat anti-mouse IgG), diluted 1:150 (Sigma) and the development of peroxidase reaction was made with 3,3'- diaminobenzidine in the presence of 0.03% H_2O_2. Finally, the cells on coverslips were counterstained with hematoxylin, dried and mounted in Canada balsam.

2.3. DETERMINATION OF CELL VIABILITY BY MTT TEST

Cells were seeded in 24-well plates at a density of 2×10^4 cells/well. After 24 hours, the medium was removed and fresh medium with different deuterium content (150 ppm, 20%, 40%, 65%, 90%) was added in quadruplicate. At different times (24h, 48h, 72h, 96h), the medium was discarded and the adherent cells were carefully washed in PBS and MTT (3-(4,5-dimethylthiazol-2-yl)-2,5-diphenyl tetrazolium bromide) solution was added to each well (MTT dissolved in culture medium at 5 mg/ml). After 3 hours incubation at 37°C, solubilization of formazan crystals formed in viable cells was achieved by adding 1 ml isopropanol to each well. After incubation at room temperature for 20 minutes under gentle agitation, the absorbance was measured at 570 nm on a UV-VIS spectrophotometer (Jasco, model V-530). The formazan formation from MTT in the deuterated variants was expressed as a percentage from the value obtained in daily control cells (150 ppm D).

2.4. CELL MORPHOLOGY

In parallel with the immunocytochemical detection of fibronectin, the cells on glass coverslips were removed from dishes and processed for Giemsa staining. After washing with PBS and cold (–20°C) methanol fixation, the coverslips with cells were stained for 20 minutes with Giemsa solution, washed with water, dried and mounted in Canada balsam.

3. RESULTS

Fibronectin was identified in the extracellular matrix of fibroblast-like cells by the indirect immunocytochemical technique, using a secondary antibody

labelled with peroxidase. The comparison of the obtained results for deuterated media and control was made with the peroxidase reaction control, where the cells were incubated with PBS instead of the primary antibody. The absence of peroxidase reaction was made evident by the lack of the brown precipitate which was characteristic for the positive reaction (Fig. 1).

In fibroblast-like embryonic cells cultured 2 days in medium with usual deuterium content (150 ppm), fibronectin had a pericellular distribution, being located as thin fibrils and spots (Fig. 2). Also in this stage it was found a fibronectin localization on the cell surface (Fig. 3), or between cell processes (Fig. 4). After 5 days, at an advanced stage as concerns the ECM organization, the FN was abundant and well structured in a three-dimensional network of interconnected fibrils of various sizes, from the thin ones to the thick ones (Fig. 5).

When the 20% D_2O experimental variant was considered, after 48 hours of exposure there were identified small aggregates of fibronectin pericellularly located (Fig. 6) or thin fibrils, parallel to the cell long axis (Fig. 7). Following 5 days exposure, FN network was more reduced and more diffuse compared to the control variant, although some thicker fibrils were found (Fig. 8).

The matrix organization was disturbed at a higher degree in the case of fibroblast exposure to a DMEM medium with 40% heavy water. After 48 h, FN distribution was diffuse being identified especially as aggregates (spots) (Fig. 9). Following 5 days exposure, a pericellular localization of FN was noticed in the form of thick fibrils (Fig. 10), the intercellular network, which is a characteristic of normal cellular matrix, being weakly developed.

Fibroblast culturing in a medium with 65% heavy water for 48 h led to a pronounced decrease in FN amount in the extracellular matrix (Fig. 11), especially observed as small, diffuse aggregates. A fibronectin altered organization was detected in some areas of the extracellular matrix cultured for 5 days, finding the presence of a diffuse intercellular network consisting of thin FN fibrils (Fig. 12).

The viability of fibroblast cells exposed to heavy water was determined using the MTT test, which measures the reduction of tetrazolium salt 3-(4,5-dimethylthiazol-2-yl)-2,5-diphenyl tetrazolium bromide (MTT) to blue insoluble formazan crystals in viable cells (15). The obtained results have shown a decrease of viability over 4 days of growth in deuterated media in a dose and time dependent manner compared to the daily control (Fig. 13). Thus, in the case of cells exposure at medium with 20% D_2O, it was observed a decrease by 22% after 4 days compared to the control, while in the culture with 40% deuterated medium the percentage of viable cells was 58%. The cytotoxic action of heavy water was more extended for the medium with 65% D_2O so only 34% viable cells were noted at the end of the considered time (Fig. 13).

In normal culturing conditions, the fibroblast cells are fusiform and flattened on glass coverslips. After 48 hours, the culture was preconfluent (Fig. 14) and at

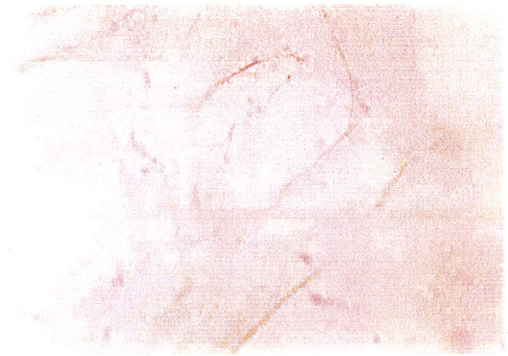

Fig. 1 – Control sample for immunocytochemical reaction. Cells were incubated with the peroxidase labelled secondary antibody, and the primary antibody was replaced by PBS. It is obvious the lack of the brown precipitate which is characteristic for the positive reaction.

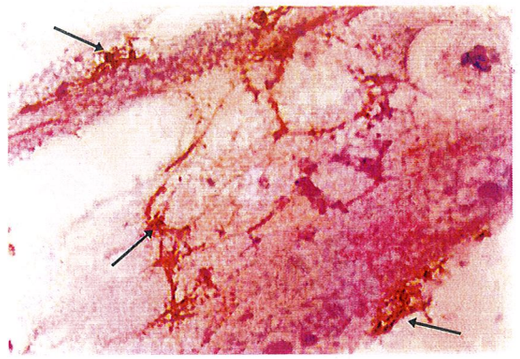

Fig. 2 – The fibronectin distribution in the extracellular matrix of fibroblasts in preconfluent culture (48 hours). The cells were cultured in normal deuterim content medium (150 ppm). Cells with positive pericellular reactivity (× 1000).

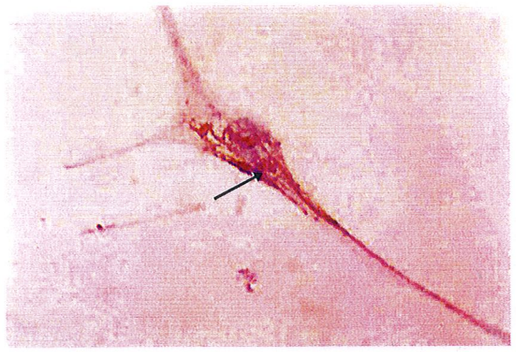

Fig. 3 – Immunocytochemical localization of FN on cell surface and on the cytoplasmic processes (2 days) (× 400) in control cells cultured in medium with normal deuterium concentrations.

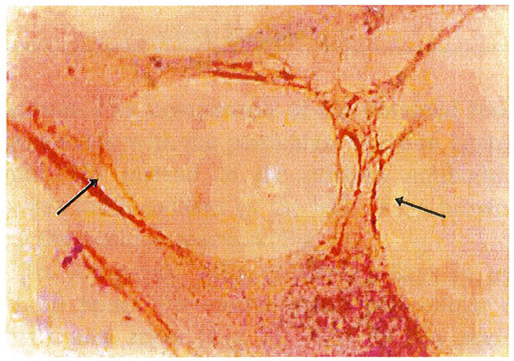

Fig. 4 – Fibronectin distribution on cytoplasmic processes between the cells after 48 hours in medium with usual deuterium concentrations (150 ppm) (×1000).

Fig. 5 – Fibronectin network immunocytochemically detected in fibroblasts cells (150 ppm D). Confluent culture (5 days) (× 400).

Fig. 6 – Fibroblasts in preconfluent culture labelled with monoclonal antifibronectin antibody after 2 days exposure to 20% deuterated medium. FN was located as small aggregates (arrow) (× 400).

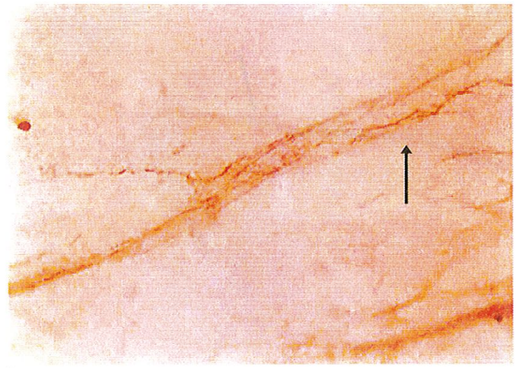

Fig. 7 – Fibroblasts in preconfluent culture labelled with monoclonal antifibronectin antibody after 2 days exposure to 20% deuterated medium. FN (arrow) was identified as thin fibrils (× 1000).

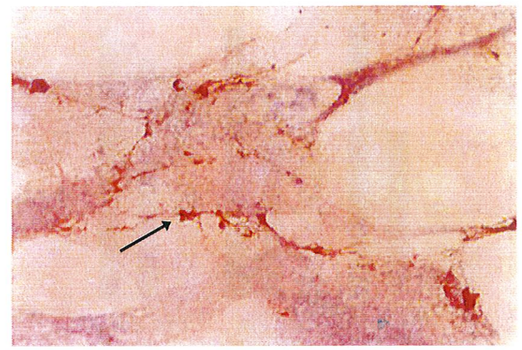

Fig. 8 – Immunocytochemical detection of FN in fibroblasts cells exposed 5 days in medium with 20% D_2O. Hematoxylin staining.

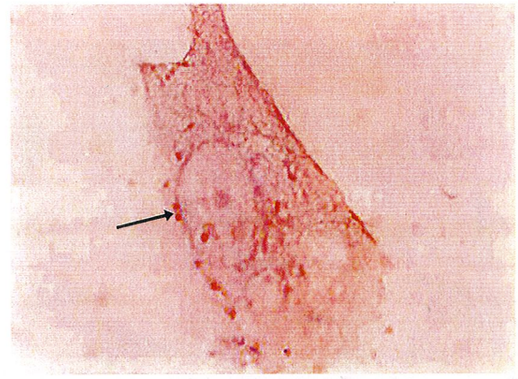

Fig. 9 – Fibronectin pattern as aggregates (arrow) in fibroblasts cells after 2 days culture in 40% deuterated medium (× 1000).

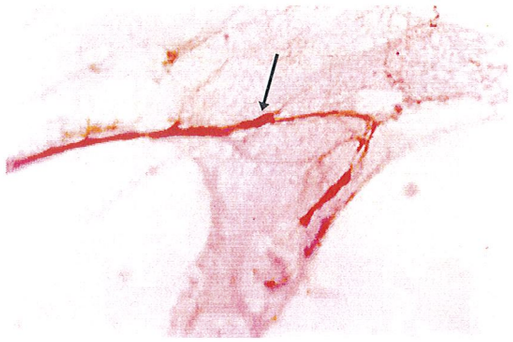

Fig. 10 – Positive pericellular reaction (arrow) after 5 days culture in medium with 40% deuterium content. Hematoxylin staining (× 400).

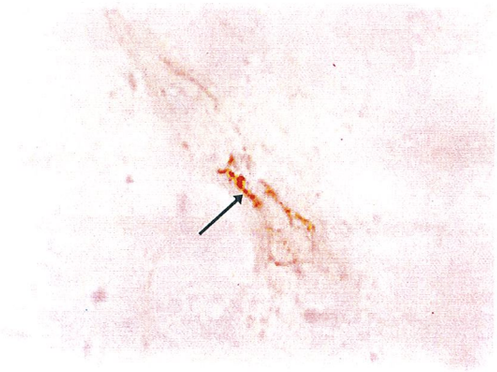

Fig. 11 – Decrease of FN amount from extracellular matrix after 2 days in 65% deuterated medium (× 1000).

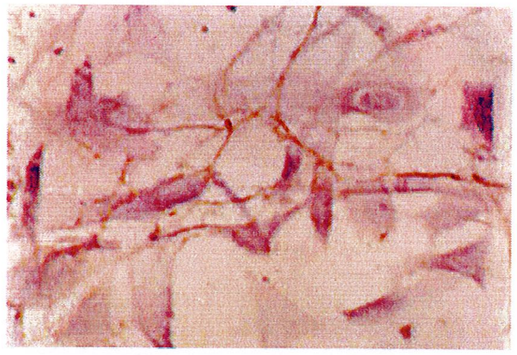

Fig. 12 – Weak distribution of FN after 5 days culture in medium with 65 % D_2O content. Poor immunochemical reaction compared with control sample. Hematoxylin staining (× 400).

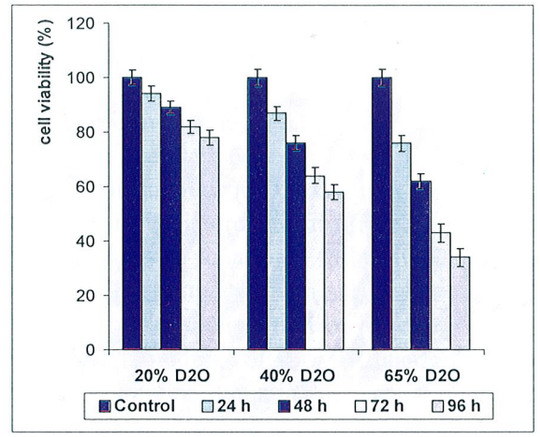

Fig. 13 – Effect of different D_2O concentrations (20%, 40%, 65%) on fibroblast cells viability determined by MTT test. The formazan formation from MTT in viable cells was expressed as a percentage from the value obtained in daily control cells (150 ppm D) which was considered 100%. The values are means of quadruplicate determination SD.

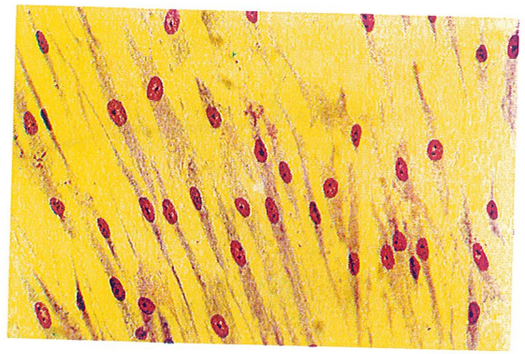

Fig. 14 – Fibroblast cells cultured for 48 hours in control medium (150 ppm D). The cells almost reached confluency. *Giemsa staining* (× 250).

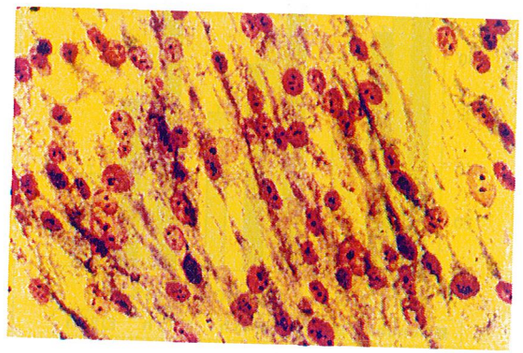

Fig. 15 – Postconfluent fibroblast cells after 5 days culture in normal deuterium content medium (1 500 ppm). *Giemsa staining* (× 250).

Fig. 16 – Fibroblast cells cultured for 5 days in medium with 65% D_2O. *Giemsa staining* (× 250).

the end of the period (5 days) it could be observed a high cell density (Fig. 15), which corresponded to a post confluent monolayer. In the presence of heavy water, the cell density compared with the control decreased with the increase of deuterium content. At 20% and 40% D_2O in medium, the remaining viable cells after 5 days were sufficient for monolayer forming (data not shown). The exposure of fibroblasts in a higher deuterium concentrations medium (65%) had determined a reduction in cell number, but groups of attached cells could still be observed even after 5 days exposure (Fig. 16).

4. DISCUSSION

Cell growth in deuterated media led to important changes in distribution and polymerization of cellular fibronectin secreted in the extracellular matrix and in cell viability.

As is known, fibronectin is one of the best characterized proteins of the extracellular matrix, being secreted by cells as a disulphide-bonded dimer of 230–250 kDa monomers that may become linked into high-order multimers in the insoluble extracellular matrix by interchain disulfide bonds (4, 5). The insoluble form of cellular FN represents the functional form involved in cell migration and adhesion during embryogenesis, tumor growth and development, angiogenesis and inflammation. Polypeptide chain organization of fibronectin is best characterized as a linear series of repetitive modules of various functional properties (3). These modules can be grouped in binding domains to fibrin, hyaluronic acid, collagens, glycosaminoglycans or domains responsible for cell-fibronectin attachment (18).

In control cells, the polymerization stage of FN in the extracellular matrix which depends on the time of fibroblast growth in culture until they reached confluency (cultures are considered confluent when the entire surface of the dishes is covered with cells).

In the presence of heavy water in the culture medium, cellular FN arrangement and location had changed depending on the time of exposure and D_2O concentration in the medium. Heavy water caused a striking reduction of FN distribution secreted by cells, this decrease being the most evident in the medium with 65% D_2O after 5 days exposure. Concerning the early state of FN network arrangement, in the case of 2 days exposure, the deuterated medium led to a pericellular distribution of FN, organized in aggregates, the fibril network being either reduced or absent.

In fibroblast cells cultured in a medium with normal deuterium concentration (150 ppm), the fibronectin polymerization process occurs in several stages. The first stage of fibronectin polymerization takes place at the nucleation site on the cell surface, which is rich in β_1 integrins and actin and corresponds to focal

adhesion (19). Fibronectin fibrils originating from the cell attachment site run parallel one to another as fine linear structures. A more advanced stage of fibronectin polymerization begins from the site of extracellular matrix nucleation, in aminoterminal domain of fibronectin itself. Assembly of a fibrillar fibronectin network is a complex process, the mechanisms of which are an area of active research. Fibril formation is cell mediated and depends on the interactions between fibronectin and integrin receptors on the cell surface (20). This final arrangement leads to the formation of a network of thick fibronectin fibrils (19) which can be noticed in the cells cultured for a longer period of time.

By binding to $\alpha_5\beta_1$ integrin, FN contributes to the activation of the signalling pathways leading to cytoskeleton reorganization (8), cell cycle progress (7) and differentiation (6).

In literature, there are some references and correlations between the proliferation rate, determined by the calculation of cell percentage in S phase of synthesis (by immunocytochemical detection of bromodeoxyuridine incorporated in DNA chain) and FN amount and its arrangement in the extracellular matrix (2). In the presence of heavy water, the disturbance of the arrangement and the relieved diffuse aspect can be also related to the low rate of multiplication. Although the viability of fibroblasts in our case was decreased to 34% from the control cells at the end of experiment, the number of cells in the culture was comparable with that at the beginning of experiments. This obstruction was determined by heavy water in medium, which is a blocking agent of microtubules (21, 22) and alters the cell cycle, the cells being arrested at interphase-prophase transition (10, 11).

As is known, the biological effects of heavy water on various biological systems (23–25) are due to isotopic and solvent effects, which alter the hydrogen bonds that are responsible for the specific configuration of macromolecules (26).

In our case, heavy water can directly act upon the FN fibril formation process due to the solvent effect exerted on FN polymerization process by cell surface direct contact with deuterated culture medium. In addition, heavy water produces an indirect effect, by action on metabolic reactions and implicitly on protein synthesis and cellular FN secretion. More recent data (9) indicate that polymerized form of extracellular matrix proteins has properties distinct from protomeric, nonpolymerized proteins. The performed experiments concerning D_2O effects on protein aggregation *in vitro* showed a stabilization of the aggregated form of oligomeric proteins (27–29), without an effective description of the mechanism by heavy water on protein structures. Since in the case of FN network formation in deuterated media, FN presence was found in the form of aggregates (spots), it might be supposed a prevalence of the solvent effect exerted by D_2O in these circumstances, whereas the reduction in FN might be due to the disturbance of protein synthesis and metabolic reactions.

REFERENCES

1. Couchman J.R., Rees D.A., Green M.R., Smith C., *Fibronectin has a dual role in locomotion and anchorage of primary chick fibroblasts and can promote entry into the division cycle*, J. Cell Biol., **93**, 402–410 (1982).
2. Grill V., Sandrucci M.A., Di Lenarda R., Dorigo E., Narducci P., Martelli A.M., Bareggi R., *Cell proliferation rates and fibronectin arrangement as parameters for biocompatibility evaluation of dental alloys in vitro*, J. Oral Sci., **42**, 1–7 (2000).
3. Hynes R. O., *Fibronectins*, Springer, Berlin, Heidelberg, New York (1990).
4. Mosher D.F., Sottile J., Wu C., McDonald J.A., *Assembly of extracellular matrix*, Curr. Opin. Cell Biol., **4**, 810–818 (1992).
5. Armstrong P.B., Armstrong M.T., *Intercellular invasion and the organizational stability of tissues: a role for fibronectin*, Biochemical and Biophysical Abstracts, **1470**, O9-O20 (2000).
6. Garcia A.J., Vega M.D., Boettinger D., *Modulation of cell proliferation and differentiation through substrate-dependent changes in fibronectin conformation*, Mol. Biol. Cell, **10**, 785–798 (1999).
7. Sechler J.L., Schwarzbauer J.E., *Control of cell cycle progression by fibronectin matrix architecture*, J.Biol. Chem., **273**, 25533–25536 (1998).
8. Schwarzbauer J.E., Sechler J.L., *Fibronectin fibrillogenesis: a paradigm for extracellular matrix assembly*, Curr. Opin. Cell Biol., **11**, 622–627 (1999).
9. Sottile J., Hocking D.C., *Fibronectin polymerization regulates the composition and stability of extracellular matrix fibrils and cell-matrix adhesions*, Molecular Biology of the Cell, **13**, 3546–3559 (2002).
10. Lamprecht J., Schroeter D., Paweletz N., *Mitosis arrested by deuterium oxide. Light microscopic, immunofluorescence and ultrastructural characterization*, Eur. J. Cell Biol., **51**, 303–312 (1990).
11. Schroeter D., Lamprecht J., Eckardt R., Futterman G., Paweletz N., *Deuterium oxide (heavy water) arrests cell cycle of PtK_2 cells during interphase*, Eur. J. Cell Biol., **58**, 365–370 (1992).
12. Andjus P.R., Kataev A.A., Alexandrov A.A., Vucelic D., Berestovsky G.N., *D_2O-induced ion channel activation in Characeae at low ionic strength*, J. Membr. Biol., **142**, 43–53 (1994).
13. Andjus P.R., Vucelic D., *D_2O-induced cell excitation*, J. Membr. Biol., **115**, 123–127 (1990).
14. Wals P.A., Katz J., *The effect of D_2O on glycolysis by rat hepatocytes*, Int. J. Biochem., **25 (11)**, 1561–1564 (1993).
15. Buzgariu Wanda, Otilia Zarnescu, Maria Caloianu, Anisoara Cimpean, Gh. Titescu, I. Stefanescu, *Effects of heavy water on ultrastructural and functional status of Hep 2 and CHO cells lysosomes*, Revue Roumaine de Biologie, **47**, 87–96 (2002).
16. Buzgariu Wanda, Otilia Zarnescu, Maria Caloianu, Coroiu Viorica, Gh. Titescu, I. Stefanescu, *Ultrastructural and functional changes in mitochondria induced by heavy water in vitro*, Revue Roumaine de Biologie, **48**, 2003.
17. Mosmann T., *Rapid colorimetric assay for cellular growth and survival: application to proliferation and cytotoxic assays*, J. Immunol. Methods, **65**, 55–63 (1983).
18. Langenbach K.J., Sottile J., *Identification of Protein-disulfide Isomerase Activity in Fibronectin*, J. Biol. Chem., **274**, 7032–7038 (1999).
19. Cristopher R.A., Kowalczyk A.P., McKeown-Longo P.J., *Localization of fibronectin matrix assembly sites on fibroblasts and endothelial cells*, J.Cell Sci., **110**, 569–581 (1997).
20. Wierzbicka-Patynowski I., Schwarzbauer J.E., *The ins and outs of fibronectin matrix assembly*, J. Cell Sci., **116**, 3269–3276 (2003).

21. Houston L.L., Odell J., Lee Y.C., Himes R.H., *Solvent isotope effects on microtubule polymerization and depolymerization,* J. Molec. Biol., **87**, 141–146 (1974).
22. Chakrabarti G., Kim S., Gupta M.L., Barton J.S., Himes R.H., *Stabilization of tubulin by deuterium oxide*, Biochemistry, **38**, 3067–72 (1999).
23. Crespi H.L., Conrad S.M., Uphaus R.A., Katz J.J., *Cultivation of microorganisms in heavy water,* Ann.N.Y.Acad.Sci., **84**, 648–666 (1960).
24. Blake M.I., Crane F.A., Uphaus R.A., Katz J.J., *The effect of deuterium oxide on the growth of peppermint (Mentha piperita)*, J. Pharm. Sci., **53**, 79–86 (1964).
25. Thompson T.J., *Physiological effects of D_2O mammals*, Ann.N.Y.Acad.Sci., **84**, 736–745 (1960).
26. Scheraga H.A., *Deuterium exchange studies and protein structure,* Brookhaven Symp Biol., **13**, 71–88 (1960).
27. Bonnete F., Madern D., Zaccai G., *Stability against denaturation mechanisms in halophilic malate dehydrogenase "adapt" to solvent conditions*. J. Mol. Biol., **244**, 436–477 (1994).
28. Henderson R.F., Henderson T.R., Woodfin B.H., *Effects of D_2O on the Association-Dissociation Equilibrium in Subunit Proteins*, J. Biol. Chem., **245**, 3733–3737 (1970).
29. Omori H, Kuroda M., Naora H., Takeda H., Nio Y., Otani H., Tamura K., *Deuterium oxide accelerates actin assembly in vitro and changes microfilament distribution in cultured cells*, Eur. J. Cell Biol., **74**, 273–280 (1997).

Received October 15, 2004.

*National Institute R-D of Biological Sciences
Bucharest, Spl. Independenței 296
E-mail: wanda@dbio.ro

**Bucharest University, Faculty of Biology,
Spl. Independenței 91–95

***NIR-DCIS Râmnicu Vâlcea

THE CYTOGENETIC STUDY OF HYBRID PROGENY OF SILVER CRUCIAN (*Carassius auratus gibelio,* Bloch.) TO UNDERSTAND ITS REPRODUCTION

LILIANA GREGORIAN*, ATENA SCRIPCARIU**

The cytogenetic study (generally based on the somatic chromosome number determination) of the progeny resulting from experimental homo- and heterospecific hybridizations, made in order to clarify the reproduction of the *C. a. gibelio* females with two morphotypes in the natural biotopes ("old form", "new form"), revealed a large aneuploid variety, from 2n(2x) = 72 to 2n(3x) = 182 somatic chromosomes. This wide range suggests the existence of both some meiotic mechanisms modified prior to the fecundation and some further desynchronizations in the male and female pronucleus evolutions, occurring in the ovule cytoplasm. The chromosome number variation of the descendants from *C. a. gibelio* heterospecific cross-breeding makes us conclude that the triploid females could generate haploid gametes (1x) by normal meioses, diploid gametes (2x) by the first or second meiotic division absence, and triploid gametes (3x) by endoreduplication. All these gametes are able of unisexual (gynogenesis) or bisexual reproduction, as well as of the combination of the two. That large reproduction strategy makes possible the reversibility of unisexual populations into bisexual ones, as well as the reverse of that, and guarantees the viability in their own evolutive system. As far as it concerns the gynogenesis, that reproduction manner leads to the surpassing of the isolation mechanisms (hybrid sterility), ensuring the stability of interspecific hybrids, on the one side. On the other side, it leads to the survival increase under unfavorable conditions and to the extension on new geographical areas, since the triploidy – or alotriploidy better said – ensures the homeostasis in the individual and species level, as well as a high degree of heterozygosis.

INTRODUCTION

The *Carassius auratus* species, mainly the *Carassius auratus gibelio* subspecies (silver crucian), have, apart from the normal, bisexual reproduction, also a controversed primitive mode of reproduction, namely gynogenesis, frequently observed in polyploid forms – a mechanism which offers a maximum reproductive adaptation. The phenomenon is possible in the absence of sex-differentiated chromosomes, the sex being determined by a "sex gene" located on some chromosomes.

REV. ROUM. BIOL. – BIOL. ANIM., TOME 49, N^{os} 1–2, P. 97–104, BUCAREST, 2004

Following the sex ratio analysis of different *Carassius auratus gibelio* populations, it resulted that both sexes could appear in some populations (bisexual), while, towards the limits of their spreading areas, the male proportion decreases, and the respective populations become unisexual (12); (13); (14). This type of unisexuality is based on gynogenesis, as sustain some authors, who described the genetic material during segmentation (8); (6); (7).

Because the silver crucian is very spread in Romania freshwaters and takes an important place among the commercialized species, its proper rearing in controlled fish culture requires the elucidation of all its particularities of reproduction, growth and development. One aspect, we proposed to explain through our cytogenetic study involves the ovogenesis mechanisms, which surely were modified by gynogenesis. Other aspects were the transfer extent of parental genomes and the measure of genotype expression in progeny.

We used indirect cytogenetic methods at progeny level, because the great chromosome number in this species may lead to uncertain meiosis analysis. In these conditions, it was possible to indirectly elucidate, by determination of somatic chromosome number in descendants resulted from intra-, interspecies or intergenus cross breeding, the polyploidy nature and the mechanisms involved in this species reproduction.

MATERIAL AND METHODS

Anterior kidney preparations were used to visualize the metaphase chromosomes. The flame dried squashes were stained by Giemsa technique.

The material was obtained from Nucet Fish Culture Station and was represented by progeny of different type fertilizations between females of *C. a. gibelio,* "old form" (o.f.) or "new form" (n.f.) fertilized with males of other species like: *C. a. auratus, C. carassius, C. carpio, A. brama,* and also with males coming from *C. a. gibelio* bisexual populations.

RESULTS AND DISCUSSION

The results are presented in Tables 1 and 2, which show the aneudiploid and triploid variation in the studied individuals and cells.

Table 1 comprises the chromosome number distribution in progeny resulted from cross breedings of *C. a. gibelio* females (o.f.) with other species males. Of 54 investigated individuals 7.41 % were diploid females (uncertain sex) and 92.59 %

Table 1

The distribution of metaphasic chromosome number in progeny from cross-breedings of *C. a. gibelio* (o.f.) females with other species males

	Fertilization variants		Studied ind. no.		Studied cell no.		Chromosome number/cell: 2n			3n		
			2n	3n	2n	3n	98	100	104	112	122	124
1	♀C.a.gibelio x ♂C.a.gibelio	♀		6		25						
		♂										
2	♀C.a.gibelio x ♂C.a.auratus	♀		5		15						
		♂										
3	♀C.a.gibelio x ♂C.carassius	♀		9		60				3		
		♂	4		13		8		5			
4	♀C.a.gibelio x ♂C.carpio	♀		11		29						
		♂										
5	♀C.a.gibelio x ♂A.brama	♀		14		30						
		♂										
6	♀C.a.gibelio x ♂Ict. Cyprinellus	♀		5	3	70	3				3	3
		♂										
TOTAL			4	50	16	229	11		5	3	3	3
%			7.41	92.59	6.53	93.47	68.75		31.25	1.31	1.31	1.31

	Fertilization variants		3n: 130	132	134	136	138	140	142	144	146	147	148	150	152	154	156	158	160	162	164	166	178
1	♀C.a.gibelio x ♂C.a.gibelio	♀												16						9			
		♂																					
2	♀C.a.gibelio x ♂C.a.auratus	♀											5				10	6					
		♂																					
3	♀C.a.gibelio x ♂C.carassius	♀			14	10										19	14						
		♂																					
4	♀C.a.gibelio x ♂C.carpio	♀	5	6					4				4		3				4			3	
		♂																					
5	♀C.a.gibelio x ♂A.brama	♀				5				5	6	5	5						4				
		♂																					
6	♀C.a.gibelio x ♂Ict. Cyprinellus	♀	3	6		3	3	4		5			3	8	4	4			4	10	4		3
		♂																					
TOTAL			8	12	14	18	3	4	4	10	6	5	17	24	7	23	24	6	12	19	4	3	3
%			3.49	5.24	6.11	7.86	1.31	1.74	1.74	4.40	2.62	2.20	7.42	10.50	3.06	10.04	10.50	2.62	5.24	8.29	1.74	1.31	1.31

Table 2

The distribution of metaphasic chromosome number in progeny from cross-breedings of *C. a. gibelio* (n.f.) females with other species males

Fertilization variants		Studied ind. no. 2n	Studied ind. no. 3n	Studied cell no. 2n	Studied cell no. 3n	2n: 72	80	82	90	92	94	98	100	3n: 116	120	122	126	128	130	132	134	136	140	142	144	146	148	150	152	154	156	158	160	164	178	180
1 ♀*C.a.gibelio x* ♂*C.a.gibelio*	♀		15		75										4		5	3								10		6	12	26			10			
	♂	3		12									12																							
2 ♀*C.a.gibelio x* ♂*C.a.auratus*	♀		11		50										7								4	8		8	9				14					
	♂																																			
3 ♀*C.a.gibelio x* ♂*C.carassius*	♀		9		57															10						12	9	5			14	7				
	♂																																			
4 ♀*C.a.gibelio x* ♂*C.carpio*	♀		15		43											5				10	5	6		6			5	6								
	♂	20		65		3	14	6	10	10	6	5	11																							
5 ♀*C.a.gibelio x* ♂*A.brama*	♀		6		59																			10	10				12		13			14		
	♂																																			
6 ♀*C.a.gibelio x* ♂*Ict. Cyprinellus*	♀		8		109									5		4		5	11	6	6	4		10	10	8			10		13			14		
	♂																																			
7 ♀(*C.a.g. x* ♂*A.brama*) *x A.brama*	♀		5		29																		11						18							
	♂																																			
8 ♀(*C.a.g. x* ♂*A.brama*) *x C.carpio*	♀		5		27																		13				14									5
	♂																																			
TOTAL		23	74	77	449	3	14	6	10	10	6	5	23	5	11	9	5	8	11	26	11	10	28	34	20	38	37	17	52	26	54	7	10	28	5	5
	%	23.71	76.29	14.63	85.37	3.90	18.20	7.80	13.00	13.00	7.80	6.49	29.87	1.11	2.44	2.00	1.11	1.78	2.44	5.79	2.44	2.22	6.23	7.57	4.45	8.46	8.24	3.38	11.58	5.80	12.00	1.55	2.22	6.23	1.11	1.11

triploid ones, as is shown in the table. Of all 245 investigated mitotic cells, 6.53% presented between 98–104 somatic chromosomes, thus they were actually diploids, 2x, while 93.47% showed aneutriploidy in wide limits, from 112 to 178 chromosomes. The lowest frequency (1.31%) was noticed at sets near these interval extremities. The highest frequency of 10.5%, within this large interval of 2n (3x), belonged to the sets with 150 and 156 chromosomes, figures characteristic of triploidy, typical of *C. a. gibelio* females.

It is also noted that only the hybridations of *C. a. gibelio* o.f. with *C. a. gibelio* and *C. a. auratus* presented no aneuploid variation. The chromosome number variation increased in other fertilization types, as the parental genomes were, from phyllogenetic point of view, at further distance of each other. This fact culminated with intraindividual polymorphism (aneusomaty) (*C. a. gibelio* x *Ict. cyprinellus*).

As regards the progeny of *C. a. gibelio* (n.f.) females with homo- and heterospecific males, Table 2 shows the chromosome number distribution in 526 analysed metaphases, belonging to 97 exemplars.

In comparison to the above-mentioned group, a number increase of 2n cells (to frequency of 14.63%), as well as of descendant males was observed. The frequency of these males (23.71%) had an aleatory character in our study. The aneudiploid variation ranged from 3.9% (2n = 72) to 29.87% (2n = 100) as regards the 2n cells.

The frequency range of aneutriploid variation was very wide in female descendance: from 1.11% at 2n = 116; 126; 178; 180, to 12% at 2n = 156, a phenomenon which imparts a strong intrapopulation polymorphism. It is observed again that the maximum frequency value belonged to the base number, namely 2n = 3x ~156.

In Fig. 1 are illustrated some metaphases of hybrid descendance with aneuploid variation between 2n = 80 and respectivelly 2n = 156 somatic chromosomes (a, b, c, d, and e).

The results shown in Tables 1 and 2, together with the literature data, allow us to consider that both diploid and triploid oocytes are formed in meiosis (1); (17); (15), (16); (4).

Thus, the hypotriploid numbers 2n(3x) which appear in all interspecific fertilization types, no matter the maternal genitor was "o.f." or "n.f.", could be explained only as the result of fecundation of diploid female gametes, formed by endoreduplication or by absence of first or second meiotic division. Aneuploidy represents the effect of a different addition, evolution and conservation of paternal genome in the egg cytoplasm (10); (11); (3).

Otherwise, eutriploid numbers presented by 40% of descendants, according to our opinion, are the result of gynogenetic evolution of 3x meiocytes. The existence of some individuals with chromosome numbers between 148 and 160 shows the conservation of three genomes. This phenomenon could appear only by intraspecific [*C. a. gibelio* (o.f.) x *C. a. gibelio* (*C. a. auratus*)], or interspecific (gynogenesis) fertilization, a condition observed in the remaining cross breedings.

The presence – indeed with low frequency of 1.11% – of some hypotriploids in descendants resulted from interspecific cross breedings: *C. a. gibelio* (n.f.) x *C. a. gibelio,* was in unconformity to the above mentioned opinion. This case could be explained only by the desynchronization of female pronucleus and homologous sperma nucleuses (2); (5).

The male appearance is correlated to the possibility of synchronization of different sex pronucleuses and of the equilibrium between sexual genes. This observation is in agreement with the data obtained by us in cross breedings: *C. a. gibelio* (n.f.) × *C. a. gibelio.* A symmetrical complement (2n = 100 chromosomes) was evidenced in these, which could be formed by normal fertilization, respectively bisexual reproduction, resulting in eudiploid fertile males.

The males resulted from fertilization of maternal genitor "n.f." with *C. carpio,* too. The appearance of individuals with chromosome numbers of 2n = 72–94, following this interspecific cross breeding, showed that they were allohybrids, hypodiploids, of which majority surely will be sterile.

The males absence in progeny of cross breedings with *C. a. gibelio* (o.f.) allowed us to suppose that "o.f." arouse unisexual populations, owing to the conspecific male absence and local conditions, as the distance from the origin site increased. This happened because they lost their capacity to realize a normal meiosis resulting in haploid oocytes.

CONCLUSIONS

- The "old form" and "new form" females generated. by intra- and interspecific fertilizations. a genetical unhomogeneous progeny, with a wide aneuploid variation, between 2n(2x) = 72 and 2n(3x) = 180 somatic chromosomes;
- The aneuploidy, especially hypoaneutriploidy, could be the result of generation of 2x female gametes which, by "pseudoamphimixis", assimilate a part of paternal genetic material;
- We consider that the existence of eutriploid values (148–162) in 40% of descendants is the result of generation of oogonies 3x which are gynogenetically controlled by heterospecific gametes, thus, the three genomes being preserved;

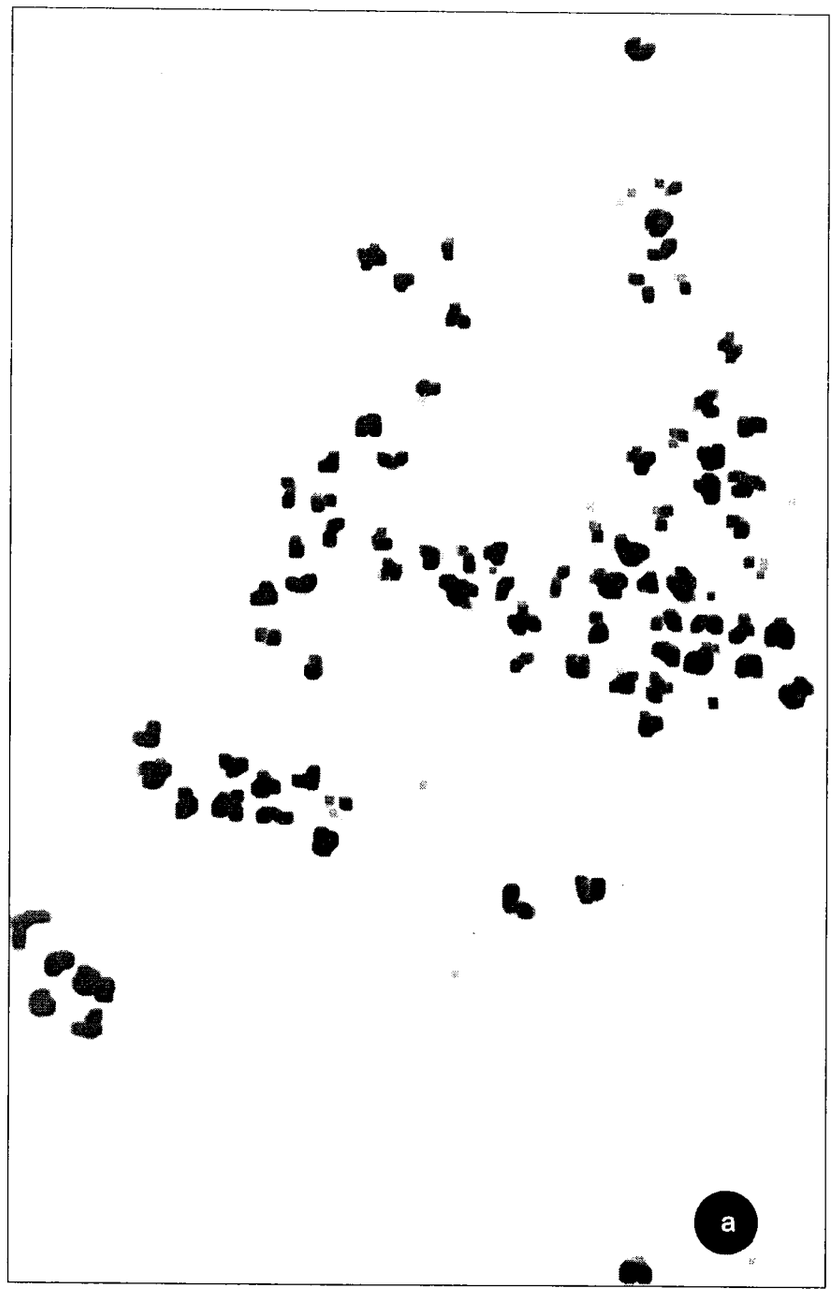

Fig. 1a

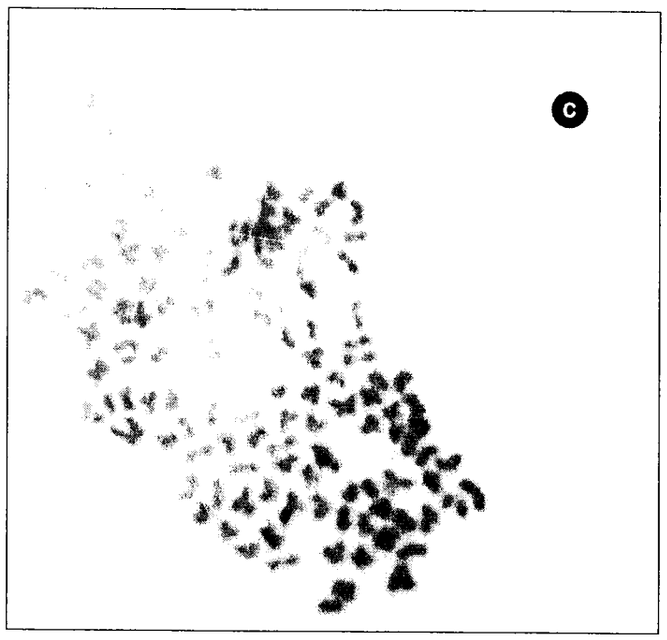

Fig. 1b, c

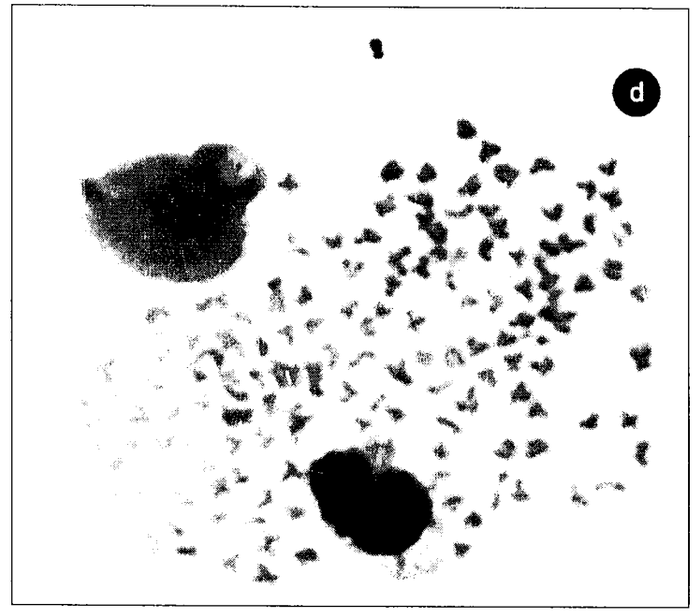

Fig. 1d

Fig. 1 – Karyotypes in progeny from fertilizations of *C. a. gibelio* females ("old form" and "new form") with other male species.
a) Metaphase with 2n = 80 somatic chromosomes.
b) Metaphase with 2n = 100 somatic chromosomes.
c) Metaphase with 2n = 120 somatic chromosomes.
d) Metaphase with 2n = 140 somatic chromosomes.
e) Metaphase with 2n = 160 somatic chromosomes.
Cytogenetic study of hybrid progeny of silver crucian (*Carassius auratus gibelio*).

• Similar eutriploid numbers were evidenced in progeny of *C. a. gibelio* (o.f.) x *C. a. gibelio* or *C. a. auratus* where the gynogenesis is excluded, because it represents an intraspecific fertilization between homologous genomes. Although, in similar conditions, from "n.f." could result hypotriploids, as a consequence of paternal and maternal pronucleus desynchronization;

• The male appearance and presence in *C. a. gibelio* populations is correlated with bisexual hybridization with female gametes (1x) which underwent a typical meiosis with two chromatic reductions. It seems that the only genetic formula 2x (♀n + ♂n), with two homospecific genomes, assures the counterbalance of feminization genes, and, in consequence, the appearance of fertile males. The blocking of this mechanism, by a stabilized time mutation, generated unisexual populations, as is the case of "old form".

REFERENCES

1. COLARES–PEREIRA, M. J., 1985, The "Rutilus alburnoides (steindachner, 1866) complex" (Pisces Cyprinidae) II First data on the karyology of a well-established diploid group. Arq. Mus. Boc. (Seria A), **III**, *5*, 69÷90.
2. DING, Y., SHAN, S. X., JIANG, Y. G., 1992, Study on the mode of primary control in the egg of gynogenetic crucian carp for inhibiting the development of two types of sperm nuclei. Sci. In China (Ser. B), **35**, *7*, p. 802÷810.
3. FAN, Z. T., SHEN, J. B., 1990, Studies on the evolution of bisexual reproduction in crucian carp (*Carassius auratus gibelio* – Bloch). Aquacult., **84**, 235÷244.
4. FENG, Z., TAKASHI, O., FUMIO, T., 1992, Chromosome synapsis and recombination during meiotic division in gynogenetic diploid ginbuna *C. a. langsdorfi*. Jap. J. Ichthyol., **39**(2): 151÷155.
5. GUI, J. F., LIANG, S. C., ZHU, L. F., JIANG, Y. G., 1993a, Discovery of tetraploids in artificially propagated populations of allogynogenetics silver crucian carp and their breeding potentialities. Chin. Sci. Bull., **38**, *4*, 327÷331.
6. -- „ --, LIANG, S. C., ZHU, L. F., JIANG, Y. G., 1993b, Discovery of two different reproductive development modes of the eggs of artificial multiple tetraploid allogynogenetic silver crucian carp. Chin. Sci. Bull., **38**, *4*, 332÷337.
7. -- „ --, J. F., LIANG, S. C., ZHU, L. F., JIANG, Y. G., 1993c. Preliminary confirmation of gynogenetic silver crucian carp. Chin. Sci. Bull., **38**, *1*, 67÷70.
8. KOBAYASI, H., 1965, A chromosome study in funa-loach hybrids. Zool. Mag. Tokyo, 201÷267.
9. -- „ --, 1971, A cytological study on gynogenesis of the triploid ginbuno (*Carassius auratus langsdorfii*). Zool. Mag., **80**: 316÷322.
10. -- „ --, OCHI, H., 1972, Chromosome studies of the hybrids, ginbuna *Carassius auratus* langsdorfii x kinbuna *Carassius auratus* subsp. and ginbuna x loach *Misgurnus anguillicandatus*. Zool. Mag., **81**: 67÷71.
11. -- „ --, 1976, A cytological study on the maturation division in the oogenic process on the triploid ginbuna *Carassius auratus langsdorfii*. Japan J. Ichthyol., **22**(*4*), 234÷240.
12. MURAMATO, Y., 1975, A note on triploidy of the funa (Cyprinidae, Pisces). Proc. Japan. Acad., **51**:583–587.
13. OJIMA, Y., ASANO, N., 1997, A cytological evidence for gynogenetic development of the ginbuna (*Carassius auratus langsdorfii*). Proc. Japan Acad., **53**(*4*), 138÷142.

14. SHIMIZU, Y., OSMIRO, T., TAKASHIMA, F., SAKAIZUMI, M., 1991, Origin of the triploid "ginbuna" *Carassius auratus langsdorfii*. Zool. Sci., **7**(*6*), 1056.
15. ZHANG, F., OSHIRO, T., TAKASHIMA, F., 1992a, Chromosome synapsis and recombination during meiotic division. Japan J. Ichthyol., **39**(*2*), 151÷155.
16. -- „ --, OSHIRO, T., TAKASHIMA, F., 1999, Fertility of triploid back-cross progeny (gengoroubuna *Carassius auratus cuvieri* ♀ x carp *Cyprinus carpio* ♂)F1 ♀ x carp or gengoroubuna ♂. Japan J. Ichthyol., **39**(*3*), 229÷233.
17. YAMASHITA, M., NAGAHAMA, Y., 1989, Mechanisms for maintaining gynogenesis: inhibition of reduction of egg chromosomes and inhibition of male pronucleus formation. Zool. Sci., **6**: 1167.

Received September 10, 2004.

*Romanian Academy

**Institute of Biology,
Bucharest
Splaiul Independenței 296

THE CHARACTERIZATION AND *IN VITRO* TESTING OF A DERMAL SHIELD CONTAINING SOLUBLE ELASTIN

OANA CRĂCIUNESCU*, LUCIA MOLDOVAN*, DANIELA BRATOSIN*, OTILIA ZĂRNESCU**, G.L. RADU*

In this study, shield variants, conditioned as membranes, containing two types of soluble elastin, collagen and glycosaminoglycans, were prepared. Cross-linking and sterilization were made by UV irradiation. All matrices were biochemically (active substance content, water-binding ability, collagenase degradability) and structurally (SEM) characterized. Their effect on dermal fibroblast morphology and viability was analyzed by flow-cytometry. *In vitro* cell attachment was also investigated. All the results showed that the membrane αEL:COL:GAG, in 1:20:4 ratio, could be used to develop a composite graft with good biostability and biocompatibility.

1. INTRODUCTION

Among skin injuries, the wound most complex and difficult to treat is that of extensive deep burn. A burn is characterized by abnormal deposition of extracellular matrix, systemic pathophysiological changes and delayed wound healing [1]. Also, scar formation is unaesthetic due to a very slow elastin regeneration. Rapid local cover is very important in burn wounds in order to replace skin functions.

The majority of matrix substitutes for wound treatment are made of collagen (COL) or collagen-glycosaminoglycans (COL-GAG) mixtures [2, 3]. The use of elastin (EL) in combination with COL is justified by several reasons. Immunological studies revealed that elastin matrix induced a lower density of activated leukocytes than COL. This reduced thrombogeneity is in favour of elastin use in tissue implants as the material that stays in contact with the blood [4]. Moreover, EL is a constitutive protein of the matrix and contributes to the morphogenesis [5] and control of cellular activity [6]. Elastic peptides stimulate elastic fibres adhesion to fibroblasts [7] and they can be adsorbed and desorbed, in particular conditions, on natural and synthetic polymers [8].

Up to the present, there have been developed various cross-linked matrices from COL and fibrillar or hydrolyzed EL [9, 10, 11]. To our knowledge, it has never been made a comparison between the presence of type α-EL and type k-EL, as a constitutive part of a dermal bioproduct.

The aim of this work was the characterization and *in vitro* testing of a membrane based on EL (type α or k), COL and GAG developed for burn and other skin lesion treatment.

REV. ROUM. BIOL. – BIOL. ANIM., TOME 49, N^os 1–2, P. 105–111, BUCAREST, 2004

2. MATERIALS AND METHODS

Isolation of matrix components. COL type I+III was isolated from bovine hides using dilute acid extraction and GAG was obtained by alkaline treatment, from bovine tracheas, as described [12]. Fibrillar EL was solubilized by acid or alkaline treatment, resulting in α-EL and k-EL solutions, respectively [13].

Preparation of EL-COL-GAG membranes. 8 variants of shields were prepared with different ratios of EL, COL and GAG and were exposed or not to UV irradiation. Non-cross-linked membranes were prepared by mixing a 0.5% COL types I+III solution, shaken at 37°C, for 30 minutes, with a 0.5% solubilized EL (type α or k) solution, incubated at 37°C, for 1h, and a 0.5% GAG suspension, in PBS, pH 7.4, in different ratios, 1:20:4 and 1:10:4 EL:COL:GAG, respectively. After 1h incubation at 37°C, the mixture was poured in a mould and dried, resulting in a flexible membrane. Cross-linking of EL-COL-GAG membranes was performed by UV irradiation. Membrane pieces were sealed in polyethylene bags and irradiated with an UV lamp for 3, 6 and 9 hours.

Characterization of the membranes

– Protein and GAG content. Membrane pieces were hydrolyzed with 6M HCl for 18 h, at 105°C. The Hyp content was determined spectrophotometrically after reaction with p-dimethylbenzaldehyde [14]. The total protein content was determined by Bradford's method [15] and the uronic acid content was determined with orcinol [12] in partially hydrolyzed samples.

– Water-binding capacity. Approx. 5 mg dry weight samples were incubated in 2 ml PBS, pH 7.4, at 20°C. After 20 h, the wet weight was determined and water-binding capacity was calculated using the equation:

$$\text{swelling ratio} = [(\text{wet weight-dry weight})/\text{dry weight}] \times 100$$

– *In vitro* degradability. Samples of approx. 5 mg of uncross-linked and cross-linked membranes were incubated in 2 ml of 10 U ml^{-1} collagenase solution (type I, Sigma, St. Louis, MO) in 0.05M Tris buffer containing 10 mM $CaCl_2$, pH 8.0, at 37°C, for 2h. The degradation degree was determined from the dissolved protein quantity measured by Bradford's method.

Scanning electron microscopy. Membrane samples were processed in the 'low vacuum' mode and visualized at a scanning electron microscope ESEM, XL-30, FEI (Philips).

In vitro biocompatibility test. A primary culture of human embryonic fibroblast cells, passage 2–4, was used in this study. Freshly trypsinized fibroblasts (1.2×10^5 cells ml^{-1}) were seeded on membranes and cultivated in cell culture medium, DMEM supplemented with 10% SFB and antibiotics, for 72 hours. Some membrane samples were treated with 1 mg/ml collagenase solution, for 10 min., at 37°C and the detached cells were analyzed at a cytofluorimeter with Cell Quest Pro software. Size/granularity assay (FSC/SSC) was performed to evaluate cell morphology and viability. Other cell-seeded membranes were fixed in Bouin buffer and embedded in paraffin. Cross sections were stained with Harris hematoxylin to evaluate cell attachment.

3. RESULTS AND DISCUSSION

Biochemical characterization of the membranes

Physico-chemical properties. Macroscopically, the membranes obtained in this study were transparent sheets, with an uneven structure. In Table 1 is given the composition of the 8 variants of membranes, before and after UV irradiation.

Table 1

The chemical composition of membranes

Membrane	EL:COL:GAG ratio	UV irradiation	Hyp content (g%)	Total protein content (g%)	Uronic acid content (g%)
αEL:COL:GAG	1:20:4	-	0.48	1.25	1.92
αEL:COL:GAG	1:20:4	+	1.34	5.12	2.20
kEL:COL:GAG	1:20:4	-	0.45	0.98	1.58
kEL:COL:GAG	1:20:4	+	1.12	4.04	1.72
αEL:COL:GAG	1:10:4	-	0.06	0.27	0.73
αEL:COL:GAG	1:10:4	+	0.21	0.86	0.85
kEL:COL:GAG	1:10:4	-	0.05	0.21	0.52
kEL:COL:GAG	1:10:4	+	0.18	0.64	0.68

The results showed that the greatest quantity of active ingredients was in the membranes containing α-EL, COL and GAG, in both ratios, 1:20:4 and 1:10:4. Also, there were small differences in Hyp and total protein content between the 8 variants, probably due to the very strong and irreversible physical interaction between EL and COL I+III [9].

Swelling test. The ability of a matrix to preserve water is very important for its properties as a dermal dressing and could be attributed to the hydrophilic character of COL [1]. The swelling ratios of different membrane variants, related to the initial weight, are given in figure 1.

These values indicated that, before UV exposure, the swelling ratio decreased while the quantity of elastin increased. However, both membranes had an absolute value over 70 times that of their initial weight, which was acceptable for a skin repair product. In the case of UV-irradiated matrices, the cross-linking process reduced the hydrophilic groups [16] and, accordingly, the porosity and the volume for water storage [17], leading to the decrease of the swelling capacity.

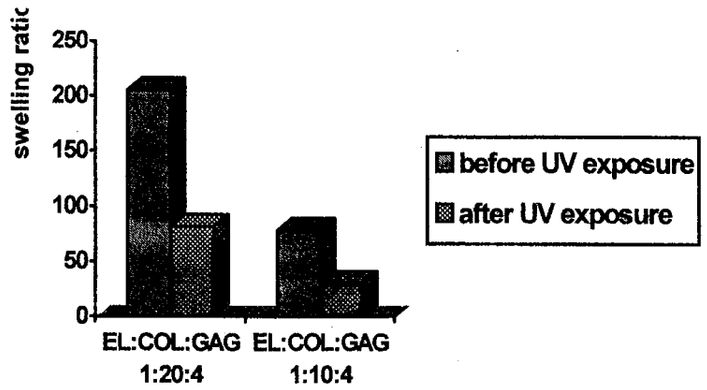

Fig. 1 – Composition and cross-linking influence on the swelling capacity.

In vitro biodegradability. An ideal biomaterial used for skin repairing should possess a controllable biodegradability [18]. The values for the degradation degree of the UV exposed and unexposed membranes are given in Table 2.

Table 2

Matrix degradation by bacterial collagenase treatment

Time (hours)	Degradation degree for αEL-COL-GAG matrix (%)	Degradation degree for kEL-COL-GAG matrix (%)
0	3.50	3.70
3	0.55	1.67
6	0.36	1.37
9	0.72	1.25

One could observe that UV exposure improved the membrane biostability, which was larger for the membranes with α-EL and smaller for k-EL membranes. Also, the UV exposure method avoids the side effects like cytotoxicity [19] and calcification [20] associated to the chemical cross-linking methods. In order to obtain cross-linked membranes, the optimal time for UV irradiation was 6 h.

From a biochemical point of view, the variants containing α-EL were selected as having the best composition and characteristics of the bioproduct.

Structural analysis of the membranes

The membranes prepared from EL:COL:GAG in 1:10:4 ratio were more fragile than those in 1:20:4 ratio, which indicated the need of a certain quantity of COL in order to obtain a stable bioproduct. Collagen may act as a glue for other components. The failure of some research teams to prepare scaffolds composed only of elastin could be due to the low number of amine groups in elastin [11].

SEM showed a fibrillar, dense, micro porous, three-dimensional structure of the membranes. The elastin presence induced the formation of a macromolecular aggregate with a different structure from that of the individual components. There was a uniform surface and the fibers were mostly orientated parallel or perpendicular to the surface, regardless of the elastin type (Fig. 2).

Fig. 2 – Scanning electron micrograph of a cross-section in the αEL membrane (× 2500).

The pore size of the membranes was not influenced by their composition. Their mean size was 2 μm. The dense microstructure of the membranes can prevent the protein and fluid loss and the bacterial invasion of skin defects. It also assures a great strength to mechanical forces and enzymes.

Cytocompatibility of the membranes in vitro

The morphology and viability of embryonic fibroblasts cultivated on the membranes were analyzed cytometrically and the computer-processed results are given in figure 3.

The results showed that the cells detached from the membrane containing k-EL presented the smallest percent of viable cells. Also, the cells from the membrane αEL:COL:GAG in 1:10:4 ratio presented some morphological changes, such as smaller size and diminished cellular content, in comparison to those from the membrane αEL:COL:GAG in 1:20:4.

Because the variant αEL:COL:GAG in 1:20:4 ratio allowed the best development of the fibroblasts, maintaining size and density values similar to the

control and greater than those for COL membranes, it was also tested by light microscopy.

We observed that dermal fibroblasts adhered after 24h (Fig. 4) and were disposed as small groups, after 72h, on the surface of the membrane (Fig. 5).

Altogether, the results presented here showed that the α-EL:COL:GAG membrane, in 1:20:4 ratio, gave the best values for the majority of tested parameters.

4. CONCLUSIONS

The best bioproduct composition had the ratio of the components EL:COL:GAG of 1:20:4, similar to that in the skin. Biochemically, the α-EL-COL-GAG membrane was superior to k-EL-COL-GAG membrane in active substance content and biodegradation rate. SEM analysis revealed a three-dimensional, fibrillar, dense structure, with a pore mean size of 2 μm. The surface was uniform, regardless the peptide type used. *In vitro* testing showed that the fibroblasts detached from the membranes, after 72h of cultivation, had no visible modifications in morphology and viability, when analyzed by flow-cytometry. Also, the α-EL:COL:GAG 1:20:4 membrane promoted the adhesion of embryonic fibroblasts in the culture.

This membrane variant can be used as a scaffold for dermal fibroblast proliferation or to develop a composite graft. Besides clinic applications, this matrix could be useful in the pharmaceutic and cosmetic fields.

Acknowledgement. This research was supported by Project No. 179 VIASAN.

REFERENCES

1. J.-E. LEE, J.-C. PARK, Y.-S. HWANG, J. K. KIM, J.-G. KIM, H. SUH, *Characterization of UV-irradiated dense/porous collagen membranes: morphology, enzymatic degradation, and mechanical properties,* Yonsei Med. J., **42**(2), 172–179 (2001).
2. L. MOLDOVAN, M. CALOIANU, O. ZARNESCU, *Membranele de colagen – substrat pentru celulele epiteliale in vitro,* Stud. Cerc. Biol., Seria Biol. Anim., **49**(1), 53–56 (1997).
3. L. MOLDOVAN, O. ZARNESCU, M. BUNEA, L. CONSTANTINESCU, *Changes induced by a collagen and glycosaminoglycan gel in corneal wound healing process*, J. Med. Biochem., **4**(1), 43–50 (2000).
4. S.Q. LIU, C. TIECHE, P.K. ALKEMA, *Neointima formation on vascular elastin and collagen matrix scaffolds implanted in the rat aorta*, Biomaterials, **25**, 101–115 (2004).
5. D.Y. LI, B. BROOKE, E.C. DAVIS, R.P. MECHAM, L.K. SORENSEN, B.B. BOAK, E. EICHWALD, M.T. KEATING, *Elastin is an essential determinant of arterial morphogenesis*, Nature, **393**, 276–280 (1998).
6. A. HINEK, *Biological roles of the non-integrin elastin/laminin receptor*, Biol. Chem., **377**, 471–480 (1996).

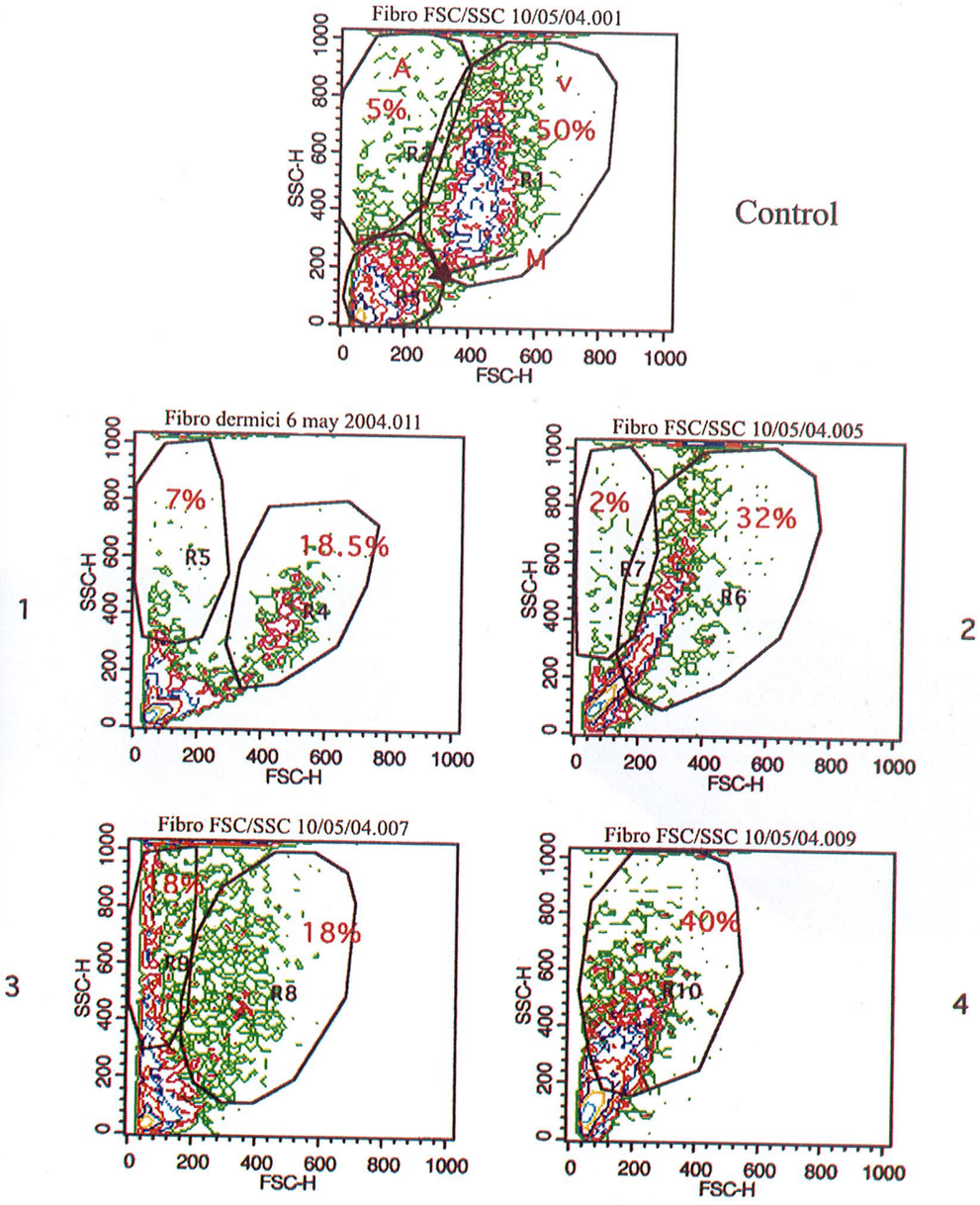

Fig. 3 – FSC/SSC system flow-cytometry analysis of embryonic fibroblasts grown on: (1) COL membrane; (2) αEL:COL:GAG 1:20:4 membrane; (3) kEL:COL:GAG 1:20:4 membrane; (4) αEL:COL:GAG 1:10:4 membrane; (control) fibroblast culture.

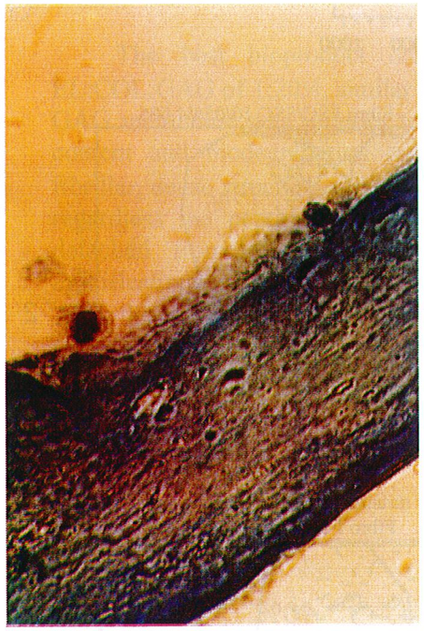

Fig. 4 – Light micrograph of the αEL membrane. There

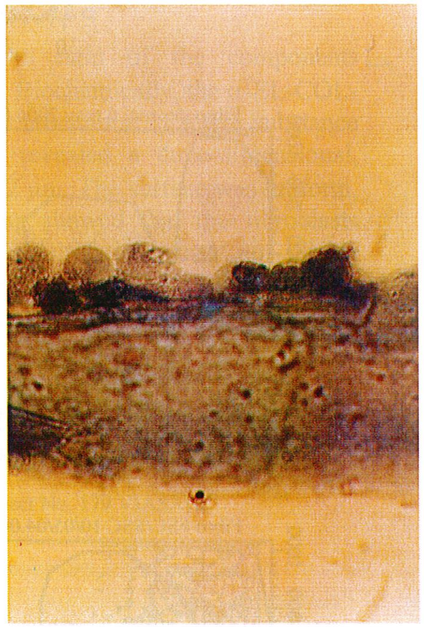

Fig. 5 – Light micrograph of the αEL membrane, after 72h in culture. A group of cells was seen on the

7. V. GROULT, W. HORNEBECK, P. FERRARI, J.M. TIXIER, L. ROBERT, M.P. JACOB, *Mechanisms of interaction between human skin fibroblasts and elastin: differences between elastin fibres and derived peptides*, Cell Biochem. Funct., **9**, 171–182 (1991).
8. S. DUTOYA, F. LEFEBVRE, C. DEMINIERES, F. ROUAIS, A. VERNA, A. KOZLUCA, A.M. LE BUGLE, *Unexpected original property of elastin derived proteins: spontaneous tight coupling with natural and synthetic polymers*, Biomaterials, **19**(1–3), 147–155 (1998).
9. M. RABAUD, F. LEFEBVRE, D. DUCASSOU, *In vitro association of type III collagen with elastin and with its solubilized peptides*, Biomaterials, **12**, 313–319 (1991).
10. N. BONZON, X. CARRAT, C. DEMINIERE, G. DACULSI, F. LEFEBVRE, M. RABAUD, *New artificial connective matrix made of fibrin monomers, elastin peptides and type I+III collagens: structural study, biocompatibility and use as tympanic membranes in rabbit*, Biomaterials, **16**, 881–885 (1995).
11. W.F. DAAMEN, H.Th.B. van MOERKERK, T. HAFMANS, L. BUTTAFOCO, A.A. POOT, J.H. VEERKAMP, T.H. van KUPPEVELT, *Preparation and evaluation of molecularly-defined collagen-elastin-glycosaminoglycan scaffolds for tissue engineering*, Biomaterials, **24**, 4001–4009 (2003).
12. G. NEGROIU, N. MIRANCEA, D. MIRANCEA, A. OANCEA, L. MOLDOVAN, *Collagen-chondroitin sulfate substrates conditioned as sponges and membranes*, *Rev. Roum. Biochim.*, **29**(1), 23–28 (1992).
13. J.M. DAVIDSON, M.G. GIRO, R.P. MECHAM, *Elastin* In: M.A. Haralson, J.R. Hassell, eds., *Extracellular Matrix*, IRL Press, Oxford, 1995, p. 241–260.
14. G. NEGROIU, L. MOLDOVAN, A. OANCEA, *Obţinerea şi caracterizarea chimică şi biochimică a colagenului tip II din cartilagiul traheal bovin*, St. Cerc. Biochim., **33**, 117–125 (1990).
15. M.M. BRADFORD, *A rapid and sensitive method for the quantitation of microgram quantities of protein utilizing the principle of protein-dye binding*, Anal. Biochem., **72**, 248–254 (1976).
16. M. REHAKOVA, D. BAKOS, K. VIZAROVA, M. SOLDAN, M.J. JURICKOVA, *Properties of collagen and hyaluronic acid composite materials and their modification by chemical cross-linking*, J. Biomed. Mater. Res., **29**, 1373–1379 (1995).
17. L. MA, C. GAO, Z. MAO, J. ZHOU, J. SHEN, X. HU, C. HAN, *Collagen/chitosan porous scaffolds with improved biostability for skin tissue engineering*, Biomaterials, **24**, 4833–4841 (2003).
18. G.P. CHEN, Y. USHIDA, T. TATEISHI, *Scaffold design for tissue engineering*, Macromolecular Biosci., **2**, 67–77 (2002).
19. L.L.H. HUANG-LEE, D.T. CHEUNG, M. NIMNI, *Biochemical changes and cytotoxicity associated with degradation of polymeric glutaraldehyde derived crosslinks*, J. Biomed. Mater. Res., **24**, 1185–1201 (1990).
20. R.J. LEVY, F.J. SCHOEN, F.S. SHERMAN, J. NICHOLS, M.A. HAWLEY, S.A. LUND, *Calcification of subcutaneously implanted type collagen sponges*, Am. J. Pathol., **122**, 71–82 (1986).

Received October 20, 2004.

*National Institute for Biological Sciences
296, Spl. Independenţei, Bucharest
e-mail: oana@dbio.ro

**Faculty of Biology, University of Bucharest
90–95, Spl. Independenţei, Bucharest

EFFECTS OF SOME BIOPRODUCTS BASED ON HYALURONATE FROM SWINE VITREOUS BODY ON THE SKIN

EUGENIA TEODOR*, VIORICA COROIU*, MARIA CALOIANU*, T. LEAU**

It is generally accepted that hyaluronan is associated with the tissue repair process. The benefits of exogenous-applied hyaluronan in tissue repair were tested. Biomaterials were prepared based on hyaluronate extracted from swine vitreous, lyophilized (freeze-dried) sponge-like and one variant of ointment, and were tested on laboratory animals (rabbits). The results (macroscopic and histology) confirmed the role of hyaluronic acid in stimulation of tissue remodeling (wounds healing).

1. INTRODUCTION

Epidermal structure, thickness, and keratinocyte turnover rate vary according to the developmental stage and physiological state of the tissue. Hyaluronan is closely involved in keratinocyte proliferation, migration, and differentiation, and therefore participates in all these regulatory changes. Accordingly, its metabolism is controlled by such signaling molecules as hormones, cytokines, and growth factors.

One of the obvious tasks for hyaluronan is maintenance of some extracellular space between the lower cells in the stratified structure of the epidermis to facilitate diffusion of nutritional supplies to and waste products from the upper cells. The tendency of this space to swell because of the presence of the high hyaluronan concentrations may destabilize desmosomes and adhere junctions between adjacent cells and enhance their turnover. Hyaluronan may thus facilitate the constant cellular remodeling through the lifetime of a keratinocyte, emerging from division of a columnar basal cell and ending as a flattened corneocyte (1).

Hyaluronan, an effective scavenger of free radicals, may also serve a protective role in epidermis by scavenging reactive oxygen species generated by ultraviolet radiation. The rapid turnover of hyaluronan may help to remove and clear noxious compounds from the epidermis.

Because hyaluronan is a hygroscopic macromolecule, hyaluronan solutions are highly osmotic, a property further increased in the presence of serum albumin as found in many tissue fluids. In the skin, this property is likely to be relevant in controlling tissue hydration during periods of change, such as embryonic development and during the inflammatory process (such as response to tissue injury) when hyaluronan levels are elevated.

REV. ROUM. BIOL. – BIOL. ANIM., TOME 49, N^{os} 1–2, P. 113–118, BUCAREST, 2004

The highly viscous nature of hyaluronan also contributes to retardation of viral and bacterial passage through the hyaluronan-rich pericellular zone (2).

Many reports have attested to the effects of exogenous hyaluronan in producing beneficial wound healing outcome. In animal experiments, topical applied hyaluronan has been shown to accelerate wound healing in rats (3) and hamsters (4), to reduce fibrotic scarring (5) and promote healing in chronic wounds such as venous leg ulcers (6).

Following injury, wound healing follows a series of tightly regulated, sequential events. These are inflammation, granulation tissue formation, reepithelization and remodeling. Hyaluronan is likely to have a multifaceted role in mediation of these cellular and matrix events (7).

The aim of this work is to show that a glycoproteic extract from swine vitreous processed into sponges and ointment stimulates wounds healing and tissue remodeling.

2. METHODS

Sponge-like biomaterials

Were working out the following species of biomaterials like lyophilized sponge:

Variant 1)

– 1% chitosan (SIGMA) solution (MW 600 000 Da) in 0.2 M CH_3COOH,

– glycoproteic extract (at least 70% hyaluronate with MW 220 000 Da), solution 0.5–1% HA in 0.2 M NaCl. The extract obtention and characterization and *in vitro* testing were previously done (8,9).

Preparation:

– 1 g chitosan dissolved in 0.2 M acetic acid are mixed with 0.5–1 g glycoproteic extract, homogenized and diluted with distilled water up to 150 ml; mixture pH = 5.5. The mixture is strongly homogenized, degassed and lyophilized 48 hours at – 40°C to an CHRIST-MARTIN, ALPHA 1–4 freeze-dryer.

Variant 2)

– 1% chitosan (FLUKA) solution (MW 60 000 Da) in 0.2 M CH_3COOH,

– glycoproteic extract (the same)

Preparation:

– 1 g chitosan from crabs shells dissolved in 0.2 M acetic acid are mixed with 0.5–1 g glycoproteic extract and 0.06 g ascorbic acid, homogenized and diluted with distilled water up to 150 ml; mixture pH = 4.5. The mixture is strongly homogenized, degassed and lyophilized 48 hours at – 40°C to an CHRIST-MARTIN, ALPHA 1–4 freeze-dryer.

Differences between the two sponge variants are the molecular weight of chitosan and a small change of composition. The biologicals obtained are homogeneous, with white-cream color, 3–4 mm thickness, good consistency, which were cut away in pieces of 3–4 cm, were mounted in transparent mounting foil and sterilized on UV on each side for 12 hours.

Gel-like and ointment biomaterials

The ointment was prepared in one variant with the following composition:

– 20 g petrolatum,

– 10 g lanolin,

– 10 ml solution of glycoproteic extract (the same), 1–5 g in distilled water,

– 0.13 g ascorbic acid.

Preparation:

The ingredients are carefully homogenized into a porcelain jar and sterilized for 12 hours on UV. It was obtained a homogeneous yellowish cream, simply to administer on the skin.

Gel composition is the same with the second variant of sponge.

Skin tolerance test (10)

Skin tolerance is determined by two tests, one using skin coating and the other applications of active substance in the shape of occlusive bandage (11).

For skin coating test rabbits were employed. After 7 days of treatment fragments of skin were assayed for histological tests (not necessarily to sacrifice the laboratory animals).

Histology

For light microscopy, fragments of skin were assayed from an experimental group of rabbits (which *a priori* had accomplished anesthesia with xyline). The samples were fixed for 72 hours, at room temperature, in Bouin fixing agent with 20% DMSO (dimethylsulfoxide) for a better permeability. After fixing, samples were washed, removed water in ethanol, clarified in xylene and included in paraplast. After cutting on a section cutter, 5μm sections were stained with haematoxylin-eosine, mounted in Canada balsam and histologically evaluated on Leitz light microscope.

3. RESULTS

Skin tolerance

The biomaterials obtained (sponge-like, gel-like and ointment) were tested for skin tolerance in animal experiments (rabbits). To animals were generated

burns and wounds (minimal, as shown in Fig. 1), which were treated with ointment and gel (or sponge), once a day for 7 days. The sponge-like materials were implanted under the skin for absorbing or rebutting observations. For each type of lesion (on the back) it was a blank zone on the left side and the treated zone on the right side.

According to the notices from daily protocols, biomaterials were perfectly tolerated and macroscopically, the healing process was faster on the gel or ointment treated zone (Fig. 2). After 7 days period of treatment, the lesions were similarly healed on the gel, sponge or ointment treated zones.

Daily observations did not notice any erythema, edema, or appearance of crusts or scars. Biomaterials were totally tolerated (level 0).

After a 7 days period, fragments of tissue were sampled for histological assays. It was not necessary to sacrifice the animals. The lesions provoked by sampling were treated further to accelerate healing. After 7 days, the lesions were completely cicatrized and zones covered with hair (Fig. 3).

Histology

After 7 days period from induced skin wounds (by burning and scarring) and their treatment with sponge-like and ointment biomaterials it was noticed that wounds were completely covered. In all analyzed cases, histology attests multi-layer epithelia organization, more or less keratinization and a vascular dermis.

After treatment with ointment of scarring skin wounds light microscopy reveal a completely remade multi-layer epithelium (Fig. 4). Basal layer is well organized, closed by subsequent layers and distinctly keratinized.

In gel variant treatment, new-formed epidermis is multi-layered, with a rough keratinized interface and a less organized basal layer.

Application of sponge-like biomaterial determined the most advanced reepithelization process. As shown in Fig. 5, epidermis is formed closed by sponge-biomaterial. Although in this stage dermal tissue does not appear completely organized, it does not contain inflammatory cells.

Instead, after the same period of time, blank-animals skin is disarranged and with a great rate of inflammatory cells (Fig. 6).

Provoked skin burns treated with biomaterials based on hyaluronic acid processed like ointment, gel or sponge are completely healed after 7 days, so confirmed by histological evaluation.

Application of ointment determined the reepithelization (new multi-layer epidermis formation and distinct keratinization, Fig. 7). Basal layer is closed by a contiguous dermis.

After 7 days application of gel, light microscopy revealed the most distinct development of a multi-layer new epithelium (5–6 layers) and an emphasized keratinization process (hyperkeratinization) (Fig. 8).

Fig. 1 – Initial lesions generated by burns (left) and scarring (right).

Fig. 2 – Untreated burn (blank- left), burn treated with ointment (right).

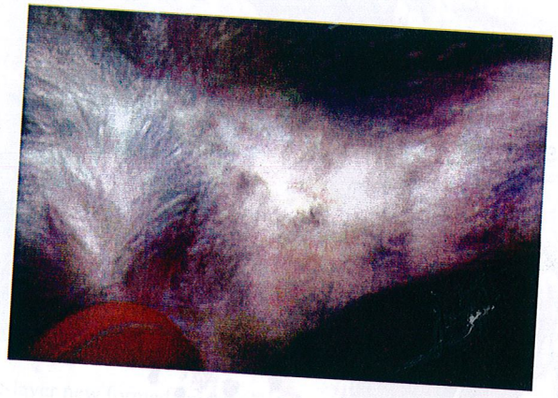

Fig. 3 – Macroscopic aspect of healed skin, after 7 days of treatment with biomaterials.

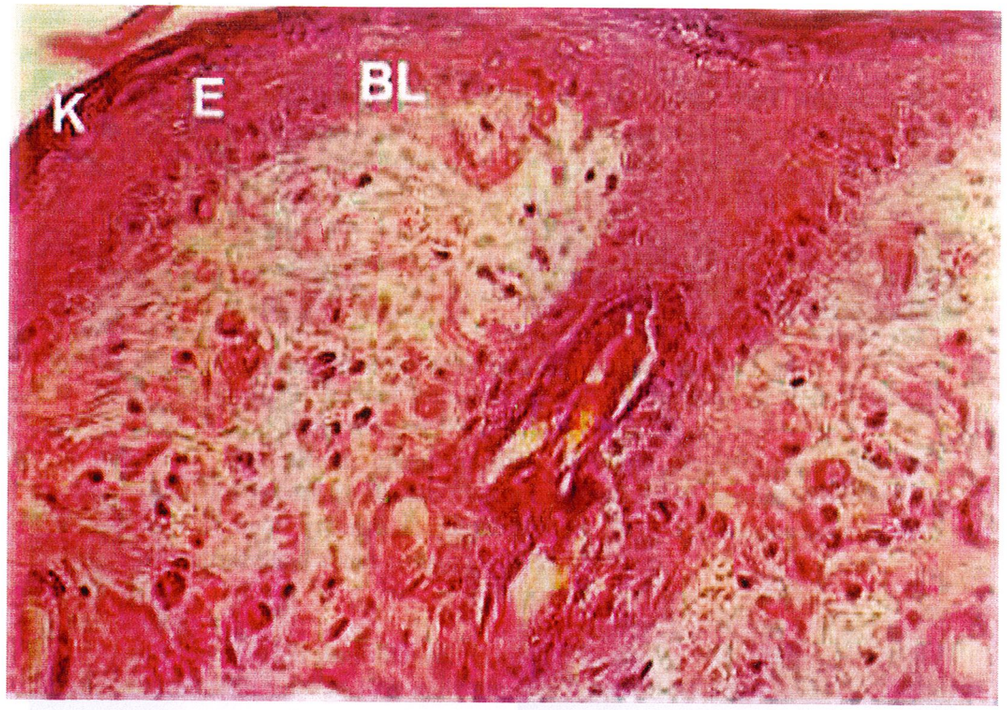

Fig. 4 – Multi-layer neo-epithelia (E). distinct keratinization (K). basal-layer well organized (BL). haematoxylin- eosine (× 160).

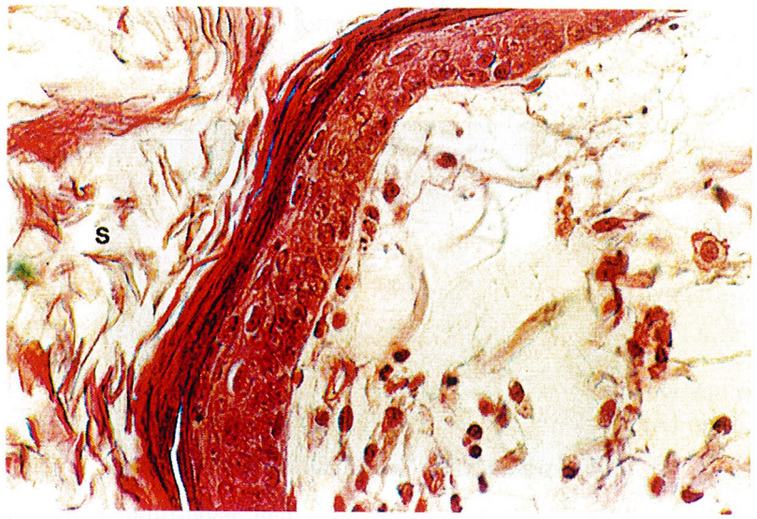

Fig. 5 – Advanced reepithelization and keratinization, sponge (S) – haematoxylin-eosine (× 400).

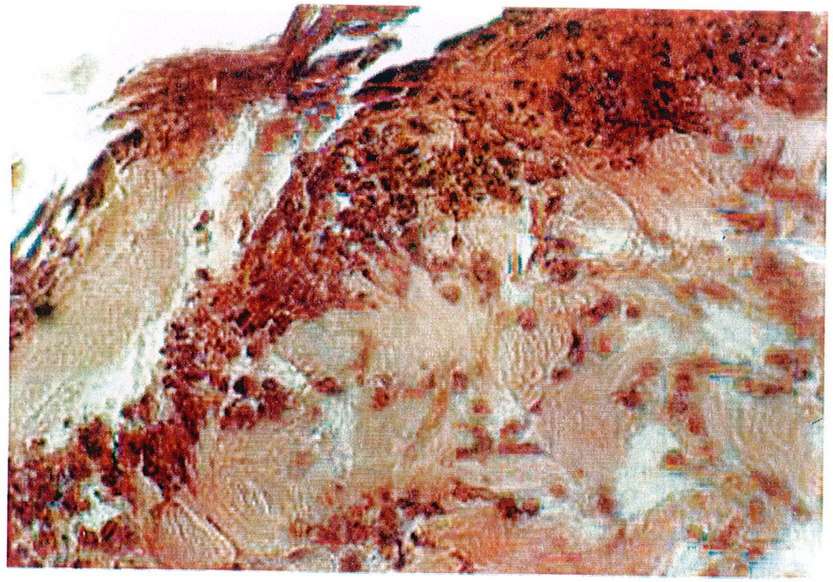

Fig. 6 – Wound site with marked cellular disorganization and inflammatory cell infiltration, haematoxylin-eosine (× 250).

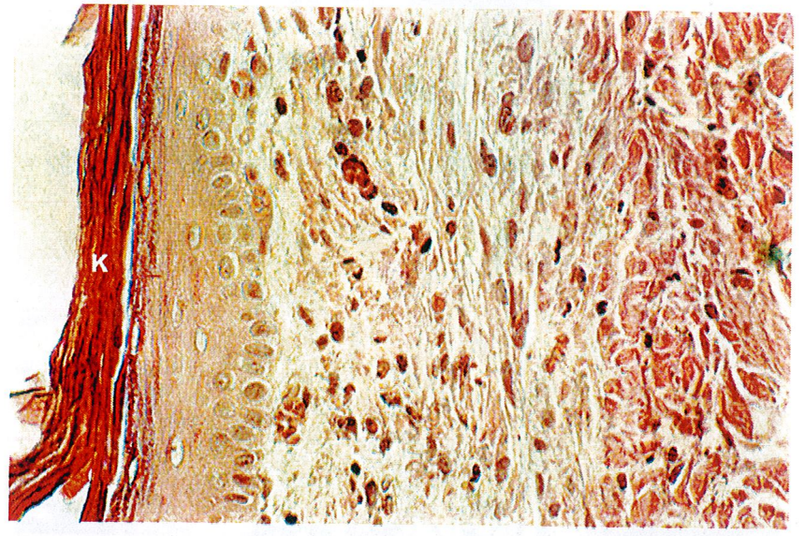

Fig. 7 – Multi-layer new formed epidermis, keratinization (K) – haematoxylin-eosine (× 400).

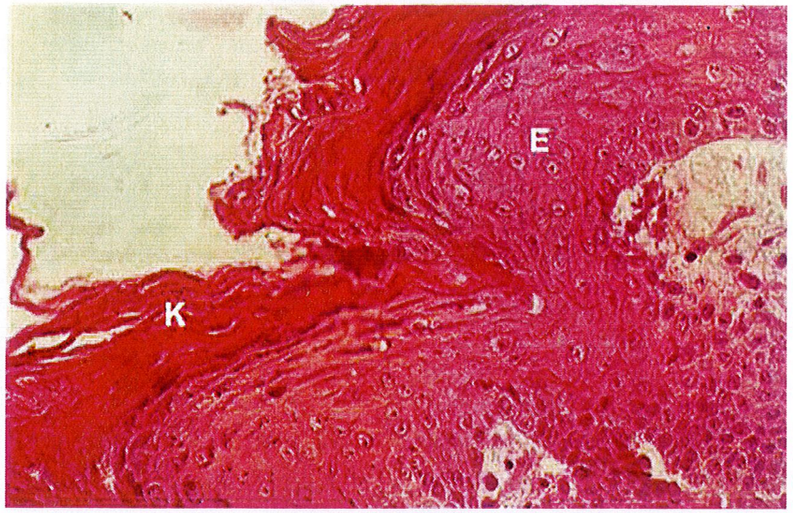

Fig. 8 – Re-epithelization completed. New-epithelia (E) multi-layered (5–6 layers). Keratinization (K) - haematoxylin-eosine (× 400).

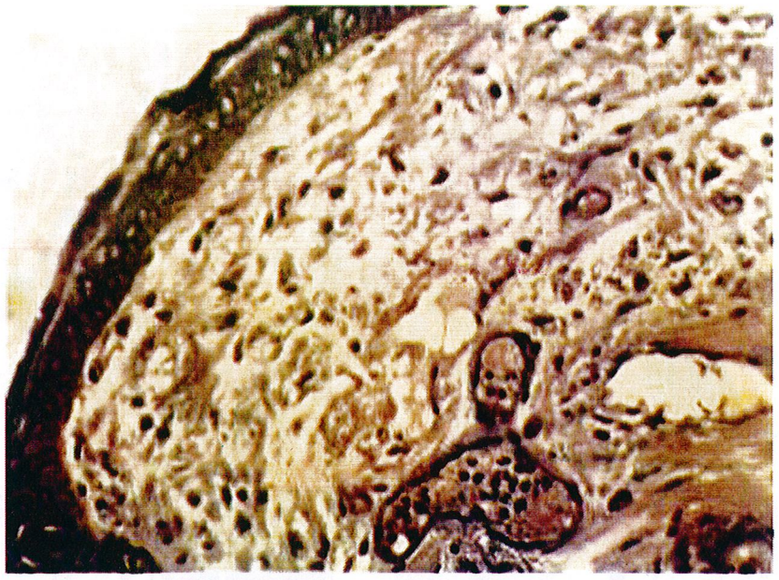

Fig. 9 – Complete epithelia, keratinization, vascular dermis. – haematoxylin (× 400).

Application of sponge-like material also determined a complete reepithelization, with a thinner epidermis formation and a basal layer well-organized but not closed by vascular underlying dermis and by wound's bed (Fig. 9).

4. DISCUSSIONS

There were fabricated biomaterials sponge-like based on glycoproteic extract from swine vitreous (hyaluronic acid) and chitosan and ointment-like with the same extract, which were tested in wounds healing experiments.

Hyaluronan is present at very high concentrations in the narrow extracellular space between the stratified keratinocytes of the epidermis and has a turnover time of less than 1 day. This dynamic metabolism suggests that hyaluronan is a space filler involved in the upwards migration and shape changes of the differentiating keratinocytes, that it provides extracellular space for the exchange of nutritional and regulatory metabolites for the upper spinous cells, and that it acts as a signaling ligand to enhance keratinocyte motility and survival. So, exogenously applied hyaluronate on the skin must be a benefit in the tissue repair process, to potentate the role of endogenous hyaluronate from early in the inflammatory activation process to granulation tissue formation and to the reepithelization process.

The biomaterials like gel, sponge and ointment, based on hyaluronate from swine vitreous, were tested on animal experiments for skin tolerance and the effects in wounds healing and tissue remodeling of skin. The results were satisfactory, daily observations (macroscopically) did not notice any erythema, edema, crusts or scars on the treated areas from animal's skin. The healing process was obviously faster on the treated areas in comparison with blank lesions.

Histological studies emphasize in all examined cases, after treatment with biomaterials based on hyaluronic acid from swine vitreous, the formation of a new multi-layer epithelium, more or less distinct keratinization and a vascular dermis.

Histology demonstrates that experimentally provoked and non-treated wounds were less reepithelized than those treated with biomaterials based on a glyco-proteic extract from swine vitreous body.

The experiments demonstrate that glyco-proteic extract with at least 70% hyaluronate of low-medium molecular mass is efficient in skin wounds healing, beside other reports with highly purified hyaluronate molecules of high molecular mass used in ocular and joint surgery (12, 13).

Similar experiments, with hyaluronic acid applied exogenously (0.9% solutions) after cervical tracheoplasty in dogs reduced postsurgical tracheal stenosis and inflammations and improved the quality of the tracheal healing (14).

REFERENCES

1. Tammi R., Tammi M., *Hyaluronan in the epidermis,* Science of Hyaluronan Today, ed. V. Hascall and M. Yanagishita, www. glycoforum.gr.jp./hyaluronan/ (2001).
2. Clarris B. J., Fraser J. R. E., Rodda S. J., *Effect of cell-bound HA in infectivity of Newcastle disease virus for human synovial cells in vitro,* Ann. Rheum. Dis., **33**, 240–2 (1970).
3. Abatangelo G., Martell M., Vecchia P., *Healing of HA-enriched wounds: histological observation,* J. Surg. Res, **35**, 410–6 (1983).
4. King S. R., Hickerson W. I., Proctor K. G., Newsome A. M., *Beneficial actions of exogenous HA on wound healing,* Surgery, **109**, 76–84 (1991).
5. Longaker M. T., Chiu E. S., Adzick N. S., Stern M., Harrison M. R., Stern R., *Studies in fetal wound healing. 5. A prolonged presence of HA characterizes fetal wound fluid,* Surg., **213**, 292–6 (1991).
6. Ortonne J. P., *A controlled study of the activity of HA in the treatment of venous leg ulcers,* J. Dermatol. Treat., **7**, 75–81 (1996).
7. Chen W. Y., Abatangelo G., *Functions of HA in wound repair,* Wound Repair Regen., **2**, 79–89 (1999).
8. Teodor E., Cutaş F., Moldovan L., Tcacenco L., Caloianu M., *"Characterization of hyaluronic acid extracted from swine vitreous humour by liquid chromatography"*, Rom. Biol. Sci., **I**, 1–2, 35–46 (2003).
9. Buzgariu W., Teodor E., Cutaş F., Ghilă L., Caloianu M., *"Effects of hyaluronan from suine eyes on fibroblastic embryonic cells"*, Rom. Biol. Sci., **I**, **1–2**, 11–22 (2003).
10. Simionovici M., Cârstea Al., Vlădescu C., *Cercetarea farmacologică şi prospectarea medicamentelor*, Ed. Medicală, 437 (1983).
11. Ghişoiu C., Sesiunea Ştiinţifică VI-ICCF, Bucureşti (1976).
12. Balasz E. A., Dorlinger J. I., *Clinical uses of hyaluronan,* In: Evered D., Whelan J., eds., *The biology of hyaluronan*, Chichester, J. Wiley & Sons, 265–80 (1989).
13. Balasz E. A., Laurent T. C., *New applications for hyaluronan*, In: Laurent TC ed: *The chemistry, biology and medical applications of hyaluronan and its derivatives*, London: Portland Press, 325–36 (1998).
14. Olmos-Zuniga J. R., Santos-Cordero J. A., Jasso-Victoria R., Sotres-Vega A., *Effect of the HA on tracheal healing. A canine experimental mode,* Acta Ottorinolaringol. Esp., **2**, 81–7 (2004).

Received August 15, 2004.

*National Institute for Biological Sciences, Bioanalyses Department, Bucharest, Spl. Independenţei 296, sector 6, dida@dbio.ro

**UASVM, Faculty of Veterinary Medicine, Bucharest, Spl. Independenţei

CYTOCHEMICAL DEMONSTRATION OF THE ACTIVATION OF ERYTHROCYTE MEMBRANE BOUND β-GALACTOSIDASE BY Ca^{2+} INDUCTION OF CELL APOPTOSIS

LAURA MITROFAN*, DANIELA BRATOSIN**, GEORGIANA C. PALII***, VLAD ARTENIE***, ALEXANDRU G. MARINESCU* and JEAN MONTREUIL****

The increase of β-D-galactosidase activity in various ageing nucleated cells has been recently proposed by Dimri et al. (1995) as a novel senescence biomarker called "senescence associated β -galactosidase" (SA-β-Gal). The demonstration was founded on a cytochemical assay using 5-bromo-4-chloro-3 indolyl-β-D-galactosid (X-Gal) a chromogene which develops a blue color due to the formation of 5-bromo-4-chloro-3 indol in the presence of β-galactosidase activity. As we have recently reported (Bratosin *et al.*, 2001) that mature human red blood cells (RBCs) undergo a rapid self-destruction process sharing several features with apoptosis in spite of the absence of mitochondria and this regulated form of programmed cell death (PCD) was induced by Ca^{2+} influx. We have extended the Dimri's cytochemical assay to senescent human RBCs. In the present paper, we demonstrate that the senescence of human RBCs induced by Ca^{2+} influx is marked by the significant increase of the cell membrane β-galactosidase activity that is well correlated with an increase of phosphatidylserine (PS) externalization.

Key words: human RBC, senescent erythrocytes, SA- β-Gal, flow cytometry, cytochemistry.

INTRODUCTION

Human red blood cells (RBCs) have a definite life span of approximately 120 days in the circulation, after which they are phagocytosed by resident macrophages. Every day, 360 billion erythrocytes are removed from the circulation or 5 million per second. This homeostatic phenomenon raises the following questions:

1. What signals the death sentence of RBCs ?
2. What molecular mechanism sequesters senescent RBCs from the bloodstream with such a precision?
3. By what signal do the macrophages distinguish between mature and senescent erythrocytes?

The progressive changes of RBCs, leading to their senescence and death, involve fundamental changes of the cell; desialylation of the RBC cell surface glycoconjugates that induce the capture of erythrocytes by macrophages and externalisation of phosphatidylserine in the membrane outer leaflet that induces the phagocytosis.

REV. ROUM. BIOL. – BIOL. ANIM., TOME 49, N^os 1–2, P. 119–127, BUCAREST, 2004

All these changes are markers of apoptosis, also called programmed cell death (PCD). We have recently reported that mature erythrocytes can undergo a rapid self-destruction process sharing several features with apoptosis: cell shrinkage, plasma membrane vesiculisation, phosphatidylserine externalization that lead to erythrocyte disintegration, or, in the presence of macrophages, to macrophage ingestion of dying erythrocytes. This regulated form of PCD was induced by Ca^{2+} influx and we demonstrated for the first time that a death programme can operate in the absence of mitochondria and nucleus, indicating that mature erythrocytes share with all other mammalian cell types the capacity to self-destruction in response to environmental signals (Bratosin *et al.*, 2001).

RBC membrane has as main functions not only the transport of oxygen and carbon dioxide between lungs and tissues, but also the control *via* the cytoskeleton of the size, shape, integrity, flexibility of the cell as well as cell-cell interactions and membrane fusion. Its architecture is typical of all living cell membranes and, interspaced within the lipid bilayer, are hundreds of integral proteins with various functions such as enzymes, transporters and receptors. Enzymes are essentially hydrolases, including glycosidases like sialidases and β-galactosidases which play a central role in RBC apoptosis and phagocytosis. In fact, sialic acids play a key role in the life span of RBCs as antirecognition signals. Desialylation of membrane glycoconjugates by sialidases well characterized by Tettamanti's group (Venerado *et al.*, 1997; Tringali *et al.*, 2001), by demasking the penultimate β-galactose residues of glycoconjugates induces the capture of the desialylated RBCs mediated by a β-galectin present in the macrophage membrane.

With regard to β-galactosidases, it is well known that they are markers of programmed cell death since Dimri's group has recently demonstrated that their activity increases with the physiological senescence of cells leading to the concept of "senescence associated β-galactosidase" (SA-β-Gal) (Dimri *et al.*, 1995). This observation was founded on a cytochemical test using chromogenic substrate, the 5-bromo-4-chloro-3-indolyl-β-D-galactoside (X-Gal) which develops *in situ* a blue color in the presence of β-galactosidase activity due to the formation of 5-bromo-4-chloro-3-indol. This discovery was confirmed by other authors (Thomas *et al.*, 1997; Xu *et al.*, 1997; Brenner *et al.*, 1998; Carman *et al.*, 1998; Litaker *et al.*, 1998; Mendez *et al.*, 1998; Naasani *et al.*, 1998; Yegorov *et al.*, 1998).

These results generated active researches, which led to the characterization of three forms of β-galactosidases: the lysosomal form (optimal pH: 4.5), the marker SA-β-Gal (optimal pH: 6) and a neutral form (Kuo *et al.*, 1978). The first and the second forms have a strong affinity for indigogenic substrate.

On the basis of our findings providing the demonstration that a regulated form of programmed cell death showing several features with apoptosis can rapidly be induced in human mature RBCs by calcium influx (Bratosin *et al.*, 2001), we hypothesized that Ca^{2+}-treated erythrocytes could express, like nucleated cells, the "senescence associated β-galactosidase" marker. We carried out the experiments by

applying the cytochemical assay proposed by Dimri *et al.* (1995) to human RBCs incubated with Ca^{2+} (2.5 mM) in the absence or presence of calcium ionophore A 23187 (0.5 μM). Results were correlated with the percentage of phosphatidylserine externalization determined by using the annexin V-FITC cytofluorimetric test.

MATERIALS AND METHODS

Chemicals

Human serum albumin, phenylmethylsulfonyl fluoride (PMSF) were purchased from Sigma Aldrich (Saint Louis, Mo, USA), fluorescein isothiocyanate (FITC) conjugated annexin V and HEPES buffer pH 7.4 containing 2.5 mM $CaCl_2$ were from Pharmingen (San Diego, CA, USA). Ca^{2+} ionophore A 23187 from *Streptomyces chartreusis* was purchased from Calbiochem (La Jolla, CA, USA) and the *Senescence Associated β-galactosidase Staining Kit* was from Cell Signaling (Beverly, MA, USA).

Cells and culture conditions

Human erythrocytes were purified from heparinized peripheral blood from healthy donors (O Rh+ blood type) supplied by the Etablissement Régional de Transfusion Sanguine de Lille. After centrifugation (2 000g, 4°C, 5 min), plasma, platelets and leukocytes were removed by pipetting. Erythrocytes were washed three times in Dulbecco's phosphate-buffered saline solution pH 7.4 (PBS: 137 mM NaCl, 2.7 mM KCl, 8.1 mM Na_2HPO_4 and 1.5 mM KH_2PO_4) and resuspended (10^7 cells per ml) in HEPES buffer (10 mM HEPES, 140 mM NaCl), pH 7.4 supplemented with 0.1% human serum albumin. Aging of red blood cells was artificially induced by incubation in HEPES buffer pH 7.4 containing 2.5 mM $CaCl_2$ in the presence or absence of ionophore A 23187 (0.5 μM) for different times points under 5% CO_2 atmosphere as previously described (Bratosin *et al.*, 2001).

Flow cytometric analysis of phosphatidylserine exposure

Human erythrocytes were suspended in HEPES (N-(2-hydroxymethyl) piperazine-N'-(2-ethane) sulfonic acid) buffer, pH 7.4, containing 2.5 mM $CaCl_2$. One hundred microliters of the cell suspension (1×10^5 cells) were incubated for 15 minutes in the dark with 10 μl (0.1 μg) FITC-annexin V solution. The suspension of cells in isotonic PBS buffer, pH 7.4 (osmolality 320–330 mosmol·kg^{-1}), was analyzed in the flow cytometer and gated for biparametric histograms FL1 (FITC fluorescence) *versus* FL2 (RBC autofluorescence). Five thousand fluorescent particles of each gated population were analyzed. Data were collected on a Becton Dickinson FACScan cytometer (Becton-Dickinson, San Jose, CA, USA), using

LYSIS software for data acquisition and analysis. The light scatter channels were set on linear gains and the fluorescence channels on a logarithmic scale.

SA β-Galactosidase staining

The senescence β-galactosidase staining kit protocol from Cell Signaling was used (Dimtri *et al.* 1995). This kit is designed to cytochemically detect β-galactosidase activity at pH 6, a known characteristic of senescent cells. The kit includes all reagents necessary for this assay. After removal of incubated medium, cells were washed once with 2ml of PBS, pH 7.4. 5×10^6 RBCs were treated with 1ml of a fixative solution (2% formaldehyde, 0.2% glutaraldehyde in PBS saline buffer pH 7.4), for 10–15 minutes at room temperature. The cells were washed twice with 2ml of PBS buffer and 1 ml of the staining solution containing 49.16 mM X-Gal was added. The plate Nunclon TM Surface with 6 wells (35 mm) was incubated overnight at 37°C under 5% CO_2 atmosphere. The cells were checked under a microscope LEICA DM IRB/E (200× total magnification) for development of blue color. The pictures were taken with a PENTAX Z 70 (Asahi Optical Co) and Fuji 200 ASA film using a blue filter. For long-term storage of stained wells, after removal of the staining solution, cells were overlaid with 70% glycerol and stored at 4°C.

RESULTS AND DISCUSSIONS

Ca^{2+} induced senescence in the erythrocyte model

As shown in Figure 1, incubation of human erythrocytes with the calcium-ionophore A 23187 in the presence of extracellular Ca^{2+} (2.5 mM) led to a rapid phosphatidylserine externalization which is time dependent since after 0.5, 1 and 2 hours incubation, 8.66, 40.3 and 73.62% of RBCs were annexin V-positive, respectively. PS externalization was associated with a marked increase in cytochemically detectable SA β-Gal activity in RBCs membrane. At 0 hour incubation time with Ca^{2+} we had a little effect on staining in cells (SA β-Gal negative cells). Incubation of human erythrocytes with Ca^{2+} (2.5 mM) alone, in the absence of A 23187, induced a slower senescence process and the percentage of annexin V-positive cells increases from 2.08 in untreated RBCs to 9.74, 32.88 and 67.82% after 24, 48 and 72 h incubation, respectively (Fig. 2) and requires 96 hours to lead to 86.62%.

The reliability and specificity of SA β-Gal staining as a biomarker for aging was tested in the same conditions and an increase of the staining was observed as evidenced by figures 1 and 2 clearly demonstrating that the enzyme activity is well correlated with the percentage of phosphatidylserine externalization and that the SA β-Gal staining increases in the aging process. Our results also indicate the reliability and efficiency of this marker as indicator of aging or environmental stress.

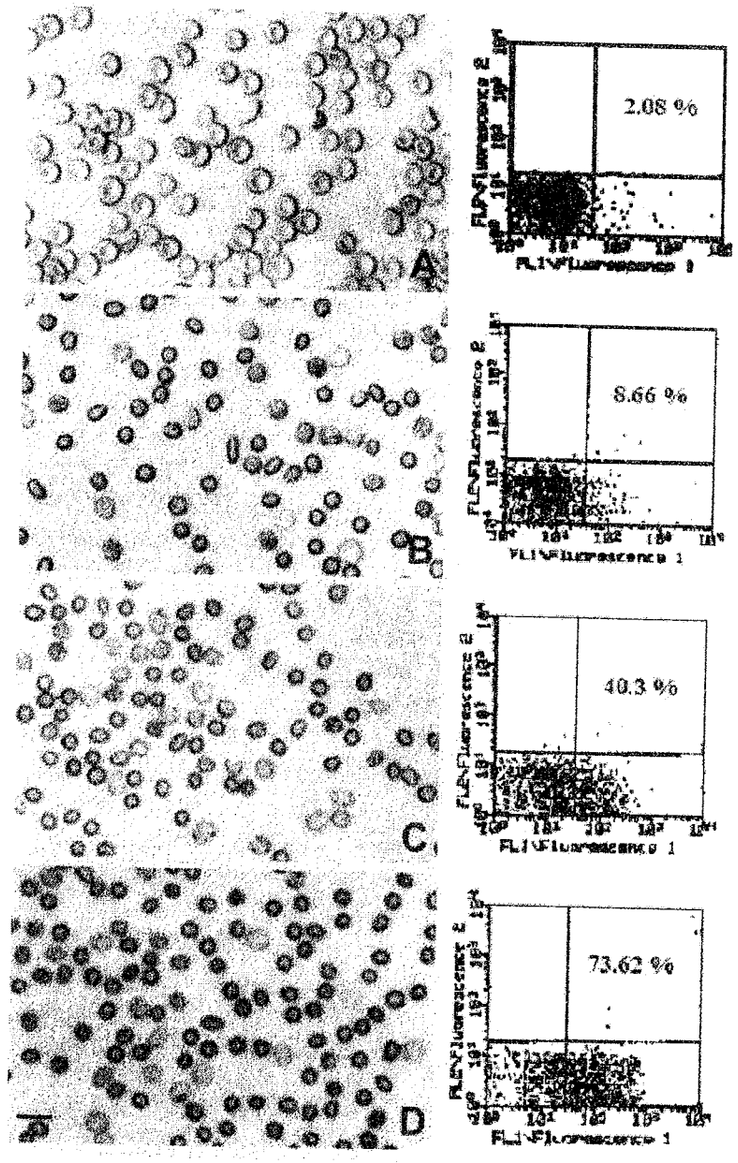

Fig. 1 – Cytochemical staining of β-galactosidase activity in erythrocyte membrane (a) correlated with the percentage of phosphatidylserine externalisation (annexin-V-FITC cytofluorimetric test) (b). Freshly isolated and purified human mature erythrocytes were analyzed after 0 hour (A), 0.5 hour (B), 1 hour (C) and 2 hours (D) time incubation in medium in the presence of 0.5 μM A 23187 and Ca^{2+} (HEPES buffer pH 7.4 containing 2.5 mM $CaCl_2$) at 37° C. Annexin V labeling: the percentages indicate the positive annexin V-positive erythrocytes (lower right quadrant). 5.000 cells were analyzed in each experimental condition. Bar: 10 μm.

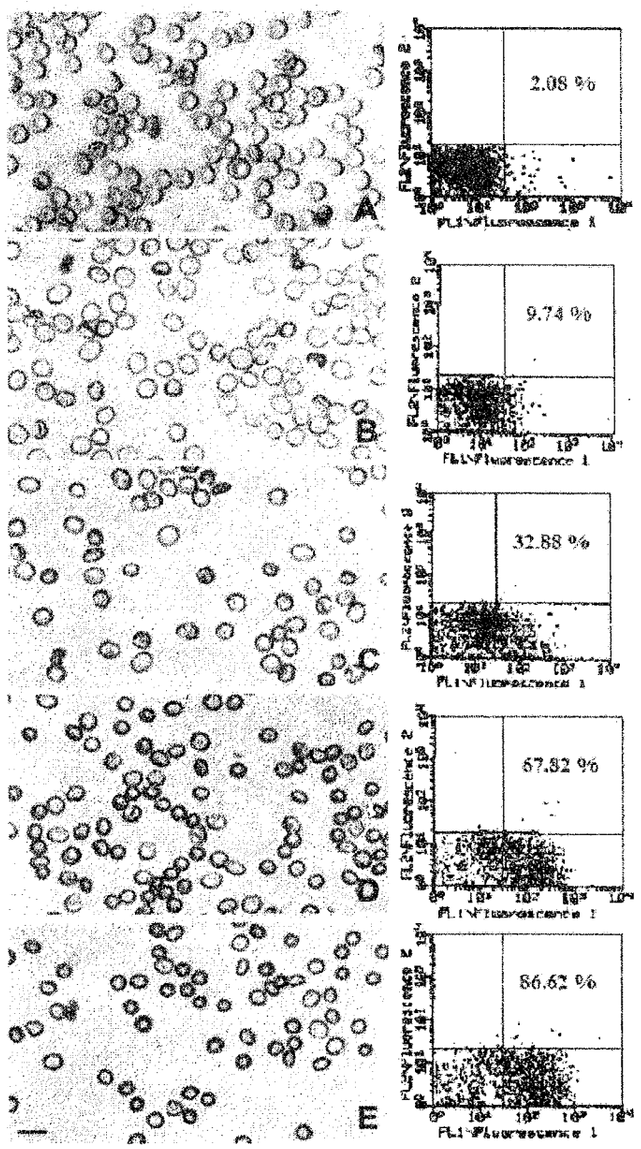

Fig. 2 – Cytochemical staining of β-galactosidase activity in erythrocyte membrane (a) correlated with the percentage of phosphatidylserine externalisation (annexin-V-FITC cytofluorimetric test) (b). Freshly isolated and purified human mature erythrocytes were analyzed after 0 hour (A), 24 hours (B), 48 hours (C), 72 hours (D) and 96 hours (E) time incubation in medium in the presence of Ca^{2+} alone (HEPES buffer pH 7.4 containing 2.5 mM $CaCl_2$) at 37° C. Annexin V labeling: percentages indicate the annexin V-positive erythrocytes (lower right quadrant). 5.000 cells were analyzed in each experimental condition. Bar: 10 μm.

These findings indicate once more that mature human RBC share, with other mammalian cell types, common features with apoptosis. In addition, they could solve the enigma raised by abnormal and unexplained results we obtained 10 years ago (Bratosin *et al.*, 1995) in the comparative study of young and aged human RBCs using FITC-labeled lectins specific for sialic acid (wheat germ, sambucus nigra and *Maackia amurensis agglutinins*) and for β-galactosyl terminal residues (*Ricinus communis* and *Erythrina crystagalli agglutinins*). In fact, analysis by flow cytofluorimetry of FITC-treated erythrocyte confirmed that aged RBCs bound less sialic acid specific lectins than young RBCs, but experiments carried out with β-galactose specific lectins led to unexpected and unexplained results with a decrease in the number of lectin-binding sites associated with increasing desialylation. On the basis of the demonstration we have brought that the β-galactosidase activity increases in senescent RBCs, we could explain these abnormal results by degalactosylation following the desialylation of membrane glycoconjugates so demasking the antepenultimate monosaccharides, *i.e.*, α- or β-N-acetylglucosamine or -galactosamine which could be the actual signals for RBC capture by macrophages. This enigma remains a fascinating and exciting challenge.

CONCLUSIONS

The results presented in this paper demonstrate the soundness of our hypothesis according to which erythrocytes constitutively express a death machinery capable of inducing plasma membrane changes associated with apoptosis of nucleated cells (Bratosin *et al.*, 2001). In fact we have shown that the Dimri's "senescence associated β-galactosidase" is a marker of ageing human erythrocyte as well as in nucleated cells undergoing programmed cell death. This view is confirmed by the demonstration we brought that the activation of the β-galactosidase present in the membrane of senescent RBCs is perfectly corroborated with the rate of phosphatidylserine externalization, a marker of erythrocyte programmed cell death. This new marker of RBC senescence represents a useful tool to estimate the erythrocyte ageing *in vitro* and, consequently, to control the quality of stored RBC in blood banks. In addition, applied to erythrocytes of aquatic animals, the "SA-β-gal test" can be an efficient ecotoxicologic biomarker.

Acknowledgements. This work was supported in part by the Université des Sciences et Technologies de Lille 1, the Ministère de l'Enseignement Supérieur de la Recherche et de la Technologie, the Centre National de la Recherche Scientifique (UMR no. 8576 du CNRS, Director: Dr. Jean-Claude Michalski), the Etablissement Régional de Transfusion Sanguine de Lille (Director: Dr. Jean-Jacques Huart), the MacoPharma Co., Tourcoing, France (Director: Dr. Francis Goudaliez) and the Romanian Academy in conformity with the collaboration agreement between the Biological

Institute of the Romanian Academy and Université des Sciences et Technologie, Lille 1. Dr. Daniela Bratosin and Laura Mitrofan are fellows of MacoPharma Co. The authors are grateful with many thanks to Dr. Jean-Jacques Huart and Hervé Dubly (Chairman of MacoPharma Co.) who provided a kind interest and financial support to this project.

REFERENCES

1. Bratosin D., Estaquier J., Petit F., Arnoult D., Quatannens B., Tissier J.P., Slomianny C., Sartiaux C., Alonso C., Huart J.J., Montreuil J., Ameisen J.C. Programmed cell death in mature erythrocytes: a model for investigating death effector pathways operating in the absence of mitochondria. Cell Death Differ 2001, **8:** 1143–1156.
2. Bratosin D., Mazurier J., Debray H., Lecocq M., Boilly B., Alonso C., Moisei M., Motas C., Montreuil J., Flow cytofluorimetric analysis of young and senescent human erythrocytes probed with lectins. Evidence that sialic acids control their life span, Glycoconj. Journal, **12**, 1995, 258–267.
3. Brenner A.J., Stampfer M.R., Aldaz C.M., Increased p16 expression with first senescence arrest in human mammary epithelial cells and extended growth capacity with p16 inactivation. Oncogene **17**, 1998, 199–205.
4. Carman T.A., Afshari C.A., Barrett J.C., Cellular senescence in telomerase expressing Syrian hamster embryo cells. Exp. Cell Res., **244**, 1998, 33–42.
5. Dimri G.P., Lee X., Basile G., Acosta M., Scott G., Roskelly C., Medrans E.E., Liskens M., Rubelj I., Pereira-Smith O., A biomarker that identifies senescent human cells in culture and in aging skin in vivo. Proc. Natl. Acad. Sci. USA, **92**, 1995, 9363–9367.
6. Goi G, Bairati C, Massaccesi L, Lovagnini A, Lombardo A, Tettamanti G., Membrane anchoring and surface distribution of glycohydrolases of human erythrocyte membranes. FEBS Lett., **4**, 2000, 473 (1):89–94.
7. Kuo C.H., Wells W.W., J. Biol. Chem., Beta-Galactosidase from rat mammary gland. Its purification, properties, and role in the biosynthesis of 6beta-O-D-galactopyranosyl myo-inositol. **253**, 1978, 3550–3556.
8. Litaker J.R., Pan J., Cheung Y., Zhang D.K., Lin Y., Wong S.C.H., Wan T.S.K., Tsao S.W., Expression profile of SA-b-galactosidase and activation of telomerase in human ovarian surface epithelial cells undergoing immortalization. Int. J. Oncol., **13**, 1998, 951–956.
9. Mendez M.V., Stanley A., Park H.Y., Shon K., Phillips T., Menzoian J.O., Fibroblasts cultured from venous ulcers display cellular characteristics of senescence. J. Vasc. Surg., **28**, 1998, 876–883.
10. Naasani I., Seimiya H., Tsurno T., Telomerase inhibition, telomerase shortening and senescence of cancer cells by tea catechins. Biochem. Biophys. Res. Commun., **249**, 1998, 391–396.
11. Thomas E., al-Baker E., Dropcova S., Denyer S., Ostad N., Lloyd A., Kill I.R., Faraggher R.G., Different kinetics of senescence in human fibroblasts and peritoneal mesothelial cells. Exp. Cell Res., **236**, 1997, 355–358.
12. Tringali C., Fiorilli A., Venerando B., Tettamnti G., Different behaviour of ghost-linked acidic and neutral sialidases during human erythrocyte ageing. Glycoconj. J., **18**, 2001, 407–418.
13. Venerando B., Fiorilli A., Croci G.L., Tettamanti G., Presence in human erythrocyte membranes of a novel form of sialidase acting optimally at neutral pH. Blood, **90**, 1997, 2047–2056.

14. Xu H.I., Zhou Y., Ji W., Perng G.S., Kruzelock R., Kong C.T., Bast R.C., Mills G.B., Li J., Hu S.X., Reexpression of the retinoblastoma protein in tumor cells induces senescence and telomerase inhibition. Oncogene **15**, 1997, 2589–2596.
15. Yegorov Y.E., Akimov S.S., Hass R., Zelenin A.V., Prudovsky I.A., Endogenous beta-galactosidase activity in continuously nonproliferating cells. Exp. Cell Res., **243**, 1998, 207–211.

Received October 12, 2004.

* *Institute of Biology of the Romanian Academy, Bucureşti*

** *National Institute of Biology Research and Development, Bucharest*

*** *"Al. I. Cuza" University, Iaşi*

**** *Université des Sciences et Technologies de Lille I, Villeneuve d'Ascq, France*

HAMSTER KIDNEY AFTER FERRUM HAUSMANN "DROPS" CHRONIC ADMINISTRATION

C-C. PRUNESCU, PAULA PRUNESCU

An original experimental model of iron loading by administration of Ferrum Hausmann "Drops" (FeHD) in the drinking water was described. Later during the experiment, symptoms of severe renal dysfunction occurred in hamsters. Histological and ultrastructural observations revealed important lesions of the renal glomerule structures and the proximal convoluted tubule epithelial cells. The amorphous material massive accumulation on the epithelial cells basal pole impeded the normal water resorption from the primary urine. In the renal interstitial tissue the fibrosis was installed.

Key words: basal membrane, epithelial cell, fibrosis, nephron, renal corpuscle.

INTRODUCTION

Numerous modalities of iron loading of the laboratory animals were conceived by the experimental pathology. Some experiments used the method of inoculations with iron saccharated solutions. Different ways of inoculation such as intravenously (iv) (9), intramuscularly (im) (2), intraperitoneally (ip) (14, 15) or subcutaneously (sc) (5, 16) were used. Other techniques used the animals feeding with the iron rich diets: Fe-carbonyl (7) or TMH-Ferrocene (6). An original method of iron overloading applied to hamster was realized by hypertransfusion with homologous blood (17).

The model of the iron overloading by adding a certain proportion of Ferrum Hausmann "Drops" (FeHD) in the drinking water was realized in our laboratory. A group of hamsters received this solution as drinking water for long periods of time. First, we studied the liver reactivity following this iron administration method (10). But, we observed that hamsters, which chronically consumed water containing FeHD, presented signs of a severe renal dysfunction: polydipsia and polyuria with dark red urine.

The data about the effects of the chronic treatment with FeHD on the hamster kidney are presented in this paper.

MATERIAL AND METHODS

The experimental group. 12 male young adult hamsters, weighing 65±3 g, were submitted to an iron loading treatment.

REV. ROUM. BIOL. – BIOL. ANIM., TOME 49 , N^{os} 1–2, P. 129–138, BUCAREST, 2004

Ferrum Hausmann "Drops" (FeHD), containing Fe (III) hydroxide polymaltose, is a pharmaceutical product (Vifor, Switzerland)' destined for human oral administration.

Drinking solution: 2 mg FeHD/1 ml tap water. The solution with this concentration represented the unique source of water for seven months. After this period, hamsters had tap water, for other five months, till the end of the experiment.

The food: consisted of concentrates MURACOM (Belgium).

The control group. 12 male young adult hamsters weighing 65±3 g received tap water and similar food to the experimental group.

The animals of the two groups were sacrificed at 4, 5, 7, 9 and 12 months from the beginning of the experiment.

Histology. Samples of kidney were processed as follows: tissue fixation using 8 % formaldehyde in saline and then standard histological methods for the embedding in paraffin were applied. The histological sections of 5 µm width were stained with Hemalum-Eosin for general observations, Perls method to make evident the ferric ion, Picro-Sirius red (PSR) stain specific for collagen fibers (8) and silver impregnation Gömöri for reticulin fibers (19).

Electron microscopy. Small fragments of hamster kidney were fixed in 2.5% glutaraldehyde solution in cacodylate buffer 0.1 M, pH 7.4 and post fixed in 1.33 % OsO_4 solution, in the same buffer. The samples washed in cold buffer and processed for the dehydration in ethyl alcohol series of growing concentrations to 100% ethyl alcohol were immersed and embedded in Epon 812. The ultrathin sections were contrasted with uranyl acetate and lead citrate and observed in transmission electron microscopy (TEM).

RESULTS

The naked eye inspection of hamsters viscera, after 5–12 months from the beginning of the experiment, made evident some macroscopic modifications of the kidney (Fig. 1) and urinary bladder (Fig. 2). The kidneys were enlarged and presented a pale-yellow colour. The organ surface was not smooth yet but presented numerous pronounced irregularities. The urinary bladder was dilated and filled with an opalescent-yellow urine.

Histological observations. After the first months of treatment, the histological sections presented a general normal aspect of the kidney. In the cortical zone, among numerous normal renal glomeruli, some presented atrophied capillaries and the Bowman's capsules like empty vesicles or containing a clear colloidal material. The renal tubules were surrounded by diffuse PSR-positive

material. The basal part of epithelial cells in the proximal convoluted tubules presented some discontinuities of striated cytoplasm. In the lumens of renal tubules, some clear or acicular material was observed.

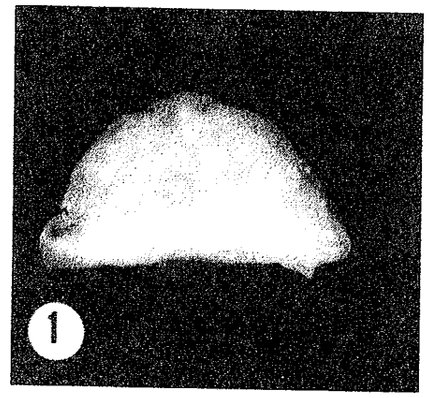

Fig. 1 – Pseudonodular deformation of the kidney. Original magnification × 2.

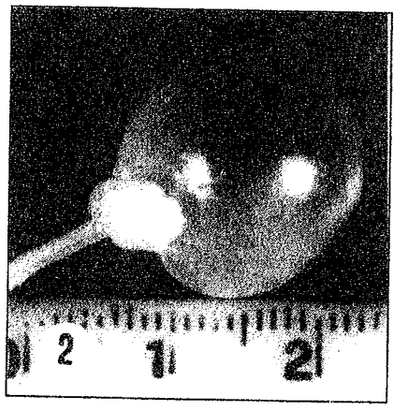

Fig. 2 – Urinary bladder at one month after iron solution administration. Original magnification × 2.

After seven months from the beginning of the experiment, important kidney damages were noted. The renal corpuscles were dilated (Fig. 3). The glomerular capillaries presented enlarged lumens. The capillaries were marked by diffuse PSR-positive material. In other zones, renal glomeruli showed destroyed capillaries

and thickened capsular epithelium. In the subcortical zones, the renal structures were covered with a fainty PSR positive material.

Fig. 3 – Alteration of the renal corpuscles and of different nephron segments. PSR-Hemalum. Original magnification × 80.

The proximal convoluted tubules presented vast damages: the brush border cells were swollen, with the nuclei placed near the apicale pole and PSR-positive cloudy cytoplasm (Fig. 4), because of the accumulation of great quantities of amorphous material at the basal pole. The lumens of ascending and descending loops of Henle, distal convoluted tubules and collecting tubules were obturated by a hyaline colloidal material (Fig. 3).

The animals, which returned to the tap water regimen after 7 months of iron solution, presented a continuous chronic evolution of the renal lesions. The Malpighi glomeruli and the proximal convoluted tubules were packed with an amorphous material. The thickening at the cells basal poles became evident in all nephrone segments. The blood vessels covered with PSR positive fibers presented thick walls.

At the end of the experiment, the active renal fibrosis was established. But functional nephrones were observed among fibrosed areas.

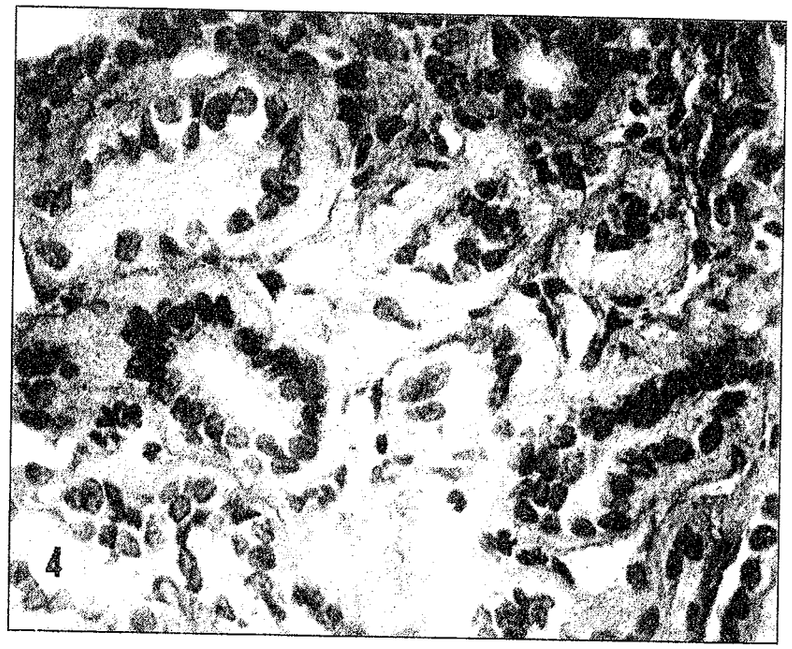

Fig. 4 – A thick amorphous material covers different nephron profiles, especially the proximal convoluted segment. PSR-Hemalum, Original magnification × 320.

Ultrastructural observations. The lesions of the renal corpuscle structures were important. However, in some cases, endothelial cells of the glomerular capillaries preserved their fenestration (Fig. 5). An amorphous material was contiguous with the basal membranes of the endothelial and mesangial cells. The endothelial cells, oriented towards the podocytes, still presented lamina densa and lamina rara of the basal membrane. Also, the amorphous material extended and united in many points the podocytes basal amorphous material. In more advanced stages, the amorphous material was so abundant that it invaded the whole corpuscle (Fig. 6).

Massive amorphous material accumulations were evident at the epithelial cells basal pole along the proximal convoluted tubules (Fig. 7). The cytoplasm and organelles were pushed towards the apical pole. The specific tubular infoldings of the cellular membrane from the basal pole were no more evident. Also, the mitochondria were absent from this zone. The nuclei were situated in the apical zone, near the microvilli (Fig. 8). The epithelial cells were of small dimensions with few bunches of short microvilli interrupted by cytoplasm blebs. The mitochondria were small, round, with small vacuoles or dense matrix.

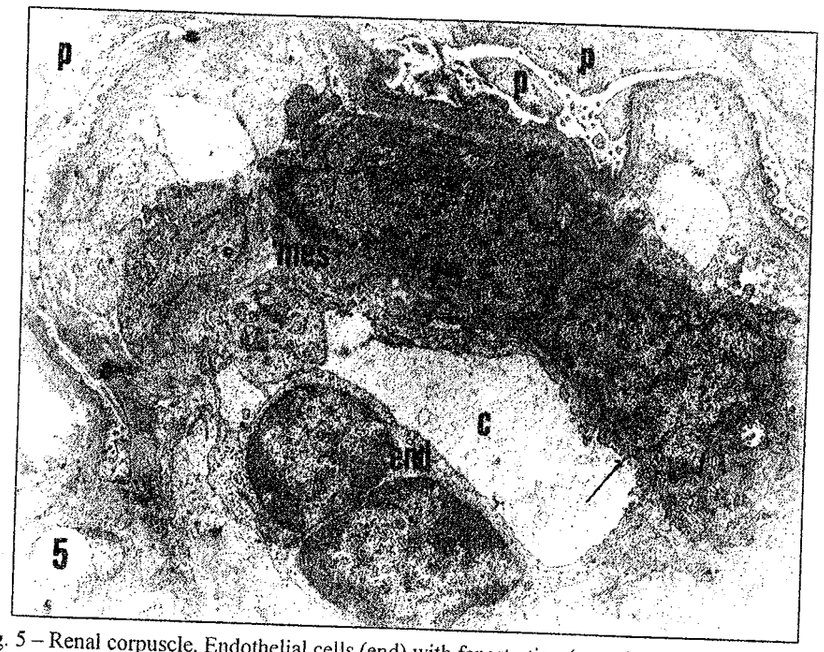

Fig. 5 – Renal corpuscle. Endothelial cells (end) with fenestration (arrow), mesangial cell (mes), capillary (c), podocyte (p). Original magnification × 4,700.

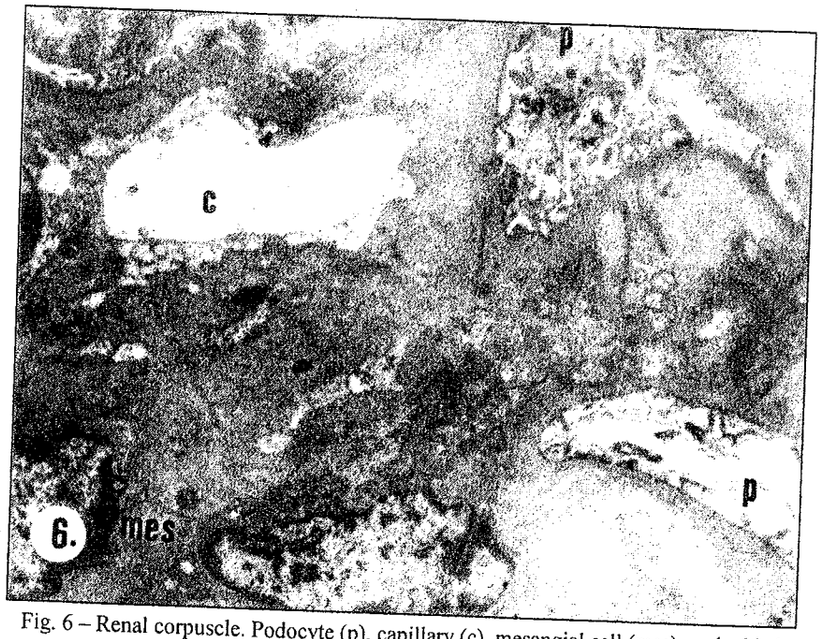

Fig. 6 – Renal corpuscle. Podocyte (p), capillary (c), mesangial cell (mes), embedded in an amorphous material. Original magnification × 6,200.

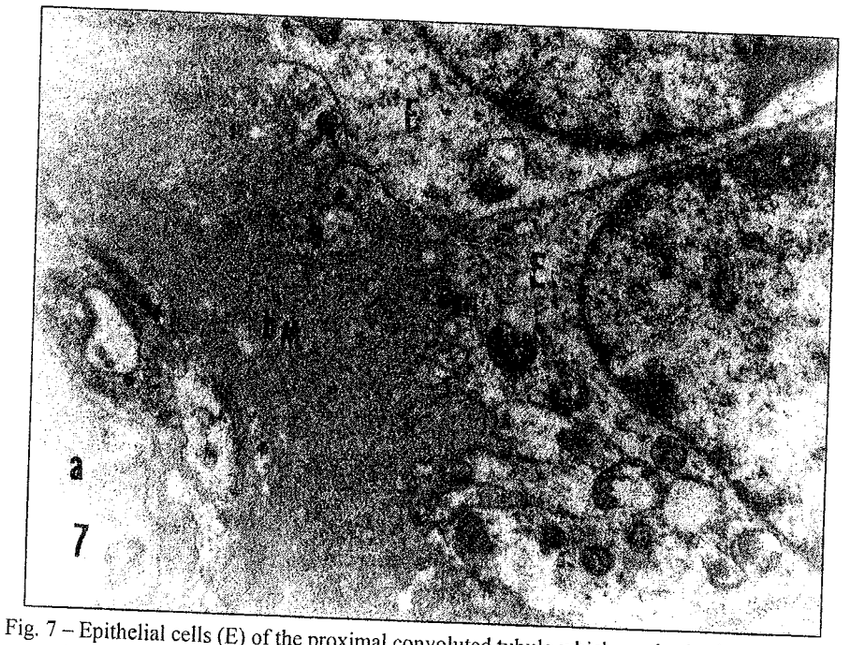

Fig. 7 – Epithelial cells (E) of the proximal convoluted tubule which synthesized and deposed amorphous material near basal membrane (bm); arteriole (a). Original magnification × 8,000.

Fig. 8 – Proximal convoluted tubule: the nucleus (n) is situated at the apical pole of the epithelial cell (E). Note cytoplasmic blebs (B) and short microvilli. Original magnification × 7,200.

DISCUSSION

After 7 months of continuous drinking of the iron solution, histological and ultrastructural observations showed the chronic damage of the nephron segments, especially the renal glomeruli and proximal convoluted tubules. The experimental hamsters were observed during other 5 months, period when they received only tap water. The maintaining of the renal damage signifies that the renal lesions became chronic. Moreover, at the experiment ceasing, the interstitial fibrosis was installed.

The main lesion of the renal corpuscles was the thickening of the cellular basal pole of the endothelial cells, podocytes and mesangial cells by an amorphous material accumulation.

The thickness of 5–10 μm attained by the basal pole of the proximal convoluted tubule may have a negative effect impeding the primary urine concentration.

The kidney damage description presented in this paper, with cellular lesions and basal membrane thickening, is similar to human diabetic nephropathy picture (3, 5). Naccarato *et al.* (1976) (10) studied the renal histology and ultrastructure in 15 patients affected by psychogenic polydipsia and diabetes insipidus syndrome. Morphological damages similar to our observations were presented. In this disease, the implication of antidiuretic hormone (ADH) was not excluded.

In a model of diabetic nephropathy obtained in rats treated with streptosotocine (12), the significant destruction of the nephron distal convoluted segments was described. The authors observed renal fibrosis eight months after diabetes induction.

An interesting experiment was realized by Smith *et al.* (1990) (20) who transfused human hemoglobin cross-linked between the alpha-chains with bis (3,5 dibromosalicyl) fumarate (DBBF-Hb) in pigs and observed the developement of specific lesions: proximal tubular necrosis and hemoglobinuria.

Some authors were interested in the collagen IV implicated in the renal cellular repair after sublethal injury (11). The collagen IV was also considered as the major structural and functional component keeping in the epithelial phenotype (21). Many renal fibroblasts were considered to derive from the conversion of the renal epithelial cells into mesenchymal cells (13). Earlier research (1) showed in cell cultures that epithelial cells originating from polycystic kidney expressed molecules of type I fibrillar collagen.

The epithelio-mesenchymal *trans*-differentiation was obtained at the moment of renal fibrosis beginning (22). Recently, this fact was demonstrated "in vitro" by elaborated experiments of collagen IV inhibition, using simultaneous induction of TGF β1. Oliver (2002) (13) showed that, besides these molecular conditions, some other parameters which work only "in vivo" must be performed: the angiotensin

and the increasing of primary urine pressure in the renal glomeruli were important fibrogenic factors, which contribute to *trans*-differentiation conditions.

Following the analysis of the collagen IV isoforms (22), it resulted that only a certain collagen IV subtype was responsible for the mesangial basal membrane abnormal extension. The progressive deposition of an amorphous basal membrane material by the mesangial cell was described in diabetic nephropathy (3). The authors homologated the mesangial cell with the hepatic perisinusoidal stellate cell.

Our morphological study revealed that the amorphous material, which made difficult the glomerular capillaries function, seemed to have the origin in the endothelial cells, but the podocytes and mesangial cells may equally produce this material.

In conclusion, after chronic and unlimited consumption of FeHD, the hamster kidney presented lesions similar to these ones of some human nephropathy. This experiment should be a model for human renal diseases presenting nephron damages and fibrosis.

Acknowledgements. We thank Vifor (Switzerland) for the kind present of Ferrum Hausmann "Drops" bottles used in this experiment.

REFERENCES

1. Altieri P., Fabretti G., Candiano G., Brisigotti M., Tiberi G., Ghiggeri G.M., Callea F., Gusmano R., 1992, *Collagen expression by tubular epithelial cells from polycystic kidneys in culture.* In: Molecular and Cell Biology of Liver Fibrogenesis, A.M. Gressner, G. Ramadori eds. Proc. Int. Falk Sump., Marburg, Germany, 22–23 Jan. 1992, Kluwer Acad. Publishers, 185–189.
2. Brissot P., Campion J.P., Guillouzo A., Allain H., Messner M., Simon M., Ferran B., Bourel M., 1983, *Experimental hepatic iron overload in the baboon: results of two years study,* Digestive Diseases and Sciences, **28**(7): 616–624.
3. Bruggeman L.A., Kopp J.B., Klotman P.E., 1992, *Progressive renal failure: role of extracellular matrix protein deposition in the renal mesangium,* Cellular and Molecular Aspects of Cirrhosis, B. Clement, A. Guillouzo eds., Colloque INSERM/ John Libbey Eurotext Ltd., **216**: 199–209.
4. Carthew P., Edwards R.E., Smith A.G., Dorman B.M., Francis J.E., 1991, *Rapid induction of hepatic fibrosis in the gerbil after parenteral administration of iron dextran complex,* Hepatology, **13**: 534–539.
5. Cohen M.P., Lauteslarger G.T., Shearman C.W., 2001, *Increased collagen IV excretion in diabetes. A marker of compromised filtration function,* Diabetes Care, **24**(5): 914-918.
6. Dullmann J., Wulfhekel U., Nielsen P., Heinrich H.C., 1992, *Iron overload of the liver by trimethylhexanoylferrocene in rats,* Acta Anat., **143**: 96–108.
7. Iancu T.C., Shiloh H., 1988, *Experimental iron overload ultrastructural studies.* In: Hemochromatosis, C.Q., Edwards and M. Krikker eds., Ann. New York Acad. Sci., **526**: 164–178.
8. Junquiera L.C.A., Bignolas G., Brentani R.R. 1979, *A simple and sensitive method for the quantitative estimation of collagen,* Ann. Biochem., **94**: 96–99.
9. Lisboa P.E., 1971, *Experimental hepatic cirrhosis in dogs caused by chronic massive iron overload,* Gut, **12**: 363–368.

10. Naccarato R., Rizzo A., Sirigu F., Bertaglia E., Previato G., Fiaschi E., 1976, *Renal histological and ultrastructural findings in psychogenic polydipsia and diabetes insipidus,* Nephron, **16**(3): 226–235.
11. Nony P. A., Schnellmann R.S., 2001, *Interactions between collagen IV and collagen binding integrins in renal cells repair after sublethal injury,* Mol. Pharmacol., **60**(6): 1226–1234.
12. Obineche E.N., Mensha-Brown E., Chandranath S.I., Ahmed I., Nasser O., Adem A., 2001, *Morphological changes in the rat kidney following long term diabetes,* Arch. Physiol. Biochem., **109**(3): 241–245.
13. Oliver J.A., 2002, *Unexpected news in renal fibrosis,* J. Clin. Invest. **110**(12): 1763–1764.
14. Prunescu C-C., Prunescu P., 1988, *Giant multinucleated iron-containing cells in the liver of polymaltosed iron injected rats,* Rev. Roum. Biochim., **25**(4): 355–362.
15. Prunescu C-C., Prunescu P., 1991, *Ferritin accumulation in nuclei of hepatocytes in polymaltosed iron injected rats,* Rev. Roum. Biochim., **28**(3–4): 169–172.
16. Prunescu C-C. Prunescu P., 1994 a, *Hepatic fibrosis and cirrhosis of hamsters overloaded with polymaltosed iron subcutaneously administered,* 7/th Internat. Symp. Cells of the Hepatic Sinusoid, Kyoto (Japan), Abstr. Book.
17. Prunescu C-C. Prunescu P., 1994 b, *Iron overloading of the liver in the hypertransfused hamsters,* Annual European Iron Club Meeting, Gargnano Del Garda (Italy), Abstr. Book.
18. Prunescu C-C., Prunescu P., 1998, *Model of hepatic fibrosis in hamster after chronic administration of ferrum Hausmann "Drops",* Annual Meeting European Iron Club, 9–11 July 1998, Zeist (The Netherlands), Abstr. Book, 38.
19. Putt A.F. 1972, *Manual of Histopathological Staining Methods,* A Wiley-Interscience Publication, John Wiley & Sons, 335 pp.
20. Smith C.D., Scuschereba S.T., Hess J.R., McKinney L.A., Bunch D., Bowman P.D., 1990, *Liver and kidney after administration of hemoglobin cross-linked with bis (3,5-dibromo-salicyl) fumarat, Biomater.* Artif Cells Artif. Organs, **18**(2): 251–261.
21. Zeisberg M., Bonner G., Marshima Y., Colorado P., Muller G.A., Strutz F., Raghu Kalluri, 2001, *Collagen composition and assembly regulated epithelial-mesenchymal trans-differentiation,* Am. J. Path., **159**(4): 1313–1321.
22. Zeisberg M., Ericksen M.B., Hamano Y., Neilson E.G., Ziyaden F., 2002, *Differential expression of type IV collagen isoformes in rat glomerular endothelial and mesangial cells,* Biochem. Biophys. Res. Commun, **295**(2): 401–407.

Received October 12, 2004.

Institute of Biology
296, Spl. Independenţei
P.O.Box 56–53 Bucharest

INGESTION OF LOW DOSES OF FUMONISIN B_1 (FB_1) INDUCES MICROSCOPIC ALTERATIONS IN SEVERAL PIGLET ORGANS

IOANA TRANDABURU*, SANDRINE BOUHET**, DANIELA E. MARIN***
IONELIA ŢĂRANU***, ISABELLE P. OSWALD**, T. TRANDABURU*

The study is focused on the microscopic alterations in the lungs, liver, ileum and cecum of weaned piglets treated twice a day by gavage with 0.75 mg/kg body weight of pure fumonisin B_1 (FB_1) for one week. Under the above experimental conditions no noticeable histopathological modifications were found in the spleen, kidney, as well as in the other examined regions of the alimentary tract (oesophagus, duodenum, jejunum and the large intestine). The mycotoxin induced relative severe pulmonary injuries consisting of proliferation of connective tissue fibers and infiltration of edematous fluid around lymphatic and blood vessels, in the interlobular septa and in the peribronchial and peribronchiolar areas. Endothelial alterations of the capillaries, widenings, disruptions and infiltrations of the alveolar walls with lymphocytes, as well as accumulations inside the alveoles of a suppurative fluid and fibrin aggregates completed the histopathological picture of pulmonary lesions. In the liver, centrolobular vein disruptions, swellings and proliferations of the sourrounding hepatocytes, but also their vacuolization and degeneration with the occurrence of autolysis foci were among the most representative alterations. To these, disorganisations and disruptions of hepatocellular cords should be added. Finally, the mycotoxin stimulated the proliferation of lymphatic nodules in the terminal ileum and cecum. The results of the study are discussed in connection with the risks of short-term exposures to low doses of FB_1 for the domestic animal and human health.

1. INTRODUCTION

The ingestion of fumonisin B_1 (FB_1), a world wide natural contaminant of corn and other crops infected with the fungus *Fusarium verticilloides*, causes species-dependent, often lethal toxicoses in lower vertebrates and homeotherms. As reported, the most sensitive organs to this mycotoxin are the equine encephal [20], porcine lung [14], mouse liver [3], and rat [27] and rabbit [10] kidney. Irrespective of the primary target organ of FB_1, the hepato-and nephro-toxicities are common features of the diseases induced by a mycotoxin both in mammals and birds [1, 11, 22, 30, 33, 34].

The mechanisms of species-and organ-specific toxicoses are still poorly and unequally understood. According to more authors [1, 4, 12, 24], they interfere with sphingolipid biosynthesis in multiple organs. As a matter of fact, as Bhandari *et al.*, (2001) have shown in mice, the accumulation of free sphingoid bases (sphingosine and sphinganine) and the modulation of cytokine levels are the two major biochemical responses to FB_1 *in vivo*.

REV. ROUM. BIOL. – BIOL. ANIM., TOME 49, N^{os} 1–2, P. 139–155, BUCAREST, 2004

Besides them, alterations of eicosanoid biosynthesis [8], of protein kinase C levels [16], of mitogen activated protein kinase expressions [32], of DNA and cell oxidative pathways [25] and of signal transduction molecular pathways [1] may explain the organ depending on various morphological expressions of the fungus toxicity.

Although the biochemical and clinical aspects of FB_1 toxicoses in swine have been investigated in detail, the available information concerning its morphological effects in different organs and tissues is still scarce, unsubstantial and even contradictory [11, 12, 15, 28, 31]. The present study was therefore designed to complete the peculiar histopathological pictures induced by the strict supervised mycotoxin ingestion in more piglet organs (lung, liver, kidney, spleen and alimentary tract).

2. MATERIAL AND METHODS

Experimental protocol

The experiments were performed according to the French National Guidelines for the care and use of animals for research purposes. Altogether 6 four-weeks-old Dalan X France hybrid piglets, all healthy males, were used in this study. They were purchased from a local commercial source at 3 weeks age, just after weaning, and were further acclimatized for one week in the animal care facilities of the INRA research center prior to initiation of the experiments. During acclimatization and experiments the animals had free access to water and were fed with a commercial starter diet, free of fumonisin B_1 (FB_1).

Three treated piglets were given by gavage, twice a day, 0.75 mg/kg body weight of purified FB_1 diluted in 10 ml sterile sweet water. The other three specimens were kept as control and received twice a day 10 ml of sterile sweet water. The experiments lasted for 7 days.

The animals were killed by electrical stunning the next day following the last gavage. Samples of lung, liver, kidney, spleen and alimentary tract (oesophagus, duodenum, jejunum, ileum and large intestine), drawn always from the same organ areas in all specimens, were processed for histological investigations.

Preparation of tissues

Small pieces of organs were immersed in Bouin's fluid for 4–5 days, dehydrated in increasing concentrations of ethanol, cleared with toluene and paraffin-embedded. Serial 6μm-thick sections, prepared on a rotary microtome, were mounted on albumin-coated slides.

The deparaffinized and rehydrated sections were stained according to hematoxylin-eosine (H-E) and hemalaun-trichrome (H-TR) techniques. The sections were finally dehydrated through a graded ethanol series, cleared with xylene and mounted in Entellan (E. Merck, Germany). The preparations were examined with an Amplival (C. Zeiss, Germany) photomicroscope.

3. RESULTS

Among the examined organs, only the lungs, liver, ileum and cecum displayed microscopic alterations ascribed to FB_1-treatment.

Lungs. As compared to the lung microscopic structure of control animals (Fig. 1), the one-week exposure of the weaned piglets to mycotoxin induced mild to severe edema in the organ, sometimes associated with the parenchyma congestion (Figs. 2–6). Thus, in all treated specimens different thickening degrees of the perivascular, interlobular and peribronchiolar areas, due to the proliferation and spacing of connective tissue fibers, could be observed (Figs. 2–4, 6).

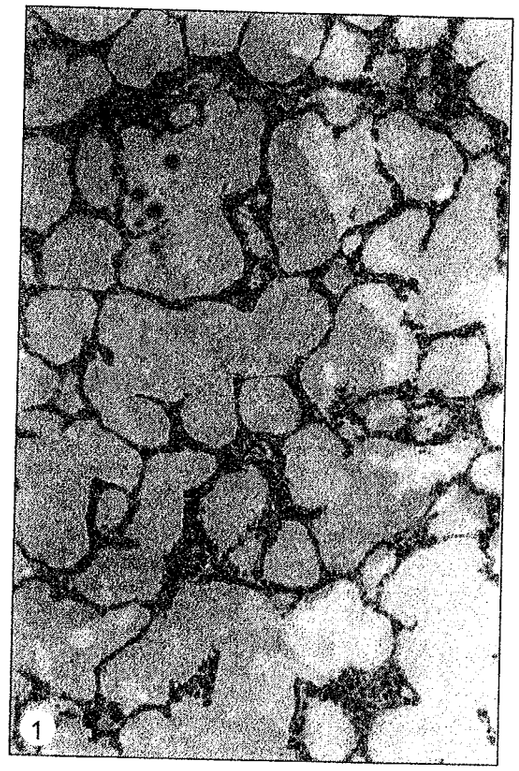

Fig. 1 – Sections through the lung of a control piglet showing moderately expanded alveoli. H-E; orig. magn. × 125.

Fig. 2 – Perivascular edema in the lung of an FB_1–treated piglet showing the enlarged lumen (L) of an artery bounded by altered endothelial cells, with pyknotic nuclei (arrowheads) or with phagocytic vacuoles (thin arrows). In the vascular lumen an agglomeration of phagocyted material (thick arrow) could also be seen. H-E; orig.magn. × 350.

Although this study was not designed to assess the evolution of histopathological changes, the thorough examination of preparations suggested that the early edema occurred around the lymph and blood vessels. The vascular lumens, often enlarged and only rarely flattened, contained macrophages, modified circulating elements, as well as cellular and membranous debris (Figs. 2, 3). The endothelial cells of capillaries showed numerous protrusions into lumens or appeared endowed in their luminal sector with multiple undulating membranous profiles (Fig. 3). Some of them displayed nuclear pyknosis and were dislocated into the blood stream (Figs. 2, 3).

Fig. 3 – Flattened lymph vessel in the proximity of an intrapulmonary bronchus. The thickening of perivascular connective tissue with accumulation of edema fluid (F) could be observed. Note also the necrotic nuclei and membraneous profiles (arrowheads) in the lumen (L) of vessel. FB_1-treated animal. C = bronchus cartilage; H-TR; orig.magn. × 135.

The occurrence of vascular edema seemed to be followed by the development of those subpleural and interlobular (Fig. 4).

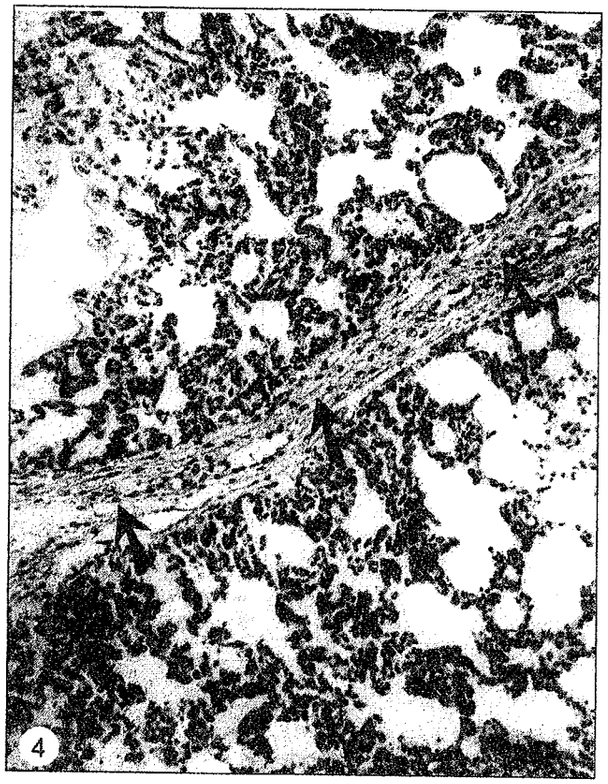

Fig. 4 – Thickened interlobular septum (thick arrows) in the lung of a FB_1-treated specimen. The alveolar walls appear also widened by edema fluid. H-E; orig.magn. × 140

Gradually, the edematous process extended to the peribronchial, peribronchiolar and alveolar areas (Figs. 5, 6). The alveolar septa appeared frequently disrupted and widened by edema fluid and the alveolar pockets filled with an amorphous suppurative material or with small fibrin aggregates (Fig. 5). In other lung areas the thickenings of the alveolar walls were accompanied by their massive, more or less punctual infiltration with lymphocytes (Fig. 6).

Fig. 5 – Photomicrograph illustrating the alterations induced by FB_1 ingestion in the piglet lung. The alveolar septa appear widened and several disrupted (thick arrows). Some alveoli contain fibrin aggregates (arrowheads), suppurative fluid (asterisks) or elastic fibers (thin arrows). H-E; orig.magn. × 145.

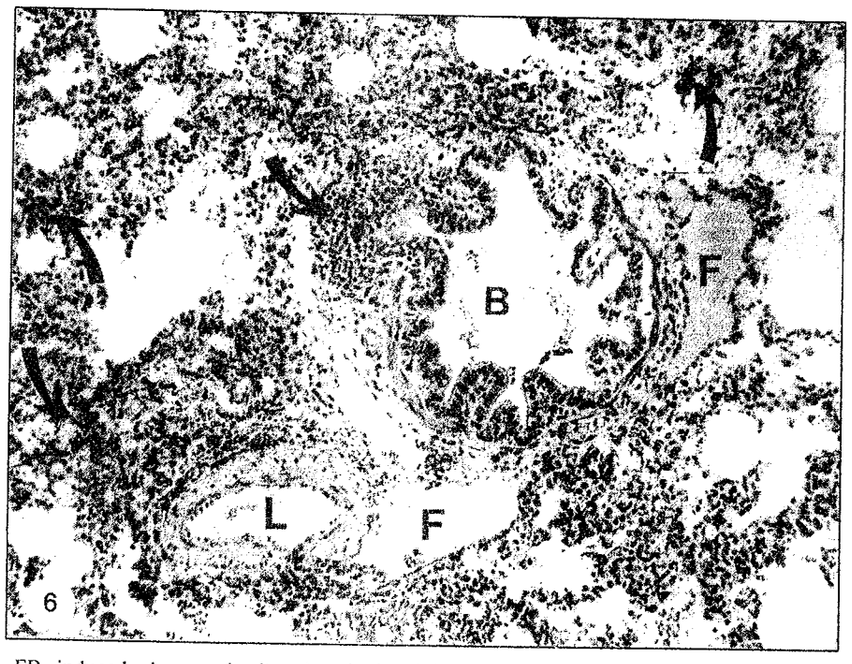

Fig. 6 – FB_1-induced microscopic alterations in the piglet lung. The alveolar septa and the dense connective tissue of a bronchiole (B) appear enlarged and punctual invaded by lymph cells (curved arrows). Note also the accumulation of edema fluid (F) near the bronchiole and of a lymphatic vessel (L). H-TR; orig.magn. × 140.

Liver. The FB_1-treatment caused multiple pathological lesions also in the hepatic tissue (Figs. 7–12).

Fig. 7 – Centrolobular zone of a hepatic lobule belonging to a control animal. The characteristic radial disposing of the hepatic cords could be observed CV = centrolobular vein. H-TR; orig.magn. × 350.

The most affected regions were the centrolobular ones, in which the hepatocellular swellings and proliferations, but also apoptoses and necroses, were often observed (Fig. 8). Disruption of centrolobular veins associated with vacuolization and dissociation of the surrounding hepatocytes, as well as the disorganization of the characteristic radial arrangement of the hepatocellular cords join the representative alterations (Figs. 8–10). The histopathological picture was completed by the high incidence of more or less extensive autolysis foci recorded in the central and midzonal regions of the hepatic lobules (Fig. 11). Finally, although the peripheral regions of the lobules appeared usually unaffected by mycotoxin, the enlargement of the interlobular spaces due to the dissociation of connective tissue fibers was also seen (Fig. 12).

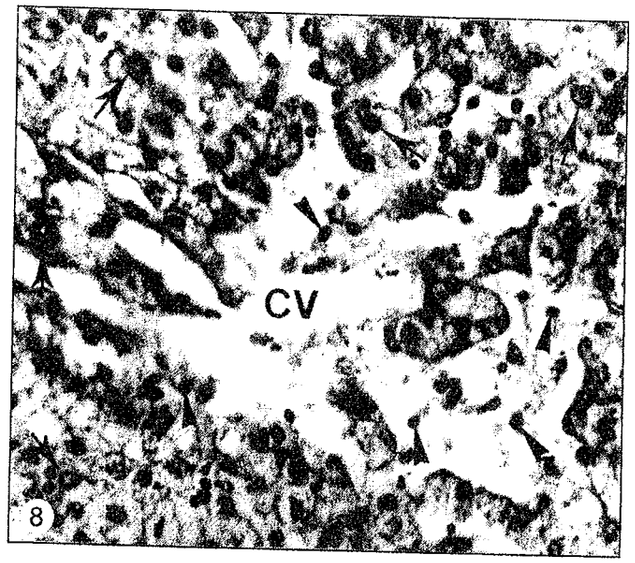

Fig. 8 – Picture illustrating the microscopic alterations induced by FB_1 in the central region of a hepatic lobule. The alterations include disruption of centrolobular vein wall (CV), hepatocyte vacuolization, their plasmalemma lysis, nuclei pyknosis (arrowheads) or hyperplasy (arrow), fragmentation of the hepatic cords and the enlargement of sinusoid spaces. The radial arrangement of the hepatocyte cords is still preserved. H-E; orig.magn. × 350.

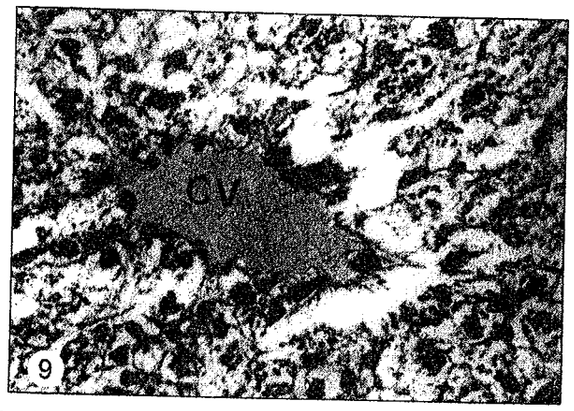

Fig. 9 – Section through a hepatic lobule less affected by FB_1 treatment. The hepatocytes surrounding the centrolobular vein (CV) display vacuolized cytoplasm. H-TR; orig.magn. × 350.

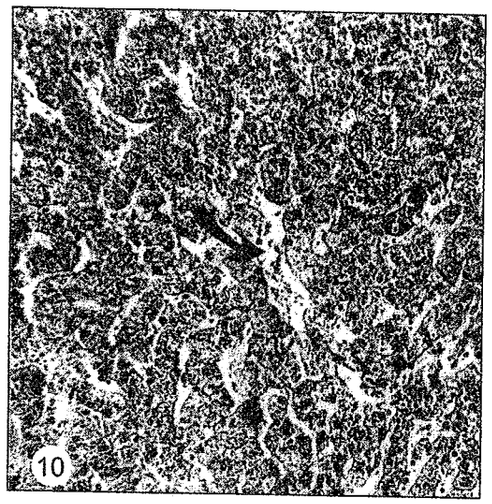

Fig. 10 – Low-power-photomicrograph illustrating the disorganization of the characteristic radial disposing of the lobule parenchymal cords in the liver of a FB_1 treated piglet. The curved arrow marks the centrolobular vein. H-TR; orig.magn. × 140.

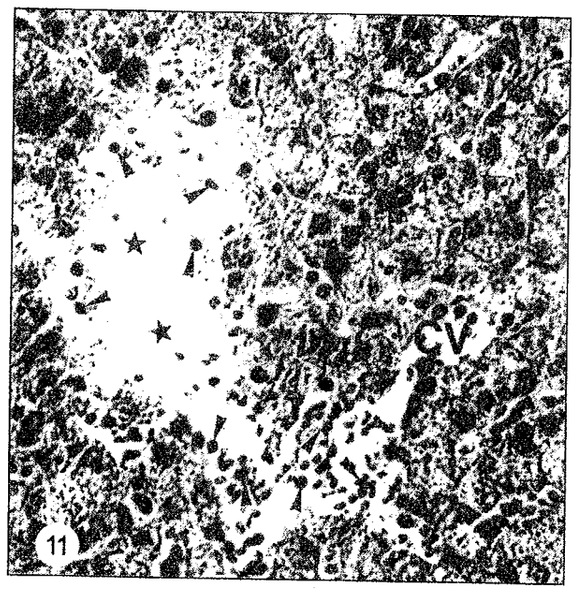

Fig. 11 – Hepatic autolysis lesion (asterisks) provoked by FB_1 ingestion in the proximity of a centrolobular vein (CV). The necrotic nuclei are marked by arrowheads. H-E; orig.magn. × 350.

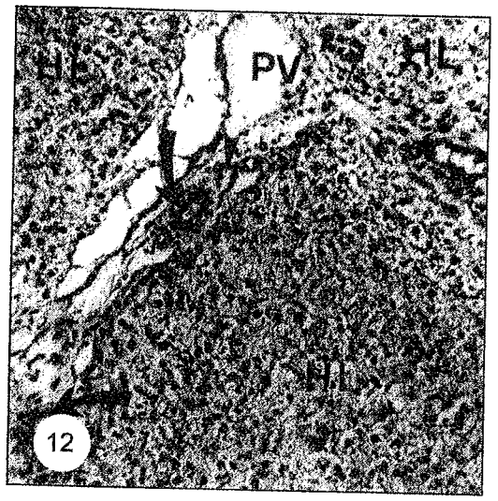

Fig. 12 – Widened interlobular space in the liver of a FB_1 treated animal achieved by dissociation of connective tissue fibers. The bile ducts are indicated by curved arrows and the hepatic artery by the arrowhead. PV = portal vein; HP = hepatic lobule; H-TR; orig.magn. × 140.

Intestine. No histological modification could be detected in the duodenum and jejunum of the pigs treated with FB_1. As regards the terminal ileum and also the cecum, the mycotoxin produced a marked proliferation of the singular or agglomerated lymphatic nodules, ordinarily present in the mucosa and only seldom in the submucosa of these intestinal regions (Figs. 13, 14). In the treated animals lymphatic nodules were placed on 2–3 rows and occupied the entire submucosa (Fig. 14). Frequently, the nodules facing the mucosa chorion appeared "broken" and discharging lymphocytes (Fig. 14). The proliferation of the lymphatic nodules ascribed to FB_1 ingestion was recorded on the background of a diffuse infiltration with lymphocytes of the intestinal chorion signaling out the chronic inflammatory reaction developed after birth in all control animals.

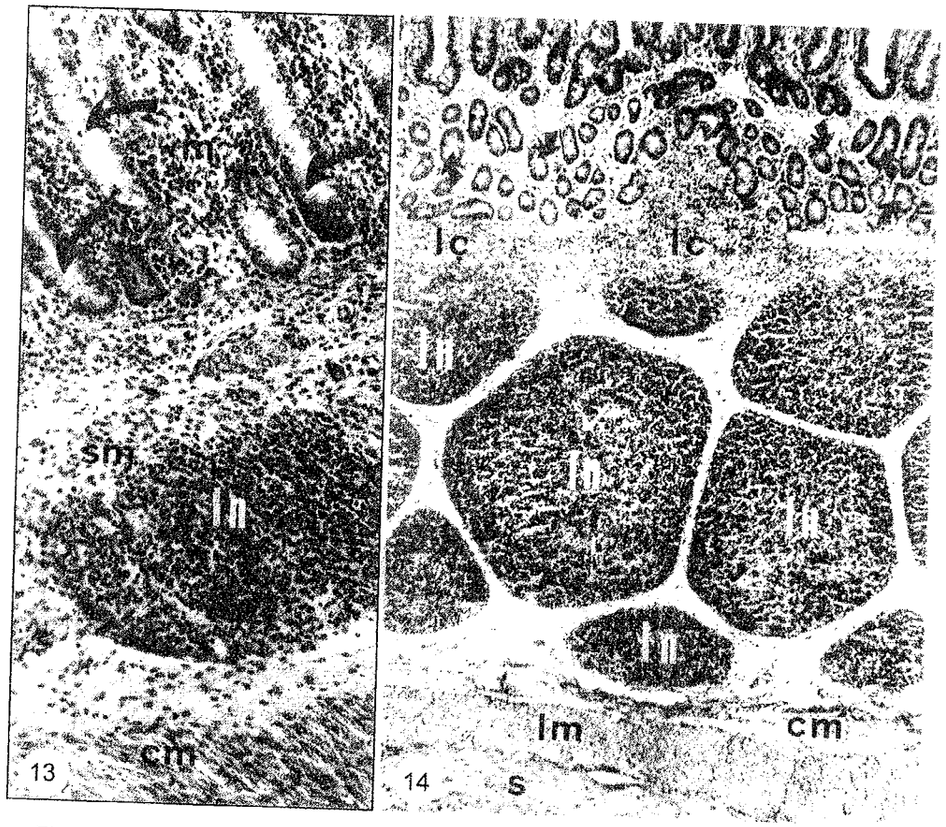

Fig. 13 – Solitary lymphatic nodule (ln) under formation in the ileum submucosa (sm) of a FB_1 treated piglet. The mucosa chorion (m) and the surrounding submucosa of nodule appear infiltrated with lymphocytes. The crypts of Lieberkühn (curved arrows) are cut in longitudinal section. cm = circular musculature. H-E; orig.magn. × 320.

Fig. 14 – Cross section through the terminal ileum of a FB_1 treated animal showing crowded lymphatic nodules (ln) in submucosa. The nodules facing mucosa discharge lymph cells (lc) The crypts of Lieberkühn (small curved arrows) appear cross sectioned. cm = circular musculature; lm = longitudinal musculature; s = serosa; H-TR; orig.magn. × 140.

4. DISCUSSION

The main target organs for fumonisin toxicity are still disputed. According to most investigators [13, 18, 22, 30], the liver and the kidney are the most sensitive organs to the fungus toxin. Contrarily, other authors [7, 11, 15, 28] consider the liver and lung the first organs affected by fumonisin, at least in swine. These divergent opinions supporting, however, the liver main role in the organism

response to mycotoxin are further contradicted by biochemical data, which proved that the drug biological activation, reflected by the kinetics of metabolizing enzyme activities, does not represent the major key of its action mechanism [24]. The evolution, severity and peculiarities of histopathological lesions induced in various organs by different doses and exposure periods to mycotoxin are also still debated, inclusively in pigs [11, 15, 31]. Finally, species-dependent organism tolerance and the route of mycotoxin administration (oral, intraperitoneal or intravenous) are other factors influencing the FB_1 induced morphological alterations. Considering the aforesaid, this study aimed the description of microscopic injuries occurred in the piglet lung, liver, ileum and cecum after repeated ingestions of purified FB_1. The detailed investigation of these organs was decided by the results of a preliminary screening showing the lack of notable histopathological modifications in the spleen, kidney, oesophagus, duodenum and jejunum of the same animals.

From many points of view, the histopathological modifications recorded by us in the lungs of weaned piglets treated with FB_1 are similar to those previously reported by other authors [11, 15, 31]. We refer firstly to the proliferation of connective tissue fibers of interlobular septa and of those around lymphatic vessels, bronchi and bronchioles, usually accompanied by accumulation of edematous fluid. Another encountered injury, such is the endothelial alteration of the lymphatic and blood capillaries, marked among others by nuclei pyknosis and accumulation of membraneous material to the luminal pole of cells, was also described by Gumprecht *et al.*, (1998, 2001) in intravenously injected animals or only after ingestion of low doses of mycotoxin that did not induce pulmonary edema. According to these authors, the alterations of vascular endothelium are specific for lung and appear only in swine. The fact that in our preparations their occurrence did not precede the development of edematous process makes unlikely the hypothesis of Gumprecht *et al.* (2001) on the important role in pathogenesis of FB_1 induced pulmonary edema. In this context, more attractive appears the opinion advanced by Haschek *et al.* (2001), according to which the pulmonary edema, as specific expresion of FB_1 toxicosis in swine, represents the consequence of an acute left-sided heart failure mediated by altered sphingolipid biosynthesis.

Finally, the microscopic alterations encountered at the level of respiratory parenchyma deserve discussion. Thus, alterations such are the widenings and disruptions of the alveolar walls, as well as the occurrence inside the alveolar pockets of edema fluid or of fibrin aggregates, reported also by other authors [11], would suggest in our opinion the development of a suppurative, more or less diffuse interstitial bronchopneumonia. On the other hand, the different histopathological picture in some relative restricted pulmonary areas, characterized by edematous thickenings of the alveolar parenchyma and punctiform infiltrations with lymphocytes, would pledge for a focal eruptive bronchopneumonia. The fact

that both histopathological pictures may coexist in the lungs of the same mycotoxin treated specimen makes heavier the accurate diagnosis of the disease.

As regards the liver, the distribution pattern of FB_1 provoked lesions appeared quite different from that recorded in the experimental aflatoxicoses of swine [23, 29] and of other mammals [2, 19 25]. Thus, unlike the microscopic alterations ascribed to aflatoxins, those induced by FB_1 were quartered in the centrolobular regions and only seldom in the midzonal regions of the hepatic lobules. In these lobule regions a part of morphological expressions such are vacuolization and deterioration of hepatocytes, disorganization of the hepatic cords, nuclear apoptosis and necrosis, as well as the occurrence of more or less expanded autolysis foci, were rather similar to those reported in mammalian [5, 23, 29] and even in aviar [6, 17] aflatoxicoses. In other words, the liver, unlike the swine lung, seems to represent a common target organ of fumonisin and aflatoxin intoxications, able to react against both metabolic aggressions through partial distinct structural expressions.

The activation of lymphatic nodule proliferation we found in the terminal ileum and cecum of FB_1 treated piglets represented the sole and major morphological effect of mycotoxin in the entire alimentary tract. Besides it, the ingestion of mycotoxin has been already linked by oesophageal and gastric cancer in humans (9,35) and oesophageal cell hyperplasia in rats (21). The effect, firstly described by us in the intestine, cannot be considered a direct and entire pathological one. In our opinion it reflects rather the local morphofunctional response against an augmented inflammatory process mediated by altered immunity of mycotoxin treated animals.

In conclusion, one week ingestion of low to moderate doses of FB_1 (in this case 0.75 mg/kg body weight) induced relative severe alterations of pulmonary and hepatic microscopic structures in weaned piglets, most probably with fatal consequences for animals under extension of experimental conditions. In addition, the strong stimulation of lymphatic nodule proliferation in the jejunum and cecum could be explained as a transient morphofunctional response of these intestinal regions to the development of local inflammatory aggressions facilitated by the low immunity of animals. The results of this experiment call attention on the risk, even of the short-term exposures to low doses of FB_1, for the health of domestic animals and humans.

Acknowledgements. This work was supported by funds from the region Midi-Pyrénées, France (DAER-Rech/99008345) and the Transversalité INRA (mycotoxins-P00263). I.Ţăranu and S.Bouhet were the recipients of an INRA post-doctoral fellowship from the "Ministère de l'Éducation Nationale, de la Recherche et de la Technologie" respectively. I. Trandaburu, D. Marin and T. Trandaburu were supported by the "Réseau Formation-Recherche", a bilateral project between France and Romania granted by the "Ministère de l'Éducation Nationale" and the "Ministère de la Recherche" (Paris, France). The skilful technical assistance of Mr. P. Pinton is gratefully acknowledged by all co-authors.

REFERENCES

1. Bailly J.D., Benard G., Jouglar J.Y., Durand S., Guerre P., (2001), Toxicity of *Fusarium moniliforme* culture material containing known levels of fumonisin B1 in ducks. Toxicology, **163:** 11–22.
2. Barton Ch., Hill A.D., Yee B.S., Barton X.A., Ganey E.P., Roth A.E. (2000) Bacterial lipopolysac charide exposure augments aflatoxin B_1-induced liver injury. Toxicol.Sci., **55:** 444–452.
3. Bhandari N., Quanren He., Sharma R.P. (2001) Gender-related differences in subacute fumonisin B_1 hepatotoxicity in BALB/c mice. Toxicology, **165:** 195–204.
4. Bucci T.J., Howard P.C., Tolleson W.H., Laborde J.B., Hansen D.K., (1998), Renal effects of fumonisin mycotoxins in animals. Toxicol. Pathol., **26:** 160–164.
5. Colvin B.M., Harrison L.R., Gosser H.S., Hall R.F. (1984) Aflatoxicoses in feeder cattle. JAVMA, **184:** 956–958.
6. Espada Y., Domingo M., Gomez J., Calvo M.A. (1992) Pathological lesions following an experimental intoxication with aflatoxin B_1 in broiler chicken. Res.Vet.Sci., **53:** 275–279.
7. Fazekas B., Bajmocy E., Glavits R., Fenyvesi A., Tany J., (1998), Fumonisin B1 contamination of maize and experimental acute fumonisin toxicosis in pigs. Zentralbl.Veterinar.med., **45:** 171–181.
8. Gelderblom W.C., Smuts C.M., Abel S., Snyman S.D., Van der Westhuizer I., Huber W.W., Swanevelder S., (1997), Effect of fumonisin B1 on the levels and fatty acid composition of selected lipids in rat liver in vivo. Food Chem.Toxicol., **35:** 647–656.
9. Groves F.D., Zhang L., Chang Y.S., Ross P.F., Gaspar H., Norred W.P., You W.C., Fraumeni J.F., (1999), Fusarium mycotoxins in corn and corn products in a high-risk area for gastric cancer in Shandong-Province, China. J.AOAC Int., **82:** 657–662.
10. Gumprecht L.A., Marcucci A., Weigel R.M., Vesonder R.F., Riley R.T., Showker J.L., Beasley V.R., Haschek W.M., (1995), Effects of intravenous fumonisin B1 in rabbits: nephrotoxicity and sphingolipid alterations. Nat.Toxins, **3:** 395–403.
11. Gumprecht L.A., Beasley V.R., Weigel R.M., Parker H.M., Tumbleson M.E., Bacon C.W., Meredith F.I., Haschek W.M., (1998), Development of fumonisin-induced hepatotoxicity and pulmonary edema in orally dosed swine: morphological and biochemical alterations. Toxicol.Pathol., **26:** 777–788.
12. Gumprecht L.A., Smith G.W., Constable P.C., Haschek W.M., (2001), Species and organ specificity of fumonisin-induced endothelial alterations: potential role in porcine pulmonary edema. Toxicology, **160:** 71–9.
13. Hard G.C., Howard P.C., Kovatch R.M., Bucci T.J., (2001), Rat kidney pathology induced by chronic exposure to fumonisin B1 includes rare variants of renal tubule tumor. Toxicol. Pathol., **29:** 379–86.
14. Harrison L.R., Covin B.M., Greene T.J., Newan L.E., Cole J.R., (1990), Pulmonary edema and hydrothorax in swine produced by fumonisin B_1, a toxic metabolite of *Fusarium moniliforme*. J.Vet.Diagn.Invest., **2:** 217–21.
15. Haschek W.M., Gumprecht L.A., Smith G., Tumbleson M.E., Constable P.D., (2001), Fumonisin toxicosis in swine: an overview of porcine pulmonary edema and current perspectives. Environ.Health.Perspect., **109**, suppl. **2:** 251–257.
16. Huang C., Dickman M., Henderson G., Jones C., (1995), Repression of protein kinase C and stimulation of cyclic AMP response elements by fumonisin, a fungal encoded toxin which is a carcinogen. Cancer Res., **55:** 1655–1659.

17. Johri T.S., Beura C.K. (2000) Efficacy of avsorb+supplement in alleviating adverse effects of aflatoxins in broilers. Poultry Times India, **4:** 1–3.
18. Kim M.S., Lee D.Y., Wang T., Schroeder J.J., (2001), Fumonisin B(1) induces apoptosis in LLC-PK (1) renal epithelial cells via a sphinganine- and calmodulin-dependent pathway. Toxicol.Appl. Pharmacol., **176:** 118–126.
19. Liu Y., Roebuck B.D., Yager J.D., Groopman J.D., Kensler T.W., (1998), Protection by 5 (pyranozinyl)-4-methyl-1,2-dithiol-3-thione (oltipraz) against the hepatotoxicity of aflatoxin B_1 in the rat. Toxicol. Appl. Pharmacol., **143:** 429–435.
20. Marasas W.F.O., Kellerman T.S., Gelderborn W.C.A., Coetzer J.A.W., Thiel P.G., Van der Lugt J.J. (1988) Leukoencephalomalacia in a horse induced by fumonisin B_1 isolated from *Fusarium moniliforme*. J.Vet.Res., **55:** 197–203.
21. Marasas W.F.O., Kriel N.P.J., Finchman J.E., Van Rensburg S.J., (1984), Primary cancer liver and oesophageal hyperplasia in rats caused by *Fusarium moniliforme*. Int.J.Cancer, **34:** 383–387.
22. Mathur S., Constable P.D., Eppley R.M., Waggoner A.L., Tumbleson M.E., Haschek W.M. (2001) Fumonisin B(1) is hepatotoxic and nephrotoxic in mild-fed calves. Toxicol.Sci., **60:** 385–396.
23. Miller D., Stuart B.P., Crowell W.A., (1981), Experimental aflatoxicosis in swine: morphological and clinical pathological results. Can.J.Comp.Meta b., **45:** 343–351.
24. Raynal M., Bailly J.D., Benard G., Guerre P., (2001), Effects of fumonisin B1 present in *Fusarium moniliforme* culture material on drug metabolising enzyme activities in ducks. Toxicol.Lett., **121:** 179–190.
25. Sahu S.C., Eppley R.M., Page S.W., Gray G.C., Barton C.N., O'Donnell M.W., (1998), Peroxidation of membrane lipids and oxidative DNA damage by fumonisin B1 in isolated liver nuclei. Cancer Lett., **125:** 117–121.
26. Seffner W., Schiller F., Lippold U., Dieter H., Hoffmann A., (1997), Experimental induction of liver fibrosis in young guinea pigs by combined application of copper sulphate and aflatoxin B_1. Toxicol.Lett., **92:** 161–172.
27. Sharma R.P., Dugyala R.R., Voss K.A., (1997), Demonstration of in-situ apoptosis in mouse liver and kidney after short-term repeated exposure to fumonisin B1. Comp.Path., **117:** 371–381.
28. Smith G.W., Constable P.D., Smith A.R., Bacon C.W., Meredith F.I., Wollenberg G.K., Haschek W.M., (1996), Effects of fumonisin-containing culture material on pulmonary clearance in swine. Am.J.Vet.Res., **57:** 1233–1248.
29. Trandaburu T., Trandaburu I., Ţăranu I., Marin D., (2003), Aflatoxin B_1(AFB_1)-induced morphological alterations in the swine organs; the alleviating effect of vitamin C. Proc.Inst.Biol., **5:** 573–581.
30. Voss K.A., Riley R.T., Norren W.P., Bacon C.W., Meredith F.I., Howard P.C., Plattner R.D., Collins T.F., Hansen D.K., Porter J.K., (2001), An overview of rodent toxicity: liver and kidney effects of fumonisins and *Fusarium moniliforme*. Environ.Health Perspect., **109** suppl. **2:** 259–266.
31. Zomborsky-Kovacs M., Vetesi F., Horn P., Repa I., Kovacs F., (2002), Effects of prolonged exposure to low-dose fumonisin B1 in pigs. J.Vet.Med. B Infect.Dis.Vet.Public Health, **49:** 197–201.
32. Wattenberg E.V., Badria F.A., Shier W.T., (1996), Activation of mitogen-activated protein kinase by the carcinogenic mycotoxin fumonisin B1. Biochem.Biophys.Res.Commun., **227:** 622–627.

33. Weibking T.S., Ledoux D.R., Bermudez A.J., Turk J.R., Rottinghause G.E., Wang E., Merrill A.H., (1993a), Effects of feeding with *Fusarium moniliforme* culture material containing known levels of fumonisin B1 on the young broiler chick. Poultry Sci., **72:** 456–466.
34. Weibking T.S., Ledoux D.R., Brown T.P., Rottinghans G.E., (1993b), Fumonisin toxicity in turkey poults. J.Vet.Diagn.Invest., **5:** 75–83.
35. Yoshizawa T., Yamashita A., Luo Y., (1994), Fumonisin occurrence in corn from high-and low-risk areas for human esophageal cancer in China. Appl.Environ.Microbiol., **60:** 1626–1629.

Received August 11, 2004.

*Institute of Biology
Spl. Independenţei 296
P.O.Box 56-63
060031-Bucharest
Romania

**INRA
Laboratoire de Pharmacologie
et Toxicologie
180 Chemin de Tournefeuille BP 3
31931-Toulouse cedex 9 France

***Institute of Biology and
Animal Nutrition, Calea Bucureşti 1
Baloteşti, Romania and INRA,
Laboratoire de Pharmacologie et
Toxicologie, 180 Chemin de
Tournefeuille, 31931-Toulouse cedex 9, France

MORPHOLOGY AND STRUCTURE OF THE TRACHEAL GILLS OF TWO SPECIES OF STONEFLIES (PLECOPTERA)

ANCA-NARCISA NEAGU

A morphological, light and electronic (SEM) examination was made of the tracheal gills of two species of stonefly (*Perla marginata* Pz. and *Dinocras cephalotes* Curt.) larvae.

The microscopic examination showed specialized structures like the coniform and floriform chloride-cells. These cellular complexes participate in osmoregulation. These results suggest that in addition to their respiratory function, the ionic transporting type cells play an important role in absorption of electrolytes to maintain a constant osmotic pressure of the haemolymph in freshwater environments. The epithelial cells of gills are respiratory in function.

1. INTRODUCTION

The perlid tracheal gills are the filamentous outgrowth of the thoracic integument of some species of larvae of aquatic insects.

The structure and ultrastructure of the gill epithelium of some species of American, Australian and European stonefly have been described. The tracheal epithelium showed many specialized cellular complexes:

- Floriform chloride-cells of *Trinotoperla irrorata* (*Gripopterygidae*) (Wichard and Eisenbeis, 1979);
- Flower-shaped sensillum of *Thaumatoperla alpina* (Kapoor and Zachariah, 1978, 1983, 1984), *Thaumatoperla alpina, Eusthenia sp., Stenoperla australis* and *Eusthenia venosa* (Kapoor and Zachariah, 1973 b);
- Caviform and bulbiform chloride-cells of *Nemoura cinerea* and *Protonemura auberti* (Wichard and Komnick, 1973);
- Coniform chloride-cells of *Perla marginata* and *Perlodes microcephalus* (Wichard and Komnick, 1973) and of *Paragnetina media* (Kapoor and Zachariah, 1973 a).

Starting from these results, we tried to identify similar structures of stoneflies larvae: *Perla marginata* and *Dinocras cephalotes*. We also assumed that such structures could change under the influence of degrading water quality.

REV. ROUM. BIOL. – BIOL. ANIM., TOME 49, N^{os} 1–2, P. 157–169, BUCAREST, 2004

2. MATERIALS AND METHODS

The *Plecoptera* larvae were collected in 2001, from the Izvorul Alb creek, one of the main tributaries of the Bicaz reservoir of the Romanian Eastern Carpathians.

For morphological examination, the gills were fixed in 70% ethanol, stained with eosine, dehydrated in ethanol and amylic alcohol, examined and photographed with a Zeiss stereomicroscope and a NOVEX microscope.

The thoracic gills were fixed for light microscopy in 10% formaldehyde, dehydrated in alcohol, embedded in paraffin and sectioned at 3 microns. They were stained with hemalaun-eosine and photographed with a NOVEX microscope with a Canon EOS 1V.

For scanning electron microscopy, the gills were fixed in 4 % glutaraldehyde in phosphate buffer and stained with silver. They were examined and photographed in a Tesla 300 BS.

3. RESULTS AND DISCUSSIONS

Shepard and Stewart (1983) have illustrated and described the American perlid gills.

Perla marginata has the next gill formula: ASC1 (anterior supracoxal) (Fig. 3), PSC1 (posterior supracoxal) (Fig. 4), AT2 (anterior thoracic) (Fig. 5), PSC2 (Fig. 6), AT3 (Fig. 7), PSC3 (Fig. 8), PT3 (posterior thoracic), A1 (abdominal) (Fig. 9) and *Dinocras cephalotes*: ASC1, PSC1, AT2, PSC2, AT3, PSC3, PT3, A1, SL (subanal), without any deviation from formula proposed by Shepard and Stewart for the American perlids. The filamentous tracheal gills of *Perla marginata* (Fig. 1) and *Dinocras cephalotes* (Fig. 2) have one (Fig. 4, Figs. 8 and 9), two (Figs. 3 and 6) or three trunks (Figs. 5 and 7).

In cross section, the gills have an epithelial wall and a haemolymphatic central space in communication with the haemocel of the body (Figs. 10 and 11).

The epithelial wall is formed by respiratory cells and specialized cells, **coniform chloride-cells** of *Perla marginata* (Fig. 12, Fig. 13, Fig. 14, Fig. 15) and it is covered by an extremely thick cuticle layer.

The tracheal surface of *Dinocras cephalotes* showed the cuticular discs of **coniform chloride-cells** (Fig. 16) and **flower-form chloride-cells** (Figs. 17 and 18).

The cuticular disc-shape structures form the interface of each chloride-cell with the external environment.

Fig. 1 – Filamentous gill of *Perla marginata* larvae.

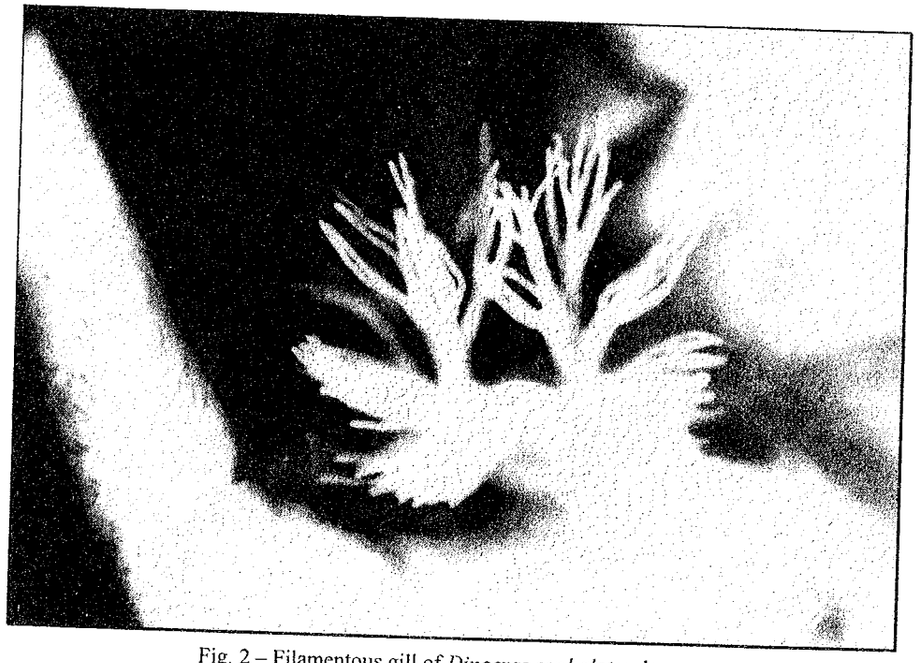

Fig. 2 – Filamentous gill of *Dinocras cephalotes* larvae.

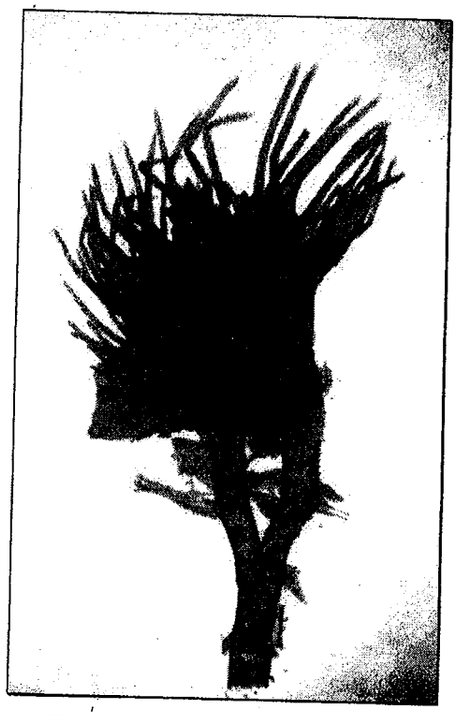

Fig. 3 – Filamentous gill of *Perla marginata* with double trunks, ASC1 (HE, 6 × 4).

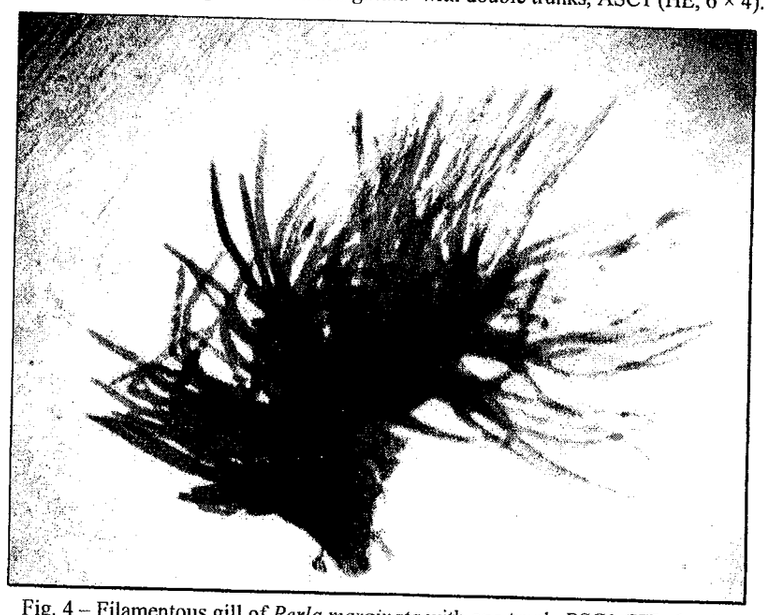

Fig. 4 – Filamentous gill of *Perla marginata* with one trunk, PSC1 (HE, 6 × 4).

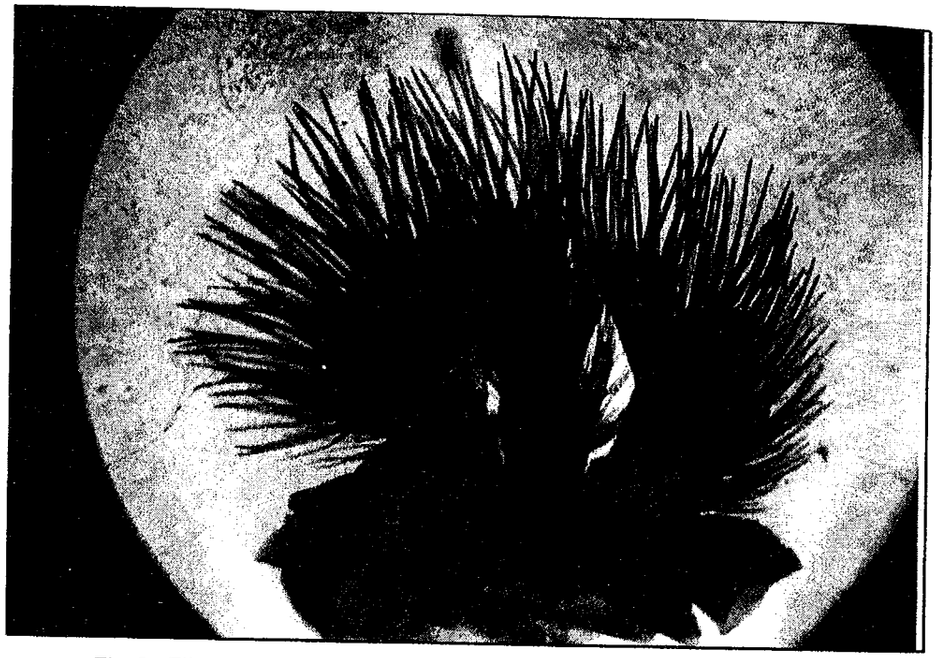

Fig. 5 – Filamentous gill of *Perla marginata* with three trunks, AT2 (HE, 5 × 4).

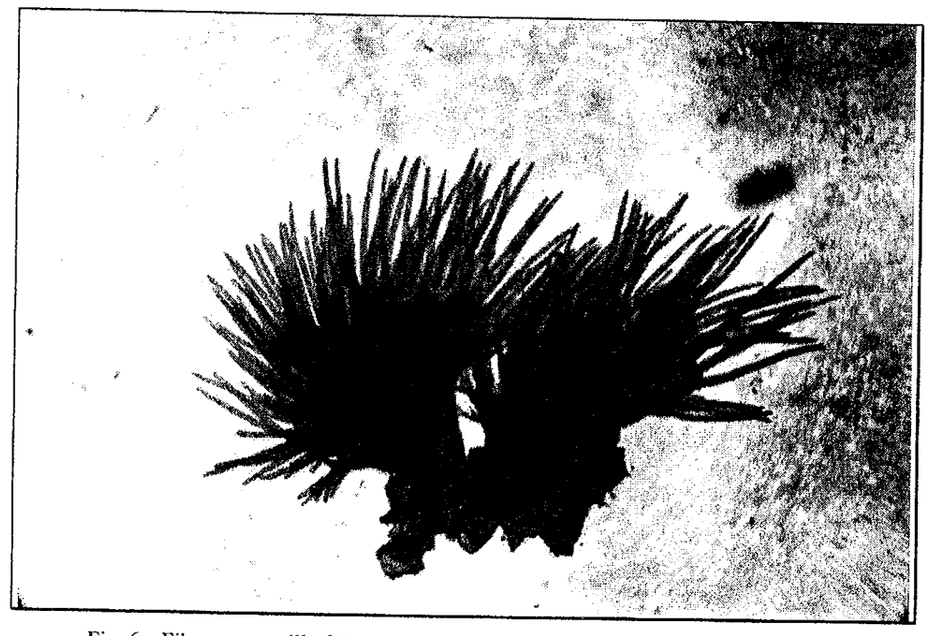

Fig. 6 – Filamentous gill of *Perla marginata* with double trunks, PSC2 (HE, 6 × 4).

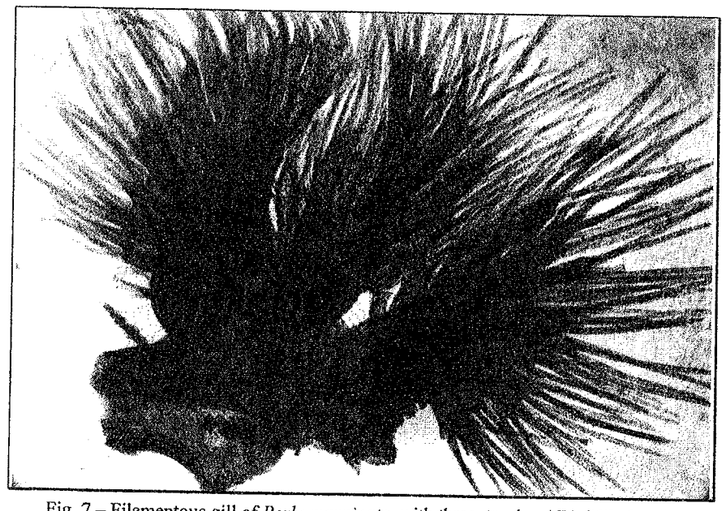

Fig. 7 – Filamentous gill of *Perla marginata* with three trunks, AT3 (HE, 6 × 4).

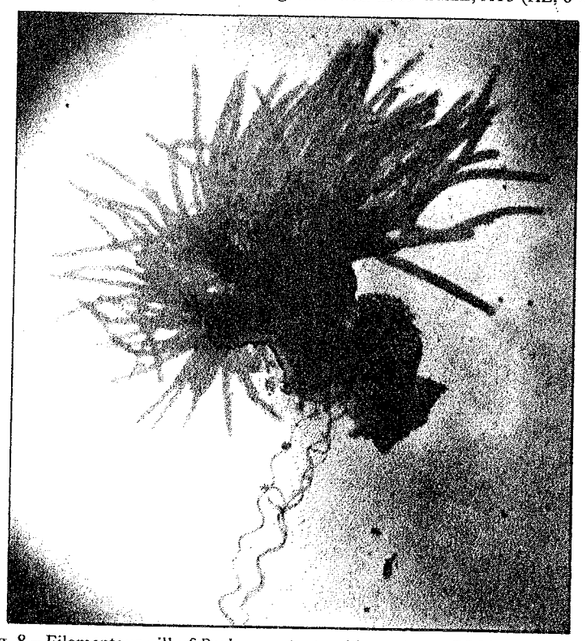

Fig. 8 – Filamentous gill of *Perla marginata* with one trunk, PSC3 (HE, 6 × 4).

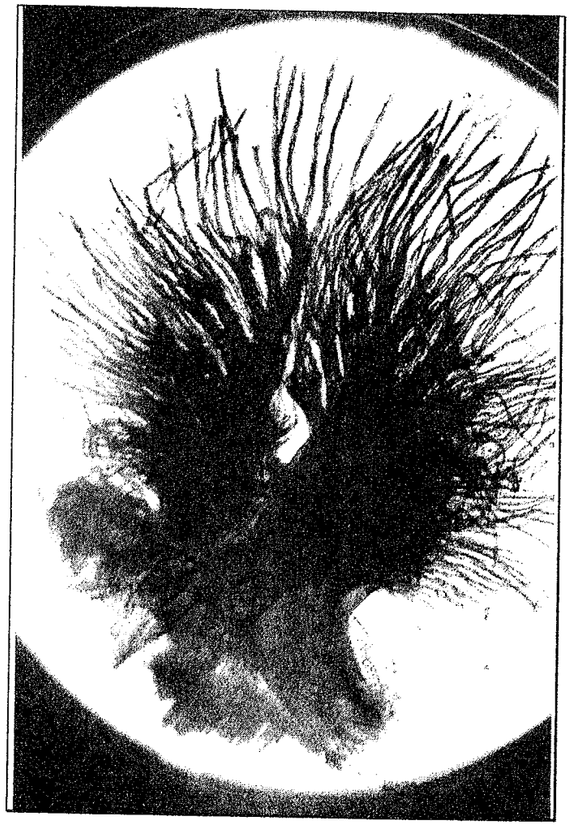

Fig. 9 – Filamentous gill of *Perla marginata* with one trunk, PT3, A1 (HE, 5 × 4).

Fig. 10 – Gill filament of *Perla marginata* (cross section, SEM, 990 ×).

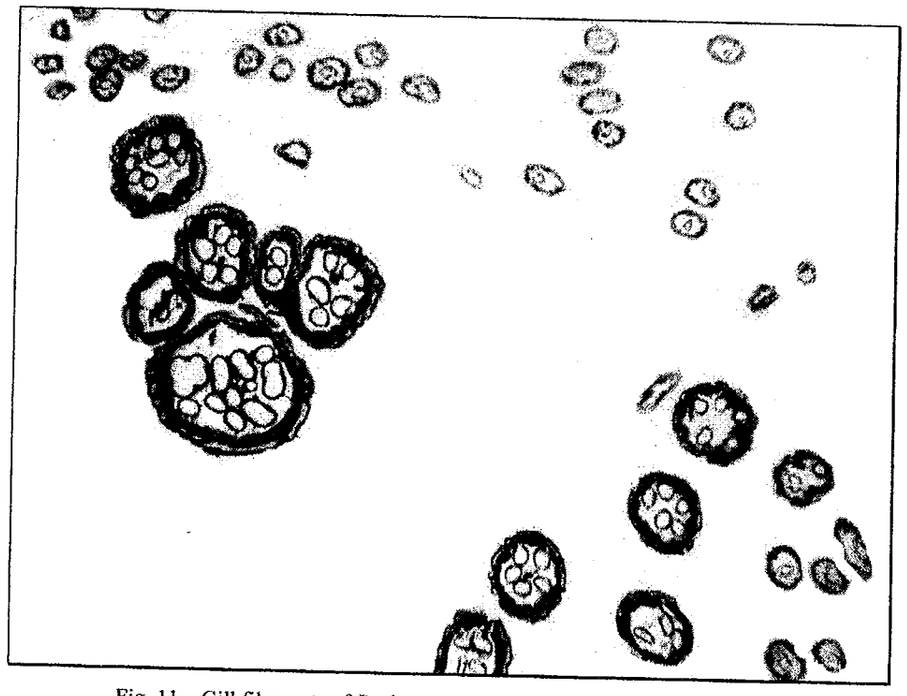

Fig. 11 – Gill filaments of *Perla marginata* (cross section, HE, 21,5 × 20).

Fig.12 – Light micrographs of the epithelial gill wall showing specialized cells of *Perla marginata* larvae (HE, 16,5 × 20).

Fig.13 – Gross morphology of the surface of gill of *Perla marginata* larvae. SEM (240 ×).

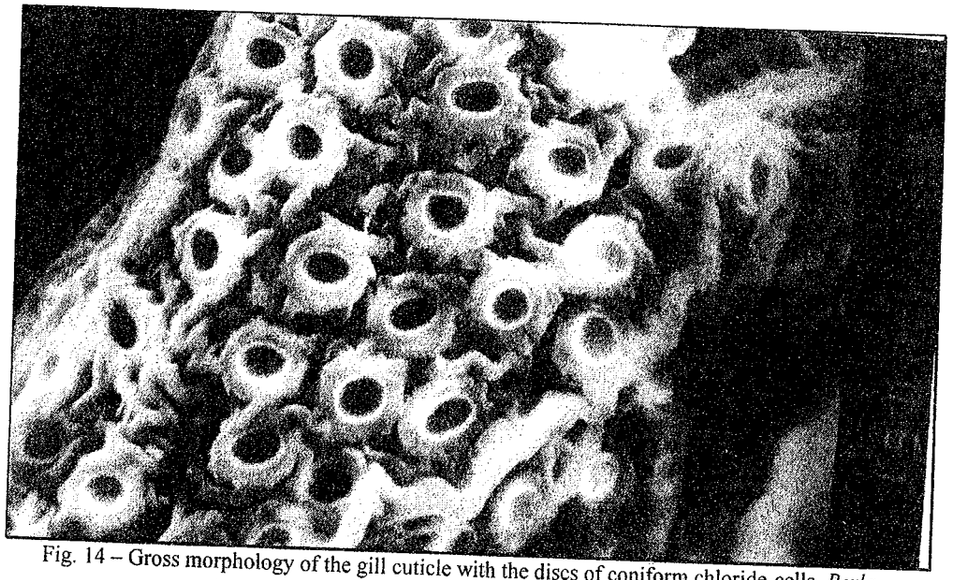

Fig. 14 – Gross morphology of the gill cuticle with the discs of coniform chloride-cells. *Perla marginata* larvae (1045 ×).

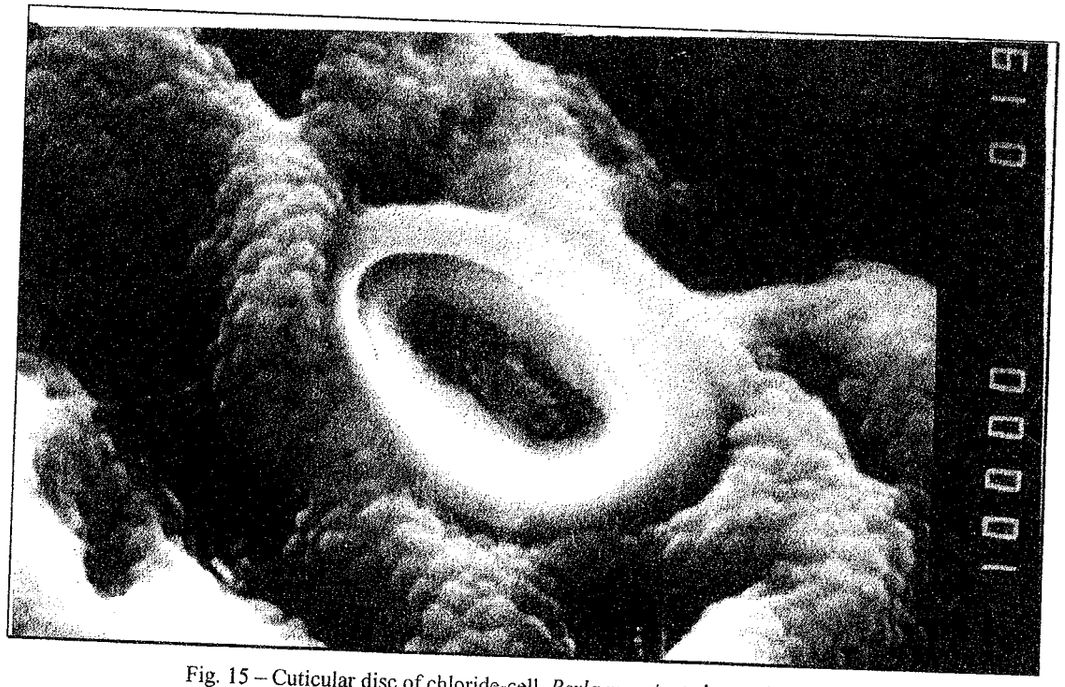

Fig. 15 – Cuticular disc of chloride-cell, *Perla marginata* larvae (6000 ×).

Fig. 16 – Gross morphology of the gill cuticle and the discs of coniform chloride-cell of *Dinocras cephalotes* larvae. SEM (2200 ×).

Fig. 17 – Gross morphology of the gill cuticle and the flower-shaped chloride-cells of *Dinocras cephalotes* larvae. SEM (7315 ×).

Fig. 18 – Gross morphology of the gill cuticle and the flower-shaped chloride-cells of *Dinocras cephalotes* larvae. SEM (6000 ×).

4. CONCLUSIONS

The morphological and structural examination of the thoracic and abdominal gill epithelium of two species of stoneflies showed specialized structures:

- Coniform chloride-cells of *Perla marginata* and *Dinocras cephalotes*;
- Flower-shaped chloride-cells of *Dinocras cephalotes*. This type of chloride cells is exclusively known in representatives of the suborder Antarctoperlaria, four families existing only in South America, Australia and New Zealand.

These cells showed their implication in the osmoregulation by the absorption of ions even if these filamentous are primarily respiratory in function.

Acknowledgements. I am grateful to Prof. dr. Ionel Miron for his aid in collecting and taxonomic determination of the larvae and for precious suggestions, to Prof. dr. Peter Zwick for references and to Engineer Dumitru Răileanu for technical assistance in electronic microscopy.

REFERENCES

1. Kapoor, N. N., Zachariah, K., 1973 a. *A study of specialized cells of the tracheal gills of Paragnetina media (Plecoptera)*. Can. J. Zool. Vol. **51:** 983–986.

2. Kapoor, N. N., Zachariah, K., 1973 b. *Abdominal gills in Eustheniidae (Plecoptera)*. Int. J. Insect Morphol. & Embriol. **2**(4)**:** 351–355.
3. Kapoor, N. N., Zachariah, K., 1984. *Scanning and transmission electron microscopy of the developmental stages af the flower-shape sensillum of the stonefly nymph, Thaumatoperla alpina* Burns *and* Neboiss *(Plecoptera: Eustheniidae)*. Int. J. Insect Morphol. & Embriol., vol. 13, **3:** 177–189.
4. Shepard, D.W., Stewart, K.K., 1983. *Comparative Study of Nymphal Gills in North American Stonefly (Plecoptera) Genera and a New, Proposed Paradigm of Plecoptera Gill Evolution.* MPEAAL **55:** 1–57.
5. Wichard, W., Eisenbeis, G., 1979. *Fine Structural and Histochemical Evidence of Chloride Cells in Stonefly Larvae 3. The Floriform Chloride Cells.* Aquatic Insects 1, **3:** 185–191.
6. Wichard, W., Komnick, H., 1973. *Feinstructureller und histochemischer Nachweis von Chloridzellen bei Steinfliegenlarven.* Cytobiologie 7, Heft **3:** 297–314.

Received May 22, 2004.

"Al.I. Cuza" University
Faculty of Biology
20 A Carol I Bvd.,
700506 Iaşi
aneagu@uaic.ro

AVIS AUX COLLABORATEURS

La «Revue roumaine de biologie – Série de biologie animale» publie des articles originaux d'un haut niveau scientifique de tous les domaines de la biologie animale: taxonomie, morphologie, physiologie, génétique, écologie, etc. Les sommaires des revues sont complétés par d'autres rubriques, comme: 1. La vie scientifique, qui traite des manifestations scientifiques du domaine de la biologie (symposiums, conférences, etc.); 2. Comptes rendus des plus récentes parutions dans la littérature.

Les auteurs sont priés de présenter leurs articles en double exemplaire, imprimés de préférence sur une imprimante laser et espacés à double interligne. Le contenu des articles sera introduit sur des disquettes dans un langage connu, préférablement Word 6.0. La composition et la mise en vedette seront faites selon l'usage de la revue: caractères de 11/13 points pour le texte, de 12/14 points pour le titre de l'article et de 9/11 pour les annexes (tableaux, bibliographie, explication des figures, notes, etc.) et le résumé en anglais de 10 lignes au maximum, qui sera placé au début de l'article. Il est obligatoire de spécifier sur les disquettes le nom des fichiers ainsi que le programme utilisé.

Le matériel graphique sera envoyé sur disquette, scanné, avec les mêmes spécifications. En l'absence d'un scanner, le matériel graphique sera exécuté en encre de Chine sur papier calque.

Les tableaux et les illustrations seront numérotés en chiffres arabes dans l'ordre de l'apparition. Les titres des revues seront abrégés conformément aux usages internationaux.

Les textes ne doivent pas dépasser 10 pages (y compris les tableaux, la bibliographie et l'explication des figures).

La responsabilité pour le contenu des articles revient exclusivement aux auteurs.